ZooKeys 1083: 1–12 (2022)
doi: 10.3897/zookeys.1083.77428
https://zookeys.pensoft.net

RESEARCH ARTICLE

A peer-reviewed open-access journal
ZooKeys
Launched to accelerate biodiversity research

A new species of *Simulium* (*Gomphostilbia*) (Diptera, Simuliidae) from Thailand, with a key to identify females of 14 species of the *Simulium varicorne* species-group

Wichai Srisuka[1], Kittipat Aupalee[2], Yasushi Otsuka[3], Masako Fukuda[4], Hiroyuki Takaoka[5], Atiporn Saeung[2]

1 *Entomology Section, Queen Sirikit Botanic Garden, P.O. Box 7, Maerim, Chiang Mai 50180, Thailand* **2** *Center of Insect Vector Study, Department of Parasitology, Faculty of Medicine, Chiang Mai University, Chiang Mai 50200, Thailand* **3** *Research Center for the Pacific Islands, Kagoshima University, Korimoto 1–21–24, Kagoshima City, Kagoshima 890–8580, Japan* **4** *Institute for Research Management, Oita University, Idaigaoka 1–1, Hasama, Yufu City, Oita, 879–5593, Japan* **5** *Higher Institution of Centre of Excellence (HICoE), Tropical Infectious Diseases Research and Education Centre, (TIDREC), Universiti Malaya, Kuala Lumpur, 50603, Malaysia*

Corresponding author: Atiporn Saeung (atisaeung.noi@gmail.com)

Academic editor: Art Borkent | Received 1 November 2021 | Accepted 5 January 2022 | Published 21 January 2022

http://zoobank.org/C4DC1800-DFA3-4490-B33B-57085534C701

Citation: Srisuka W, Aupalee K, Otsuka Y, Fukuda M, Takaoka H, Saeung A (2022) A new species of *Simulium* (*Gomphostilbia*) (Diptera, Simuliidae) from Thailand, with a key to identify females of 14 species of the *Simulium varicorne* species-group. ZooKeys 1083: 1–12. https://doi.org/10.3897/zookeys.1083.77428

Abstract

Simulium (*Gomphostilbia*) *khelangense* **sp. nov.** is described on the basis of females, collected by a sweeping net in Lampang, Phitsanulok and Chiang Mai Provinces, Thailand. This new species is placed in the *S. chumpornense* subgroup of the *S. varicorne* species-group in the subgenus *Gomphostilbia* Enderlein by having the antenna with eight flagellomeres, pleural membrane bare, and female subcosta lacking hairs. It is similar to *S. kuvangkadilokae* Pramual & Tangkawanit from Thailand in the same subgroup but is barely distinguished from the latter species by the head width relative to the greatest width of the frons and length of the labrum relative to the clypeus. A genetic analysis using the COI gene sequences similarly shows that *S. khelangense* **sp. nov.** is most closely related to *S. kuvangkadilokae*, with a genetic distance of 1.23–2.81%. A revised key to identify females of 14 species of the *S. varicorne* species-group is provided.

Keywords

Aquatic insects, biodiversity, blackflies, sweeping net, taxonomy

Introduction

The *Simulium varicorne* species-group, one of the 15 species-groups of the subgenus *Gomphostilbia* Enderlein of the genus *Simulium* Latreille, redefined by Takaoka (2012), is small, consisting of 14 species, of which 12 have been recorded in the Oriental region and the remaining two in the Palearctic region (Adler 2021). In Thailand, five species of this group are recorded: *Simulium burtoni* Takaoka & Davies, *S. chumpornense* Takaoka & Kuvangkadilok, *S. kuvangkadilokae* Pramual & Tangkawanit, *S. novemarticulatum* Takaoka & Davies, and *S. piroonae* Takaoka & Srisuka (Kuvangkadilok and Takaoka 2000; Takaoka and Choochote 2004; Pramual and Tangkawanit 2008; Takaoka et al. 2010, 2014).

Biting habits and other biological aspects of these species remain unknown, although females of *S. burtoni* and *S. chumpornense* were captured using human attractants at low and medium elevations in Doi Inthanon National Park in Chiang Mai (Choochote et al. 2005), and females of *S. chumpornense* were natural vectors of protozoan parasites of the genera *Leucocytozoon* Berestneff and *Trypanosoma* Gruby (Thaijarern et al. 2019; Pramual et al. 2020).

Recently, we found a female of an unnamed species of the *S. varicorne* species-group, for which hereafter we call "*Simulium* sp." as used by Aupalee et al. (2020), when morphologically and molecularly investigating parasites in adult female black flies collected by a sweeping net at Ban Pang Dang, Chiang Mai Province, Thailand. An unknown filarial species (probably a new species) was found in this unnamed species (Aupalee et al. 2020). *Simulium* sp. is placed in the *S. chumpornense* subgroup in the same species-group by lacking hairs ventrally on the subcosta, as defined by Takaoka (2012). It is morphologically similar to *S. kuvangkadilokae* of the same subgroup by having the hind tibia darkened on the apical half (Takaoka et al. 2014) and also genetically close to the latter species with a genetic distance of 1.99–2.36% (Aupalee et al. 2020).

In this study, we aimed to evaluate the status of *S.* sp. by morphologically and molecularly examining additional adult females collected by a sweeping net while they were flying around a human attractant, and to provide a revised key to identify females of 14 species of the *S. varicorne* species-group.

Materials and methods

Morphological analysis

Nine females of adult black flies (with eight antennal flagellomeres and without hairs ventrally on their subcosta) preserved in 80% ethanol after collection at three localities were used in this study. All were morphologically examined for color of legs, and heads and abdomens of three females (from each site) were treated with KOH solution overnight and observed in detail. The methods of collection, description and

illustration, as well as terms for morphological features, followed those of Takaoka (2003). The type specimens are deposited at the Entomology Section, Queen Sirikit Botanic Garden, Chiang Mai, Thailand.

All but two were separated into three parts, head, thorax, and abdomen, and the thoraces were used for DNA analysis. The localities, number of females, designated numbers for DNA analysis are as follows:

- Site 1 at Pratoo Pha, Mueang, Lampang Province: three females (CPPT–1, CPPT–2, CPPT–3)
- Site 2 at Ban Lek, Fang District, Chiang Mai Province: three females (CPPH-1, two females not dissected)
- Site 3 at Ban Romklao Botanic Garden, Chat Trakan, Phitsanulok Province: three females (CPRK–1, CPRK–2, CPRK–3).

Genetic analysis

The procedures for DNA extraction, PCR amplification, and sequencing followed those of Aupalee et al. (2020). In brief, total DNA was extracted from the thorax of individual adult black flies, using the Gene JET Genomic DNA Purification Kit (Thermo Fisher Scientific, Waltham, MA). DNA amplification of the COI gene using the LCO1490 forward primer and HCO2198 reverse primer (Folmer et al. 1994) was carried out with a reaction mixture of 20 µl consisting of 2 µl of DNA template, 0.5 U of *Taq* DNA polymerase, 3 mM of $MgCl_2$, 0.25 mM dNTPs and 0.2 µM of each primer. The thermal cycling for PCR was as follow: 94 °C for 2 min followed by 40 cycles of 94 °C for 30 sec, 50 °C for 45 sec, and 72 °C for 45 sec, with a final extension at 72 °C for 5 min. After PCR amplification, the amplified products were subjected to electrophoresis on 1.5% agarose gel, stained with Ultrapower (BioTeke, Beijing, China) dye, and 100 bps DNA marker was used as standard. PCR products were purified and sequenced using the BigDyeTerminator v.3.1 cycle sequencing kit (First BASE, Selangor, Malaysia) and run on an ABI 3730XL Genetic Analyzer (Applied Biosystems Inc., Foster City, CA, USA).

After DNA sequencing, sequence assembly and alignment were conducted using Geneious Prime 2021.1.1 (Kearse et al. 2012). Genetic distance was estimated using the Kimura 2-parameter (K2P) model, implemented in MEGA 7 (Kumar et al. 2016). Phylogenetic analysis based on the COI gene sequences was performed using neighbor-joining (NJ) and Bayesian inference (BI) methods. The NJ tree was built in MEGA 7 with 1000 bootstrap replications (Kumar et al. 2016). The BI tree was constructed in MrBayes v.3.2.7 (Ronquist et al. 2012) and was run for two million generations with sampling every 100 generations and a burnin of 25%. GTR+I was selected as the best-fit model for BI method based on the Akaike Information Criterion (AIC) by using jModelTest v.2.1.10 (Guindon and Gascuel 2003; Darriba et al. 2012). The DNA sequence of *S. asakoae* belonging to the *S. asakaoae* species-group of the subgenus *Gomphostilbia* was used as the outgroup species. The COI gene sequences deposited

in GenBank of *S*. sp. (MT262583), *S. chumpornense* (MT262567, MT262569–MT262570), *S. kuvangkadilokae* (MT262571–MT262573) and *S. piroonae* (MT262574–MT262576) were used for comparison. Newly generated COI gene sequences were registered in GenBank (NCBI) database under the accession numbers: MZ543397–MZ543403.

Nomenclature

This paper and the nomenclatural acts have been registered in ZooBank (www.zoobank.org), the official register of the International Commission on Zoological Nomenclature. The Life Science Identifier (LSID) numbers are noted under the new species of black flies.

Results

Morphological analysis

All females seem to be indistinguishable from one another in many features except the mandible, which had three or four distinct outer teeth in six females (CPPH-1, CPPT-1, CPPT-2, CPPT-3, CPRK-2 and CPRK3), but had a few weak outer teeth in one female (CPRK-1).

All females of *S*. sp. have the subcosta lacking hairs ventrally indicating that these females are placed in the *S. chumpornense* subgroup in the *S. varicorne* species-group. Among six known species of the *S. chumpornense* subgroup, *S. kuvangkadilokae* and *S. piroonae*, both from Thailand, are similar to *S*. sp. in having the hind tibia darkened on the apical half. However, *S*. sp. is distinguished from *S. kuvangkadilokae* by the width of the head relative to the greatest width (4.21–4.66 versus 3.78–4.05), length of the labrum relative to the clypeus (0.65–0.69 versus 0.57–0.59), and length of the fore basitarsus relative to its greatest width (6.29–6.38 versus 5.56); from *S. piroonae* by the length of the sensory vesicle relative to the third segment (0.33–0.39 versus 0.25–0.30), and length of the fore basitarsus relative to its greatest width (6.29–6.38 versus 5.54–5.68) (Takaoka and Srisuka 2010; Takaoka et al. 2014).

Genetic analysis

A genetic analysis using the COI gene sequences shows two clear clades, one consisting of *S. kuvangkadilokae* and *S*. sp. including the sample previously reported (MT262583), and the other consisting of *S. chumpornense* and *S. piroonae* (Fig. 1). Genetic analysis similarly shows that *S*. sp. is most closely related to *S. kuvangkadilokae*, with a genetic distance of 1.23–2.81%. Intraspecific divergence for *S.* sp. ranged from 0.30 to 1.54%. Considering the morphological and genetic evidence, we conclude that *S*. sp. is new to science, thus being described here.

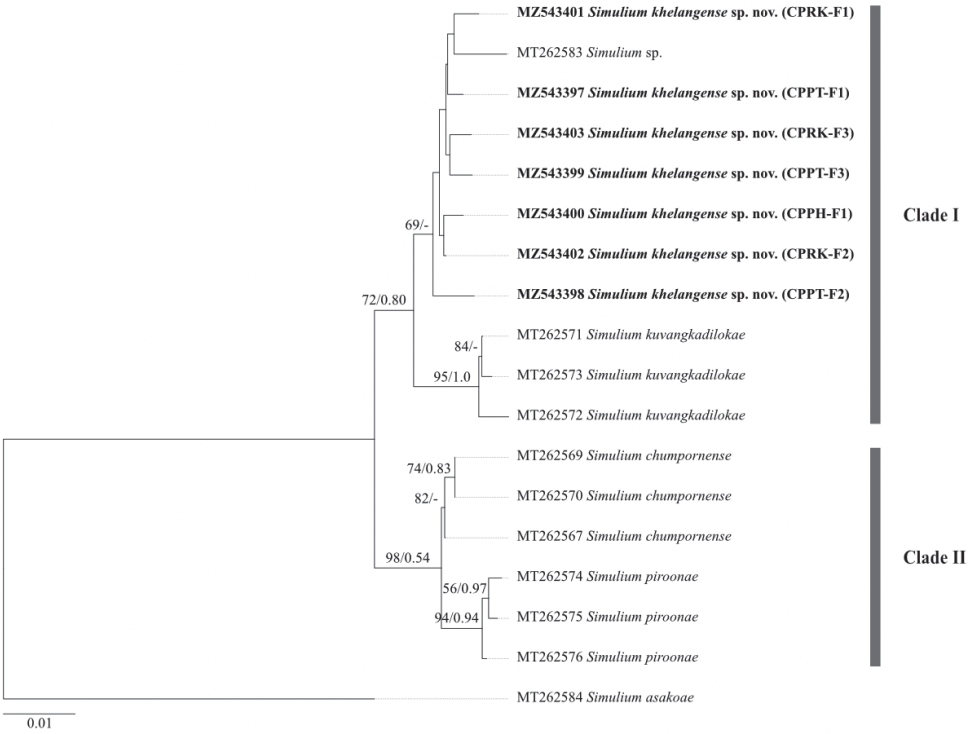

Figure 1. Neighbor-joining tree of the four Thai species in the *S. chumpornense* subgroup of the *S. varicorne* species-group based on 658 bp COI gene sequences. Bootstrap and posterior probability values (NJ/BI) are shown above each branch. The scale bar represents 0.01 substitutions per nucleotide position. Sequences in bold type are generated in this study.

Descriptions of new species

***Simulium* (*Gomphostilbia*) *khelangense* Takaoka, Srisuka & Saeung, sp. nov.**
http://zoobank.org/A2B76F93-9D05-4CA7-A03C-2FB789155495

Material examined. *Holotype*: Female (whole body) captured by a sweeping net, at Ban Lek, Fang District, Chiang Mai Province, 20°04'36.3"N, 99°10'53.0"E, 1571 m in elevation, 29 III 2018, by Wichai Srisuka (Site 2). ***Paratypes*:** One female and one female (except thorax), same data and date as for the holotype, three females (except thorax), collected at Pratoo Pha, Mueang, Lampang Province (Site 1); three females (except thorax) collected at Ban Romklao Botanic Garden, Chat Trakan, Phitsanulok Province (Site 3).

Diagnosis. Female adult: the only species of the *S. chumpornense* subgroup with antenna with eight flagellomeres, pleural membrane bare, subcosta bare, and hind tibia darkened on apical half, with dark subbasal marking and relatively slender fore basitarsus (6.29–6.38 times as long as its greatest width).

Description. Female (*N* = 9). Body length 2.3–2.5 mm.

***Head*.** Slightly narrower than thorax. Frons brownish black, dull, densely covered with yellowish-white scale-like recumbent short hairs; frontal ratio 1.35–1.44:1.00:1.71–2.09; frons:head ratio 1.00:4.21–4.66. Fronto-ocular area well developed, directed laterally and slightly upward. Clypeus brownish black, densely covered with yellowish-white scale-like short hairs interspersed with several dark unbranched longer hairs along lateral margin on each side. Labrum 0.65–0.69 times as long as clypeus. Antenna (Fig. 2A) composed of scape, pedicel and eight flagellomeres, dark brown to brownish black except scape, pedicel and base of first flagellomere yellowish white, rest of first flagellomere and third flagellomere medium to dark brown, and second and fourth flagellomeres yellow to dark yellow (sometimes light brown). Maxillary palpus composed of five segments, light brown, proportional lengths of third, fourth and fifth segments 1.00:1.00–1.03:2.34–2.48; third segment (Fig. 2B) somewhat swollen apically; sensory vesicle (Fig. 2B) ellipsoidal, 0.33–0.39 times length of third segment, with medium-sized opening. Maxillary lacinia with 9–12 inner, and 12–14 outer, teeth. Mandible with 20–22 inner teeth and with three or four outer teeth at some distance from apex, though outer teeth very weakly developed in one female. Cibarium (Fig. 2C) with pair of short stout submedian projections directed dorsally on dorsal margin.

***Thorax*.** Scutum brownish black (except anterolateral calli ochreous), shiny, gray-pruinose with three longitudinal nonpruinose vittae (one medial and two submedial), densely covered with yellowish-white scale-like recumbent short hairs intermixed with brownish similar hairs. Scutellum dark brown, covered with yellowish-white short hairs and dark brown upright long hairs. Postnotum dark brown, bare, slightly shiny and gray-pruinose when illuminated at certain angle. Pleural membrane bare. Katepisternum dark brown, longer than deep, moderately covered with yellowish fine hairs interspersed with dark brown hairs.

***Legs*.** Foreleg: coxa and trochanter yellowish white; femur medium brown though apical tip yellow; tibia medium brown, except base yellow, and median large portion on outer surface and apex light brown; tarsus brownish black, with moderate dorsal hair crest; basitarsus somewhat dilated, 6.29–6.38 times as long as its greatest width. Midleg: coxa dark brown; trochanter light brown; femur medium to dark brown though apical tip yellow; tibia (Fig. 2D) light brown on basal two-fifths except base yellow and with or without faint subbasal dark marking, and medium to dark brown on apical three-fifths; tarsus light brown except basal three-fourth of basitarsus, basal half of second tarsomere and base of third tarsomere yellowish white. Hind leg: coxa dark brown; trochanter yellowish; femur dark brown with base and apical tip yellowish; tibia (Fig. 2E) dark brown to brownish black on apical half, and yellowish on base, with distinct medium brown subbasal marking (though dark yellow to light brown between subbasal marking and dark apical half, and sometimes subbasal dark marking connected along posterior margin to dark apical half); tibia densely covered with whitish-yellow fine hairs on outer and posterior surface of basal three-fourths; tarsus medium brown except little more than basal two-thirds (though base light brown)

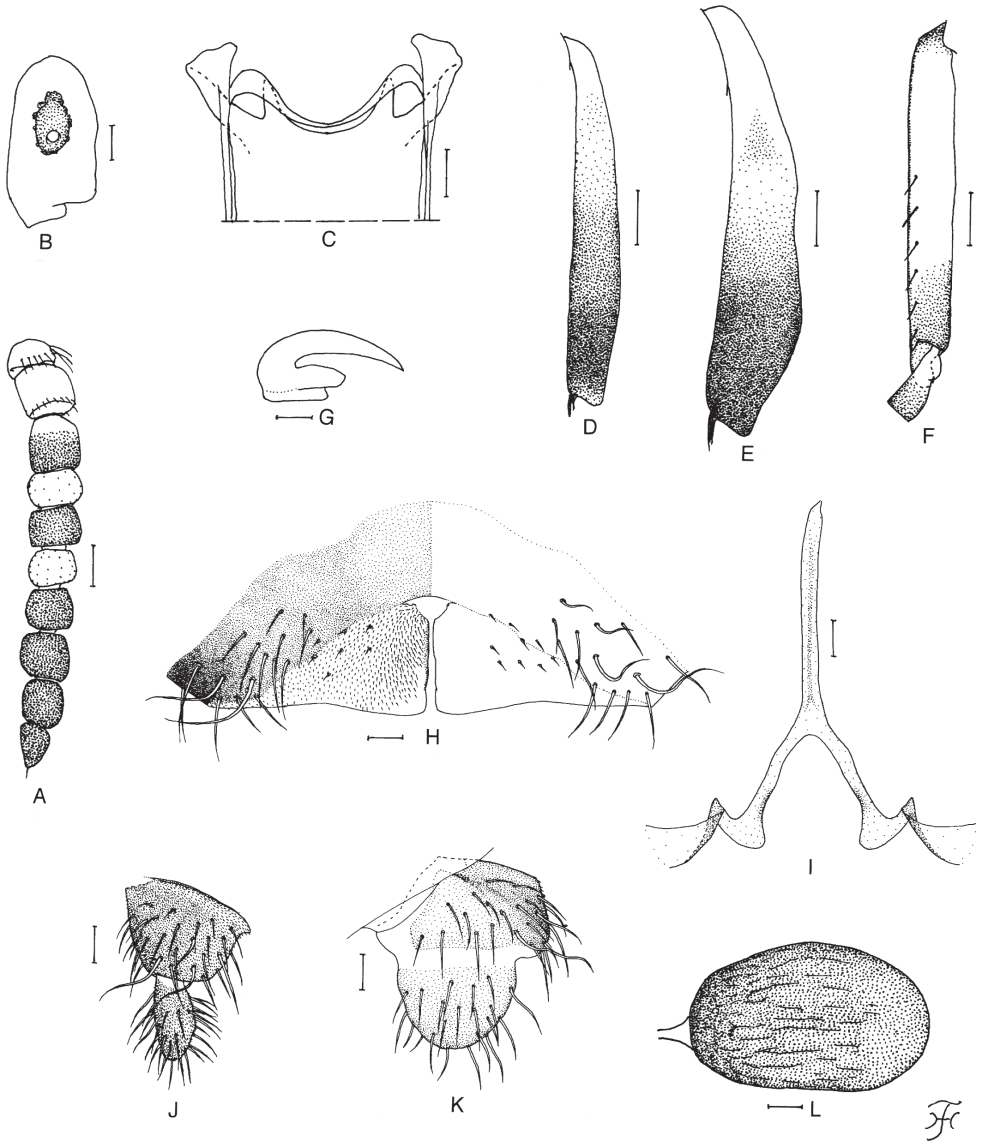

Figure 2. Female of *Simulium khelangense* sp. nov. **A** antenna (left side; dorsal view) **B** third palpal segment with sensory vesicle (right side; front view) **C** cibarium **D** mid tibia (left side; outer view) **E** hind tibia (left side; outer view) **F** hind basitarsus and second tarsomere (left side; outer view) **G** claw of hind tarsus (lateral view) **H** eighth sternite and ovipositor valves (ventral view) **I** genital fork (ventral view) **J, K** paraprocts and cerci (right side; **J** ventral view **K** lateral view) **L** spermatheca. Scale bars: 0.1 mm (**D–F**); 0.05 mm (**A**); 0.02 mm (**B, C, H–L**); 0.01 mm (**G**).

of basitarsus and basal half of second tarsomere yellowish white; basitarsus (Fig. 2F) narrow, nearly parallel-sided, 6.55–7.05 times as long as wide, and 0.58–0.61 and 0.48–0.52 times as wide as greatest width of tibia and femur, respectively; calcipala

(Fig. 2F) 1.3 times as long as wide, and 0.45–0.47 times as wide as width of basitarsus; pedisulcus (Fig. 2F) well marked. Hind tarsal claw (Fig. 2G) with large basal tooth 0.46–0.47 times length of claw.

Wing. Length 2.0 mm. Costa with dark brown spinules and dark brown hairs except basal portion with patch of white hairs. Subcosta bare. Hair tuft on base of radial vein white. Basal portion of radius fully haired. Basal cell absent.

Halter. White with base of stem darkened.

Abdomen. Basal scale light brown, with fringe of yellowish-white fine hairs. Dorsal surface of abdomen medium brown to brownish black except little less than basal one-half lighter, moderately covered with yellowish-white short hairs interspersed with dark brown long hairs; tergites of segments 2 and 6–8 shiny; sternal plate on segment 7 undeveloped.

Genitalia. Sternite 8 (Fig. 2H) bare medially, with 14–16 long stout hairs and two to five short setae on each side. Ovipositor valves (Fig. 2H) nearly triangular, thin, membranous, each moderately covered with microsetae interspersed with five or six short setae; inner margins slightly sinuous, moderately sclerotized. Genital fork (Fig. 2I) of usual inverted-Y form, with narrow arms; arm folded medially. Paraproct in ventral view (Fig. 2J) rounded outwardly and tapered medially, with 26–31 long hairs on ventral and lateral surfaces, and with five sensilla on anteromedial surface; paraproct in lateral view (Fig. 2K) moderately produced ventrally beyond ventral margin of cercus, 0.58–0.68 times as long as wide. Cercus in lateral view (Fig. 2K) rounded posteriorly, 0.44–0.68 times as long as wide. Spermatheca (Fig. 2L) ellipsoidal, 1.67–1.88 times as long as wide, well sclerotized except duct unsclerotized, and with many fissures on surface; internal setae absent; both accessory tubes slender, slightly larger in diameter than major one.

Male, pupa and larva. Unknown.

Etymology. The species name *khelangense* refers to Khelang, an old name of Lampang Province, where this new species was collected.

Distribution. Thailand (Lampang, Phitsanulok and Chiang Mai).

Ecological note. Females of this new species were captured while attracted to a human, though they have a large claw tooth, a characteristic suggesting that this species is ornithophilic (Adler et al. 2004).

Discussion. *Simulium khelangense* sp. nov. is placed in the *varicorne* species-group in the subgenus *Gomphostilbia* by having the antenna with eight flagellomeres (Fig. 2A). It is further placed in the *chumpornense* subgroup by having the pleural membrane bare, and female subcosta lacking hairs ventrally, as defined by Takaoka (2012).

The female of this new species is distinguished from those of *S. kuvangkadilokae* and *S. piroonae* of the *S. chumpornense* subgroup, as noted above. This species is also distinguished from the four other members of the same subgroup: *S. chumpornense* from Thailand, *S. sumbaense* Takaoka & Suana from Sumba, Indonesia, *S. tomae* Takaoka from Sulawesi, Indonesia, and *S. varicorne* Edwards from Sumatra and Java, Indonesia, and Peninsular Malaysia, by the hind tibia darkened on the apical half (darkened on the apical one-third in the latter four species) (Kuvangkadilok and Takaoka 2000; Takaoka 2003; Takaoka et al. 2018a, b).

Key to females of 14 species of the varicorne species-group of the subgenus *Gomphostilbia*

The female of *S. breviflagellum* Takaoka & Sofian-Azirun from Vietnam is not included because its female is unknown.

1 Antenna with seven flagellomeres **2**
– Antenna with eight flagellomeres **3**
2 Sensory vesicle 0.29–0.31 times length of third palpal segment ..... ***S. charlesi* Takaoka**
– Sensory vesicle 0.21–0.25 times length of third palpal segment ..... ***S. novemarticulatum* Takaoka & Davies**
3 Pleural membrane haired ..... ***S. trirugosum* Davies & Györkös**
– Pleural membrane bare **4**
4 Subcosta haired ventrally **5**
– Subcosta bare **8**
5 Abdominal segments 5–8 shiny dorsally **6**
– Abdominal segments 6–8 shiny dorsally **7**
6 Flagellomeres darkened except basal one-third of first flagellomere yellow ..... ***S. huangi* Takaoka**
– Flagellomeres 3 and 5–8 darkened and others yellow ..... ***S. burtoni* Takaoka & Davies**
7 Hind femur entirely darkened ..... ***S. shogakii* Rubtsov**
– Hind femur darkened on apical one-third ..... ***S. synanceium* Chen & Cao**
8 Hind tibia darkened on apical half **9**
– Hind tibia darkened on apical one-third **11**
9 Fore basitarsus 6.29–6.38 times as long as its greatest width ..... ***S. khelangense* sp. nov.**
– Fore basitarsus 5.54–5.68 times as long as its greatest width **10**
10 Head 3.78–4.05 times as wide as greatest width of frons ..... ***S. kuvangkadilokae* Pramual & Tangkawanit**
– Head 4.30–4.54 times as wide as greatest width of frons ..... ***S. piroonae* Takaoka & Srisuka**
11 Head 6.7 times as wide as greatest width of frons ..... ***S. tomae* Takaoka**
– Head 3.7–5.2 as wide as greatest width of frons **12**
12 Head 4.7–5.2 times as wide as greatest width of frons ..... ***S. varicorne* Edwards**
– Head 3.9–4.0 as wide as greatest width of frons **13**
13 Height of frons 1.7 times as long as narrowest width ..... ***S. chumpornense* Takaoka & Kuvangkadilok**
– Height of frons 1.3–1.4 times as long as narrowest width ..... ***S. sumbaense* Takaoka & Suana**

Conclusions

Considering the morphological and genetic evidence, we conclude that *S*. sp. *sensu* Aupalee et al. (2020), is new to science, thus being described here. Females of *S*. (*G*.) *khelangense* sp. nov. were captured while attracted to a human. This new species is distributed in northern and central Thailand.

Acknowledgements

We are grateful to Dr Peter H. Adler (Professor Emeritus, Clemson University, Clemson, SC, USA) for reading the current manuscript and providing valuable comments. We acknowledge funding from the Ministry of Education, Malaysia, under the Higher Institution of Centre of Excellence (HICoE) niche area vector and vector-borne diseases (Project no. MO002–2019). This research was funded by the Office of Research Administration, Chiang Mai University, Thailand (A. Saeung).

References

Adler PH (2021) World Blackflies (Diptera: Simuliidae): A Comprehensive Revision of the Taxonomic and Geographical Inventory 2021, 144 pp. https://biomia.sites.clemson.edu/pdfs/blackflyinventory.pdf [accessed on 10 June 2021]

Adler PH, Currie DC, Wood DM (2004) The Black Flies (Simuliidae) of North America, Cornell University Press, Ithaca, New York, USA, [xv +] 941 pp.

Aupalee K, Saeung A, Srisuka W, Fukuda M, Streit A, Takaoka H (2020) Seasonal filarial infections and their black fly vectors in Chiang Mai province, northern Thailand. Pathogens 9: e512. https://doi.org/10.3390/pathogens9060512

Choochote W, Takaoka H, Fukuda M, Otsuka Y, Aoki C, Eshima N (2005) Seasonal abundance and daily flying activity of black flies (Diptera: Simuliidae) attracted to human baits in Doi Inthanon National Park, northern Thailand. Medical Entomology and Zoology 56: 335–348. https://doi.org/10.7601/mez.56.335

Darriba D, Taboada GL, Doallo R, Posada D (2012) jModelTest 2: more models, new heuristics and parallel computing. Nature methods 9: e772. https://doi.org/10.1038/nmeth.2109

Folmer O, Black M, Hoeh W, Lutz R, Vrijenhoek R (1994) DNA primers for amplification of mitochondrial cytochrome c oxidase subunit I from diverse metazoan invertebrates. Molecular Marine Biology and Biotechnology 3: 294–299. https://www.mbari.org/wp-content/uploads/2016/01/Folmer_94MMBB.pdf

Guindon S, Gascuel O (2003) A simple, fast, and accurate algorithm to estimate large phylogenies by maximum likelihood. Systematic Biology 52: 696–704. https://doi.org/10.1080/10635150390235520

Kearse M, Moir R, Wilson A, Stones-Havas S, Cheung M, Sturrock S, Buxton S, Cooper A, Markowitz S, Duran C, Thierer T (2012) Geneious Basic: an integrated and extendable

desktop software platform for the organization and analysis of sequence data. Bioinformatics 28: 1647–1649. https://doi.org/10.1093/bioinformatics/bts199

Kumar S, Stecher G, Tamura K (2016) MEGA7: molecular evolutionary genetics analysis version 7.0 for bigger datasets. Molecular Biology and Evolution 33: 1870–1874. https://doi.org/10.1093/molbev/msw054

Kuvangkadilok C, Takaoka H (2000) Taxonomic notes on Simuliidae (Diptera) from Thailand: Description of a new species and new distributional records of nine known species. Japanese Journal of Tropical Medicine and Hygiene 28: 167–175. https://doi.org/10.2149/tmh1973.28.167

Pramual P, Tangkawanit U (2008) A new species of *Simulium* (*Gomphostilbia*) (Diptera: Simuliidae) from Northeastern Thailand. Medical Entomology and Zoology 59: 297–303. https://doi.org/10.7601/mez.59.297

Pramual P, Tangkawanit U, Kunprom C, Vaisusuk K, Chatan W, Wongpakam K, Thongboonma S (2020) Seasonal population dynamics and a role as natural vector of *Leucocytozoon* of black fly, *Simulium chumpornense* Takaoka & Kuvangkadilok. Acta Tropica 211: e105617. https://doi.org/10.1016/j.actatropica.2020.105617

Ronquist F, Teslenko M, Van Der Mark P, Ayres DL, Darling A, Höhna S, Larget B, Liu L, Suchard MA, Huelsenbeck JP (2012) MrBayes 3.2: efficient Bayesian phylogenetic inference and model choice across a large model space. Systematic Biology 61: 539–542. https://doi.org/10.1093/sysbio/sys029

Takaoka H (2003) The Black Flies (Diptera: Simuliidae) of Sulawesi, Maluku and Irian Jaya. Kyushu University Press, Fukuoka, [xxii +] 581 pp.

Takaoka H (2012) Morphotaxonomic revision of *Simulium* (*Gomphostilbia*) (Diptera: Simuliidae) in the Oriental Region. Zootaxa 3577: 1–42. https://www.biotaxa.org/Zootaxa/article/view/zootaxa.3577.1.1

Takaoka H, Choochote W (2004) A list of and keys to black flies (Diptera: Simuliidae) in Thailand. Tropical Medicine and Health 32: 189–197. https://doi.org/10.2149/tmh.32.189

Takaoka H, Davies DM (1995) The Black Flies (Diptera: Simuliidae) of West Malaysia. Kyushu University Press, Fukuoka, Japan, [viii +] 175 pp.

Takaoka H, Huang YT (2017) A new black fly species of *Simulium* (*Gomphostilbia*) (Diptera: Simuliidae) from Taiwan, with keys to all 13 species of the *Simulium varicorne* species-group. Zootaxa 4312: 438–448. https://doi.org/10.11646/zootaxa.4312.3.2

Takaoka H, Otsuka Y, Choochote W, Aoki C, Hayakawa H, Thongsahuan S (2010) Descriptions of the male, pupa and larva of *Simulium* (*Gomphostilbia*) *novemarticulatum* (Diptera: Simuliidae) from Peninsular Malaysia and Thailand. Medical Entomology and Zoology 61: 59–67. https://doi.org/10.7601/mez.61.59

Takaoka H, Sofian-Azirun M, Chen CD, Lau KW, Halim MRA, Low VL, Suana IW, (2018a) Three new species of black flies (Diptera: Simuliidae) from the Lesser Sunda Archipelago, Indonesia. Tropical Biomedicine 35: 951–974. https://www.msptm.org/files/Vol35No4/951-974-Hiroyuki-Takaoka.pdf

Takaoka H, Srisuka W (2010) Description of the female of *Simulium* (*Gomphostilbia*) *kuvangkadilokae* (Diptera: Simuliidae) from Thailand. Medical Entomology and Zoology 61: 39–47. https://doi.org/10.7601/mez.61.39

Takaoka H, Srisuka W, Saeung A, Choochote W (2014) A new species of *Simulium* (*Gomphostilbia*) (Diptera: Simuliidae) from Thailand, with keys to 11 species of the *Simulium varicorne* species-group. Journal of Medical Entomology 51: 314–322. https://doi.org/10.1603/ME13171

Takaoka H, Ya'cob Z, Sofian-Azirun M (2018b) Classification, annotated list and keys for the black flies (Diptera: Simuliidae) of Peninsular Malaysia. Zootaxa 4498: 1–65. https://doi.org/10.11646/zootaxa.4498.1.1

Thaijarern J, Tangkawanit U, Wongpakam K, Pramual P (2019) Molecular detection of *Trypanosoma* (Kinetoplastida: Trypanosomatidae) in black flies (Diptera: Simuliidae) from Thailand. Acta Tropica 200: e105196. https://doi.org/10.1016/j.actatropica.2019.105196

ZooKeys 1083: 13–88 (2022)
doi: 10.3897/zookeys.1083.75624
https://zookeys.pensoft.net

RESEARCH ARTICLE

A peer-reviewed open-access journal
ZooKeys
Launched to accelerate biodiversity research

Notes on the taxonomic status and distribution of some Cylindrotomidae (Diptera, Tipuloidea), with emphasis on Japanese species

Levente-Péter Kolcsár[1], Nikolai Paramonov[2], Yume Imada[3], Daichi Kato[4], Maribet Gamboa[5], Dai Shinoka[1], Makoto Kato[6], Kozo Watanabe[1]

1 *Center for Marine Environmental Studies (CMES), Ehime University, Matsuyama, Ehime 790-8577, Japan* **2** *Zoological Institute, Russian Academy of Sciences, 1 Universitetskaya Emb., St Petersburg 199034, Russia* **3** *Graduate School of Science and Engineering, Ehime University, 2–5 Bunkyo-cho, Matsuyama, Ehime, 790-8577 Japan* **4** *Echigo-Matsunoyama Museum of Natural Sciences, 'Kyororo', 1712-2 Matsunoyama, Tôkamachi, 942-1411, Japan* **5** *Department of Ecology, Faculty of Sciences, Universidad Católica de la Santísima Concepción, 409054 Concepción, Chile* **6** *Graduate School of Human and Environmental Studies, Kyoto University, Sakyo-ku, Yoshida-nihonmatsu-cho, Kyoto, 606-8501 Japan*

Corresponding author: Levente-Péter Kolcsár (kolcsar.peter@gmail.com)

Academic editor: F. L. da Silva | Received 27 September 2021 | Accepted 28 December 2021 | Published 24 January 2022

http://zoobank.org/D263A9C3-D2EB-4A2D-9D7F-ECAC41AFD710

Citation: Kolcsár L-P, Paramonov N, Imada Y, Kato D, Gamboa M, Shinoka D, Kato M, Watanabe K (2022) Notes on the taxonomic status and distribution of some Cylindrotomidae (Diptera, Tipuloidea), with emphasis on Japanese species. ZooKeys 1083: 13–88. https://doi.org/10.3897/zookeys.1083.75624

Abstract

A morphological and molecular study of 17 Cylindrotomidae species revealed that the two subspecies of *Cylindrotoma distinctissima*, the Nearctic *C. americana* Osten Sacken, 1865, **stat. reval.** and the Palearctic *C. distinctissima* (Meigen, 1818), represent separated lineages and consequently are raised to species level. *Cylindrotoma japonica* Alexander, 1919, **syn. nov**. and *C. distinctissima alpestris* Peus, 1952, **syn. nov.** are now known to be junior synonyms of *C. distinctissima*. *Triogma kuwanai limbinervis* Alexander, 1953, **syn. nov.** and *T. nimbipennis* Alexander, 1941, **syn. nov.** are now placed into synonymy under *Triogma kuwanai* (Alexander, 1913). The Japanese Cylindrotomidae are all redescribed and all available literature and distribution data are summarised. Supplementary descriptions and illustrations for male and female terminalia of *Cylindrotoma nigriventris* Loew, 1849, *Diogma dmitrii* Paramonov, 2005, *Liogma nodicornis* (Osten Sacken, 1865), *Phalacrocera replicata* (Linnaeus, 1758), *P. tipulina* Osten Sacken, 1865, and *Triogma trisulcata* (Schummel, 1829) are provided. The following new distribution records are outlined; *Diogma caudata* Takahashi, 1960 from Arkhangelsk Oblast, Russia; *D. glabrata* (Meigen, 1818) from Belarus, Latvia, and Altai Republic, Amur Oblast, Novgorod Oblast, Magadan Oblast, Samara Oblast,

and Kuril Islands (Shikotan I and Paramushir I) in Russia; *Liogma serraticornis* Alexander, 1919 from Khabarovsk Krai, Russia; *Phalacrocera replicata* from Khabarovsk Krai, Russia; and the presence of *Cylindrotoma nigriventris* in Altai Republic, Russia is confirmed.

Keywords
Barcode, COI sequences, comparison, Cylindrotominae, ovipositor, terminalia, Tipulomorpha

Introduction

The Cylindrotomidae, the so-called long-bodied crane flies, are the smallest crane fly family within the superfamily Tipuloidea, with 70 extant species and 18 extinct species (Greenwalt et al. 2019; Krzemiński et al. 2019; Kania-Kłosok et al. 2021; Oosterbroek 2021). The family is subdivided into two subfamilies, the Cylindrotominae (50 extant spp.) which are distributed in the Northern Hemisphere, and the Stibadocerinae (20 spp.) which occur in the Oriental, Australasian, and Neotropical Regions (Oosterbroek 2021).

The Cylindrotominae are characterised by the following character combinations: (head) 16-segmented antennae; (thorax) the transverse V-shaped suture of the scutum is less apparent than other crane flies; (abdomen) this is slender and elongated; (male terminalia) unbranched gonostylus; large aedeagal complex with trifid or secondary bifid (*Diogma* Edwards, 1938) aedeagus; relatively short and broad female terminalia with leaf- or blade-like cerci and hypogynial valves (Alexander 1928; Peus 1952; Brodo 1967; Ribeiro 2009). Although Cylindrotomidae are also characterised by reduction of radial wing veins (i.e., R_1 and R_3), this character is highly variable among species and specimens (Peus 1952; Brodo 1967). Cylindrotominae larvae are very distinctive and resemble parts of lower plants such as bryophytes to a remarkable degree, due to the following trait complexes: elongated cuticular outgrowths, body colourations (green to brown) and dorsal patterns (Alexander 1920; 1928; Peus 1952; Takahashi 1960; Brodo 1967; Imada 2020). The biology and morphology at the immature stages, with ecomorphological analyses of the elongated lobes are recently detailed for 11 species in five genera (Imada 2020).

Members of the subfamily Stibadocerinae are primarily separated from the Cylindrotominae based on the following characters in adults: very elongated antenna, usually longer than their entire body, and highly reduced number of wing veins, particularly, the lack of vein R_{4+5} (Ribeiro 2009).

Despite the low species diversity of Cylindrotominae, both genus- and species-level taxonomy are still problematic areas. Most of the Eastern Palearctic and Oriental species were originally described based upon characteristics of wing venation and body colouration (see species descriptions of C.P. Alexander). Later revisions of European and Nearctic Cylindrotomidae revealed that these characters were highly variable among specimens (Peus 1952; Brodo 1967). The monophyly and validity of the different genera as *Cylindrotoma*, *Liogma*, and *Phalacrocera*, and the systematic position of several Eastern Palearctic and Oriental species have been in question for some time (Peus 1952; Takahashi 1960; Brodo 1967).

This article clarifies taxonomic status of some Cylindrotominae at species level, based on morphological comparison and molecular (mtDNA COI) data. The species that occur in Japan are redescribed, including the review of the species' literature and distribution data. An elevation of a subspecies and new synonyms are proposed. The genus-level taxonomy and species classification will be presented in the future with the phylogeny of the Cylindrotominae.

Materials and methods

A total of 456 Cylindrotominae specimens belonging to 17 taxa of five genera was investigated. The specimens were identified in reference to the original literature (Peus 1952; Takahashi 1960; Brodo 1967; Nakamura 2001; Paramonov 2006) and by comparing with type specimens. Terminology follows Cumming and Wood (2017). For preparation of male and female terminalia, caudal end of abdomen was cut off and macerated with 10–15% KOH at room temperature and neutralised with 3% acetic acid; then the terminalia was placed in glycerol and observed under a stereomicroscope. The cleared terminalia was preserved in tubes containing glycerol. Wings and entire bodies of specimens were photographed using a Zeiss Stemi 508 stereomicroscope equipped with Canon Kiss M digital camera; the photos were stacked using the Zerene Stacker version 1.04. Illustrations were drawn with Adobe Photoshop CC 2019. For providing distribution maps, an approximate spatial coordinate was selected on Google Earth Pro and with QGIS version 3.6 Noosa for each sampling locality in literature.

Specimens from the following depositories were examined:

BLKU Biosystematics Laboratory, Kyushu University.
CKLP Private Collection of L.-P. Kolcsár.
CYI Private Collection of Y. Imada.
EUMJ Ehime University Museum, Matsuyama, Japan.
FAUK Entomological Laboratory, Faculty of Agriculture, Kyushu University.
LMM Regional Museum of Lapland, Rovaniemi, Finland.
ZIN Zoological Institute, Russian Academy of Science, Saint-Petersburg, Russia.
ZFMK Zoological Research Museum Alexander Koenig, Bonn, Germany.
USNM U.S. National Museum of Natural History, Smithsonian Institution, Washington, D.C., USA.

DNA isolation, amplification, sequencing, and alignment

Mitochondrial DNA was extracted using DNeasy Blood & Tissue kits (Qiagen GmbH, Hilden, Germany). Extracted DNA was amplified using LCO-1490 and HCO-2198 primers (Folmer et al. 1994) on the 658 bp region of the mitochondrial cytochrome oxidase I (COI, cox1) gene, with an annealing temperature of 38^{0}C and 40 PCR cycles. The PCR products were purified using the QIAquick PCR Purification Kit (Qia-

gen GmbH, Hilden, Germany) and sequenced by Eurofins Operon (Tokyo, Japan) in both directions using the same primer set as above. Forward and reverse reads were assembled and edited using CodonCode Aligner v 3.5 (Codon Code Corporation, Dedham, USA). All sequences were submitted to GenBank, and also transferred to BoldSystems. BoldSystems ID was used as sequence identifier.

The newly sequenced (for this study) and published (public) Cylindrotominae sequences from BoldSystems (http://www.boldsystems.org) (Table 1) in multiple COI alignments were used in this study. All sequences were aligned using ClustalW (Thompson et al. 1994) and the phylogenetic search was conducted using a maximum likelihood approach in PhyML v 3.0 (Guindon and Gascuel 2003) under a GTR model of evolution (as determined by Modeltest v 3.7; Posada and Crandall 1998) and 1000 bootstrap analysis. Specimens of Limoniidae: *Limonia phragmitidis* (Schrank, 1781) (FINTI876-12), Pediciidae: *Pedicia rivosa* (Linnaeus, 1758) (FINTI657-12), and Tipulidae: *Tipula maxima* Poda, 1761 (FINTI636-12) were used as outgroups. The genetic distance between species groups was determined using DnaSP v 5.1 (Librado and Rozas 2009).

Results

Molecular analyses

A maximum likelihood tree based on the COI barcode sequences is shown in Figures 1 and 2. To make viewing easier the tree was divided into two parts, with Figure 1 showing the *Cylindrotoma* clade, and Figure 2 consisting of *Diogma*, *Liogma*, *Triogma*, and *Phalacrocera* representing the sister clade.

The tree (Fig. 1) illustrates *Cylindrotoma nigriventris* Loew, 1849 as the sister group of *C. distintissima* which consists of two subspecies, *Cylindrotoma d. americana* Osten Sacken, 1865 in the Nearctic and *Cylindrotoma d. distinctissima* (Meigen, 1818) in the Palearctic. Validity of *C. japonica* Alexander, 1919 was not supported because *Cylindrotoma d. distinctissima* (Meigen, 1818) formed a clade together with *C. japonica* Alexander, 1919.

The monophyly of *Phalacrocera* was recovered based on the sequences of two species, *P. replicata* (Linnaeus, 1758) and *P. tipulina* Osten Sacken, 1865. The sequences from the Nearctic and Western Palearctic specimens of *P. replicata* formed the respective clades.

Within Figure 2 *Liogma mikado* (Alexander, 1919) is placed as sister to *Diogma*. In the case of *Diogma*, *D. dmitrii* Paramonov, 2005 represented the sister species of *D. caudata* Takahashi, 1960 and *D. glabrata* (Meigen, 1818). The sequences from the latter species were not separated, and the two sequences of *D. caudata* from Finnish specimens were closely related to the clade of sequences of *D. glabrata* of Finnish specimens, while the sequences of *D. glabrata* from Japanese specimens formed a separate clade.

Although two species of *Triogma* were monophyletic, the clade was nested in the clade of *Liogma* spp., with exception of the aforementioned *L. mikado*. Four species,

Table 1. Barcode sequences included this study.

Species name – BoldSystems	Species name (new)	Genebank ID	BOLD ID	BOLD BIN	country	latitude	longitude	date	collectors
New sequences for this study									
Cylindrotoma d. distinctissima	*Cylindrotoma distinctissima*	MT151834	GBMNB25014-20	BOLD:AAD0770	Finland	63.92	26.869	2008/6/18-7/13	J. Salmela
Cylindrotoma japonica	*Cylindrotoma distinctissima*	MT151788	GBMNB24968-20	BOLD:AAD0770	Japan	39.94	140.86	2014.09.20	D. Kato
		MT151789	GBMNB24969-20	BOLD:AAD0770	Japan	35.74	139.18	2019.05.11	L.P. Kolcsár
		MT151790	GBMNB24970-20	BOLD:AAD0770	Japan	43.65	142.82	2019.07.24	L.P. Kolcsár
		MT151791	GBMNB24971-20	BOLD:AAD0770	Japan	43.39	143.96	2019.07.27	L.P. Kolcsár
		MT151805	GBMNB24985-20	BOLD:AAD0770	Japan	35.32	133.59	2015.05.17	D. Kato
		MT151806	GBMNB24986-20	BOLD:AAD0770	Japan	40.5	140.2	2013.09.18	D. Kato
		MT151807	GBMNB24987-20	BOLD:AAD0770	Japan	36.11	137.56	2016.07.22	D. Kato
Cylindrotoma nigriventris		MT151830	GBMNB25010-20	BOLD:ABV9491	Finland	60.6	23.959	2018.06.09	Kato D.
		MT151826	GBMNB25006-20	BOLD:AED8500	Russia	51.06	85.59	2016/06/27-30	N.E. Vikhrev
Diogma dmitrii		MT151827	GBMNB25007-20	BOLD:AED6086	Russia	44	39.994	2012.06.11	N.E. Vikhrev
Diogma glabrata		MT151828	GBMNB25008-20	BOLD:ABV3921	Finland	63.43	21.074	2019.07.02	L.P. Kolcsár
		MT151829	GBMNB25009-20	BOLD:ABV3921	Finland	60.56	27.838	2016.07.25	E. Viitanen
		MT151792	GBMNB24972-20	BOLD:AED4669	Japan	44.05	145.1	2019.07.26	L.P. Kolcsár
		MT151793	GBMNB24973-20	BOLD:AED4669	Japan	44.05	145.1	2019.07.26	L.P. Kolcsár
		MT151808	GBMNB24988-20	BOLD:AED4670	Japan	35.86	137.51	2016.07.22	D. Kato
		MT151809	GBMNB24989-20	BOLD:AED4670	Japan	35.86	137.51	2016.07.22	D. Kato
		MT151810	GBMNB24990-20	BOLD:AED4670	Japan	39.94	140.86	2015.08.05	D. Kato
		MT151825	GBMNB25005-20	BOLD:ABV3921	Russia	55.36	36.74	2014.06.29	D. Kato
Liogma brevipecten		MT151794	GBMNB24974-20	BOLD:AED7661	Japan	33.56	132.93	2019.06.17	L.P. Kolcsár
		MT151795	GBMNB24975-20	BOLD:AED3259	Japan	33.75	133.15	2019.06.05	L.P. Kolcsár
		MT151803	GBMNB24983-20	BOLD:AED3259	Japan	33.71	133.1	2019.05.18	L.P. Kolcsár
		MT151811	GBMNB24991-20	BOLD:AED7662	Japan	39.94	140.86	2014.07.15	D. Kato
		MT151812	GBMNB24992-20	BOLD:AED8471	Japan	34.59	132.14	2015.05.18	D. Kato
		MT151813	GBMNB24993-20	BOLD:AED7662	Japan	42.92	141.17	2014.06.23	D. Kato
Liogma mikado		MT151796	GBMNB24976-20	BOLD:AED6113	Japan	33.48	130.93	2019.05.21	L.P. Kolcsár
		MT151797	GBMNB24977-20	BOLD:AED6113	Japan	33.76	133.12	2019.06.05	L.P. Kolcsár
		MT151814	GBMNB24994-20	BOLD:AED6113	Japan	33.49	130.96	2016.04.22	D. Kato
		MT151815	GBMNB24995-20	BOLD:AED6114	Japan	40.68	140.1	2014.05.11	D. Kato
		MT151816	GBMNB24996-20	BOLD:AED6114	Japan	40.53	140.48	2013.05.31	D. Kato
Liogma nodicornis		MT151832	GBMNB25012-20	BOLD:AAK8889	Canada	45.2	-75.83	2011.06.07	F. Brodo
Liogma serraticornis		MT151798	GBMNB24978-20	BOLD:AED5489	Japan	33.48	130.93	2019.05.21	L.P. Kolcsár
		MT151799	GBMNB24979-20	BOLD:AED5489	Japan	33.75	133.15	2019.06.16	L.P. Kolcsár
		MT151817	GBMNB24997-20	BOLD:AED5489	Japan	33.43	130.23	2015.04.23	D. Kato

Species name – BoldSystems	Species name (new)	Genebank ID	BOLD ID	BOLD BIN	country	latitude	longitude	date	collectors
Liogma serraticornis		MT151818	GBMNB24998-20	BOLD:AED5489	Japan	40.51	140.43	2013.06.08	D. Kato
		MT151819	GBMNB24999-20	BOLD:AED5489	Japan	35.73	138.83	2014.07.08	D. Kato
		MT151820	GBMNB25000-20	BOLD:AED5489	Japan	35.23	137.15	2016.05.04	D. Kato
		MT151824	GBMNB25004-20	BOLD:AED5489	Russia	43.1	131.54	2007.06.13	N.M. Paramonov
Phalacrocera replicata		MT151833	GBMNB25013-20	BOLD:AAD9776	Canada	45.2	-75.83	2017.05.10	F. Brodo
Phalacrocera tipulina		MT151831	GBMNB25011-20	BOLD:AED8285	USA	37.36	-80.53	2018.02.25	Y. Imada
Triogma kuwanai kuwanai	*Triogma kuwanai*	MT151787	GBMNB24967-20	BOLD:AED6747	Japan	40.52	140.34	2013.05.24	D. Kato
		MT151802	GBMNB24982-20	BOLD:AEE0240	Japan	33.75	133.15	2019.06.05	L.P. Kolcsár
		MT151821	GBMNB25001-20	BOLD:AEE0245	Japan	35.35	133.58	2015.05.17	D. Kato
		MT151822	GBMNB25002-20	BOLD:AEE0240	Japan	33.43	130.36	2015.05.02	D. Kato
		MT151823	GBMNB25003-20	BOLD:AED6747	Japan	40.94	140.46	2014.05.15	D. Kato
Triogma kuwanai limbinervis	*Triogma kuwanai*	MT151800	GBMNB24980-20	BOLD:AED7834	Japan	33.86	132.77	2019.03.31	L.P. Kolcsár
		MT151801	GBMNB24981-20	BOLD:AED7834	Japan	33.86	132.77	2019.03.31	L.P. Kolcsár
		MT151804	GBMNB24984-20	BOLD:AED7834	Japan	33.86	132.76	2019.04.06	L.P. Kolcsár
Sequences from BOLDSystems									
Cylindrotoma borealis	*Cylindrotoma distinctissima*		FINTI044-11	BOLD:AAD0770	Finland	60.492	22.302	2011.08.10	J. Salmela
			FINTI045-11	BOLD:AAD0770	Finland	60.223	22.905	2009.08.01	J. Penttinen
			FINTI046-11	BOLD:AAD0770	Finland	62.076	22.492	2010.07.27	J. Salmela, T. Tuovinen
			FINTI047-11	BOLD:AAD0770	Finland	61.066	22.272	2010.08.18	L. Paasivirta
			FINTI054-11	BOLD:AAD0770	Finland	61.34	23.25	2006.08.11	E. Saarela
			FINTI491-12	BOLD:AAD0770	Finland	61.871	24.188	2005.07.30	J. Salmela, J. Kirjavainen
			FINTI507-12	BOLD:AAD0770	Finland	66.373	29.319	2001.08.09	Oulanka Biological Station
			FINTI588-12	BOLD:AAD0770	Finland	60.56	24.218	2011.08.05	E. Viitanen
Cylindrotoma cf. *distinctissima*	*Cylindrotoma distinctissima*		SATIP608-09	BOLD:AAD0770	Germany	47.832	11.793	2009.05.21	C. Young
			SATIP609-09	BOLD:AAD0770	Germany	47.832	11.793	2009.05.21	C. Young
			SATIP610-09	BOLD:AAD0770	Germany	47.832	11.793	2009.05.21	C. Young
			SATIP611-09	BOLD:AAD0770	Germany	47.832	11.793	2009.05.21	C. Young
			SATIP612-09	BOLD:AAD0770	Germany	47.832	11.793	2009.05.21	C. Young
			SATIP613-09	BOLD:AAD0770	Germany	47.832	11.793	2009.05.21	C. Young
			SATIP614-09	BOLD:AAD0770	Germany	48.115	11.206	2009.05.20	C. Young
			SATIP619-09	BOLD:AAD0770	Germany	48.115	11.206	2009.05.20	C. Young
			SATIP1838-12	BOLD:AAD0770	Poland	49.444	21.685	1988.08.25	C. Young
			SATIP1839-12	BOLD:AAD0770	Poland	54.389	18.752	1988.09.04	C. Young
			SATIP1840-12	BOLD:AAD0770	Poland	54.389	18.752	1988.09.04	C. Young
			SATIP1841-12	BOLD:AAD0770	Poland	54.389	18.752	1988.09.04	C. Young

Species name – BoldSystems	Species name (new)	Genebank ID	BOLD ID	BOLD BIN	country	latitude	longitude	date	collectors
Cylindrotoma d. americana	*Cylindrotoma americana*		BBTIP172-10	BOLD:AAV1805	Canada	49.074	-125.8	2010.07.08	BIObus 2010
			BBTIP183-10	BOLD:AAV1805	Canada	49.042	-125.7	2010.07.05	BIObus 2010
			BBTIP220-10	BOLD:AAV1805	Canada	51.265	-117.5	2010.07.16	BIObus 2010
			BBTIP221-10	BOLD:AAV1805	Canada	51.265	-117.5	2010.07.16	BIObus 2010
			CNCDI077-11	BOLD:ABA1601	Canada	52.617	-117.9	2003.07.22	F. Brodo
			CNTMC2308-14	BOLD:AAV1805	Canada	58.451	-62.8	2013.08.16	D. Whitaker
			POSPA900-15	BOLD:AAV1805	Canada	49.301	-123.1	2014.05.26	B. Titaro
			RBNII437-13	BOLD:ABA1601	Canada	53.124	-117.8	2012.06.14	BIOBus 2012
			SSJAA1387-13	BOLD:ABA1601	Canada	53.124	-117.8	2012.06.14	BIOBus 2012
			SSJAA1478-13	BOLD:ABA1601	Canada	53.124	-117.8	2012.06.14	BIOBus 2012
			SSJAA1499-13	BOLD:ABA1601	Canada	53.124	-117.8	2012.06.14	BIOBus 2012
			SSJAA904-13	BOLD:ABA1601	Canada	53.124	-117.8	2012.06.14	BIOBus 2012
			SSJAD5274-13	BOLD:ABA1601	Canada	53.124	-117.8	2012.07.21	BIOBus 2012
			SSJAD6461-13	BOLD:ABA1601	Canada	53.124	-117.8	2012.07.21	BIOBus 2012
			SSJAD6463-13	BOLD:ABA1601	Canada	53.124	-117.8	2012.07.21	BIOBus 2012
			SSJAD6464-13	BOLD:ABA1601	Canada	53.124	-117.8	2012.07.21	BIOBus 2012
			SSJAD6465-13	BOLD:ABA1601	Canada	53.124	-117.8	2012.07.21	BIOBus 2012
			SSJAD6466-13	BOLD:ABA1601	Canada	53.124	-117.8	2012.07.21	BIOBus 2012
			SSJAD6467-13	BOLD:ABA1601	Canada	53.124	-117.8	2012.07.21	BIOBus 2012
			SSJAD6468-13	BOLD:ABA1601	Canada	53.124	-117.8	2012.07.21	BIOBus 2012
			SSJAD6469-13	BOLD:ABA1601	Canada	53.124	-117.8	2012.07.21	BIOBus 2012
			SSJAD6471-13	BOLD:ABA1601	Canada	53.124	-117.8	2012.07.17	BIOBus 2012
			FINTI050-11	BOLD:AAV1805	USA	58.31	-134.4	1988.06.07	F. Brodo
Cylindrotoma d. distinctissima	*Cylindrotoma distinctissima*		FINTI053-11	BOLD:AAD0770	Czech Rep.	50.03	17.51	2011.05.24	J. Stary
			FINTI042-11	BOLD:AAD0770	Finland	69.035	20.839	2006.07.01	J. Jakovlev, J. Penttinen
			FINTI043-11	BOLD:AAD0770	Finland	69.035	20.839	2006.07.01	J. Jakovlev, J. Penttinen
			FINTI061-11	BOLD:AAD0770	Finland	67.83	26.052	2009.06.30	J. Salmela
			FINTI062-11	BOLD:AAD0770	Finland	67.588	24.214	2006.07.01	J. Penttinen, J. Jakovlev
			FINTI078-11	BOLD:AAD0770	Finland	68.636	22.784	2009.07.22	J. Salmela
			FINTI517-12	BOLD:AAD0770	Finland	63.924	26.869	2008.07.13	J. Salmela
			FINTI743-12	BOLD:AAD0770	Finland	61.926	22.436	2008.07.02	J. Salmela
			FINTI040-11	BOLD:AAD0770	Lithuania	54.115	24.28	2011.08.06	S. Podenas
			FINTI041-11	BOLD:AAD0770	Lithuania	54.115	24.28	2011.08.06	S. Podenas
			FINTI563-12	BOLD:AAD0770	Russia	49.127	154.48	2000.07.28	A.S. Lelej S.Y. Storozhenko

Species name – BoldSystems	Species name (new)	Genebank ID	BOLD ID	BOLD BIN	country	latitude	longitude	date	collectors
Cylindrotoma d. distinctissima			FINTI565-12	BOLD:AAD0770	Russia	43.624	132.22	2001.08.26	V.S. Sidorenko
			FINTI566-12	BOLD:AAD0770	Russia	51.791	87.228	2006.07.15	N.M. Paramonov
			FINTI567-12	BOLD:AAD0770	Russia	42.937	133.93	2007.07.16	N.M. Paramonov
			FINTI568-12	BOLD:AAD0770	Russia	55.874	48.723	2010.06.10	N.M. Paramonov
			FINTI569-12	BOLD:AAD0770	Russia	44.154	40.041	2004.06.13	N.M. Paramonov
	Cylindrotoma distinctissima		FINTI570-12	BOLD:AAD0770	Russia	44.19	40.066	2007.08.06	N.M. Paramonov
			FINTI571-12	BOLD:AAD0770	Russia	55.911	48.729	2009.06.15	N.M. Paramonov
			FINTI572-12	BOLD:AAD0770	Russia	55.911	48.729	2009.06.15	N.M. Paramonov
			FINTI573-12	BOLD:AAD0770	Russia	60.233	29.163	2007.07.24	N.M. Paramonov
			CNCDI078-11	BOLD:AAD0770	Sweden	60.05	17.333	1992.06.10	F. Brodo
			FINTI1082-12	BOLD:AAD0770	Sweden	68.334	18.794	2002.07.17	J. Kramer
Cylindrotoma distinctissima	*Cylindrotoma americana*		SSBAB2554-12	BOLD:AAV1805	Canada	51.35	-116.1	2012.06.19	BIOBus 2012
			SSBAB3039-13	BOLD:AAV1805	Canada	51.35	-116.1	2012.06.20	BIOBus 2012
			SSBAE1284-13	BOLD:AAV1805	Canada	51.35	-116.1	2012.07.28	BIOBus 2012
			SSBAE1285-13	BOLD:AAV1805	Canada	51.35	-116.1	2012.07.28	BIOBus 2012
			SSBAE1289-13	BOLD:AAV1805	Canada	51.35	-116.1	2012.07.28	BIOBus 2012
			SSBAE1292-13	BOLD:AAV1805	Canada	51.35	-116.1	2012.07.28	BIOBus 2012
			SSBAE1293-13	BOLD:AAV1805	Canada	51.35	-116.1	2012.07.28	BIOBus 2012
			SSBAE1294-13	BOLD:AAV1805	Canada	51.35	-116.1	2012.07.23	BIOBus 2012
			SSBAE1295-13	BOLD:AAV1805	Canada	51.35	-116.1	2012.07.23	BIOBus 2012
			SSGBB7185-14	BOLD:AAV1805	Canada	49.429	-57.74	2013.07.20	BIObus 2013
Cylindrotoma nigriventris			FINTI048-11	BOLD:ABV9491	Finland	61.109	24.264	2009.06.24	J. Penttinen
			FINTI049-11	BOLD:ABV9491	Finland	60.427	24.922	2009.06.24	J. Penttinen
			FINTI745-12	BOLD:ABV9491	Finland	62.075	22.492	2010.06.17	J. Salmela, T. Tuovinen
Diogma caudata			FINTI080-11	BOLD:ABV3921	Finland	66.335	29.513	2005.08.03	J. Salmela
			FINTI087-11	BOLD:ABV3921	Finland	66.335	29.513	2005.08.03	J. Salmela
Diogma cf. *glabrata*			FINTI1135-12	BOLD:ABV3921	Finland	60.491	22.302	2011.05.23	J. Salmela
			FINTI1136-12	BOLD:ABV3921	Finland	60.491	22.302	2011.05.23	J. Salmela
			AMTPD3808-15	BOLD:ABV3921	Germany	47.387	10.344	2014.07.20	D. Doczkal
Diogma glabrata			FINTI1025-12	BOLD:ABV3921	Finland	61.837	24.064	2006.08.03	J. Salmela
			FINTI235-12	BOLD:ABV3921	Finland	63.407	28.2	2008.07.14	J. Salmela
			FINTI842-12	BOLD:ABV3921	Finland	63.941	26.663	2008.07.13	J. Salmela
			FINTI918-12	BOLD:ABV3921	Finland	62.201	22.454	2008.08.08	J. Salmela
Liogma cf. *nodicornis*			SATIP1842-12	BOLD:AAK8889	USA	40.422	-80.17	1998.05.20	D. Koenig
			SATIP1845-12	BOLD:AAK8889	USA	41.558	-80.2	1998.05.18	C. Young, D. Koenig, T. Tomon
			SATIP268-09	BOLD:AAK8889	USA	40.612	-79.95		C. Young

Species name – BoldSystems	Species name (new)	Genebank ID	BOLD ID	BOLD BIN	country	latitude	longitude	date	collectors
Liogma nodicornis			BBTIP158-10	BOLD:AAK8889	Canada	48.593	-86.29	2010.06.10	BIObus 2010
			BBTIP162-10	BOLD:AAK8889	Canada	48.593	-86.29	2010.06.10	BIObus 2010
			CNCTI002-12	BOLD:AAK8889	Canada	45.4	-75.85	1995.06.09	F. Brodo
			CNCTI003-12	BOLD:AAK8889	Canada	45.4	-75.85	1995.06.09	F. Brodo
			CNCTI006-12	BOLD:AAK8889	Canada	45.267	-75.8	2011.06.07	F. Brodo
			CNCTI007-12	BOLD:AAK8889	Canada	45.267	-75.8	2011.06.07	F. Brodo
			CNFNE3074-14	BOLD:AAK8889	Canada	48.857	-64.38	2013.07.05	F. Tremblay
			CNRGK935-15	BOLD:AAK8889	Canada	43.822	-79.19	2014.06.10	K. Kerr, A. Sritharan
			CNTIC6257-15	BOLD:AAK8889	Canada	44.453	-75.87	2014.06.11	M. Brown
			JSDIQ829-10	BOLD:AAK8889	Canada	44.621	-75.77	2010.05.30	J. Sones
			OPPAM1198-17	BOLD:AAK8889	Canada	45.256	-77.19	2014.06.18	CBG Collections Staff
			SSEIC5992-13	BOLD:AAK8889	Canada	53.663	-112.8	2012.07.01	BIOBus 2012
			SSROC9031-15	BOLD:AAK8889	Canada	43.811	-79.16	2013.06.09	BIObus 2013
			GMFRQ424-15	BOLD:AAK8889	USA	38.892	-78.17	2014.06.02	K.J. Anderson
Phalacrocera replicata			CNTIA2077-15	BOLD:AAD9776	Canada	44.453	-75.87	2014.05.14	M.B. Lynch
			CNTIA2078-15	BOLD:AAD9776	Canada	44.453	-75.87	2014.05.14	M.B. Lynch
			CNTIA2079-15	BOLD:AAD9776	Canada	44.453	-75.87	2014.05.14	M.B. Lynch
			CNTIA2081-15	BOLD:AAD9776	Canada	44.453	-75.87	2014.05.14	M.B. Lynch
			CNTIB1805-15	BOLD:AAD9776	Canada	44.453	-75.87	2014.05.14	M. Brown
			OPPOA298-17	BOLD:AAD9776	Canada	44.283	-77.8	2014.05.23	CBG Collections Staff
			PHTCH356-08	BOLD:AAD9776	Canada	58.741	-93.82	2008.07.16	C.W.Young
			PHTCH357-08	BOLD:AAD9776	Canada	58.741	-93.82	2008.07.16	C.W.Young
			PHTCH358-08	BOLD:AAD9776	Canada	58.741	-93.82	2008.07.16	C.W.Young
			PHTCH359-08	BOLD:AAD9776	Canada	58.741	-93.82	2008.07.16	C.W.Young
			PHTCH385-08	BOLD:AAD9776	Canada	58.741	-93.82	2008.07.16	C.W.Young
			FINTI310-12	BOLD:AAD9776	Finland	69.746	27.822	2007.02.07	J. Salmela
			FINTI805-12	BOLD:AAD9776	Finland	63.433	27.53	2008.06.04	J. Salmela
			CNCDI081-11	BOLD:AAD9776	Norway	60.6	7.5	1992.07.17	F. Brodo
			CNCTI005-12	BOLD:AAD9776	Norway	60.6	7.5	1992.07.17	F. Brodo
Triogma trisulcata			FINTI801-12	BOLD:ABW4579	Finland	63.433	27.53	2008.06.04	J. Salmela
			FINTI928-12	BOLD:ABW4579	Finland	62.215	25.742	2005.06.09	J. Salmela
Limonia phragmitidis			FINTI876-12	BOLD:ABV3744	Finland	62.22	25.77	2006.08.10	J. Salmela
Pedicia rivosa			FINTI657-12	BOLD:ABW1968	Finland	69.751	27.88	2006.07.03	J. Salmela
Tipula maxima			FINTI636-12	BOLD:AAD6106	Finland	60.333	24.501	2007.07.19	J. Ilmonen

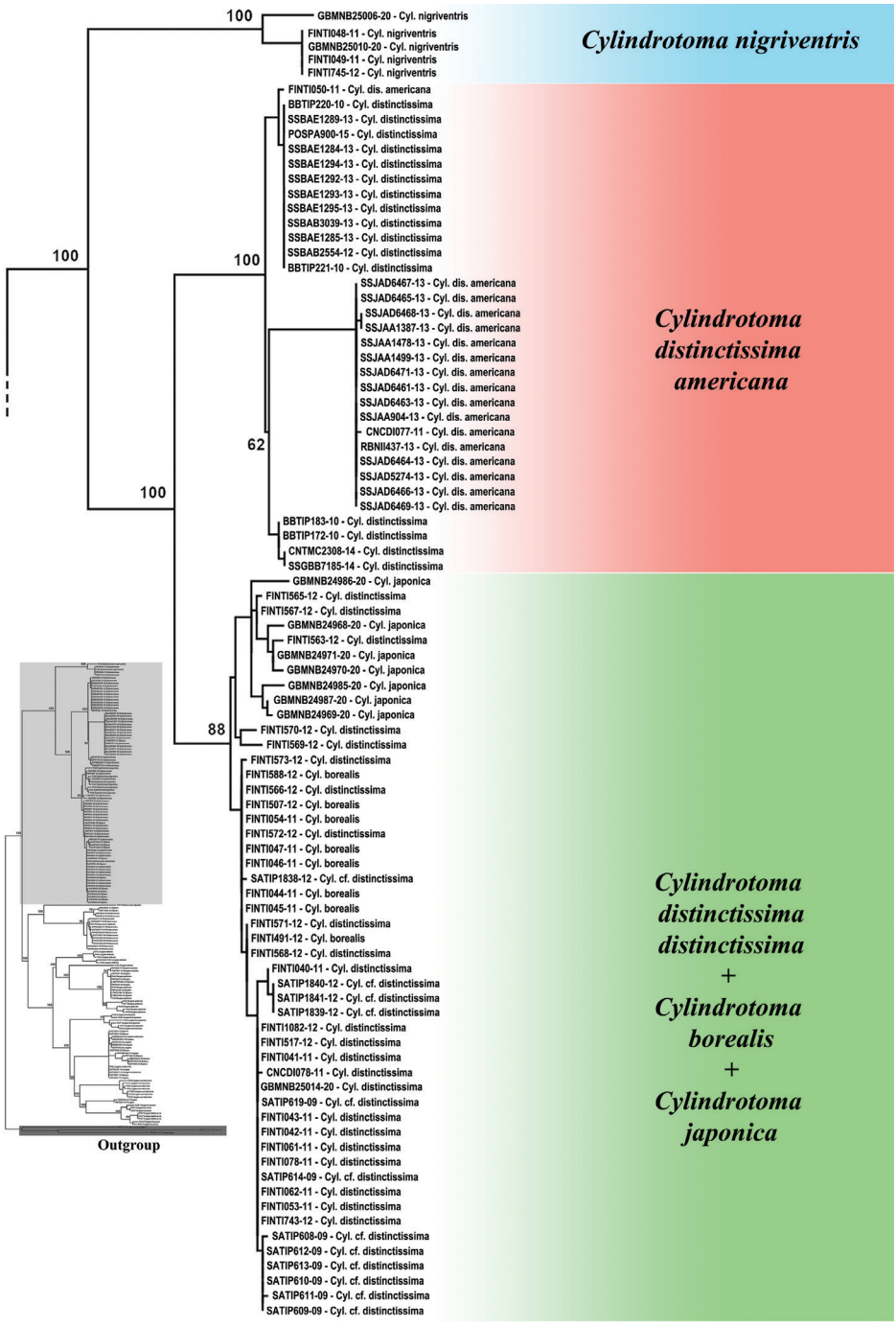

Figure 1. Partial maximum likelihood tree based on COI marker showing the clade of *Cylindrotoma* sequences, which is magnified from the entire tree on the left as highlighted with pale grey. Outgroup highlighted with dark grey. Numbers at nodes indicate bootstrap values of major clades. Sequence identifiers are BoldSystems numbers, see Table 1 for further information.

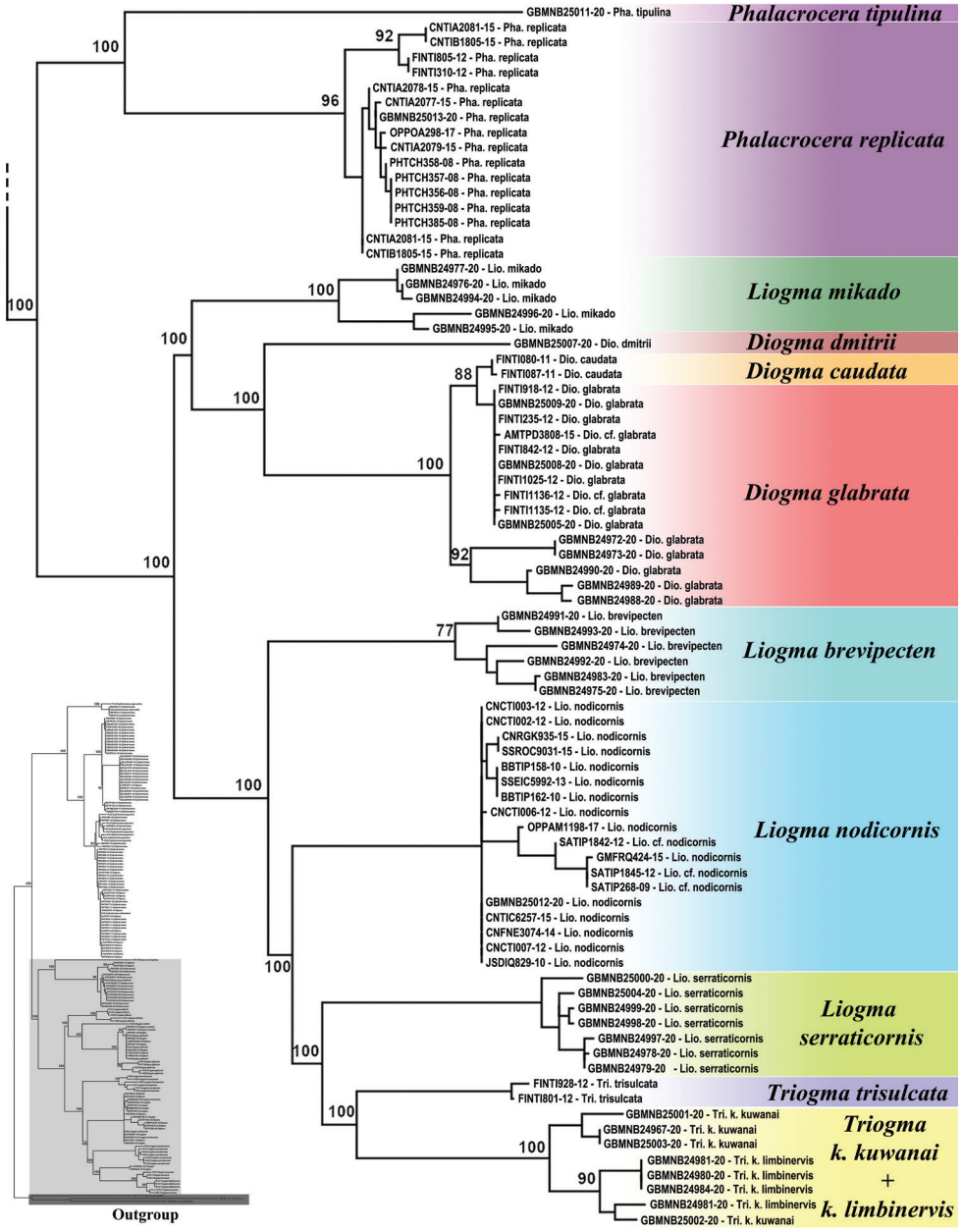

Figure 2. Partial maximum likelihood tree based on COI marker showing the clades of *Phalacrocera*, *Diogma*, *Liogma*, and *Triogma* sequences, which is magnified from the entire tree on the left as highlighted with pale grey. Outgroup highlighted with dark grey. Numbers at nodes indicate bootstrap values of major clades. Sequence identifiers are BoldSystems numbers, see Table 1 for further information.

Liogma brevipecten Alexander, 1932, *L. nodicornis* (Osten Sacken, 1865), *L. serraticornis* Alexander, 1919, and *Triogma trisulcata* (Schummel, 1829), represented a distinct clade. Two subspecies of *Triogma kuwanai* (Alexander, 1913), *T. k. kuwanai* and *T. k. limbinervis*, were not clearly distinguished.

Taxonomic treatment

Based upon our morphological comparison and genetic analyses, the two subspecies of *Cylindrotoma distinctissima*, the Palearctic *C. d. distinctissima* and the Nearctic *C. d. americana* represent separate lineages. Therefore, we propose the elevation of these subspecies to species rank as *C. americana* stat. reval. and *Cylindrotoma distinctissima*. Furthermore, *Cylindrotoma japonica* syn. nov. and *C. distinctissima alpestris* Peus, 1952 syn. nov. are treated as junior synonyms of *C. distinctissima*. Similarly, *Triogma kuwanai limbinervis* syn. nov. and *T. nimbipennis* Alexander, 1941 syn. nov. are junior synonyms of *Triogma kuwanai*. Each case is discussed in detail under the corresponding species discussion.

Cylindromine species that occur in Japan are redescribed, along with their habitus and wing photographs and the illustrations of male and female terminalia. The male and female terminalia of *Cylindrotoma nigriventris* Loew, 1849, *Diogma dmitrii* Paramonov, 2005, *Liogma nodicornis* (Osten Sacken, 1865), *Phalacrocera replicata* (Linnaeus, 1758), *P. tipulina* Osten Sacken, 1865, and *Triogma trisulcata* (Schummel, 1829) are also illustrated and described in detail.

Cylindrotoma Macquart, 1834
Cylindrotoma distinctissima (Meigen, 1818)

Figs 3, 4A, 5A, 6, 7, 8A

Tipula brevicornis (Zetterstedt, 1838)
Cylindrotoma tenebrarum Krogerus, 1937
Cylindrotoma distinctissima borealis Peus, 1952
Cylindrotoma japonica Alexander, 1919, syn. nov.; Alexander 1919: 344–345: original description; Alexander 1924: 595: faunistic records; Alexander 1928: 9: distribution, illustrations; Esaki 1950: 1513: illustration; Ishida 1955: 77: distribution; Takahashi 1960: 81: distribution; Alexander 1966: 122: distribution, faunistic records; Sidorenko 1999: 68–70: identification key, illustration, distribution; Nakamura 2001: 23–29: identification key, illustration, distribution, faunistic records; Pilipenko and Sidorenko 2004: 12 faunistic records; Boldgiv 2006: phylogeny, faunistic records; in Paramonov 2006 as *Cylindrotoma distinctissima japonica*: 888: stat. nov., identification key, illustration, distribution; Gelhaus et al. 2007: 64 comparison; Sasakawa 2008: 131: faunistic records; Nakamura 2014: 54: distribution; Kato and Suzuki 2017: 16: faunistic records, distribution; Imada 2020: biology and ecology of larvae.

Cylindrotoma distinctissima alpestris Peus, 1952, syn. nov.: Peus 1952: original description.

Type material examined. *Cylindrotoma japonica* Alexander, 1919: ***Paratype***. **Japan** • ♀; Saitama Pref., Saitama; 31 May 1919; R. Takahashi leg.; USNM.

Non-type material examined. *Cylindrotoma distinctissima distinctissima* (Meigen, 1818): **Finland** • 1 ♂; Vieremä, Mammonhauta; 63.924404°N, 26.869023°E; alt. 135; 18 Jun. 2008 – 13 Jul. 2008; J. Salmela leg.; CKLP. **Russia** • 1 ♂, 1 ♀; Krasnodar Krai, Apsheronsky District, Mezmay Settlement, Kamyshanova polyana, Mezmaika River; 44.16989°N, 40.05181°E; alt. 1200 m; 11 Jun. 2004; N.M. Paramonov leg.; CKLP.

Cylindrotoma japonica Alexander, 1919: **Japan** • 1 ♂; Mt. Shirouma Alps, 36.78°N, 137.7°E; 8 Aug. 1931; J. Machida leg.; USNM. • 1 ♀; Aomori, Towada, Sakura Spa, Okuse; 40.627315°N, 140.909831°E; alt. 854 m; 21 Jun. 2014, D. Kato leg.; BLKU. • 1 ♂, 1 ♀; Aomori, Nishimeyamura, Okawa Path, Kawaratai; 40.500625°N, 140.204058°E; alt. 300 m; 18 Sep. 2013; D. Kato leg.; BLKU. • 1 ♂, reared from larva; Gifu, Takayama, Nigorikawa; 36.0545°N, 137.55818°E; 1375 m; larva collected: 5 Aug. 2015, emerged: 26 May. 2015; M. Kato leg.; CYI. • 1 ♂; Gifu, Mt. Norikura, Japanese Alps; 36.12°N, 137.5°E; 26 Jun. 1929; J. Machida leg.; USNM. • 1 ♀; Hokkaido, Sapporo, Minami-ku, Jozankei, trail of Mt. Sapporo; 42.92392°N, 141.17688°E; alt. 450–860 m; 3 Sep. 2018; D. Kato leg.; BLKU. • 2 ♂, 3 ♀; Hokkaido, Higashikawa, Asahidake, River Yukomabetsu; 43.65226°N, 142.80229°E; alt. 1120 m; 23 Jul. 2019; L.-P. Kolcsár leg.; CKLP. • 2 ♂; Hokkaido, Higashikawa, Asahidake; 43.65582°N, 142.82608°E; alt. 1100–1500 m; 24 Jul. 2019; L.-P. Kolcsár, leg.; CKLP. • 1 ♂; Hokkaido, Ashoro, Meakan Moutain, small sandy/muddy stream; 43.3907°N, 143.96821°E; alt. 365 m; 27 Jul. 2019; L.-P. Kolcsár leg.; CKLP. • 1 ♀; Iwate, Hachimantai, Toshiti Spa; 39.94253°N, 140.86804°E; alt. 1344 m; 3 Aug. 2013; • 1 ♀; same locality; 1 Jul. 2014; • 1 ♂; same locality; 5 Aug. 2014; • 2 ♀; same locality; 20 Sep. 2014; • 1 ♀; same locality; 5 Aug. 2015; D. Kato leg.; BLKU. • 3 ♂; Nagano, Matsumoto, Azumi, Mt. Norikura, near Kuraigahara-Sansou; 36.11987°N, 137.5692°E; alt. 2370 m; 22 Jul. 2016; D. Kato leg.; BLKU. • 1 ♂; Nagano, Ueda, Daimyozin stream, Sugadaira MRC; 36.51992°N, 138.3539°E; alt. 1315 m; 27 Aug. 2012; D. Kato leg.; BLKU. • 2 ♂; Nagano, Sakae-mura, Sakai, Koakazawa-gawa River; 36.85352°N, 138.66358°E; alt. 1320–1600 m; 19. Sep. 2019; D. Kato leg.; BLKU. • 1 ♂; Nagano, Chino, Shibunoyu; 36.03582°N, 138.32771°E; alt. 1863 m; 21 Jul. 2013; M. Kato leg.; CYI. • 2 ♂; Nagano, Miyada, Kisokomagatake; 35.76917°N, 137.8357°E; alt. 1683 m; 13 Aug. 2013; M. Kato leg.; CYI. • 1 ♂; Nagano, Matsumoto, Kamikouchi; 36.20966°N, 137.60662°E; alt. 1320 m; 3 Aug. 2014; M. Kato leg.; CYI. • 1 ♀; Niigata, Yuzawa, Mitsumata, Mt. Naeba; 36.85616°N, 138.71041°E; alt. 1500–1900 m; 8 Aug. 2019; D. Kato leg.; BLKU. • 1 ♂; Niigata, Kurokawa, Echigo; 38.05°N, 139.47°E; 19 May 1954; B. Kintaro leg.; USNM. • 1 ♀; Okayama, Maniwa, Hiruzen-Shimotokuyama; 35.32931°N, 133.59725°E; alt. 784 m; 17 May. 2015; D. Kato leg.; BLKU. • 2 ♀; Tokyo, Tokyo, Akiruno, rocky river and stream; 35.74766°N, 139.18466°E; alt. 288 m; 11 May. 2019; L.-P. Kolcsár leg.; CKLP. • 1

♂; Tokyo, Tokyo, Mitake; 35.78°N, 139.14°E; 10 May. 1931; B. Oda leg.; USNM. • 1 ♂; Toyama, Kurobegoro; 36.38°N, 137.47°E; 8 Aug. 1931; Imanishi leg.; USNM. • 1 ♀; Yamagata, Yonezawa, Shirabu-onsen; 37.77646°N, 140.11964°E; alt. 888 m; 26 Jun. 2015; Y. Imada leg.; CYI. **Russia** • 1 ♂; Saghalien [Far East, Sakhalin Oblast], Shimizu; 1922.07.27, T. Esaki leg.; USNM.

Redescription. Colouration very variable, base colour whitish yellow to dark orange, with pale brown to black markings.

Head. Vertex and occiput with dark area, size variable among specimens, larger on "*borealis*" and "*japonica*" form; yellowish around eye (Fig. 3C, D, F). Rostrum short, yellow to brown, without nasus, but with tuft of hairs (Fig. 3F, E). Palpus five segmented, last segment 2 × longer than penultimate segment. Antenna yellowish brown to black (Fig. 3F, E); scape short, as long as wide; pedicel short, subspherical to drop-shaped; flagellum 14 segmented (Fig. 4A). Flagellar segments simple in both sexes, not expanded ventrally, covered with dense, whitish setae (sensilla), especially in ventral side (Figs 3E, F, 4A); sensilla less dense in female; first flagellomere longer than second in both sexes; verticels black, relatively long.

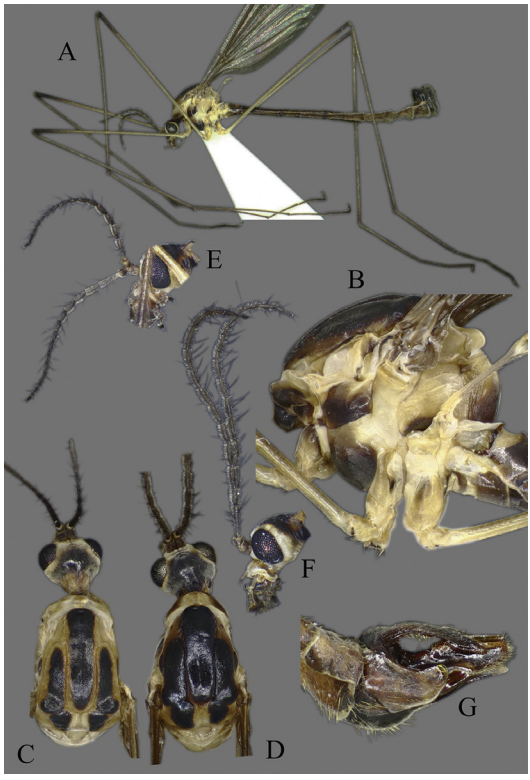

Figure 3. *Cylindrotoma distinctissima* (Meigen, 1818) **A** habitus of male, lateral view (colouration of wings is artefact) **B** thorax of male, lateral view **C** head and thorax dorsal view of pale "*distinctissima*" form **D** head and thorax dorsal view of dark, "*japonica*" form **E** head of female, lateral view **F** head of male, lateral view **G** female terminalia lateral view.

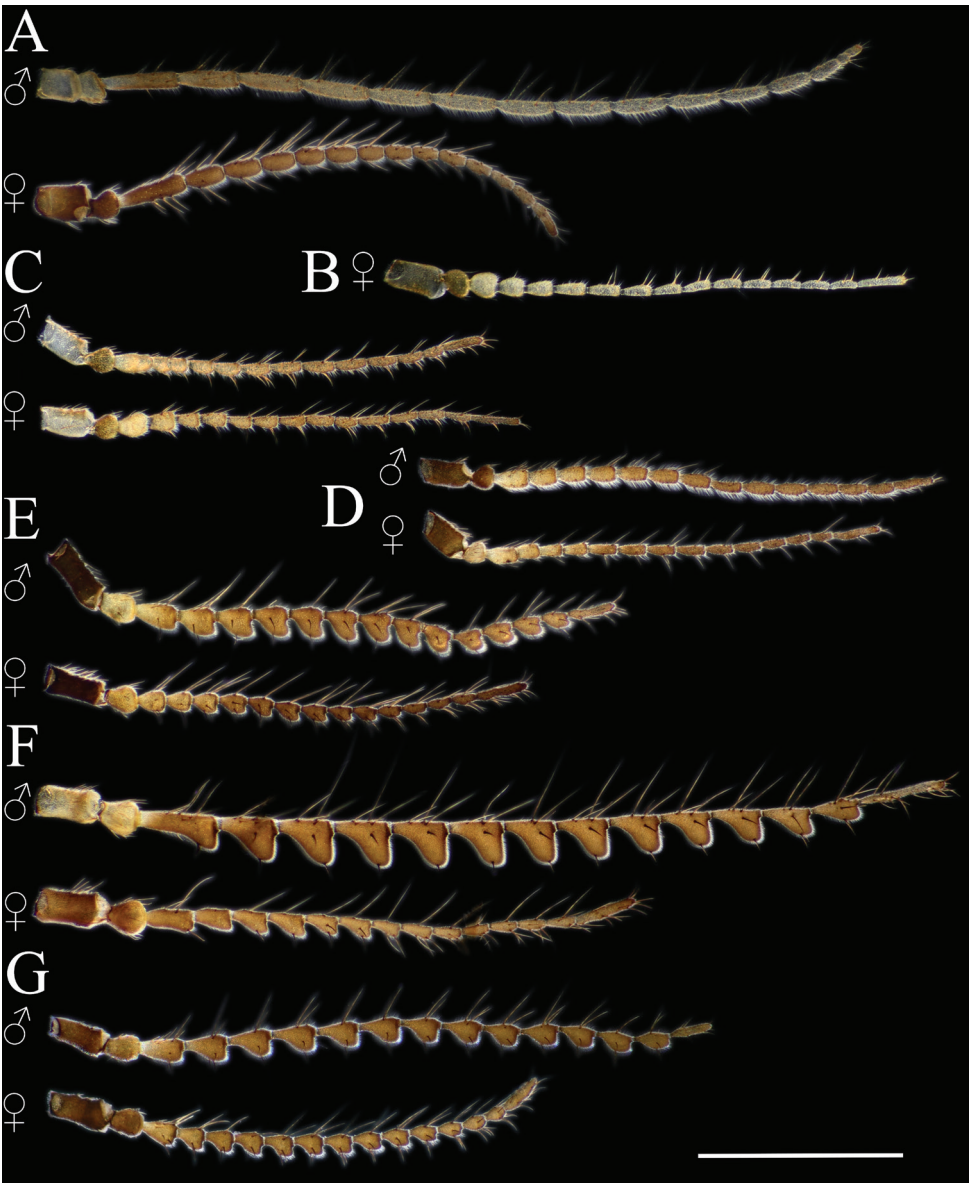

Figure 4. Antennae **A** *Cylindrotoma distinctissima* (Meigen, 1818) **B** *Diogma caudata* Takahashi, 1960 **C** *Diogma glabrata* (Meigen, 1818) **D** *Liogma mikado* (Alexander, 1919) **E** *Liogma brevipecten* Alexander, 1932 **F** *Liogma serraticornis* Alexander, 1919 **G** *Triogma kuwanai* (Alexander, 1913). Scale bar: 1 mm.

Thorax. Whitish yellow to dark orange, with contrasting black marks. Cervical sclerites brown to black. Pronotum pale in middle, darker laterally (Fig. 3B, C, D). Mesonotal pattern variable, from three longitudinal, pale brown ("*alpestris*" form) to black (the typical "*distinctissima*" form Fig. 3C) markings to one large patch ("*japonica*" form Fig. 3D); longitudinal mesonotal suture distinct, formed by deep groove

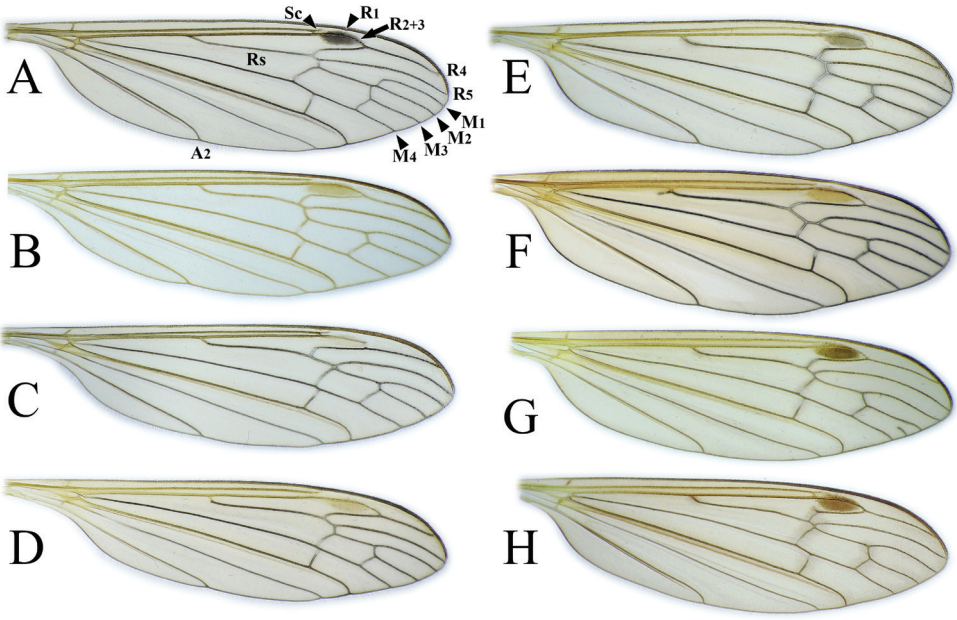

Figure 5. Wing **A** *Cylindrotoma distinctissima* (Meigen, 1818) **B** *Diogma caudata* Takahashi, 1960 **C** *Diogma glabrata* (Meigen, 1818) **D** *Liogma mikado* (Alexander, 1919) **E** *Liogma brevipecten* Alexander, 1932 **F** *Liogma serraticornis* Alexander, 1919 **G** *Triogma kuwanai* (Alexander, 1913) of "*kuwanai*" form **H** *Triogma kuwanai* (Alexander, 1913) of "*limbinervis*" form.

(Fig. 3C, D). Scutellum yellow, triangular (Fig. 3C, D). Mediotergite yellow, posterior part black (Fig. 3B). Anepisternum and katepisternum separated, both darker ventrally (Fig. 3B). Katatergite yellow, black above posterior spiracle, with creases. Coxa base yellow to pale brown, apically yellow, trochanter yellowish (Fig. 3B); femur and tibia yellowish, with distinct and wide, black ring at tip; tarsus uniformly black. Stem of halter yellow, knob usually darker. Wing hyaline, with yellowish brown to brown tinge; veins brown to black; pterostigma brown to black (Fig. 5A); wing membrane with interference patterns, visible with dark background (Fig. 3A). Four branches of M reaching wing margin. Cell a2 less than 6 × longer than wide.

Abdomen. Yellow ("*alpestris*" form) to almost black ("*japonica*" form); gradually lightening caudally, without clear pattern or with narrow longitudinal line medially.

Male terminalia. Black, directed dorsally (Fig. 3A). Tergite 9 partly fused with gonocoxite (Fig. 6C). Caudal margin of tergite 9 with deep V-shaped notch at middle (Fig. 6A); posterior edge of tergite 9 forming dorsal and ventral portion in lateral view (Fig. 6C), shapes variable among specimens. Gonocoxite fused with sternite 9 (Fig. 6B, C); gonocoxite with ventral crescent-shaped lobe (Fig. 6A, B: vl); apical lobe of gonocoxite (al) prominent, well separated, directed inward; both ventral and inner lateral margins sclerotised, shape variable (Fig. 6A, D, E). Gonostylus undivided; twisted, widening in caudal view, shape variable among and within population(s) (Fig. 6F, Japan; Fig. 6G, Finland). Interbase small, without membranous or sclerotised lobe between in-

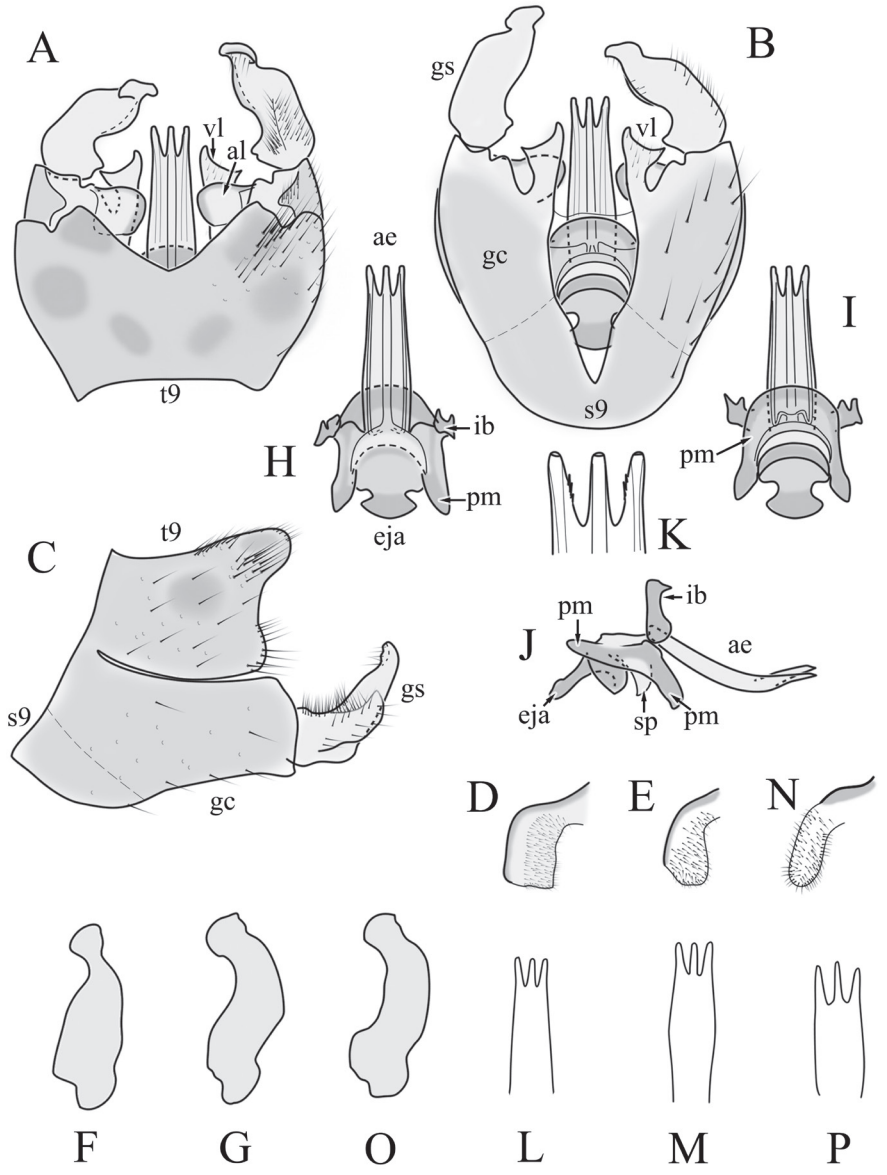

Figure 6. Male genital structures of *Cylindrotoma distinctissima* (Meigen, 1818) (**A–M**), in comparison to *C. americana* Osten Sacken, 1865 (**N–P**) **A** terminalia, dorsal view **B** terminalia, ventral view **C** terminalia, lateral view; **D** Apical lobe of the gonocoxite (Japan) **E** apical lobe of the gonocoxite (Finland) **F** shape of the gonostylus caudal view (Japan) **G** shape of the gonostylus caudal view – Finland **H** aedeagus complex, dorsal view **I** aedeagus complex, ventral view **J** aedeagus complex, lateral view **K** tip of the aedeagus **L** shape of the aedeagus (Japan) **M** shape of the aedeagus (Finland); *C. americana* Osten Sacken **N** apical lobe of the gonocoxite **O** shape of the gonostylus caudal view **P** shape of the aedeagus. Abbreviations: ae – aedeagus; al – gonocoxite apical lobe; eja – ejaculatory apodeme; gc – gonocoxite; gs – gonostylus; ib – interbase; pm – paramere; sp – sperm pump; s9 – sternite 9; t9 – tergite 9; vl – gonocoxite ventral lobe.

terbases (Fig. 6H, I). Aedeagus dorsoventrally flattened, gently curved dorsally (Fig. 6J), gradually narrowing to tip, shape variable among and within population(s) (Fig. 6H, I, L, Japan; Fig. 6M, Finland); tip divided into three short, nearly equal tubes in last 1/4 of its length (Fig. 6L, M). Spines on lateral branch of aedeagus small, indistinct (Fig. 6K).

Female terminalia. Brown to black, strongly sclerotised (Fig. 3G). Tergite 8 separated in middle by membranous area (Fig. 7A). Tergite 9 larger than tergite 8 in lateral view (Fig. 7B). Tergite 10 with elongated Y-shaped projection, shape variable among specimens (Fig. 7A, Japan; Fig. 7C, Russia (Krasnodar Krai), Fig. 7D, Finland). Cercus with serrate, cutting edge on inner-dorsal surface (Fig. 7A, B). Hypogynial valve on dorsal side with bulbous or triangular projection near middle, shape variable within specimens (Fig. 7B, F); distal part of hypogynial valve narrowing to tip. Three, relatively large spermathecae present, diameter ~ 0.15–0.2 of wide of sternite 8; duct of spermatheca straight or curved (Fig. 7I, J). Sperm ducts simple, without darkened areas (Fig. 7H). Sternite 10 with a small notch at tip, less sclerotised at midline (Fig. 7G).

Distribution. Widely distributed species in Palearctic, known from: Austria, Belarus, Belgium, Bulgaria, Croatia, Czech Rep., Denmark, Estonia, Finland, France, Germany, Great Britain, Hungary, Ireland, Italy, Kazakhstan, Lithuania, Luxembourg, Mongolia, Netherlands, Norway, Poland, Romania, Russia (North European territory, Central European territory, South European territory, West Siberia (Altay), Far East (Kamchatka Krai, Primorsky Krai, Sakhalin Oblast (incl. Kuril I), Serbia, Slovakia, Slovenia, Spain, Sweden, Switzerland, Ukraine, and Turkey (Paramonov and Lobkova 2013; Devyatkov 2021; Oosterbroek 2021). Distribution records of *C. japonica* transferred to *C. distinctissima*: Mongolia and Japan (Hokkaido I, Honshu I, and Kyushu I) (Fig. 8A).

Comments. The species was originally described 250 years ago from Europe, where it is among the most widespread of cylindrotomines. The colour polymorphisms of *C. distinctissima* have been described as separate species or subspecies. Peus (1952) separated three subspecies, the nominate subspecies *C. d. distinctissima* (Meigen, 1818), widespread in Europe, *C. d. borealis* Peus, 1952 from Norway, and *C. d. alpestris* Peus, 1952 from Italian Alps. Later, *Cylindrotoma d. borealis* was raised to species rank based on the generally darker habitus and slightly different genital characters (Salmela and Autio 2007). As the COI gene sequence's genetic distance between *C. d. distinctissima* and *C. borealis* was low, the species was later synonymised with *C. d. distinctissima* (Salmela 2013). In our ML tree, *C. borealis* sequences were also not separated from *C. d. distinctissima* sequences. *Cylindrotoma d. alpestris* was treated as species in CCW (2018–2021), because it showed the sympatric distribution with *C. d. distinctissima* in Alps (Italy). This subspecies was designated based on very pale colouration, compared with the nominative subspecies, but the male terminalia does not show any differentiation, which was highlighted in the original description by Peus (1952). Peus noted that this subspecies maybe just a local colour variation, as *Cylindrotoma* specimens showed colour polymorphisms, especially in mountain specimens (as noted by the personal experience of N. Paramonov), but there is no genital differentiation between the two species, and therefore we synonymise *C. d. alpestris* syn. nov. with *C. distinctissima*.

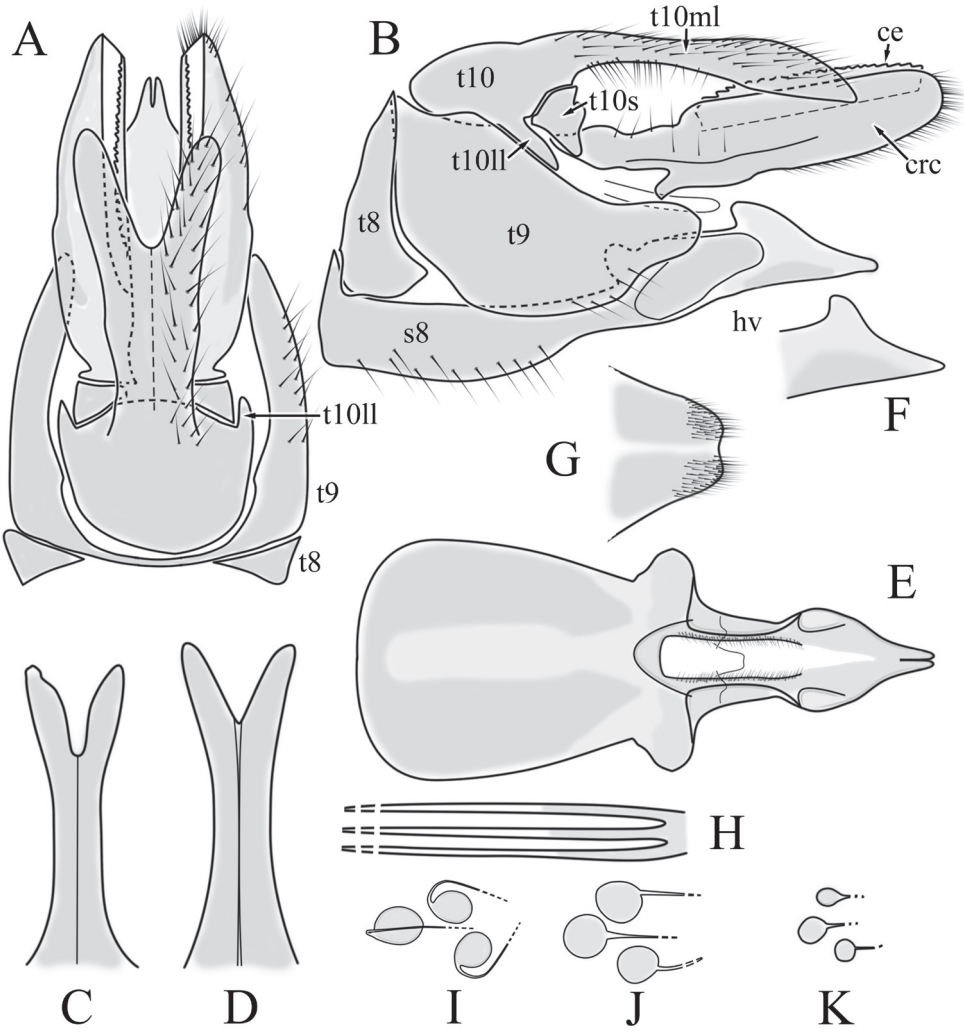

Figure 7. Female genital structures of *Cylindrotoma distinctissima* (Meigen, 1818) (**A–J**) and *C. americana* Osten Sacken, 1865 (**K**) **A** terminalia, dorsal view **B** terminalia, lateral view **C** shape variant of median lobe of tergite 10 (Krasnodar Krai, Russia) **D** shape variant of median lobe of tergite 10 (Finland) **E** sternite 8 and hypogynial valves, inner dorsal view **F** shape variant of tip of the hypogynial valve **G** sternite 10 **H** genital opening and sperm ducts **I** spermathecae (Japan) **J** spermathecae (Finland) **K** spermathecae of *C. americana* Osten Sacken, 1865. Abbreviations: ce – cutting edge; crc – cercus; hv – hypogynial valve; t8 – tergite 8; t9 – tergite 9; t10 – tergite 10; t10s – tergite 10 triangular sclerite; t10ll – tergite 10 lateral lobe; s8 – stergite 8.

Another species related to *C. distinctissima* was described from Japan. The description of *Cylindrotoma japonica* Alexander, 1919, was based on the darker colouration of the thorax (Fig. 3D) (Alexander 1919). The rank of this species was first questioned by Paramonov (2006), who referred to it as a subspecies of *C. distinctissima* in his identifi-

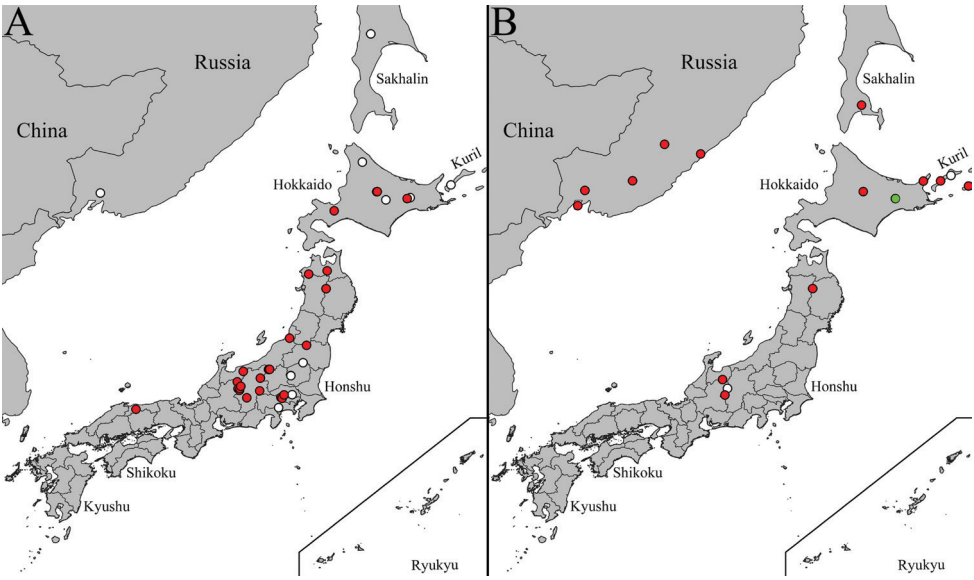

Figure 8. Occurrence data in Japan and surrounding areas of **A** *Cylindrotoma distinctissima* (Meigen, 1818) **B** *Diogma glabrata* (Meigen, 1818) and *D. caudata* Takahashi, 1960. Red dots indicate locations of investigated specimens, white dots indicate approximate locations of literature data. Green dot indicate approximate location of type locality of *D. caudata* Takahashi, 1960.

cation key of The Cylindrotomidae of Far East Russia. Our morphological and genetic comparisons suggest that *C. japonica* does not differ significantly from *C. distinctissima*, even at the subspecies level. The colouration of *C. japonica* shows a high level of variability in Japan. The specimens collected in Hokkaido Island, have, typically, three separated black marks on the mesonotum (Fig. 3C). Small genital differences occur between the typical examples of *C. distinctissima* and *C. japonica*, in the shape of the apical gonocoxal lobe (rectangular in Japanese specimens (Fig. 6D) and less sclerotised and rounded in studied European specimens Fig. 6E), the shape of aedeagus (evenly narrowing in Japanese specimens Figure 6L, and broader at the middle in examined European specimens Fig. 6M), as well as the shape of the gonostylus in caudal view (Fig. 6F, G). However, these also show variability amongst specimens (see illustrations by Peus 1952: fig. 27; Salmela and Autio 2007; figs 1e, 2b, e). Ujvárosi et al. (2011: fig. 2) illustrated the high variability level of the ventral lobe of the gonocoxite in Bulgarian and Romanian populations in the case of *C. d. distinctissima*, but we did not find that similar variability in *C. japonica* specimens examined. *C. japonica* syn. nov. and *C. distinctissima* are now synonymised based on the high colour variability level, the minimal genital differences, and the small genetic differentiation between the species.

Four species of *Cylindrotoma* have been described from the Nearctic, which are related to *C. distinctissima*, namely *C. americana* Osten Sacken, 1865, *C. juncta* Coquillett, 1900, *C. splendens* Doane, 1900, and *C. pallescens* Alexander, 1931. After the revision of North American Cylindrotomidae, these later three species were syn-

onymised with *C. americana*, and the latter species was treated as a subspecies of *C. distinctissima* as *C. distinctissima americana* Osten Sacken, 1865, as their male terminalia were highly similar to each other (Brodo 1967). Molecular analysis shows a relatively high (~ 4.6%) genetic distance between the Nearctic and Palearctic subspecies, and a slight genital difference between these two clades was found in our study (see below the comparative diagnosis of *C. americana*). Based upon the two subspecies' genetic and geographic separation, the two subspecies are now raised to species rank, *C. americana* stat. reval. and *C. distinctissima*. Furthermore, the Nearctic *C. americana* shows an additional molecular differentiation, as specimens from Jasper National Park, Alberta, Canada were found to belong to a separate barcode BIN (BOLD:ABA1601), and the remaining sequences, both from western and eastern parts of North America represent another barcode BIN (BOLD:AAV1805). The phylogenetic relationship between these clades is not resolved in the molecular tree and lowly supported (Bootstrap: 65) in our analysis.

***Cylindrotoma americana* Osten Sacken, 1865, stat. reval.**
Figs 6N, O, P, 7K

Cylindrotoma juncta Coquillett, 1900
Cylindrotoma splendens Doane, 1900
Cylindrotoma pallescens Alexander, 1931.

Non-type material examined. Canada • 1 ♂; British Columbia, Cowichan Valley, Upper Carmanah Valley; 48.616°N, 124.733° W; alt. 95 m; 4 Jul. 1991 – 15 Aug. 1991; N. Winchester leg.; CKLP. • 1 ♀; British Columbia, Cowichan Valley, Upper Carmanah Valley; 48.67°N, 124.69° W; alt. 160 m; 4 Jul. 1991 – 15 Aug. 1991; N. Winchester leg.; CKLP. **Usa** • 1 ♂, 1 ♀; Alaska, Juneau; 58.37°N, 134.54° W; alt. 330 m; 14 Jun. 1988; F. Brodo leg.; CKLP.

Comparative diagnosis. General appearance, colouration, antennal structure, and male and female terminalia are very similar to *C. distinctissima*. Differences: only the ventral margin of the inner gonocoxal lobe are sclerotised (Fig. 6N) (the lateral margin is also sclerotised in *C. distinctissima* (Fig. 6D, E)**.** Sheath of aedeagus shorter and wider (Fig. 6P) than in *C. distinctissima* (Fig. 6L, M). Aedeagus does not narrow to the tip in this species, the lateral margin being almost straight (Fig. 6P) (in *C. distinctissima* the aedeagus clearly narrows to the tip, starting from around the middle in Japanese specimens (Fig. 6M). Spermathecae small (Fig. 7K), diameter ~ 0.07–0.1 of the width of sternite 8 (in *C. distinctissima* relatively large, 0.15–0.2 of the width of sternite 8).

For a detailed species description see Brodo (1967) under "*Cylindrotoma distinctissima americana*".

Distribution. Widely distributed species in Nearctic, known from Canada and USA (Alaska to Oregon and Colorado, in the east from Labrador and Newfoundland to Ontario and Pennsylvania) (Oosterbroek 2021).

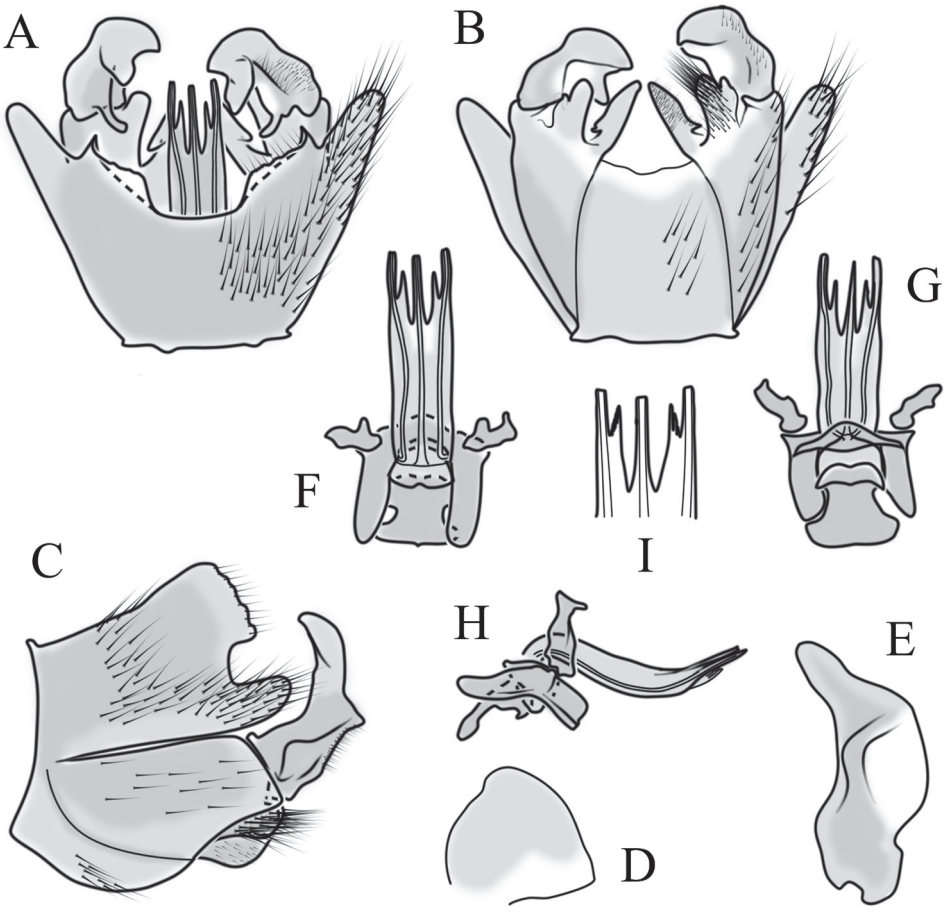

Figure 9. Male genital structures of *Cylindrotoma nigriventris* Loew, 1849 **A** terminalia, dorsal view **B** terminalia, ventral view (aedeagus complex removed) **C** terminalia, lateral view **D** ventral lobe of the gonocoxite, lateral view **E** shape of the gonostylus, caudal view **F** aedeagus complex, dorsal view **G** aedeagus complex, ventral view **H** aedeagus complex, lateral view **I** tip of the aedeagus.

Cylindrotoma nigriventris Loew, 1849

Figs 9, 10

Non-type material examined. **Finland** • 1 ♂; Lohja, Karkola; 60.60841°N, 23.95901°E; alt. 125 m; 9 Jun. 2018; E. Viitanen leg.; CKLP. **Russia** • 1 ♂; Altai Republic, Ongudaysky District, Onguday, Seminsky Pass; 51.06°N, 85.59°E; alt. 1650 m; 27 Jun. 2016 – 30 Jun. 2016; N.E. Vikhrev leg.; CKLP. • 1 ♀; Altai Republic, Kupchegen Settlement, Chike-Taman Pass; 50.64477°N, 86.3117°E; alt. 1266 m; 28 Jun. 1964; E.P. Narchuk leg.; CKLP.

Supplementary description. Male terminalia: Directed dorsally. Tergite 9 partly fused with gonocoxite (Fig. 9C). Posterior margin of tergite 9 with deep, U-shaped notch (Fig. 9A). Posterior edge of tergite 9 forming dorsal and ventral portion in lateral

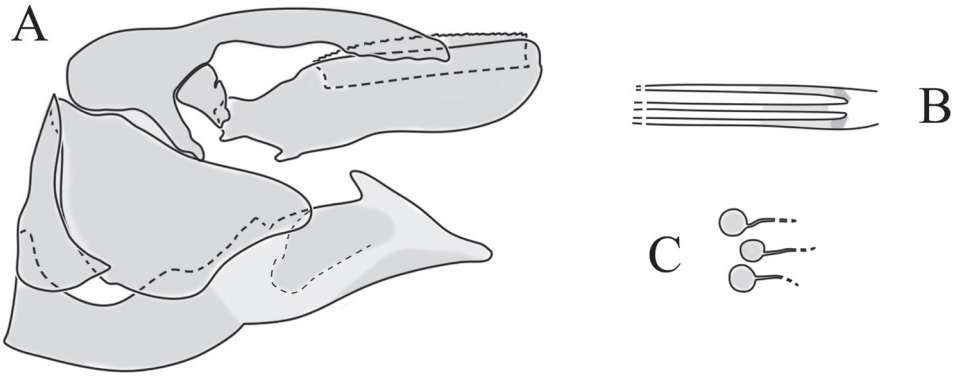

Figure 10. Female genital structures of *Cylindrotoma nigriventris* Loew, 1849 **A** terminalia, lateral view **B** sperm ducts **C** Spermathecae.

view (Fig. 9C). Ventral part produced caudally, forming finger-like lobe, covered by long hairs; dorsal portion wavy, formed by posterior margin of tergite 9 (Fig. 9C); lateral part of dorsal portion bent under tergite 9, forming a gently curved plate, covered with few fine setae, visible in caudal view. Gonocoxite fused with sternite 9 (Fig. 9B, C); sternite 9 sclerotised with few long hairs. Gonocoxite ventral lobe, laterally flattened, directed dorso-laterally, shape as in Fig. 9D; apical lobe of gonocoxite directed caudally, not inward as in *C. distinctissima* or *C. americana*; covered by long hairs, except small bare portion at base, next to gonostylus, visible in ventral view (Fig. 9B). Gonostylus undivided, twisted; base wide, with a small gently curved finger-like lobe directed inward; inner ventral part paler, slightly membranous; in caudal view medially with outgrowth ridge (Fig. 9E); gonostylus narrowing to tip in caudal view. Interbase small, without membranous median part (Fig. 9F). Aedeagus dorsoventrally flattened, gently curved dorsally (Fig. 9H), tip divided into three short, equal tubes in last 1/4 of its length (Fig. 9F, G). Spines on inner side of lateral branch of aedeagus large, distinct, forming spike-like outgrowth (Fig. 9I); in lateral view individual spine can be separated (Fig. 9H).

Female terminalia: (Fig. 10A)**.** Very similar to terminalia of *C. distinctissima* and *C. americana* stat. reval. The only clear difference is the sclerotisation of lateral sperm ducts (Fig. 10B), corresponding to the position of large spines on lateral branches of aedeagus (Fig. 9I). Spermathecae small (Fig. 10C), diameter ~ 0.08–0.12 × width of sternite 8 (in inner dorsal view).

Distribution. Palearctic species, distributed from Finland to Far East Russia. Reported from Finland, Kazakhstan, Mongolia, and Russia: North European Russia, West Siberia (Altai Republic), East Siberia (Irkutsk Oblast), Far East Russia (Sakhalin Oblast, Primorsky Krai) (Oosterbroek 2021). The species was reported from the Altai Republic (Russia) by Soós and Oosterbroek (1992), but without any collection data, here we publish the first confirmatory record from the Altai Republic.

Comments. Besides the apparent terminal differences in male specimens, the only distinct difference between *C. nigriventries*, *C. distinctissima*, and *C. americana* stat. reval. noted in our study, was the colouration of the scutellum, which is yellow in the latter

two species, and with a median brown stripe or patch in *C. nigriventries*. Salmela and Autio (2007) and Gelhaus et al. (2007) note that these species also differ in the colouration of the abdomen (dark brown, almost black in *C. nigriventries*, and yellowish brown in *C. distinctissima*), however, some of the Japanese species of *C. distinctissima* have a very dark brown abdomen (Fig. 3A). The illustration of the female terminalia of *C. nigriventris* by Gelhaus et al. (2007: fig. 9) shows a high similarity to the drawing of the female terminalia of *C. distinctissima* by Peus (1952: fig. 21b), making the former suspect.

Diogma caudata Takahashi, 1960

Figs 4B, 5C, 8B, 11, 12, 13

Diogma caudata in Takahashi 1960: 82–84: original description; Siitonen 1984: 203: faunistic record; Sidorenko 1999: 68–70: identification key, illustration, distribution; Oosterbroek et al. 2001: 122: distribution; Paramonov 2004a: 258: faunistic record; Paramonov 2005: 211: comparison; Mukkala et al. 2005: 7: faunistic record; Bartsch et al. 2005: red list status, faunistic record; Paramonov 2006: 888–889: identification key, illustration, distribution; Polevoi 2006: 96: faunistic records; Sandström 2008: red list status; Salmela 2008: 12: ecology; Salmela 2012a: 242: distribution; Salmela 2012b: 16: distribution; Salmela and Petrašiūnas 2014: 31: checklist; Nakamura 2014: 54: distribution.

Type material examined. *Diogma caudata* Takahashi: ***Holotype***: • ♂; Japan, Hokkaido, Mount Meakandake; 5 Jul. 1958; M. Takahashi leg.; ELUK.

Non-type material examined. **Finland** • 3 ♂, 1 ♀; Kaavi, Kalalamminpuro; 63.11458°N, 28.67255°E; alt. 140 m; 20 Jun. 2008 – 17 Jul. 2008; J. Salmela leg.; LMM, CKLP. **Russia** • 1 ♂, 1 ♀; Arkhangelsk Oblast, Plesetsk District, Obozersky Settlement, around the settlement; 63.44231°N, 40.30789°E; alt. 100 m; 26 Jun. 1959; N.P. Krivosheina leg.; CKLP. • 1 ♂; Karelia Republic, Kon: 6909:550, Kondopoga District, Kivach Nature Reserve, spruce forest; 62.26766°N, 33.97975°E, alt. 42 m; 19 May. 1993 – 23 Jun. 1993; A.V. Polevoi leg.; window trap; ZIN. • 1 ♂; Karelia Republic, Karelia, Kon: 6982:570, Medvezhyegorsk Urban Settlement, 3 km NW Medvezhyegorsk City, point №6; 62.93364°N, 34.38467°E; alt. 130 m; 19 Jul. 2002; A.V. Polevoi leg.; ZIN. • 1 ♂; Perm Krai, Kungur Urban Okrug, Kungur City, forest station; 57.42881°N, 56.944206°E; alt. 219 m; 16 Jun. 1960; K.B. Borisova leg.; ZIN. • 1 ♂; Tuva Republic, Tandinsky District, north slope of Tannu-Ola mountains, near Chagytaj Lake; 50.99591°N, 94.6764°E; alt. 1500 m; 24 Jun. 1963; N.A. Violovich leg.; ZIN. **Sweden** • 2 ♂; Lule Lappmark, Kaltbacken bei Messaure; 66.67347°N, 20.32239°E; alt. 240 m; 23 Jun. 1969 – 26 Jun. 1969; • 1 ♀; same locality; 22 Jun. 1970 – 24 Jun. 1970; • 2 ♂; same locality; 23 Jun. 1971 – 30 Jun. 1971; • 31 ♂, 4 ♀; same locality; 12 Jun. 1972 – 13 Jul. 1972 / 21. Aug. 1972 – 28 Aug. 1972; • 2 ♂; same locality; 19 Jun. 1973 – 25 Jun. 1973; • 1 ♂, 1 ♀; same locality; 17 Jun. 1974 – 8 Jul. 1974; K. Müller leg.; ZFMK.

Redescription. Head. Dorsally dark brown, ventrally brown. Frons with white pubescence noticeable only in dry specimens (Fig. 11C, D). Rostrum pale brown, short, without nasus, with few hairs. Mouthparts pale brown to brown (Fig. 11C, D). Palpus pale brown to brown, short, five segmented; last segment slightly longer than penultimate segment (Fig. 11B). Scape cylindrical, 2 × as long as pedicel; pedicel ovate, slightly darker than scape; flagellum 14-segmented, gradually darkening from base to tip; segments simple in both sexes, not expanded ventrally (Figs 4B, 11E, F); in male, first flagellomere as long as wide, remaining segments cylindrical; last segment 1.2–1.3 × as long as penultimate segment; flagellomeres with short, relative sparse whitish setae (sensilla), just slightly denser in ventral and lateral sides (Fig. 11E); in female, last flagellomere 1.8–2 × as long as penultimate; last 4–6 segments without sensilla (Figs 4B, 10F). Verticels black, shorter than length of flagellomere; usually one verticel in ventral surface and two or three in dorsal/dorsolateral sides, first segment with 4–6 verticels.

Thorax. General colouration yellowish brown with contrasting, shiny black markings. Mesonotum pale brown, greenish yellow in fresh, living specimen (Takahashi 1960), with three separated, broad, longitudinal black markings (Fig. 11C); several small yellow setae along pale strips. Scutellum yellow. Posterior part of mediotergite black. Anepisternum and katepisternum separated, both ventral parts dark brown to black. Ventral corner of laterotergite black. Additional small darker patch on posterior basalare, and on ventral part of meron. Coxa and trochanter yellowish, darker on anterior- dorsal parts (Fig. 11B); femur pale brown; tibia gradually darkening from pale brown to dark brown/black; tarsus uniformly black. Wing hyaline; veins pale brown to brown; pterostigma pale (Fig. 5B); three branches of M reaching wing margin; M1 in same level as M1+2; cell a2 narrow, > 7 × longer than wide (Fig. 5B); membrane with interference patterns, visible with dark background (Fig. 11A). Halter monochrome, yellow or pale brown.

Abdomen. Tergites and sternites pale brown to brown, tergite 8 and sternite 8 darker than others (Fig. 11A). Pleural parts greenish in living specimen (Takahashi 1960).

Male terminalia: Black, large, complex, directed caudally. Tergite 9 not fused with gonocoxite, partly cover gonocoxite (Fig. 12C); medial part rounded with small tuft of hairs (Fig. 12A); lateral lobe of tergite 9 greatly extended, complex; as long as basal part of tergite 9; ventral portion of lateral lobe elongated, finger-like in lateral view (Fig. 12C); lateral margin almost straight or weakly divergent in dorsal view (Fig. 12A, B); ventral base of lateral lobe with small, black, heavily sclerotised lobe (Fig. 12C, E) – named lamina by some authors – shape variable; posterior margin of tergite 9 between median round part and lateral lobe covered with dense short, blunt ended setae (Fig. 12A). Gonocoxite complex; apical lobe with dense hairs (Fig. 12B–D); ventral lobe round, almost bare (Fig. 12B, D); inner part of gonocoxite with basally directed lobe, with hairs on margin (Fig. 12D). Gonostylus simple, wider at middle (Fig. 12F); with finger-like membranous lobe on inner side, poorly visible in dry specimens (Fig. 12G). Aedeagus bifid; aedeagus with apical branches long, curved ventrally almost in right angle, then curved in right angle posteriorly, then turn dorsally in right angle in lateral view (Fig. 12J); dorsal lobe between interbases complex, sclerotised (Fig. 12H, J); interbase with ventral projec-

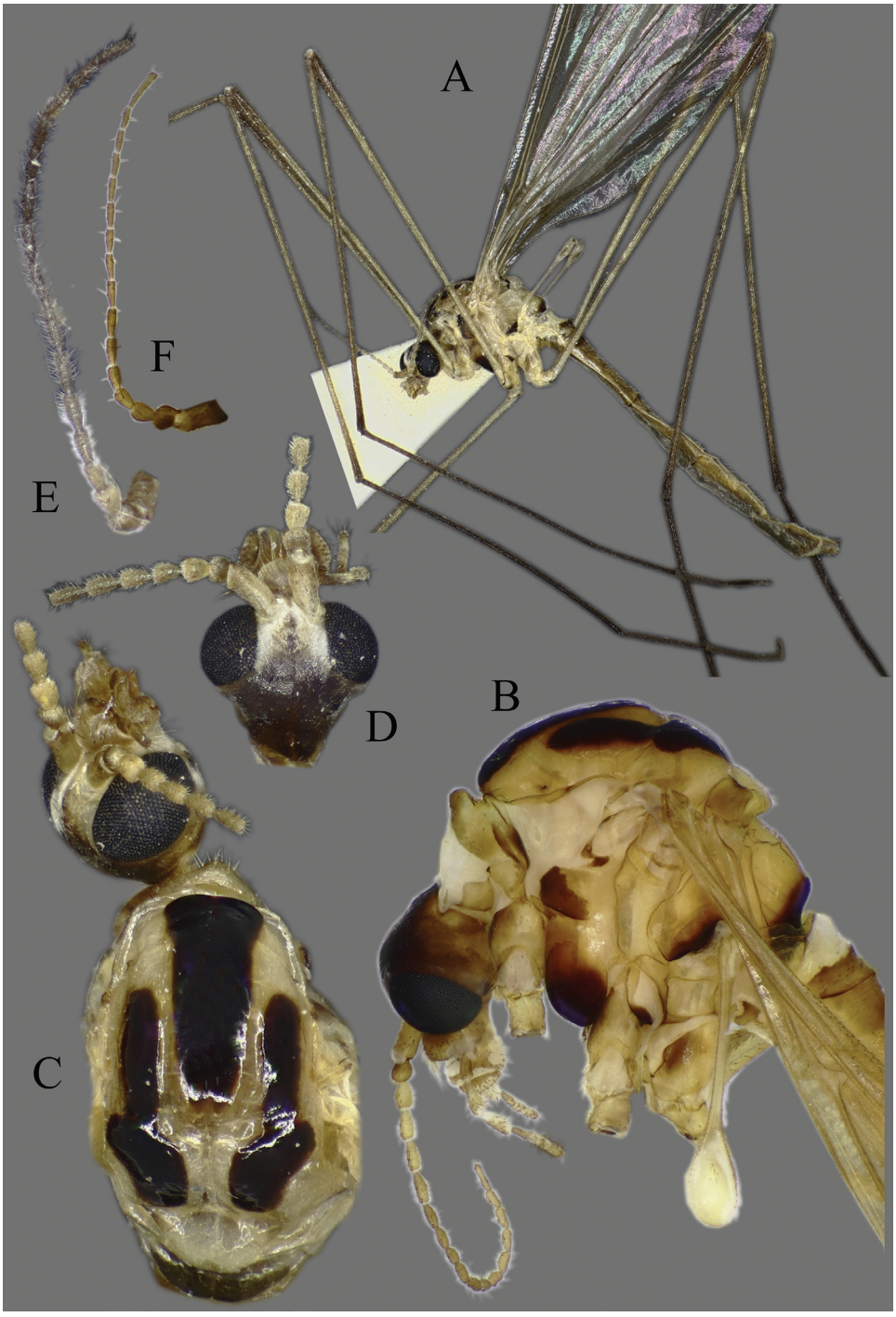

Figure 11. *Diogma caudata* Takahashi, 1960 **A** habitus of the holotype male, lateral view (colouration of wings is artefact) **B** head and thorax of female, lateral view **C** head and thorax of female, lateral and dorsal views **D** head of female, dorsal view **E** antenna of holotype male **F** antenna of female.

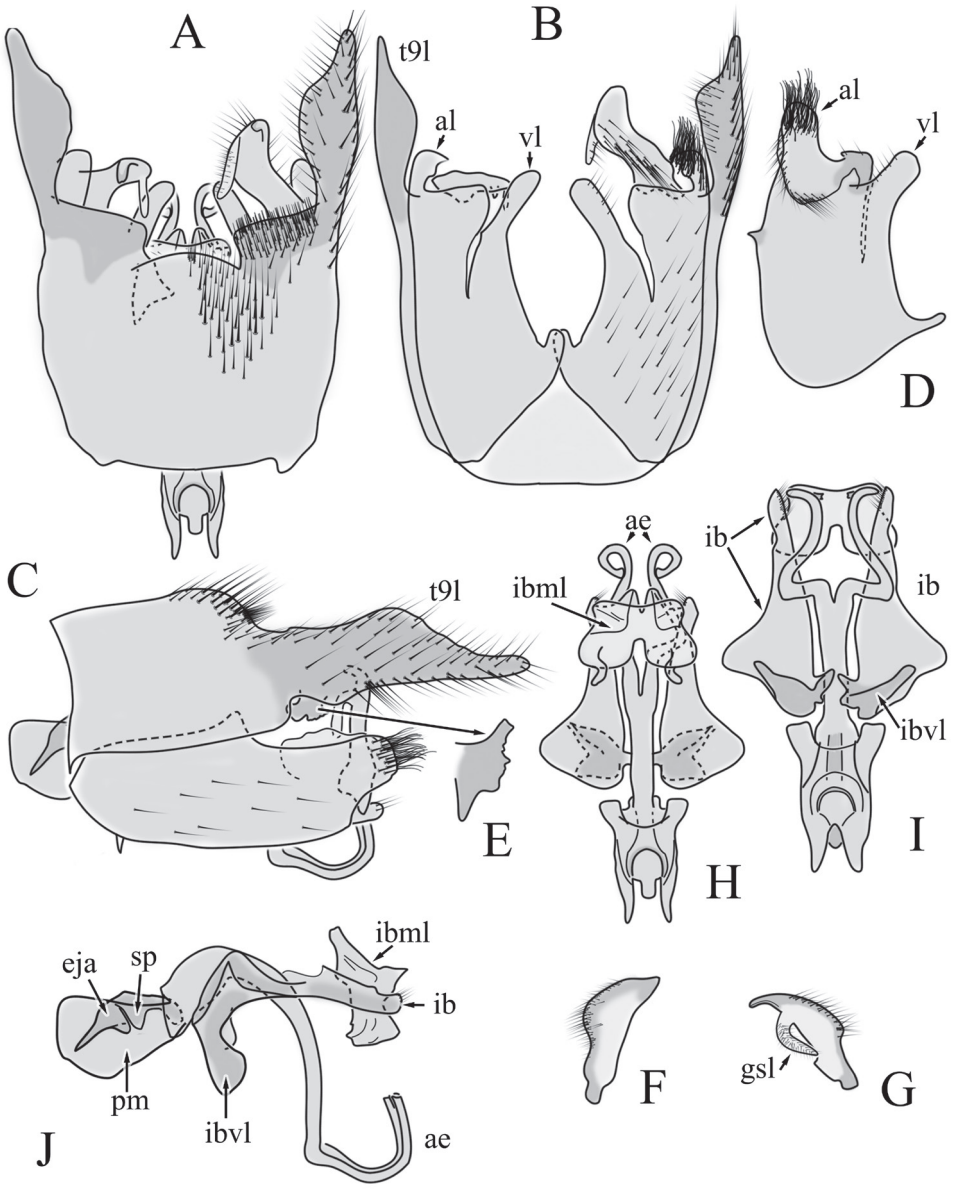

Figure 12. Male genital structures of *Diogma caudata* Takahashi, 1960 **A** terminalia, dorsal view **B** terminalia, ventral view (aedeagus complex removed) **C** terminalia, lateral view **D** gonocoxite, inner lateral view **E** shape of heavily sclerotised lobe (lamina) of tergite 9 **F** shape of the gonostylus, caudal view **G** shape of the gonostylus, inner ventral view **H** aedeagus complex, dorsal view **I** aedeagus complex, ventral view **J** aedeagus complex, lateral view. Abbreviations: ae – aedeagus; al – gonocoxite apical lobe; eja – ejaculatory apodeme; gsl – lobe of gonostylus; ib – interbase; ibml – interbase median lobe; ibvl – interbase ventral lobe; pm – paramere; sp – sperm pump; t9l – tergite 9 lateral lobe; vl – gonocoxite ventral lobe.

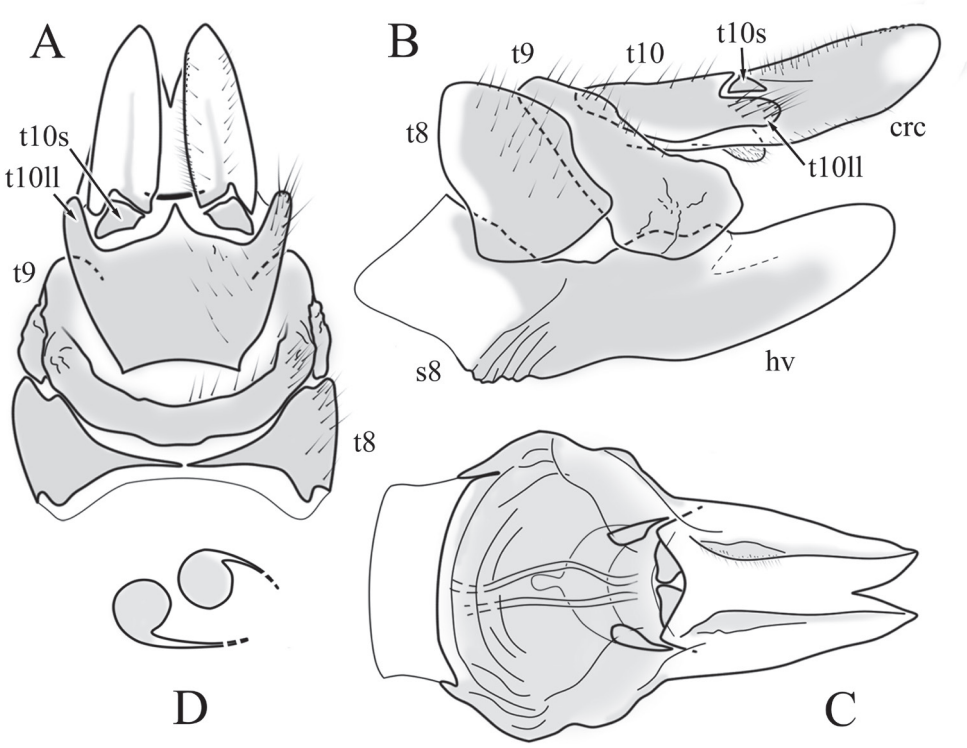

Figure 13. Female genital structures of *Diogma caudata* Takahashi, 1960 **A** terminalia, dorsal view **B** terminalia, lateral view **C** sternite 8, hypogynial valve, genital fork, and sperm ducts, inner dorsal view **D** spermathecae. Abbreviations: crc – cercus; hv – hypogynial valve; t8 – tergite 8; t9 – tergite 9; t10 – tergite 10; t10s – tergite 10 triangular sclerite; t10ll – tergite 10 lateral lobe; s8 – stergite 8.

tion (Fig. 12J). Sperm pump and ejaculatory apodeme small (Fig. 12H–J), covered by parameres in lateral view (Fig. 12J).

Female terminalia: Brown, tip of cercus and hypopygial valve yellowish brown. Tergite 8 separated at middle by membranous area (Fig. 13A). Tergites 8 and 9 similar in size (Fig. 13B). Ventral corner of tergite 9 rugged (Fig. 13B). Triangular sclerite separated from tip of tergite 10 (Fig. 13A). Lateral lobes of tergite 10 elongated, with few longer hairs (Fig. 13A, B). Cercus and hypogynial valve simple, wide, blade-shaped, tips rounded (Fig. 13B). Dorsal apical surface of cercus rough, formed by few blunt, pyramid or round teeth (Fig. 13A, B). Base of sternite 8, weakly sclerotised, extended laterally at middle, with transverse creases (Fig. 13AC). Two round spermathecae present, duct curved (Fig. 13D). Lateral sclerite of genital fork elongated; two sperm ducts simple, without any clear markings (Fig. 13D).

Distribution. Finland, Japan (Hokkaido I, Fig. 8B), Sweden, and Russia (Kareliya Republic, Perm Krai and Tuva) (Oosterbroek 2021). First records from Arkhangelsk Oblast, Russia.

Comments. The species was initially described from Hokkaido, Japan. However, no additional Japanese data has been published, and the species was not found in the type locality in our study. The species later was reported from Finland, Sweden, and Russia (Karelia Republic, Perm Krai, and Tuva). Morphologically it is a well separated species from the close related *Diogma glabrata*, but the Finnish specimens show only a small COI genetic difference from it and form a clade together with the West Palearctic *D. glabrata*. No significant morphological differences were found between the Finnish and Russian specimens and the Japanese holotype.

***Diogma glabrata* (Meigen, 1818)**
Figs 4C, 5C, 8B, 14, 15, 16

Phalacrocera megacauda in Alexander 1931: 349–350: original description.
Diogma glabrata megacauda in Alexander 1949: 196: comparison; Ishida 1955: 76: distribution; Takahashi 1960: 82: distribution, comparison, illustration; Alexander 1966: 122: distribution, faunistic records; Sidorenko 1999: 68–70: identification key, illustration, distribution.
Diogma glabrata (*glabrata megacauda*) in Paramonov 2006: 888–889: identification key, illustration, distribution.
Diogma glabrata megacauda, *D. glabrata* in Gelhaus et al. 2007: synonymy, comparison, ecology, distribution, illustration.
Diogma glabrata in Nakamura 2014: 54: distribution; Imada 2020: biology and ecology of larvae.

Non-type material examined. Belarus • 2 ♂, 1 ♀; Brest Oblast; Kamenets District, Belavezhskaya Pushcha National Park; 52.58807°N, 23.81746°E; alt. 160 m; 4 Aug. 1961; E.P. Narchuk leg.; ZIN. **Denmark** • 1 ♂; ?Upilbo; 27 Jul. 1917; P. Nielsen leg.; USNM. **Estonia** • 1 ♀; Ida-Viru County, Narva-Jõesuu Town [Gungerburg]; 59.45°N, 28.03°E; 18 Jul. 1909; A.I. Chekini leg.; ZIN. **Finland** • 1 ♂, 2 ♀; Pihtipudas, Valkeispuro; 63.41082°N, 26.05336°E; alt. 170 m; 12 Jul. 2008 – 14 Aug. 2008; J. Salmela leg.; Malaise trap; LMM. • 1 ♂; Luvia, Niemenkyla; 61.39108°N, 21.56586°E; 12 m; 18 Jul. 2012; E. Viitanen leg.; CKLP. • 1 ♂; Mustasaari, Valassaaret; 63.43103°N, 21.07421°E; alt. 1 m; 2 Jul. 2019; E. Viitanen leg.; CKLP. • 1 ♀; Virolahti, Kurkela; 60.56858°N, 27.83847°E; alt. 8 m; 25 Jul. 2016; E. Viitanen leg.; CKLP. • 1 ♀; Fennia, Kb: 698:72, Ilomantsi, Tapionaho; 62.86016°N, 31.48371°E; alt. 190 m; 7 Jul. 1993 – 28 Jul. 1993; J.B. Jakovlev leg.; ZIN. • 1 ♀; Sotkamo, Iso-Matojarvi, Window trap №3, Kn: 7086:590; 63.86638°N, 28.85971°E; alt. 210 m; 1 Jul. 1997 – 14 Jul 1997; Kuussaari leg.; ZIN. **Japan** • 2 ♂; Hokkaido, Higashikawa, Asahidake, River Yukomabetsu; 43.65226°N, 142.80229°E; alt. 1120 m; 23 Jul. 2019; L.-P. Kolcsár leg.; CKLP. • 4 ♂, 1 ♀; Hokkaido, Shari, Shiretoko Pass; 44.05331°N, 145.10166°E; alt. 716 m; 26 Jul. 2019; L.-P. Kolcsár leg.; CKLP. • 1 ♂; Iwate, Hachimantai, Toshiti Spa; 39.94253°N, 140.86804°E; alt. 1344 m; 3 Aug. 2013; • 2 ♀; same locality; 5 Aug.

2015; D. Kato leg.; BLKU. • 4 ♂; Nagano, Otakimura, Mt. Ontake; 35.86894°N, 137.51421°E; alt. 1990 m; 22 Jul. 2016; D. Kato leg.; BLKU. • 1 ♂; Toyama, Toyama, Arimine Jurodani; 36.46063°N, 137.42198°E; alt. 1130 m; 28 Aug. 2009 – 1 Sep. 2009; • 1 ♀; same locality; 1 Sep. 2009 – 8 Sep. 2009; M. Watanabe leg; Malaise trap; BLKU. **Latvia** • 1 ♀; Dolesmuiža, Doles sala; 56.866°N, 24.2014°E; alt. 4 m; 20 Jul. 2018; L.-P. Kolcsár leg.; CKLP. • 1 ♂, 1 ♀; Skaistkalne, small stream; 56.411°N, 24.637°E; alt. 12 m; ; L.-P. Kolcsár leg.; birch-spruce forest; CKLP. **Russia** • 1 ♂; Altai Republic, Turochak District, near Artybash Settlement; 51.79299°N, 87.26535°E; alt. 430 m; 15 Jul. 2006; N.M. Paramonov leg.; ZIN. • 1 ♀; Amur Oblast, Shimanovsk District, Urochishche Samodon, 100 km W Svobodny City; 51.29°N, 126.83°E; alt. 320 m; 6 Aug. 1959; A.G. Zinovjev leg.; ZIN. • 1 ♂; Amur Oblast, Shimanovsk District, Simonovo Settlement, 75km W Svobodny City; 51.46°N, 126.98°E; alt. 305 m; 27 Jul. 1959; A.G. Zinovjev leg.; ZIN. • 1 ♂; Leningrad Oblast, Luga District, Jashhera Village; 58.89°N, 29.82°E; alt. 40 m; 23 Jul. 1963; A.A. Stackelberg leg.; ZIN. • 2 ♂, 1 ♀; Leningrad Oblast, Gobzhicy Village; 58.83°N, 30.13°E; 7 Jul. 1934 -16 Jul. 1934; A.A. Stackelberg leg.; ZIN. • 1 ♂, 2 ♀; Leningrad Oblast, Tolmachyovo Urban Locality; 58.86°N, 29.91°E, alt. 60 m; 16 Jul. 1935 – 26 Jul. 1935; A.A. Stackelberg leg.; ZIN. • 1 ♂; Leningrad Oblast, Kamenka River; 58.88°N, 29.76°E; alt. 65 m; 8 Jul. 1935 ; A.A. Stackelberg leg.; ZIN. • 2 ♂, 5 ♀, Leningrad Oblast, Vsevolozhsk District, Jukki Village; 60.11°N, 30.27°E; alt. 58 m; 13 Jul. 1931 – 22 Jul. 1933; A.A. Stackelberg leg.; ZIN. • 1 ♂; Leningrad Oblast, Vsevolozhsk District, Ostrovki Village; 59.81°N, 30.82°E; alt. 13 m; 21 Jun. 1906 – 22 Jun. 1906; G.G. Jakobson leg.; ZIN. • 1 ♂; Magadan Oblast, Magadan Urban Okrug, near Sokol Urban Settlement; 59.92°N, 150.71°E; alt. 177 m; 11 Jul. 2014 – 19 Jul. 2014; N.E. Vikhrev leg.; ZIN. • 2 ♀; Moscow Oblast, Naro-Fominsk District, Naro-Fominsk City, near Vostochnyy Community; 55.39094°N, 36.68878°E; alt. 195 m; 29 Jun. 2011; • 1 ♂; same locality, 29 Jun. 2014; D.I. Gavryushin leg.; ZIN. • 1 ♀; Moscow Oblast, Naro-Fominsky District, Vostochnyy [Oriental] settlement, within the settlement; 55.3741°N, 36.4984°E; alt. 205 m; 29 Jun. 2011; D.I. Gavryushin leg.; CKLP. • 1 ♂, Moscow Oblast, Naro-Fominsk, Nara River; 55.36075°N, 36.7404°E; alt. 174 m; 29. Jun. 2014; D.I. Gavryushin leg.; CKLP. • 1 ♀; Novgorod Oblast, Novgorod District, 1.5 km SE Glebovo Settlement; 58.54893°N, 31.83198°E; alt. 40 m; 2010; N.M. Paramonov leg.; ZIN. • 1 ♂; Primorsky Krai, Vladivostok City; 43.11553°N, 131.88548°E; alt. 20 m; 8 Aug. 2003; V.V. Sidorenko leg.; ZIN. • 1 ♂; Primorsky Krai, Chuguyevka District, Verchneussuri station; 44.067°N, 133.979°E; alt. 330 m; 30 Jul. 1979; A.G. Zinovjev leg.; ZIN. • 1 ♂; Primorsky Krai, Krasnoarmeysk District, Udegeyskaya Legenda National Park, apiary; 45.46052°N, 135.20451°E; alt. 700 m; 19 Jul. 2009; A.N. Ovtshinnikov leg.; ZIN. • 1 ♀; Primorsky Krai, Terney District, Terney Urban-type Settlement, Lower Serebryanka [Sanhobe] River; 45.09°N, 136.58°E; alt. 60 m; 6 Aug. 1941; K.J. Grunin leg.; ZIN. • 1 ♂; Primorsky Krai,Ussuriysk Urban Settlement, Gorno-Tajozhnoe Settlement, 25 km SE Ussuriysk; 43.69°N, 132.15°E; alt. 120 m; 3 Aug. 1963; E.P. Narchuk leg.; ZIN. • 1 ♀; Sakhalin Oblast, Severo-Kurilsky District, Kuril Islands, Paramushir Island, Rifovaya Bay; 50.4594°N, 156.0138°E; alt. 130 m; 30 Aug. 1999;

A.S. Lelej, S.Y. Storozhenko leg.; ZIN. • 1 ♂; Sakhalin Oblast, Yuzhno-Kurilsk Urban Settlement, Kuril Islands, Kunashir Island, near Lagunnoe Lake; 44.062°N, 145.759°E; alt. 20 m; 25 Jul. 1955; N.A. Violovich leg.; ZIN. • 1 ♀; Sakhalin Oblast, Kuril Islands, Shikotan Island, near Malokurilskoye Village; 43.866°N, 146.827°E; alt. 30 m; 21 Aug. 1963; G.O. Krivoluckaja leg. ZIN. • 1 ♂; Sakhalin Oblast, Sakhalin Island, Yuzhno-Sakhalinsk City; 46.95°N, 142.73°E; alt. 50 m; 29 Jul. 1959; N.A. Violovich leg.; ZIN. • 1 ♀; Samara Oblast, Zhigulyovsk Urban Okrug, Zhiguli Nature Reserve, Bakhilova Polyana; 53.43543°N, 49.66252°E; alt. 45 m; 24 Jun. 2006; N.M. Paramonov leg.; ZIN. • 1 ♀; Tver Oblast, Udomlya District, 1,5 km NW Kaskovo Village; 57.98475°N, 35.03497°E; alt. 167 m; 19 Jul. 2017; A.G. Korobkov leg.; ZIN. • 1 ♂; Tver Oblast, Udomlya District, Moldino Settlement; 57.74807°N, 35.24965°E; alt. 155 m; 4 Jul. 2018; • 1 ♂; same locality; 5 Jul. 2018; A.G. Korobkov leg.; ZIN. • 1 ♂; Yaroslavl Oblast, Tutayev District, near former railway station Pustovo; 57.81438°N, 39.56016°E; alt. 122 m; 30 Jun. 2012; M.A. Klepikov leg.; pine forest, stream; ZIN.

Redescription. Head. Dorsal part brown, ventral part yellowish brown (Fig. 14B, C). Frons with white to yellowish-grey pubescence, visible only in dry specimens (Fig. 14C, F). Rostrum yellowish brown, short without nasus; mouthparts pale brown to brown. Palpus pale brown to brown, 5 segmented; last segment slightly longer than penultimate segment (Fig. 14F). Scape cylindrical 1.8–2 × longer than pedicel; pedicel ovate; pedicel and scape same colour or pedicel slightly darker (Figs 4C, 14E, F); flagellum 14 segmented, gradually darkening from base to tip; flagellar segments simple in both sexes, not expanded ventrally; male flagellomere cylindrical, with short sparse whitish setae – sensilla, slightly denser in ventral and lateral sides; last segment 1.5–1.8 × longer than penultimate (Figs 4C, 14E); female flagellomeres oval to cylindrical, first 4–6 flagellomeres oval, rest of segments cylindrical, sometimes all segment elongated, cylindrical as in male; only first 8–10 flagellomeres with sensilla; last flagellomere 1.8–2.8 × longer than penultimate (Figs 4C, 14F); verticels black, shorter than length of flagellomere; generally one verticel in ventral surface and two or three in dorsal/dorsolateral sides of flagellomeres, first segment with 4–6 shorter verticels.

Thorax. General colouration yellowish with contrasting, shiny black markings. Pronotum yellow, middle part pale brown. Mesonotum yellow to pale brown with three separated black markings (Fig. 14C) or one big black patch (Fig. 14D). Scutellum yellow. Posterior part of mediotergite black (Fig. 14B). Anepisternum and katepisternum well separated; ventral part of katepisternum black; ventral part of anepisternum yellowish (Japan, Fig. 14B) or pale brown to brown (Finland, Russia). Ventral part of meron pale brown (Japan, Fig. 14B) or brown to black (Finland, Russia). Laterotergite black at ventral corner. Coxa and trochanter yellow, femur pale brown; tibia gradually darkening from pale brown to dark brown/black; tarsus uniformly black; tarsomeres each with one spur. Wing hyaline; veins pale brown to brown; pterostigma pale; three branches of M reaching wing margin, M_1 at same level as M_{1+2}, cell a_2 narrow, > 7 × longer than wide (Fig. 5C); wing membrane with interference patterns, visible with dark background. Halter monochrome or knob darker, yellow to pale brown.

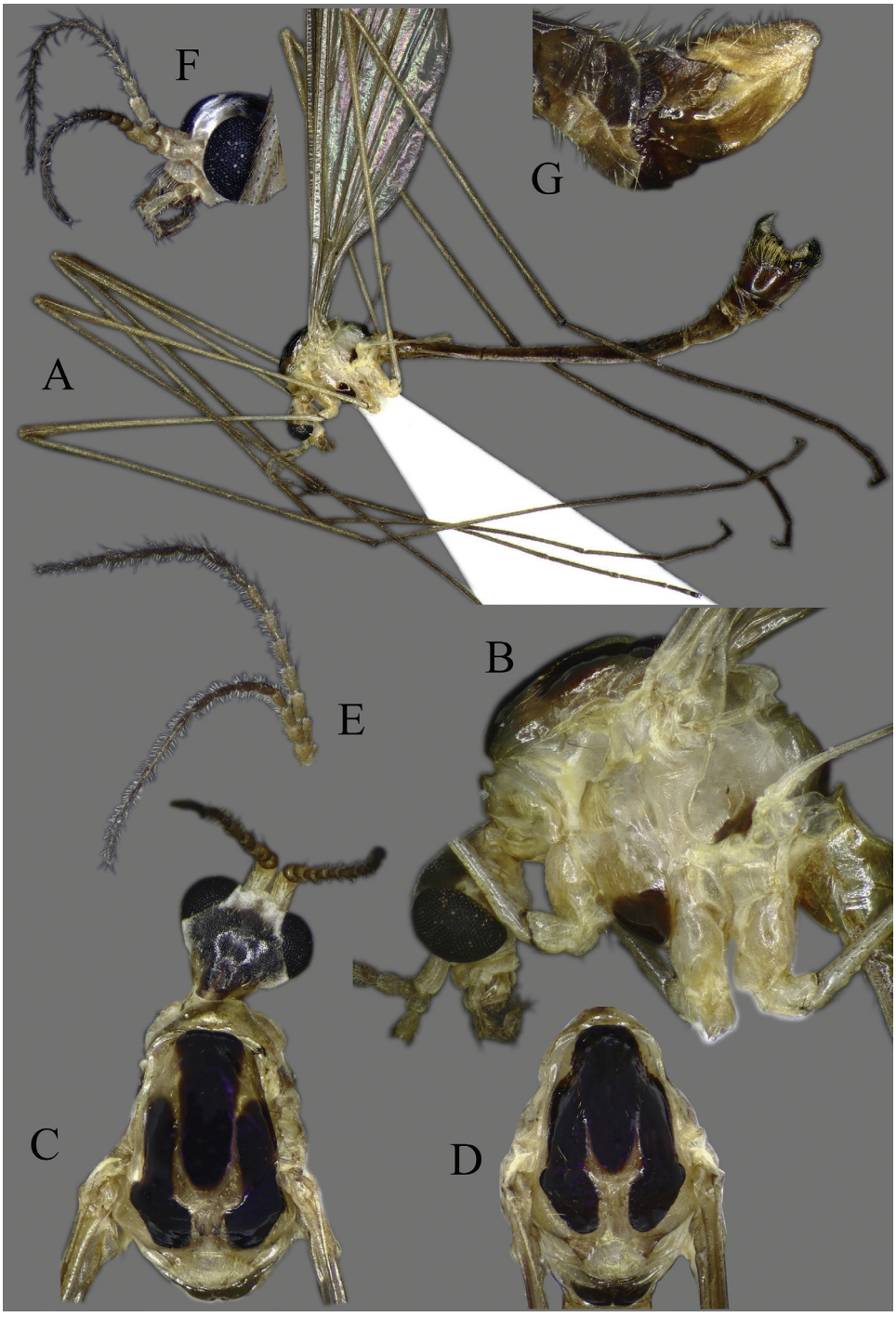

Figure 14. *Diogma glabrata* (Meigen, 1818) **A** habitus of male, lateral view (colouration of wings is artefact) **B** head and thorax, lateral view **C** head and thorax, dorsal view of pale form **D** thorax, dorsal view – dark form **E** antenna of male, dorsal view **F** head of female, lateral view **G** female terminalia lateral view.

Abdomen. Tergites and sternites pale brown to brown, with paler longitudinal median line, poorly visible in dry specimens. Tergites and sternites 7 and 8 darker (Fig. 14A). Pleural parts yellow to greenish yellow in living specimen.

Male terminalia. Large, black directed caudally (Fig. 14A). Tergite 9 not fused with gonocoxite, partly cover gonocoxite (Fig. 15C); medial part of tergite 9 rounded, with small tuft of hairs (Fig. 15A); lateral lobe of tergite 9 greatly extended, complex, shorter than basal part of tergite 9; shape variable, rectangular to triangular in lateral view (Fig. 15C); margin wavy, especially in caudal end (Fig. 15C, see also Gelhaus et al. 2007: figs 12–15); weakly curved inward in dorsal view (Fig. 15A); ventral base of lateral lobe with small, black, heavily sclerotised lobe (named lamina by some authors)

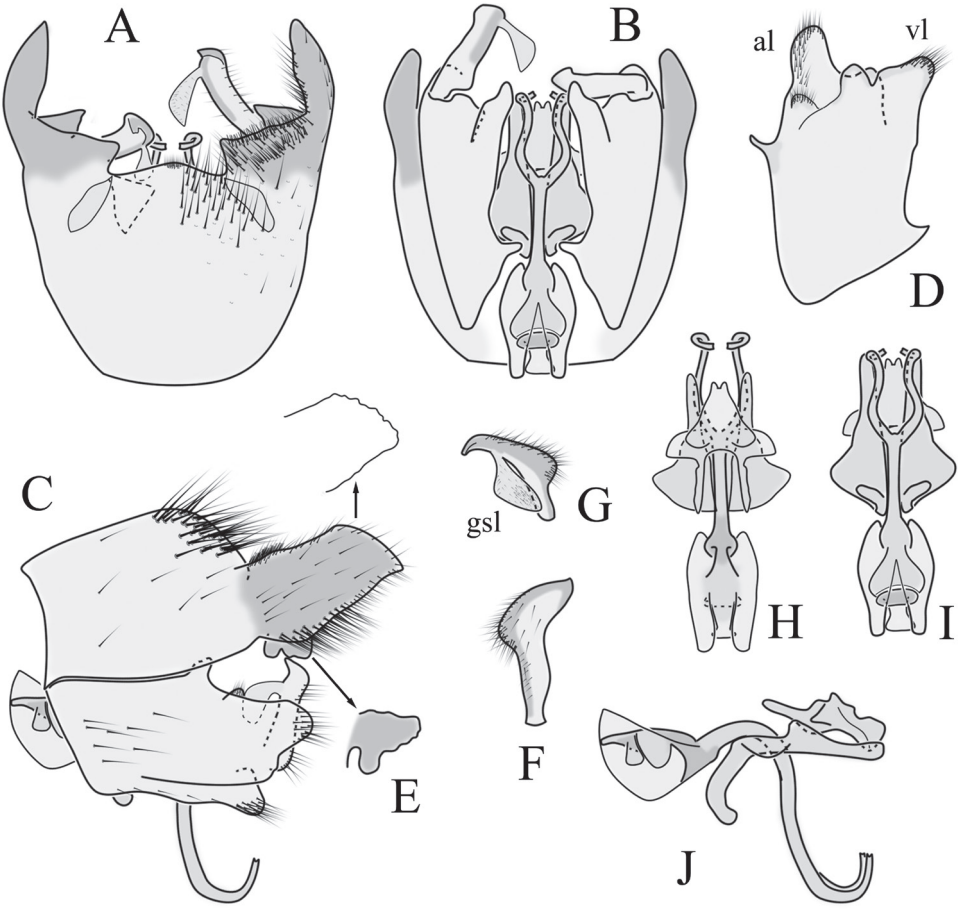

Figure 15. Male genital structures of *Diogma glabrata* (Meigen, 1818) **A** terminalia, dorsal view **B** terminalia, ventral view **C** terminalia, lateral view **D** gonocoxite, inner lateral view **E** shape of heavily sclerotized lobe (lamina) of tergite 9 **F** shape of the gonostylus, caudal view **G** shape of the gonostylus, inner ventral view **H** aedeagus complex, dorsal view **I** aedeagus complex, ventral view **J** aedeagus complex, lateral view. Abbreviations: al – gonocoxite apical lobe; gsl – gonostylar lobe; vl – gonocoxite ventral lobe.

considerably variable in shape (Fig. 15E, see also, Gelhaus et al. 2007: figs 16–20, Takahashi 1960: figs 2, 3). Posterior margin of tergite 9 between median round part and lateral lobe with dense short, blunt ended setae (Fig. 15A). Gonocoxite complex; apical and ventral lobe tips rounded with hairs; inner part of gonocoxite with less defined lobe, directed apically with hairs on tip (Fig. 15D). Gonostylus simple, outer half wider (Fig. 15F), with triangular, membranous lobe at inner side, poorly visible in dry specimens (Fig. 15G). Sperm pump and ejaculatory apodeme small (Fig. 15H–J), covered by parameres in lateral view (Fig. 15J). Dorsal lobe between interbases complex, sclerotised (Fig. 15H, J); interbase with ventral projection (Fig. 15J). Aedeagus bifid, branches long, curved ventrally almost in right angle, then turned dorsally (Fig. 15J).

Female terminalia. Brown, tip of cercus and hypopygial valve yellowish brown (Fig. 14G). Tergite 8 separated at middle by membranous area (Fig. 16A). Ventral corner of tergite 9 weakly rugged and with hairs (Fig. 16B). Triangular sclerite separated from tip of tergite 10 (Fig. 16A). Lateral lobe of tergite 10 relatively small, with long hairs (Fig. 16A, B). Cercus and hypogynial valve simple, wide, blade-shaped, tips

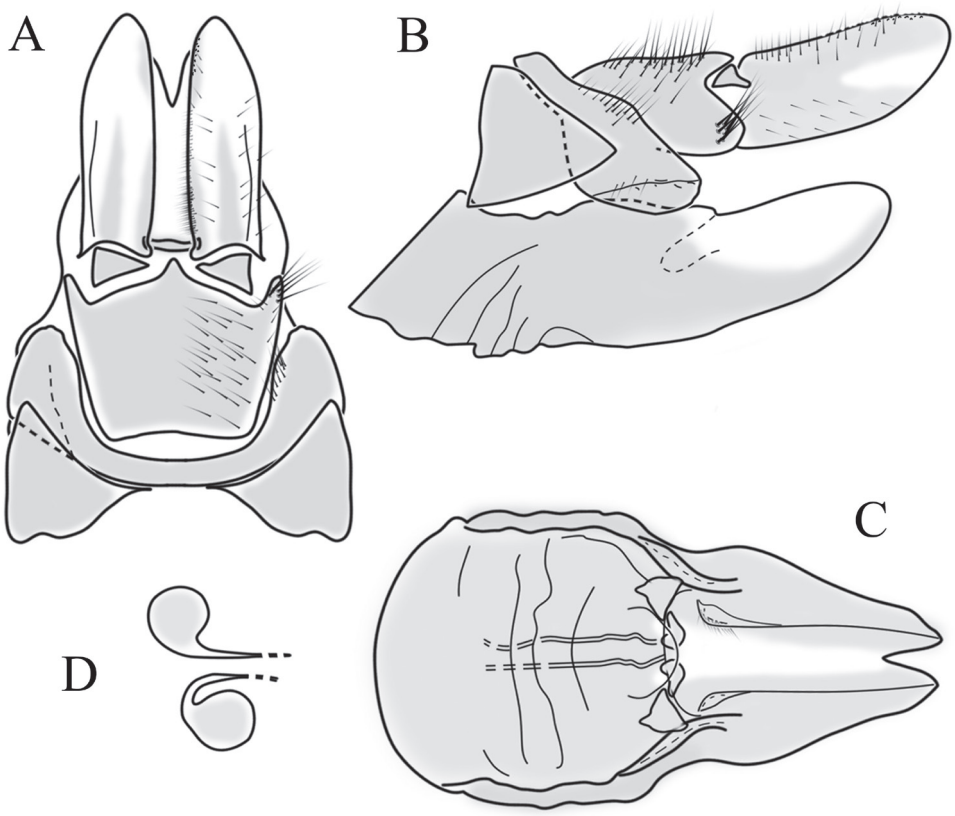

Figure 16. Female genital structures of *Diogma glabrata* (Meigen, 1818) **A** terminalia, dorsal view **B** terminalia, lateral view **C** sternite 8, hypogynial valve, genital fork, and sperm ducts, inner dorsal view **D** spermathecae.

rounded (Fig. 16B). Dorsal apical surface of cercus rough, formed by few blunt pyramid or round teeth (Fig. 16A, B). Base of sternite 8 sclerotised (Fig. 16B), lateral margins almost straight in ventral and inner dorsal view (Fig. 16C), with transverse creases (Fig. 16B, C). Two round spermathecae present, duct curved (Fig. 16D). Lateral sclerite of genital fork triangular, two sperm ducts simple, without any clear markings (Fig. 16C).

Distribution. Austria, Belgium, Czech Rep., Denmark, Estonia, Finland, France, Germany, Great Britain, Ireland, Japan: Hokkaido I, Honshu I, Korea (North Korea or South Korea), Lithuania, Luxembourg, Netherlands, Norway, Poland, Romania, Slovakia, Sweden, Switzerland, and Russia (North European territory, Central European territory (Yaroslavl Oblast), Far East (Amur Oblast, Primorsky Krai, Sakhalin Oblast (Kuril Is: Kunashir I) (Oosterbroek 2021).

First records from Belarus, Latvia, and Russia: Altai Republic, Amur Oblast, Novgorod Oblast, Magadan Oblast, Samara Oblast, and Kuril Islands (Shikotan I and Paramushir I). Occurrence data in Japan and surrounding areas are presented in Figure 8B.

Comments. *Diogma glabrata* is a relatively common species in Europe, with a similar distribution to *Cylindrotoma distinctissima*. However, it is rarer or seemingly absent from southern Europe (Kolcsár et al. 2018; Oosterbroek 2021). Alexander (1931) described the species *Phalacrocera megacauda* from Japan, based on the external morphological characters, without describing or illustrating the male terminalia. Later, Edwards (1938) designated a new genus, *Diogma*, for *Cylindrotoma glabrata*, which was previously included in *Liogma* by Osten Sacken (1859). Later, Alexander (1949) moved *Phalacrocera megacauda* to *Diogma* and mentioned it as a subspecies of *Diogma glabrata*, without detailing the difference or the reason for transferring it to subspecies rank. Takahashi (1960) illustrated the structural difference of the ventral lobe of tergite 9, called "lamina", between *Diogma glabrata megacauda*, and *Diogma glabrata glabrata*. This lobe's morphological variability was discussed and illustrated in detail by Gelhaus et al. (2007). They concluded that the two *D. glabrata* subspecies did not significantly differ in stable features and synonymised *D. megacauda* with *D. glabrata*. After morphological comparisons of the Japanese specimens with the West Palearctic specimens, our conclusion is the same. Only the body colouration shows slight differences between the two groups, however, colour variation is common among different populations of Cylindrotominae species. In this study, the European specimens are found to be genetically separated from the Japanese specimens, and the *D. caudata* sequences joined the Finnish *D. glabrata* clade. Additional sequences are needed for both *Diogma* species, from different areas of their distribution ranges, to resolve this genetic contradiction.

Diogma dmitrii Paramonov, 2005

Figs 17, 18

Non-type material examined. Russia • 1 ♂; Krasnodar Krai [Republic of Adygea, Maykopsky District], Khamyshki, Lagonaki Plateau; 44.009°N, 39.994°E; alt. 1700 m; 11 Jun. 2012; N.E. Vikhrev leg.; CKLP. • 1 ♀; Krasnodar Krai, Apsheronsky Dis-

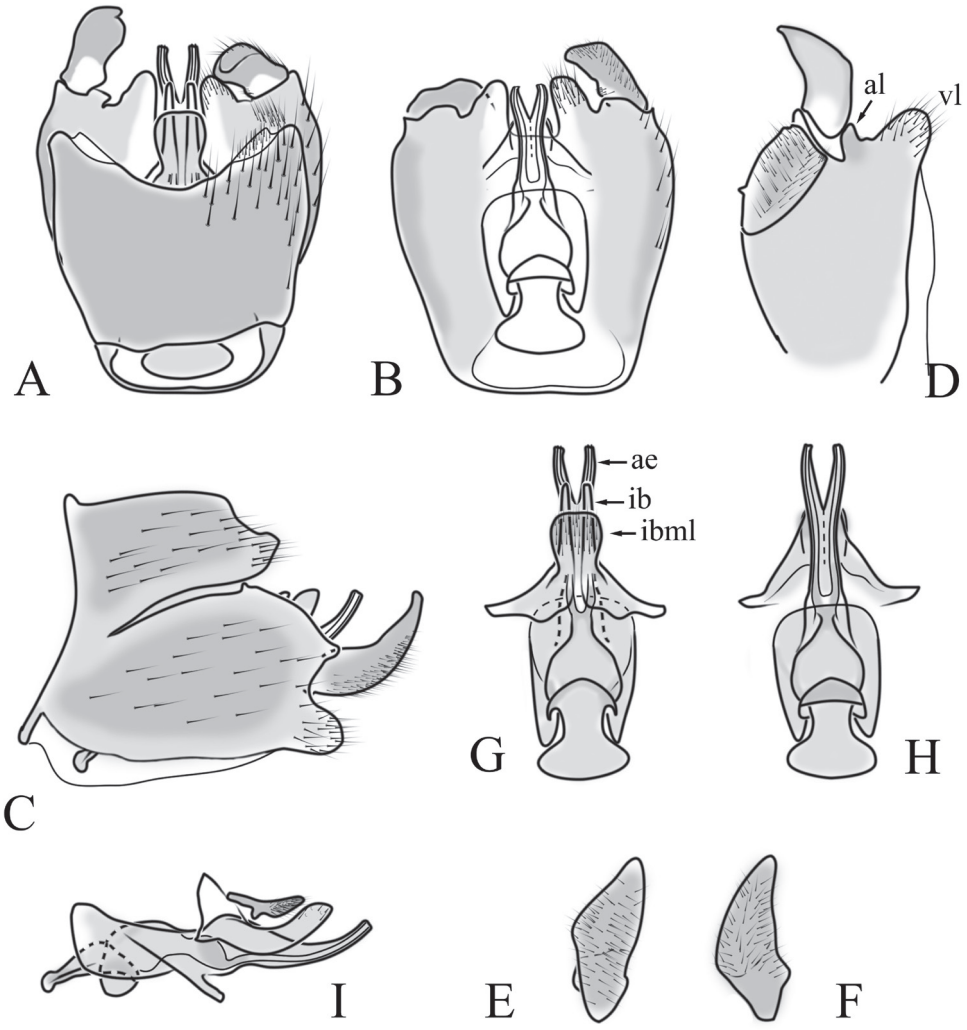

Figure 17. Male genital structures of *Diogma dmitrii* Paramonov, 2005 **A** terminalia, dorsal view **B** terminalia, ventral view **C** terminalia, lateral view **D** gonocoxite and gonostylus, inner lateral view **E** shape of the gonostylus, caudal view **F** shape of the gonostylus, inner dorsal view **G** aedeagus complex, dorsal view **H** aedeagus complex, ventral view **I** aedeagus complex,

trict, Mezmay Settlement, Kamyshanova polyana, Mezmaika River; 44.16989°N, 40.05180°E; alt. 1200 m; 13 Jun. 2004; N.M. Paramonov leg.; CKLP.

Supplementary description. Male terminalia: Medium sized and relatively simple, directed caudally. Tergite 9 fused with gonocoxite (Fig. 17C). Tergite 9 posterior margin convex in dorsal view (Fig. 17A), lateral lobe very small, triangular, ~ 1/4 ×total length of tergite 9 in lateral view (Fig. 17C); covered with relative long setae; posterior margin of tergite 9 with subhyaline, ventrally directed plate, next to lateral

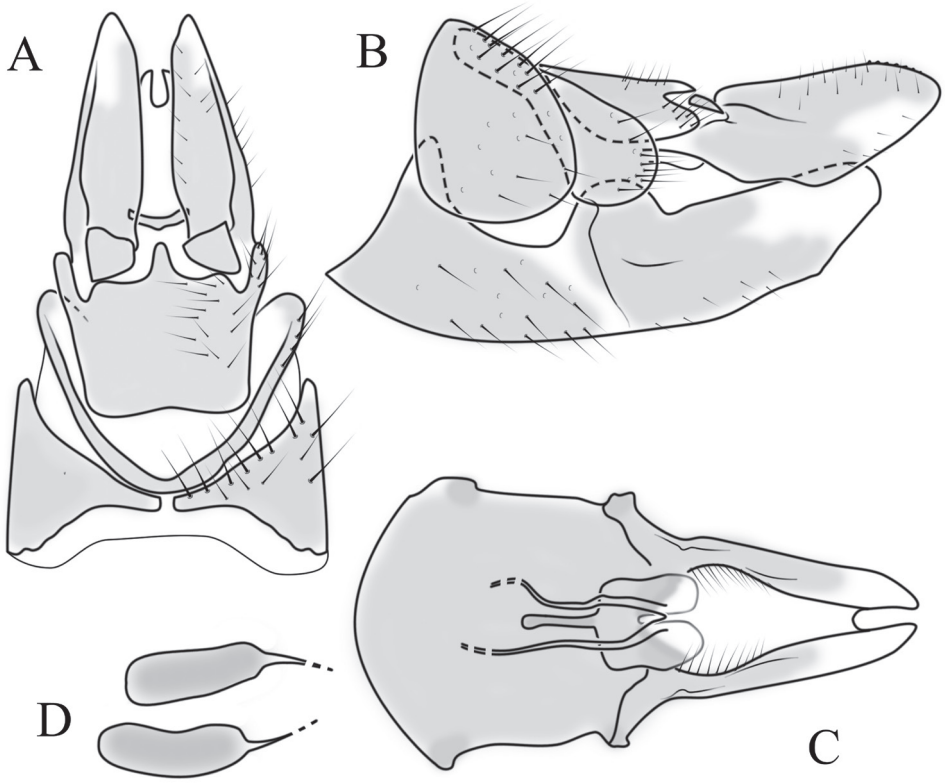

Figure 18. Female genital structures of *Diogma dmitrii* Paramonov, 2005 **A** Terminalia, dorsal view **B** terminalia, lateral view **C** sternite 8, hypogynial valve, genital fork, and sperm ducts, inner dorsal view **D** Spermathecae.

lobe; shape approximately triangular, covered with short pale setae (Fig. 17A). Sternite 9 fused with tergite 9 and gonocoxites, present as a narrow but continuous ring (Fig. 17A–C). Gonocoxite longer than tergite 9 in lateral view. Ventral lobe of gonocoxite well visible, without deep separation from gonocoxite (as in *D. caudata* and *D. glabrata*); inner half pale, partly membranous, covered by long pale hairs (Fig. 17B); apical lobe very small, mostly bare; inner part of gonocoxite forming a plate with hairs on all surface (Fig. 17D). Membranous area between gonocoxites reach base of ventral lobe (Fig. 17B). Gonostylus simple, without lobe in inner side; claw-like in lateral view (Fig. 17D); widened in middle length in caudal view (see Fig. 17E, F from different angles), with small, rounded bulge in inner ventral base (Fig. 17E). Sperm pump and ejaculatory apodeme large, partly covered by paramere in lateral view (Fig. 17I). Dorsal lobe between interbases dorso-ventrally flattened, posterior margin almost straight, covered by dense short hairs (Fig. 17G, I); interbase simple, with a few hairs, curved dorsally, without ventral projection, (Fig. 17I). Aedeagus bifid, branches short, slightly curved dorsally; base wide, evenly narrowing to tip in lateral view (Fig. 17I).

Female terminalia: Brown, tip of cercus and hypopygial valve yellowish brown. Tergite 8 separated at middle by membranous area (Fig. 18A). Tergite 8 larger than tergite 9 in lateral view (Fig. 18B). Ventral corner of tergite 9 not rugged, with few hairs (Fig. 18B). Triangular sclerite separated from tip of tergite 10, but close situated (Fig. 18A). Lateral lobes of tergite 10 finger-like with few long hairs (Fig. 18A). Cercus and hypogynial valve simple, wide, blade-shaped, tips rounded (Fig. 18B). Dorsal apical surface of cercus rough, formed by few, blunt pyramid teeth (Fig. 18B). Sternite 8 simple, without transverse creases (Fig. 18B, C). Two very large, elongated spermathecae present with duct almost straight (Fig. 18D). Two sperm ducts simple, without any clear markings, genital fork with a rod-shaped median part, posterior part pale (Fig. 18C).

Distribution. Russia: North Caucasus (Krasnodar Krai, Karachay-Cherkessia Republic); Georgia, Turkey (Asiatic part: Manisa, Rize, Samsun, Trabzon) (Oosterbroek 2021).

Liogma brevipecten Alexander, 1932

Figs 4E, 5E, 19, 20, 21, 22A

Liogma brevipecten in Alexander 1932: 110–111: original descriptions; Ishida 1955: 75: distribution; Takahashi 1960: 84–85: distribution, additional description, faunistic records, illustration; Sidorenko 1999: 68–70: identification key, illustration, distribution; Nakamura 2001: 23–29: identification key, illustration, distribution, faunistic records; Paramonov 2006: 888–889: identification key; Nakamura 2014: 54: distribution; Imada 2020: biology and ecology of larvae.

Non-type material examined. Japan • 1 ♂, 1 ♀; Aomori, Towada, Okuse, Tsutanuma Path; 40.59084°N, 140.95705°E; alt. 468 m; 23 May. 2014; • same locality; 1 Jun. 2014; D. Kato leg.; BLKU. • 1 ♂; Ehime, Kumakogen, small valley; 33.60489°N, 132.85584°E; alt. 580 m; 19 May. 2019; L.-P. Kolcsár leg.; CKLP. • 1 ♂; Ehime, Kumakogen, headwaters, stream; 33.56476°N, 132.93501°E; alt. 1387 m; 17 Jun. 2019; L.-P. Kolcsár leg.; CKLP. • 1 ♂; Ehime, Saijo, spring and mosses rocks; 33.75504°N, 133.15377°E; alt. 1480 m; 5 Jun. 2019; • 2 ♂; same locality; 16 Jun. 2019; L.-P. Kolcsár leg.; CKLP. • 1 ♂; Ehime, Wakayama, small waterfall; 33.71591°N, 133.10839°E; alt. 930 m; 18 May. 2019; L.-P. Kolcsár leg.; CKLP. • 1 ♀; Fukuoka, Soeda, rocky streem and moss covered cliff; 33.48309°N, 130.93289°E; alt. 900 m; 21 May. 2019; L.-P. Kolcsár leg.; CKLP. • 1 ♂; Fukui, Fukui, Mt. Ifuri; 35.96928°N, 136.4459°E; alt. 387 m; larva collected: 22 Apr. 2015, emerged: 3 May. 2015; Y. Imada leg.; CYI. • 1 ♂; Fukui, Ono, Aburazaka-touge; 35.87298°N, 136.82297°E; alt. 735 m; larva collected: 28 Apr. 2012, emerged: 3 May. 2012; M. Kato leg.; CYI. • 1 ♂; Hiroshima, Akiota, Yokogo; 34.59419°N, 132.14497°E; alt. 892 m; 18 May. 2015; D. Kato leg.; BLKU. • 1 ♂; Hokkaido, Chitose, Komukara-toge, small stream; 42.837°N, 141.7505°E; alt. 55 m; 14 Jun. 2015 – 27 Jun. 2015; N. Kuhara leg.; Malaise-trap; EUMJ. • 1 ♂; Hok-

kaido, Kamikawa, Aizankei; 43.73521°N, 142.7923°E; alt. 762 m; 25 Aug. 2015; M. Kato leg.; CYI. • 1 ♂, 1 ♀; Hokkaido, Sapporo, Minami-ku, Jozankei, trail of Mt. Sapporo; 42.92392°N, 141.17688°E; alt. 450–860 m; 23 Jun. 2014; D. Kato leg.; BLKU. • 1 ♀; Iwate, Hachimantai, Matsuoyoriki; 39.89958°N, 140.89155°E; alt. 1200 m; larva collected: 14 Jun. 2014, emerged: 4 Jul. 2014; Y. Imada leg.; CYI. • 2 ♂; Iwate, Hachimantai, Toshiti Spa; 39.94253°N, 140.86804°E; alt. 1344 m; 3 Aug. 2013; • 4 ♂; same locality; 15 Jul. 2014; • 1 ♀; same locality; 5 Aug. 2014; D. Kato leg.; BLKU. • 1 ♂; Kyoto, Kyoto, Kibune; 35.13681°N, 135.76622°E; alt. 458 m; larva collected: 3 Apr. 2016, emerged: 1 May. 2016; • 1 ♀; same locality; larva collected: 13 May. 2016, emerged: 20 May. 2016; Y. Imada leg.; CYI. • 1 ♂; Nagano, Ichiromata, Mt. Jonen; 36.3°N, 137.76°E; 27 Jul. 1951; Inoue leg.; USNM. • 1 ♂; Nagano, Iida, Jabora-rindo; 35.44865°N, 138.00905°E; alt. 1337 m; larva collected: 27 Apr. 2014, emerged: 6 May. 2014; M. Kato leg.; CYI. • 1 ♂; Nagano, Iida, Shirabiso-touge; 35.43801°N, 138.03053°E; alt. 1830 m; larva collected: 19 Oct. 2015, emerged: 18 Dec. 2015; Y. Imada leg.; CYI. • 1 ♀; Nagano, Sakae, Akiyama-gou; 36.85447°N, 138.64803°E; alt. 1125 m; larva collected: 3 May. 2015, emerged: 14 Apr. 2015; Y. Imada leg.; CYI. • 1 ♀; Shizuoka, Shizuoka, Tsudono; 35.08929°N, 138.35618°E; alt. 175 m; 3 May. 2015; M. Kato leg.; CYI. • 1 ♂; Tokushima, Naka, Mt. Takashiro, Kisawamura; 33.90468°N, 134.23315°E; alt. 1300 m; 16 May. 2016; M. Kato leg.; CYI. • 1 ♂; Tokushima, Yamagata, Yonezawa, Shirabu-onsen; 37.77646°N, 140.11964°E; alt. 888 m; larva collected: 19 Oct. 2013, emerged: 25 Apr. 2014; M. Kato leg.; CYI. • 1 ♀; Yamanashi, Koshu, Enzankamihagihara, Kaminichikawa Pass; 35.7316°N, 138.8321°E; alt. 1580 m; 8 Jul. 2014; D. Kato leg.; BLKU.

Redescription. Head. Black with greyish pubescence (Fig. 19B–E). Rostrum short without nasus, but with patch of hairs (Fig. 19B, E); rostrum and mouthparts dark brown to black. Palpus pale brown to black, five segmented; first two segments always darker (Fig. 19E, D); last segment 1.3–1.5 × longer than penultimate. Scape cylindrical, 2 × as long as pedicel, and usually darker than pedicel; pedicel ovate; flagellum 14 segmented, gradually darkening to tip (Figs 4E, 19D, E); flagellomeres expanded ventrally in both sexes, more prominent in male (Figs 4E, 19D); only flagellomeres 2 or 3–9 extended evidently ventrally in female (Figs 4E, 19E), remaining segments elongated; last flagellomere cylindrical in both sexes; extended flagellomeres covered with dense whitish sensilla, denser on ventral side; six verticels on each flagellomere, two long verticels on dorsal surface, two verticels in lateral surface, two shorter on ventral side; first flagellomeres always bearing additional 2–4 verticels; second to sixth flagellomeres sometimes with additional one or two shorter verticels on dorsal surface.

Thorax. Uniformly black with weak greyish pruinosity, except pleural area, base of wing, and halter which yellowish especially in living specimens (Fig. 19B). Scatter pale short hairs on mesonotum present, forming two lines. Anterior 1/3–1/2 of mediotergite and anterior half of pleurotergite with creases and rugoses (Fig. 19B). Trochanter yellow; femur gradually darkening apically, basal part yellowish, apically dark brown; tibia brown to dark brown; tarsus uniformly brown to black (Fig. 19A). Wing pale, tinged

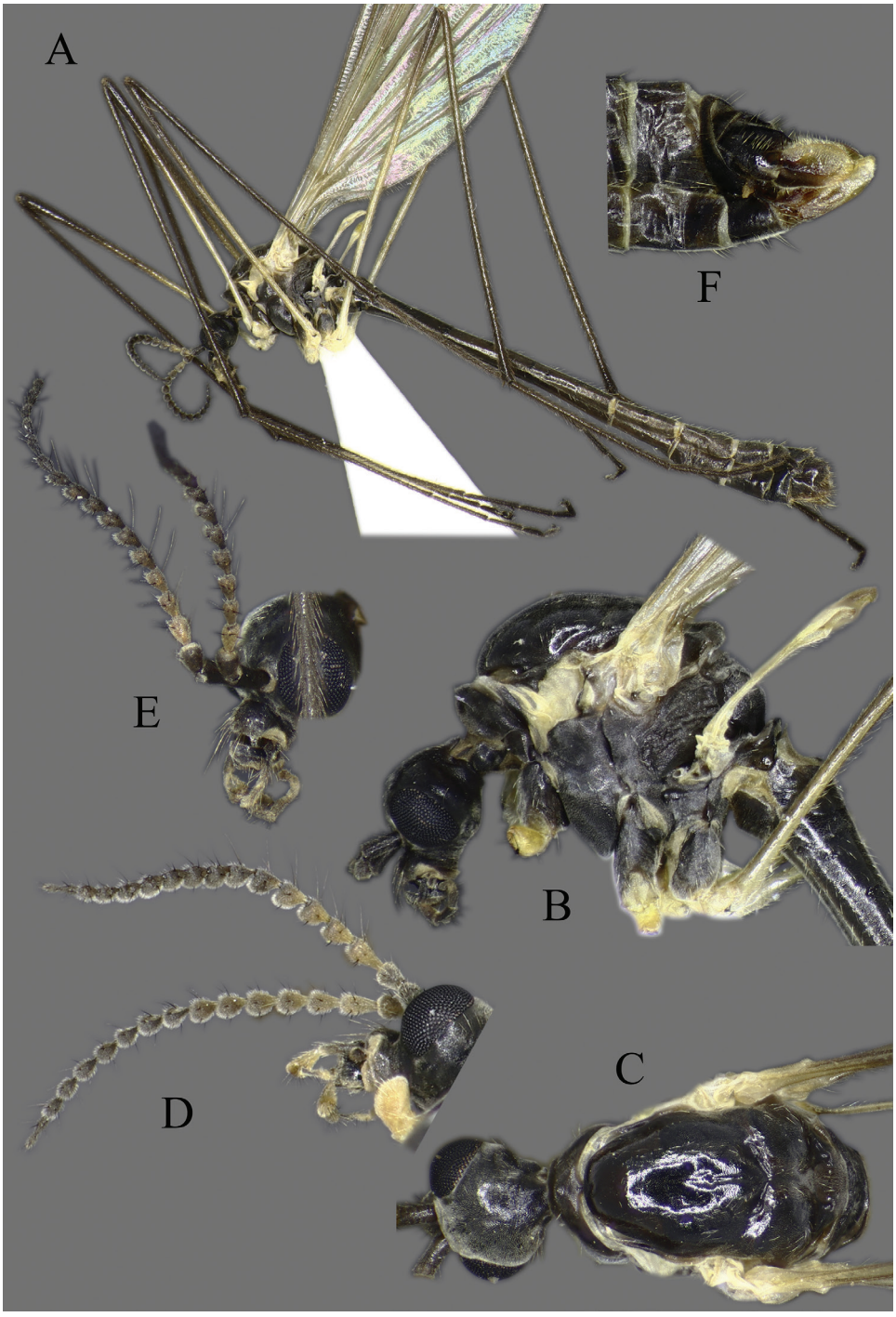

Figure 19. *Liogma brevipecten* Alexander, 1932 **A** habitus of male, lateral view (colouration of wings is artefact) **B** head and thorax, lateral view **C** head and thorax, dorsal view **D** antenna of male **E** head of female, lateral view **F** female terminalia lateral view.

with brown; pterostigma brown, well defined; veins brown; three branches of M reaching wing margin; M_1 at same level as M_{1+2}, cell a_2 less than 6 × longer than wide (Fig. 5E); membrane with interference patterns, visible with dark background (Fig. 19A).

Abdomen. Dark brown to black (Fig. 19A). Pleura yellowish especially in females and living specimen.

Male terminalia: Uniformly dark brown to black, relatively small, directed caudally (Fig. 19A). Tergite 9 fused with gonocoxite (Fig. 20C); caudal margin straight, without prominent outgrowth, only a small lateral lobe present at lateral corner (Fig. 20A, C). Sternite 9 membranous (Fig. 20B). Gonocoxite large, 1.5–1.6 × longer than tergite 9, with long ventral lobe (Fig. 20B, C); inner surface of gonocoxite simple, without lobe (Fig. 20A). Gonostylus simple, tapering to distal end. Aedeagal complex large, 1.2–1.3 × longer than gonocoxite (Fig. 20D–F); ejaculator apodeme and sperm pump large, together 1/2 × length of aedeagal complex, not covered by parameres in lateral view (Fig. 20F); tip of interbase finger-like, with round lobe dorsally in lateral view (Fig. 20F); interbase wide and rounded in dorsal view (Fig. 20D); dorsal lobe between interbases globular, membranous (Fig. 20D, F); aedeagus trifid, median branch slightly longer (Fig. 20G); sperm ducts branching from elongated portion of sperm pump, branching area dark (Fig. 20F).

Female terminalia: Brown to black, end of cercus and hypogynial valve yellowish (Fig. 19F). Tergite 8 three times larger than tergite 9 (Fig. 21B), not divided medially (Fig. 21A). Tergite 9 narrow band-shaped in lateral view (Fig. 21B). Triangular sclerite relatively large, 1/4 ×length of tergite 10; sclerite separated from tip of tergite 10; lateral lobe of tergite 10 medium sized, with few long hairs (Fig. 21A, B). Cercus and hypogynial valve broad, blade-like, tips rounded (Fig. 21B). Cercus on dorsal surface close to apical end with small notch; area before notch rough, with short and dense setae, and with few short sharp teeth (Fig. 21A, B); ventral margin of cercus before mid-length with notch (Fig. 21B). Common spermathecal duct present after genital opening; sperm ducts extended, inner wall rugose (Fig. 21C); three spermathecae laterally elongated, base of duct wide, curved, suddenly tapering suddenly (Fig. 21D).

Distribution. Japan (Honshu I and Kyushu I) and Russia (Far East: Sakhalin Oblast) (Oosterbroek 2021). First records from Japan: Hokkaido I and Shikoku I (Fig. 22A).

Comments. This species differs from the closely related *Liogma serraticornis* in details of the antennae, male and female terminalia, and colouration, though these are slight. Both sexes of this species can be separated from *L. serraticornis* based upon the first flagellomere length. It is always longer than the second flagellomere in *L. serraticornis* (Fig. 4F) and similar size in *L. brevipecten* (Fig. 4E). The ventral extensions of the flagellomeres of male *L. brevipecten* are relatively short and shout (Fig. 4E), while *L. serraticornis* has more elongated flagellomeres (Fig. 4F). The pedicel's colouration and wing venation characters mentioned by Takahashi (1960) were not useful for species separation here because these characters show high variability levels. The two species differ in details of male and female terminalia: the ventral lobe of the gonocoxite has several pale spine-like setae in *L. serraticornis* (Fig. 29B, C), whereas *L. brevipecten* is without these spine-like setae (Fig. 20B, C); the middle branch of the aedeagus is

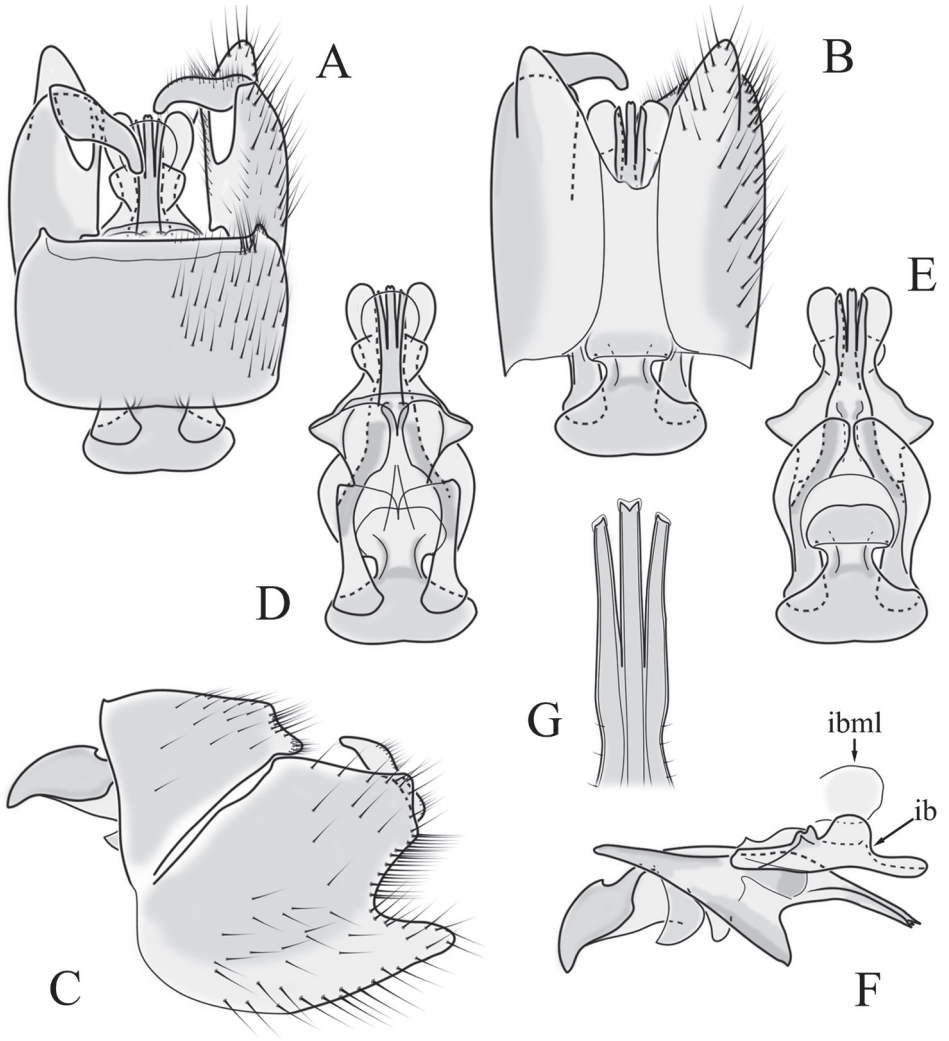

Figure 20. Male genital structures of Liogma brevipecten Alexander, 1932 **A** terminalia, dorsal view **B** terminalia, ventral view **C** terminalia, lateral view **D** aedeagus complex, dorsal view **E** aedeagus complex, ventral view **F** aedeagus complex, lateral view **G** tip of the aedeagus. Abbreviations: ib – interbase; ibml – interbase median lobe.

longer than the lateral ones in *L. brevipecten* (Fig. 20G) but shorter than the lateral branches in *L. serraticornis* (Fig. 29G). The female terminalia of *L. brevipecten* is narrow and long in dorsal view (Fig. 21C), but widens ventrally in *L. serraticornis* (Fig. 30C). In *L. serraticornis* the lateral lobes of tergite 10 are 2 × longer than wide (Fig. 30B), but only as long as wide in *L. brevipecten* (Fig. 21B). Inner genital structures also show differences among the species in the spermathecae shapes (see Figs 21D, 30D) and sperm ducts. The base of the sperm duct is readily discernible in *L. brevipecten* (Fig. 21C), while it is short or very poorly discernible in *L. serraticornis* (Fig. 30C); and the sperm

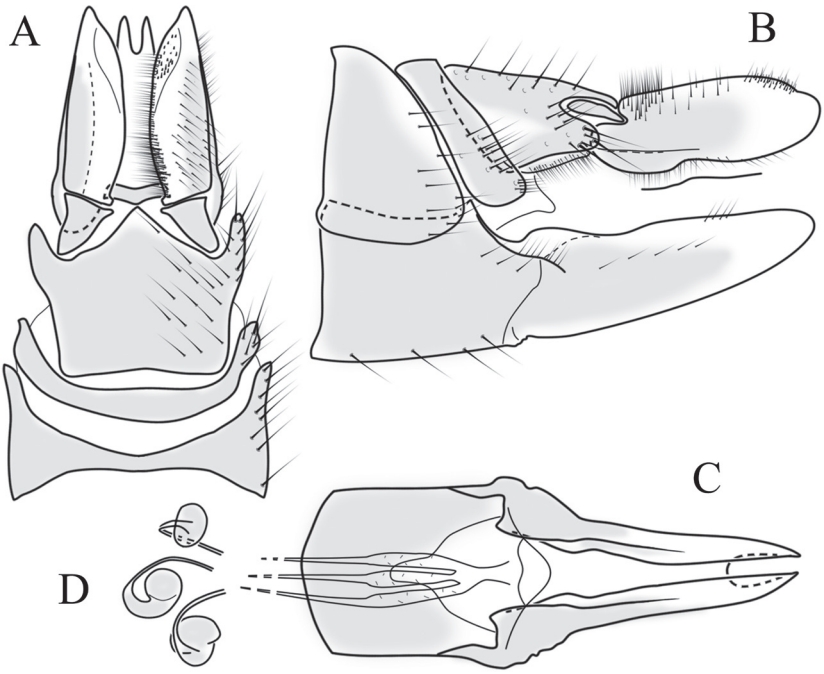

Figure 21. Female genital structures of *Liogma brevipecten* Alexander, 1932 **A** aerminalia, dorsal view **B** terminalia, lateral view **C** sternite 8, hypogynial valve, genital fork, and sperm ducts, inner dorsal view **D** spermathecae.

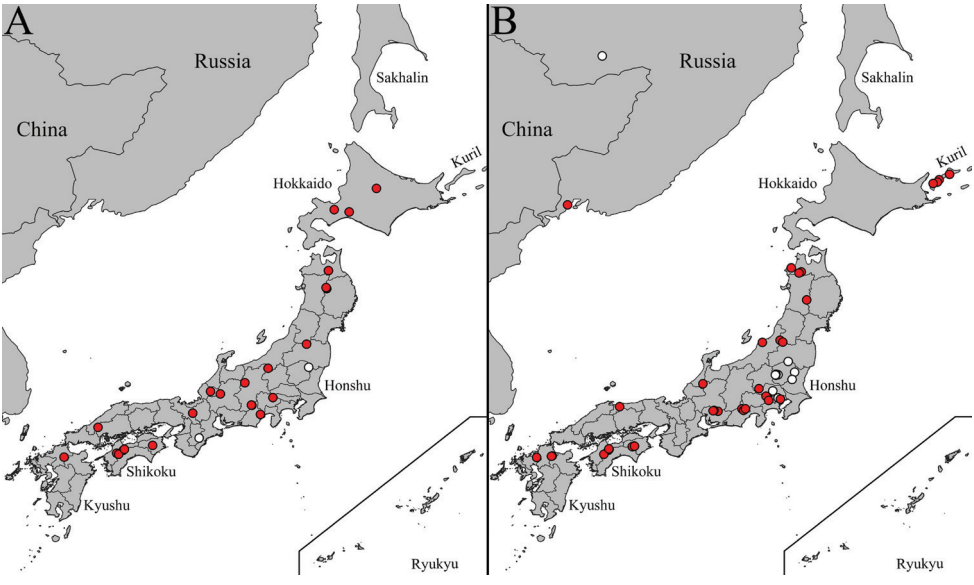

Figure 22. Occurrence data in Japan and surrounding areas of **A** *Liogma brevipecten* Alexander, 1932 **B** *Liogma mikado* (Alexander, 1919). Red dots indicate locations of investigated specimens, white dots indicate approximate locations of literature data.

ducts house three inflated areas the shape of golf tees in *L. serraticornis* (Fig. 30C), but these are much less well developed in *L. brevipecten* (Fig. 21C).

Liogma mikado (Alexander, 1919)

Figs 4D, 5D, 22B, 23, 24, 25

Phalacrocera mikado in Alexander 1919: 346: original description; Alexander 1928: 10: distribution, illustration; Alexander 1953a: 57: faunistic record; Ishida 1955: 77: distribution.

Liogma mikado in Takahashi 1960: 85–90: new combination, distribution, faunistic records, larva and pupa description, illustrations; Sidorenko 1999: 68–70: identification key, illustration, distribution; Nakamura 2001: 23–29: identification key, illustration, distribution, faunistic records; Paramonov 2004b: 69: faunistic record; Paramonov 2006: 888–889: identification key, distribution; Nakamura 2014: 54: distribution; Kato and Suzuki 2017: 16: distribution; Paramonov 2019: 120: faunistic data; Imada 2020: biology and ecology of larvae; Kim and Bae 2020: distribution.

Type material examined. *Phalacrocera mikado* Alexander: ***ALLOTYPE*** ♂: • **Japan,** Tokyo, Tokyo metropolis, 1919.04.?, leg. R. Takahashi (USNM).

Non-type material examined. Japan • 2 ♀; Aichi, Toyota, Kawashimo, triburary of Yahagi River; 35.20376°N, 137.3012°E; alt. 140 m; 4 May. 2014; D. Kato leg.; BLKU. • 1 ♀; Aichi, Seto, Iwaya-cho, near Iwayada Park; 35.23957°N, 137.15084°E; alt. 300 m; 4 May. 2016; D. Kato leg.; BLKU. • 1 ♀; Aichi, Seto, Minamiazuma; 35.223213°N, 137.1131°E; alt. 150 m; 5 May. 2014; D. Kato leg.; BLKU. • 3 ♀; Aomori, Hirosaki, Koguriyama, Inekari River; 40.53658°N, 140.48701°E; alt. 170 m; 28 May 2013; • 1 ♂; same locality; 31 May. 2013; D. Kato leg.; BLKU. • 1 ♂; Aomori, Fukaura, Mt. Takanio; 40.68993°N, 140.10285°E; alt. 140 m; 11 May. 2014; D. Kato leg.; BLKU. • 1 ♂; Aomori, Hirosaki, Soma Path; 40.49479°N, 140.40231°E; alt. 392 m; 31 May. 2013; D. Kato leg.; BLKU. • Ehime, Kumakogen, River Myogadani springs, 1275 m, 33.55808°N, 132.93805°E, 2019.05.19, 2 ♂ 1 ♀, L.-P. Kolcsár leg.; CKLP. • 5 ♂, 11 ♀; Ehime, Wakayama, Mount Ishizuchi; 33.76491°N, 133.12948°E; alt. 1600 m; 5 Jul. 2019; L.-P. Kolcsár leg.; CKLP. • 1 ♂; Ehime, Wakayama, small waterfall and stream; 33.74519°N, 133.13714°E; alt. 1305 m; 18 May. 2019; L.-P. Kolcsár leg.; CKLP. • 2 ♀; Ehime, Wakayama, small waterfall; 33.71591°N, 133.10839°E; alt. 930 m; 18 May. 2019; L.-P. Kolcsár leg.; CKLP. • 2 ♂; Fukuoka, Fukuoka, Sawara-ku, Itaya, Mt. Sefuri; 33.43811°N, 130.36673°E; alt. 970 m; 2 May. 2015; • 1 ♂; same locality; 13 May. 2015; D. Kato leg.; BLKU. • 1 ♂; Fukuoka, Miyako, Saigawa-Hobashira, Notoge Pass; 33.49565°N, 130.96156°E; alt. 740 m; 22 Apr. 2016; D. Kato leg.; BLKU. • 1 ♀; Fukuoka, Soeda, rocky streem and moss covered cliff; 33.48309°N, 130.93289°E; alt. 900 m; 21 May. 2019; L.-P. Kolcsár leg.; CKLP. • 2 ♂; Ishikawa, Hakusan, near to Hakusan National Park;

36.25869°N, 136.72558°E; alt. 678 m; 27 May. 2015; M. Kato leg.; CYI. • 1 ♀; Iwate, Nishiwaga, Mahirudake; 39.46511°N, 140.69365°E; alt. 900 m; 19 Jun. 2015; Y. Imada leg.; CYI. • 1 ♂; Niigata, Echigo, Sugatani, Kitakanbara; 37.84°N, 139°E; 8 May. 1955; H. Koike leg.; USNM. • 1 ♀; Saitama, Ogano, Mt. Futago; 36.06994°N, 138.86753°E; alt. 942 m; larva collected: 28 Nov. 2014, emerged 15 Dec. 2014; M. Kato leg.; CYI. • 1 ♀; Shizuoka, Aoi-ku, Umegashima, Akamizu; 35.27455°N, 138.32731°E; alt. 680 m; larva collected: 8 Jan. 2007, emerged: 22 Feb. 2007; leg. Y. Sato EUMJ. • 9 ♂; Shizuoka, Shizuoka, Hatanagi; 35.2976°N, 138.21557°E; alt. 828 m; 12 May. 2013; M. Kato leg.; CYI. • 1 ♂; Shizuoka, Shizuoka, Abenoootaki; 35.30031°N, 138.35084°E; alt. 930 m; larva collected: 15 Jan. 2014, emerged: 19 Apr. 2014; M. Kato leg.; CYI. • 8 ♂, 1 ♀; Shizuoka, Ikawa-touge; 35.24094°N, 138.28156°E; alt. 1471 m; 10 May. 2015; M. Kato / Y. Imada leg.; CYI. • 1 ♂; Tokushima, Awa, Mt. Tsurugi; 33.87°N, 134.11°E; 30 May. 1950; Issiki-Ito leg.; USNM. • 1 ♂; Tokushima, Mima, Koyadaira; 33.87543°N, 134.09571°E; alt. 1340 m; 30 Apr. 2016; D. Kato leg.; BLKU. • 1 ♂; Tokushima, Miyoshi, Higashiiya-Sugeoi, near Nagoro Dam; 33.85182°N, 134.0234°E; 29 Apr. 2016; D. Kato leg.; BLKU. • 2 ♂; Tokyo, Mt. Mitake; 35.78°N, 139.14°E; 10 May. 1931; B. Oda leg.; USNM. • 1 sex unknown; Tokyo, Mt. Takao; 35.62°N, 139.24°E; alt. 300–600 m; 7 May. 1922; Esaki leg.; USNM. • 1 ♀; Tokyo, Tokyo, Akiruno, rocky river and stream; 35.74766°N, 139.18466°E; alt. 288 m; 11 May. 2019; L.-P. Kolcsár leg.; CKLP. • 1 ♂; Tottori, Mt. Daisen; 35.38°N, 133.54°E; 7 Jun. 1930; Hibi leg.; USNM. • 1 ♂; Yamagata, Iide, Mt. Iide; 37.85122°N, 139.78064°E, alt. 600 m; 23 May. 2015; Y. Imada leg.; CYI. • 2 ♂, 1 ♀; Yamagata, Oguni, Nukumidaira; 37.92293°N, 139.67546°E; alt. 433 m; larvae collected: 9 Nov. 2014, emerged: 22 Apr. 2014; Y. Imada leg.; CYI. **Russia** • Primorsky Krai, Khasansky District, Primorsky Settlement, Zolotistyy [Golden] Stream; 43.10075°N, 131.54862°E; alt. 62 m; 10 Jun. 2007 – 11 Jun. 2007; N.M. Paramonov leg.; CKLP. • 2 ♂; Sakhalin Oblast, Yuzhno-Kurilsk Urban Settlement, Kuril/Kunashir Island, near Lagunnoe Lake; 44.0623°N, 145.759°E; alt. 20 m; 11 Jul. 1954 – 12 Jul. 1954; leg. N.A. Violovich ZIN. • 1 ♂; Sakhalin Oblast, Kunashir Island, Mendeleevo Settlement; 43.971°N, 145.694°E; alt. 220 m; 28 Jun. 1973; I.M. Kerzhner leg.; ZIN. • 1 ♀; Sakhalin Oblast, Kunashir Island, Alekhino Settlement [uninhabited]; 43.91°N, 145.52°E; alt. 5 m, 29 Jun. 1962; G.O. Krivoluckaja leg.; ZIN. • 2 ♂; Sakhalin Oblast, Kunashir Island, the mouth of the Tjatina River; 44.2711°N, 146.1583°E; alt. 15 m; 21 Jul. 2014; Y.N. Sundukov leg.; ZIN.

Redescription. Head. Dark brown to black, with greyish pubescence (Fig. 23B–D). Rostrum short without nasus. Mouth parts pale brown to brown. Palpus brown to dark brown, five segmented; last segment 1.2–1.4 × longer than penultimate (Fig. 23B, D). Scape cylindrical, 1.6–1.8 × longer than pedicel; pedicel ovate; pedicel brown, scape yellow to brown (Figs 4D, 23B, D); flagellum 14-segmented, pale brown to brown, monochrome or gradually darkening from base to tip. Flagellar segments simple, cylindrical in both sexes, not expanded ventrally; all male flagellomeres and 2–8 female flagellomeres covered with sparse whitish setae/sensilla; sensilla slightly denser

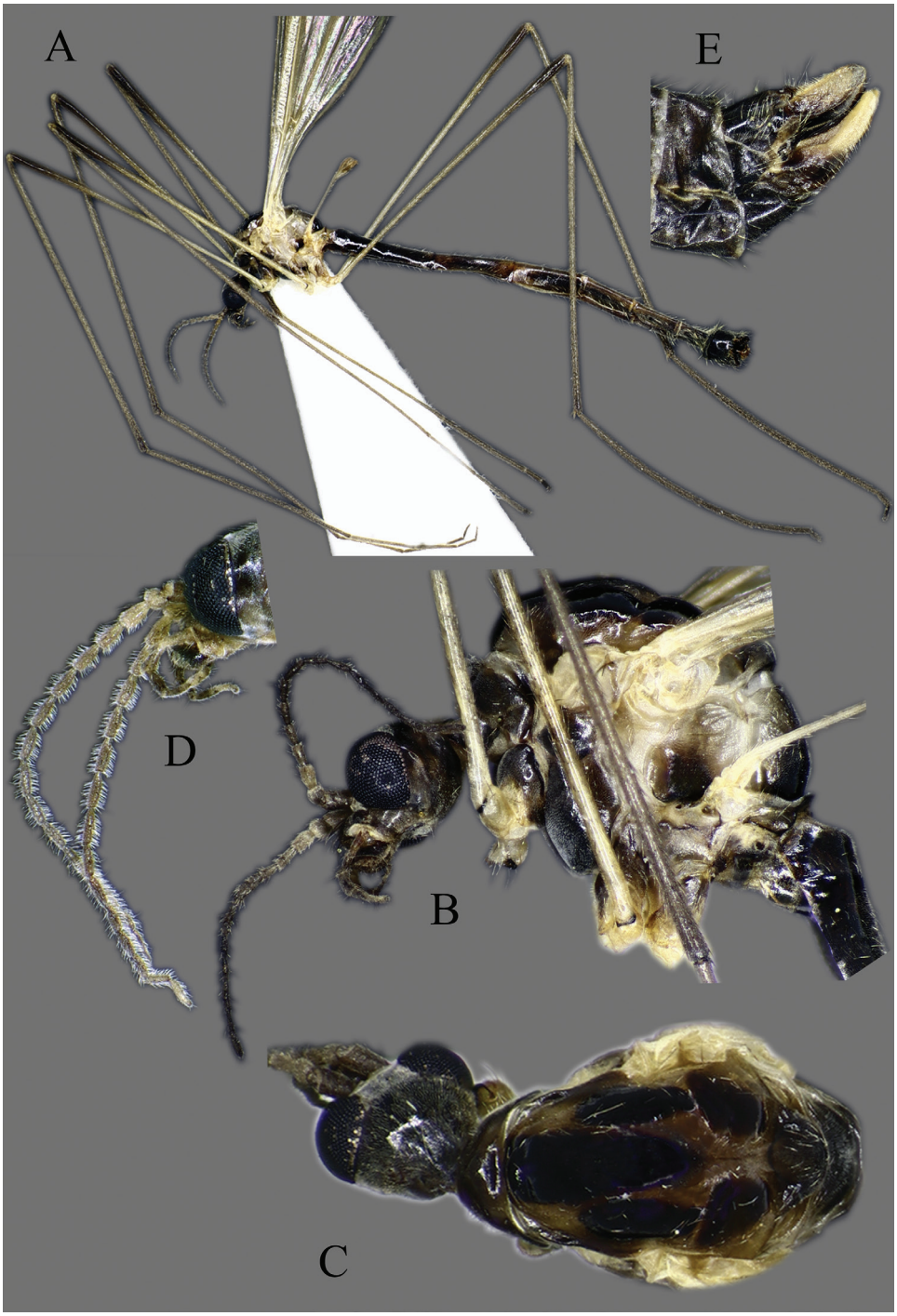

Figure 23. *Liogma mikado* (Alexander, 1919) **A** habitus of male, lateral view (colouration of wings is artefact) **B** head and thorax of female, lateral view **C** head and thorax, dorsal view **D** head of male, dorsal view **E** female terminalia lateral view.

in ventral side; verticels less prominent, 4–6 verticels not showing clear arrangement (Figs 4D, 23B, D).

Thorax. General colour shiny dark brown to black, with yellowish area in lateral side. Pronotum dark brown to black. Anterior part of mesonotum brown with black stripes or patches, usually forming three longitudinal, black markings on presutural area of scutum, and two drop-shaped black markings on postsutural area of scutum (Fig. 23C) or one large marking; black parts bare and shiny; paler parts with pubescence and with several long yellow hairs, forming longitudinal lines (Fig 23C). Dorsal pleural area, base of wing, anepimeron, and base of halter yellowish. Coxa black, ventrally paler (Fig. 23B); trochanter yellow; femur gradually darkening distally, basal part yellowish, apical part dark brown to black; tibia and tarsus dark brown. Wing hyaline; veins brown; pterostigma pale; three branches of M reaching wing margin, M_1 at same level as M_{1+2}, cell a_2 narrow, > 8 × longer than wide (Fig. 5D); membrane with interference patterns, visible with dark background (Fig. 23A). Halter stem pale brown, knob brown.

Abdomen. Black, without any distinct patterns (Fig. 23A).

Male terminalia: Relatively small, uniformly black, directed caudally (Fig. 23A). Tergite 9 fused with gonocoxite and sternite 9 (Fig. 24C); tergite 9 with median lobe, with notch at middle (Fig. 24A); lateral lobes of tergite 9 not prominent. Sternite 9 reduced to narrow band (Fig. 24B, C). Gonocoxite relatively large, 1.2–1.4 × longer than tergite 9, in lateral view (Fig. 24C); without any distinct lobes (Fig. 24B, C); inner side of gonocoxite membranous; small round sclerotised patch on membranous area between gonocoxites present (Fig. 24B), triangular in lateral view (Fig. 24C, F); holding base of aedeagal complex if it moved dorsally. Gonostylus with a strongly sclerotised, claw-like outgrowth; tip of gonostylus finger-like (Fig. 24A, C). Aedeagus complex as long as gonocoxite and sternite 9 together; sperm pump and ejaculatory apodeme, partly covered by parameres (Fig. 24F); interbase simple L-shaped, both in lateral and dorsal/ventral views (Fig. 24D–F); posterior part blade-like, with a small notch on dorsal side, in lateral view (Fig. 24F); aedeagus widened and curved dorsally at right angle in midlength, covered with prominent spines on ventral and lateral sides; membranous area on ventral side behind ventral spines, make flexible the aedeagus and able to straighten, probably during copulation (Fig. 24D, F); aedeagus with apical branches short, directed caudally; median branch slightly longer and wider than lateral ones (Fig. 24D, F).

Female terminalia: Black, tips of cercus and hypopygial valve yellowish (Fig. 23E). Tergite 8, 2 × larger than tergite 9 in lateral view (Fig. 25B); not divided at middle (Fig. 25A). Caudal margin of tergite 9 straight in lateral view (Fig. 25B). Lateral lobe of tergite 10 finger-like, 3 × longer than wide, well separated from tergite 10 (Fig. 25A); triangular sclerite large, separated from tergite 10 (Fig. 25A). Cercus and hypogynial valve blade-like, relative narrow compared to other cylindrotomines (Fig. 25B); rough surface on dorsal tip of cercus hardly recognisable, only a few small pyramid teeth present. Genital fork large, heavily sclerotised plate; common sperm duct after genital opening relatively short, hardly recognisable; sperm ducts carrot-shaped; wall of sperm wrinkled (Fig 25C); three round spermathecae present, diameter ~ 1/3–1/2 × width of genital fork (Fig. 25D).

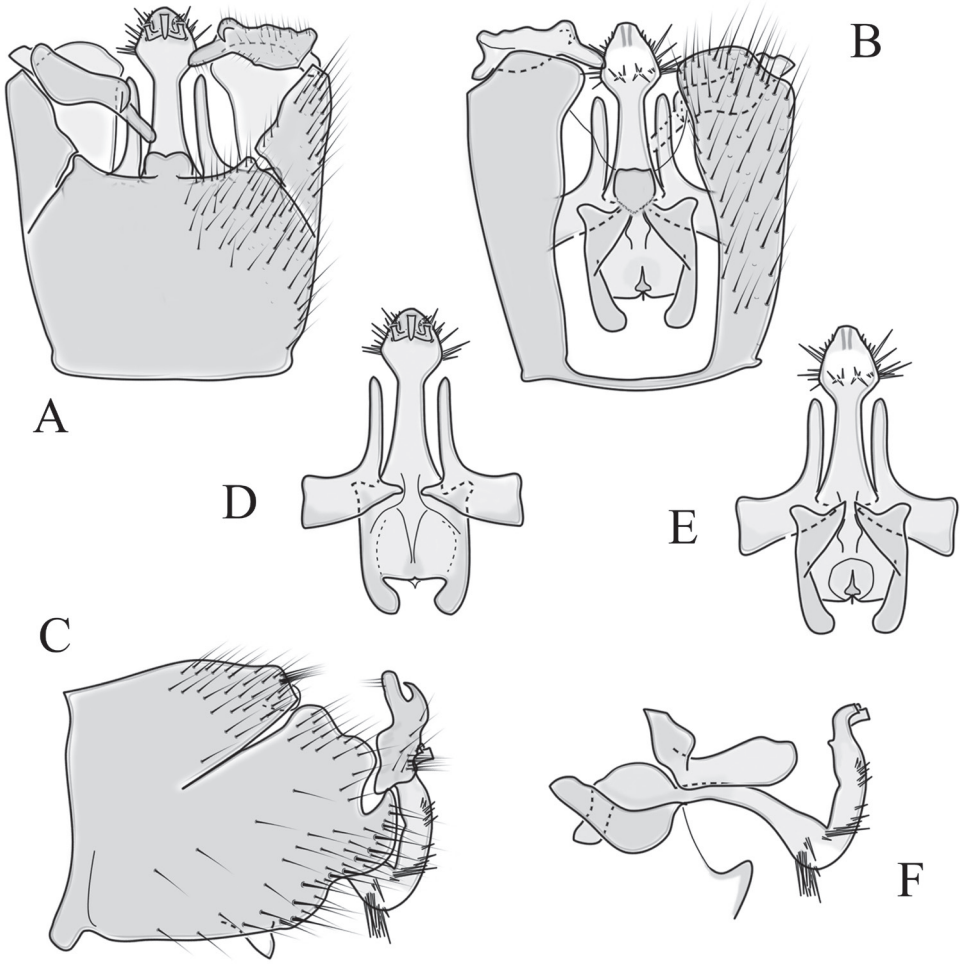

Figure 24. Male genital structures of *Liogma mikado* (Alexander, 1919) **A** terminalia, dorsal view **B** terminalia, ventral view **C** terminalia, lateral view **D** aedeagus complex, dorsal view **E** aedeagus complex, ventral view **F** aedeagus complex, lateral view.

Distribution. South Korea, Japan (Honshu I and Shikoku I), and Russia (Jewish Autonomous Oblast, Sakhalin Oblast (Kuril Is: Kunashir I) (Oosterbroek 2021). First records from Japan: Kyushu I (Fig. 22B).

Comments. As with other Cylindrotominae species that have simple antennae and three M vein branches, this species was also originally described as *Phalacrocera* (Alexander 1919). Later Takahashi (1960) moved this species to the *Liogma* genus based on the morphological similarity of the immature stages with *Liogma nodicornis* (Osten Sacken, 1865). However, *L. mikado* is a morphologically and genetically quite distinct species from the other *Liogma* species, and the exact phylogenetic position remains unclear.

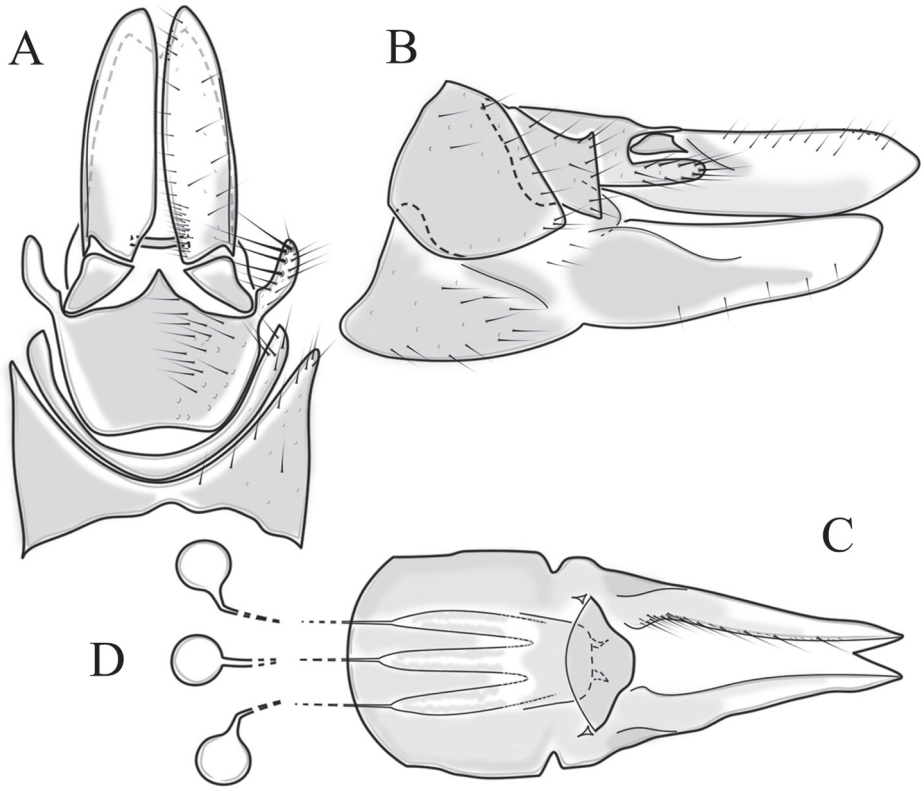

Figure 25. Female genital structures of *Liogma mikado* (Alexander, 1919) **A** terminalia, dorsal view **B** terminalia, lateral view **C** sternite 8, hypogynial valve, genital fork, and sperm ducts, inner dorsal view **D** spermathecae.

***Liogma nodicornis* (Osten Sacken, 1865)**
Figs 26, 27

Liogma flaveola Alexander, 1919.

Non-type material examined. Canada • 1 ♀; Manitoba, Winnipeg, Birds Hill Park, cedar bog; 50.03°N, 96.91° W; alt. 250 m; 20 Jun. 2003; F. Brodo leg.; CKLP. • 1 ♂, 2 ♀; Ontario, Ottawa, Stony Swamp; 45.3°N, 75.83° W; alt. 115 m; 7 Jun. 2011; • 1 ♂; same locality; 30 May. 2011; F. Brodo leg.; CKLP. **Usa** • 1 ♂; New Hampshire, Twin mountains, vochtig loofbos; 44.218°N, 71.415° W; alt. 600 m; 20 Jun. 1982; P. Oosterbroek / I. Tangelder leg.; CKLP. • 1 ♂; • 1 ♂; Michigan, Delta Co., 11 Jun. 1860; R. and K. Dreisbach leg; « Green label under the geographical label: *Liogma nodicornis* (O.S.). NOTE genotype of *Liogma* ».

Supplementary description. Male terminalia directed caudally. Tergite 9 fused with gonocoxite at base (Fig. 26C); caudal margin of tergite 9 with prominent lat-

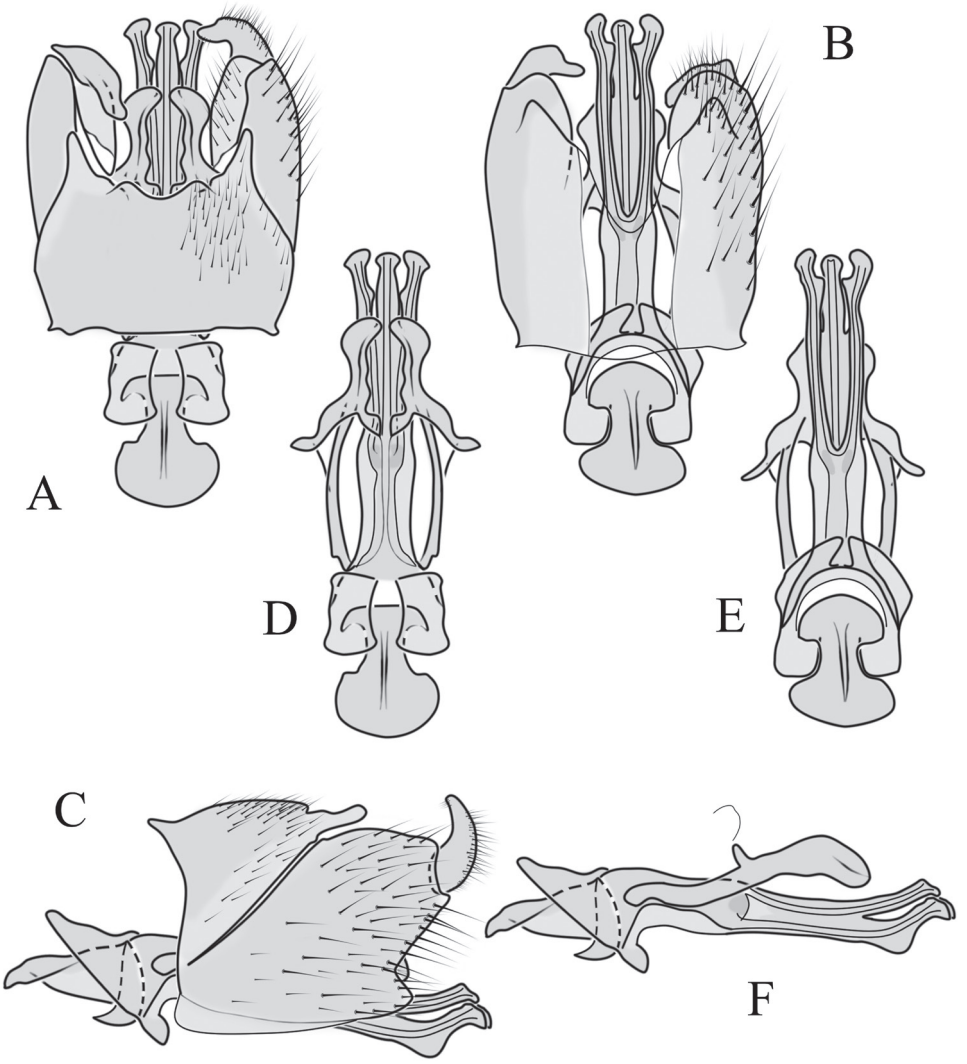

Figure 26. Male genital structures of *Liogma nodicornis* (Osten Sacken, 1865) **A** terminalia, dorsal view **B** terminalia, ventral view **C** terminalia, lateral view **D** aedeagus complex, dorsal view **E** aedeagus complex, ventral view **F** aedeagus complex, lateral view.

eral lobe, finger-like in lateral view (Fig. 26C), elongated, triangular in dorsal view (Fig. 26A); posterior margin with additional small, triangular outgrowth (Fig. 26A). Sternite 9 membranous (Fig. 26B). Gonocoxite 1.3–1.5 × longer than tergite 9 (including lobe); ventral lobe relatively small, triangular both lateral and ventral views, covered by few setae (Fig. 26B, C); inner surface of gonocoxite with hairs, proximal corner with hairless, paler area (Fig. 26A). Gonostylus simple, tapering to distal end. Aedeagus complex very large, 1.8–1.9 × longer than gonocoxite, in lateral view (Fig. 26C); ejacu-

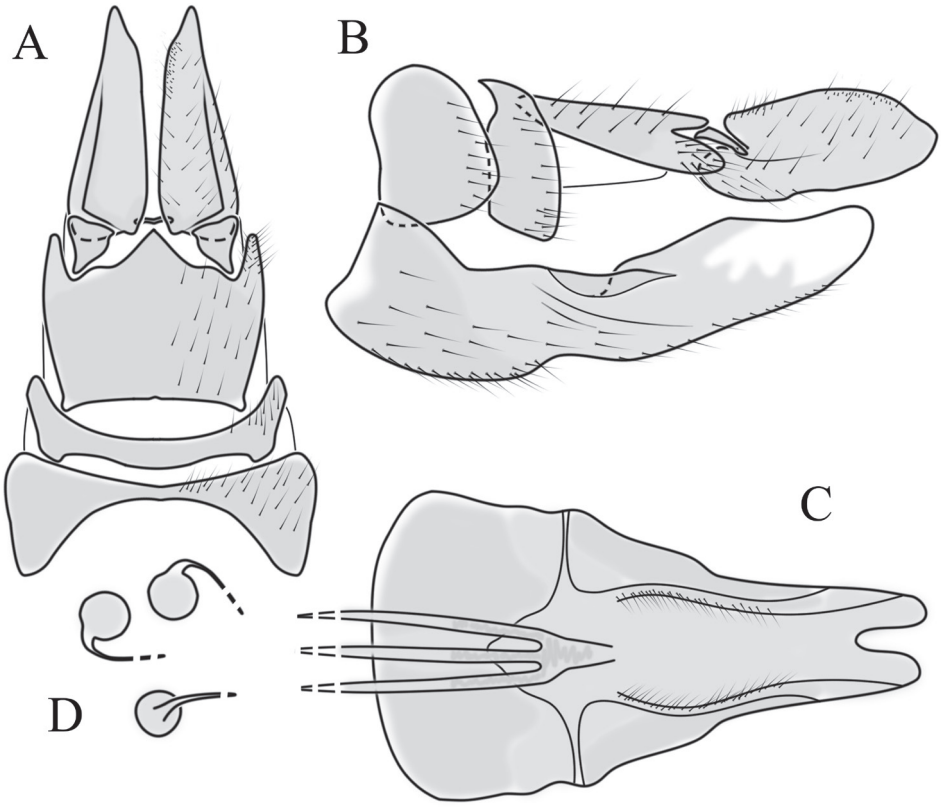

Figure 27. Female genital structures of *Liogma nodicornis* (Osten Sacken, 1865) **A** terminalia, dorsal view **B** terminalia, lateral view **C** sternite 8, hypogynial valve, and sperm ducts, inner dorsal view **D** spermathecae.

lator apodeme large, not covered by paramere in lateral view (Fig. 26F); tip of interbase directed inward in dorsal view (Fig. 26D), and ventrally in lateral view (Fig. 26F); dorsal lobe between interbases small, membranous, hardly noticeable (Fig. 26F); aedeagus long, trifid, median branch slightly shorter (Fig. 26D–F); lateral branch prolonged ventrally/caudally (Fig. 26F); tips of branch flattened; sperm ducts branching from elongated portion of sperm pump, branching area dark (Fig. 26F).

Female terminalia: Tergite 8, ~ 1.7–1.8 × wider than tergite 9 in lateral view (Fig. 27B), not divided medially (Fig. 27A). Triangular sclerite ~ 1/4 of length of tergite 10; sclerite separated from tip of tergite 10; lateral lobe of tergite 10 medium sized, 2 × as long as wide, with few long hairs (Fig. 27B). Cercus wide, with blunt notches on dorsal, close to tip and ~ 1/3 of mid-length on ventral margin. Hypogynial valve relative long, dorsal margin close to tip concave (Fig. 27B). Common spermathecal duct recognisable; sperm ducts simple, narrow tubes, (Fig. 27C); three round spermathecae with curved, suddenly tapering ducts (Fig. 27D).

Distribution: Canada and USA from (Alberta to Newfoundland, south to South Dakota, South Carolina and Georgia) (Oosterbroek 2021).

Liogma serraticornis Alexander, 1919

Figs 4F, 5F, 28, 29, 30, 31A

Liogma serraticornis in Alexander 1919: 345–346: original description; Alexander 1928: 11: distribution, illustration.; Alexander 1949: 195 comparison.; Esaki 1950: illustration.; Alexander 1953b: 77: faunistic record, distribution.; Ishida 1955: 75–76: distribution.; Takahashi 1960: 84: distribution.; Sidorenko 1999: 68–70: identification key, illustration, distribution.; Nakamura 2001: 23–29: identification key, illustration, distribution, faunistic records.; Paramonov 2004b: 69: faunistic record.; Paramonov 2006: 888–889: identification key, distribution.; Nakamura 2014: 54: distribution.; Kato and Suzuki 2017: 16: distribution.; Imada 2020: biology and ecology of larvae.

Liogma fuscipennis in Alexander 1932 111–112: original description; Alexander 1953a: 55–56, syn. nov.

Type material examined. *Liogma serraticornis* Alexander: ***Paratype***: **Japan** • ♂; Saitama, 29 May. 1919; R. Takahashi leg.; USNM.

Non-type material examined. Japan • 1 ♂; Aichi, Seto, Iwaya-cho, near Iwayada Park; 35.23957°N, 137.15084°E; alt. 300 m; 4 May. 2016; D. Kato leg.; BLKU. • 1 ♂; Aichi, Toei, Futto; 35.10117°N, 137.6607°E; alt. 390 m; larva collected: 9 Mar. 2014, emerged: 1 Apr. 2014; M. Kato leg.; CYI. • 1 ♀; Aichi, Toyota, Kawashimo, triburary of Yahagi River; 35.20376°N, 137.30125°E; alt. 140 m; 4 May. 2014; D. Kato leg.; BLKU. • 1 ♀; Aomori, Hirosaki, Ichinowatari-washinosu; 40.51923°N, 140.43889°E; alt. 205 m; 7 Jun. 2013; D. Kato leg.; BLKU. • 1 ♀; Aomori, Hirosaki, Koguriyama, Inekari River; 40.53658°N, 140.48701°E; alt. 170 m; 7 Jun. 2013; D. Kato leg.; BLKU. • 1 ♀; Ehime, Matsuyama, forest seep and stream; 33.86152°N, 132.82591°E; alt. 180 m; 20 Apr. 2019; L.-P. Kolcsár leg.; CKLP. • 1 ♂; Ehime, Odamiyama; 33.53°N, 132.86°E; 26 May. 1963; M. Miyatake leg.; EUMJ. • 5 ♂; Ehime, Saijo, spring and mosses rocks; 33.75504°N, 133.15377°E; alt. 1480 m; 16 Jun. 2019; L.-P. Kolcsár leg.; CKLP. • 1 ♂, 1 ♀; Ehime, Toon-shi, Saragamine; 33.72361°N, 132.88602°E; alt. 955 m; 21 May. 2017; K. Kuroda leg.; EUMJ. • 1 ♂, 1 ♀; Ehime, Wakayama, Mount Ishizuchi; 33.76491°N, 133.12948°E; alt. 1600 m; 5 Jun. 2019; L.-P. Kolcsár leg.; CKLP. • 2 ♀; Ehime, Wakayama, River Omogo gorge; 33.72581°N, 133.10291°E; alt. 750 m; 5 Jun. 2019; L.-P. Kolcsár leg.; CKLP. . • 1 ♀; Ehime, Kumakogen, headwaters, stream; 33.56476°N, 132.93501°E; alt. 1387 m; 17 Jun. 2019; L.-P. Kolcsár leg.; CKLP. • 1 ♀; Fukuoka, Miyako, small stream and Japanese cedar forest; 33.49796°N, 130.95861°E; alt. 686 m; 21 May. 2019; L.-P. Kolcsár leg.; CKLP. • 1 ♀; Fukuoka, Soeda, rocky streem and moss covered cliff; 33.48309°N, 130.93289°E; alt. 900 m; 21 May. 2019; L.-P. Kolcsár leg.; CKLP. • 1 ♂; Fukushima, Hinoemata, Ozebunanomori Museum;

36.99082°N, 139.27803°E; alt. 1230 m; 28 Jun. 2015; M. Kato leg.; CYI. • 1 ♂, 1 ♀; Iwate, Hachimantai, Matsuoyoriki; 39.89958°N, 140.89155°E; alt. 1200 m; larvae collected: 14 Jun. 2014, emerged: 4 Jul. 2014; Y. Imada leg.; CYI. • 1 ♂; Kagoshima, Inaodake; 31.12°N, 130.88°E; 11 May. 1952; Ito-Issiki leg.; USNM. • 1 ♀; Kagoshima, Kirishima, around Amori-gawa River, Hayato-cho-Kareigawa; 31.79821°N, 130.75275°E; 80 m; 28 Apr. 2018; D. Kato leg.; BLKU. • 1 ♂; Kumamoto, Gokanosho; 32.53°N, 130.86°E; 5 May. 1926; S. Issiki leg.; USNM. • 1 ♀; Kumamoto, Yatsushiro, Izumimachi-Momiki; 32.4915°N, 130.99084°E; alt. 1060 m; 11 May. 2016; T. Hosoya, S. Kakizoe leg.; BLKU. • 1 ♀; Kumamoto, Yatsushiro, Momiki-gawa river, Izumimachi-Momiki and Hagi; 32.51417°N, 130.93927°E; alt. 530 m; 11 May. 2016; D. Kato leg.; BLKU. • 1 ♂; Kyoto, Kyoto, Kibune; 35.13681°N, 135.76622°E; alt. 458 m; 1 May. 2016; Y. Imada leg.; CYI. • 1 ♂; Nagano, Oshika, Oike; 35.4887°N, 138.0219°E; alt. 1250 m; 19 Oct. 2015; Y. Imada leg.; CYI. • 1 ♂; Nagano, Ueda, Sanada-machi, Irikaruizawa; 36.47441°N, 138.25481°E; alt. 777 m; 16 May. 2012; D. Kato leg.; BLKU. • 1 ♂; Nagasaki, Unzen; 32.8°N, 130.23°E; May 1926; E. Svenson leg.; USNM. • 1 ♂; Oita, Kokonoe, Tano; 33.11621°N, 131.23541°E; alt. 1150 m; 7 May. 2016; D. Kato leg.; BLKU. • 2 ♂; Saga, Kanzaki, springs; 33.43401°N, 130.36866°E; alt. 980 m; 23 May. 2019; L.-P. Kolcsár leg.; CKLP. • 1 ♂; Saga, Karatsu, Tsubakiyama Pond, Hamatama-machi-torisu; 33.40414°N, 130.1064°E; alt. 630 m; 26. Apr. 2015; D. Kato leg.; BLKU. • 1 ♂, 1 ♀; Saga, Saga, Kase river near Hokuzan Dam, Fujimachi-sekiya; 33.43322°N, 130.23212°E; alt. 325 m; 23 Apr. 2015; D. Kato leg.; BLKU. • 1 ♂; Tokushima, Miyoshi, around Matsuogawa Dam, Higashiiya-Ochiai; 33.96478°N, 133.93908°E; alt. 900 m; 15 May. 2015; D. Kato leg.; BLKU. • 2 ♂; Tokushima, Minokosi, Mt. Tsurugi; 33.87°N, 134.11°E; alt. 1400 m; 1 Jun. 1950; Issiki-Ito leg.; EUMJ. • 1 ♂; Wakayama, Kozagawa, Takinohai; 33.6058°N, 135.76127°E; alt. 80 m; 13 Apr. 2014; M. Kato leg.; CYI. • 1 ♀; Yamanashi, Koshu, Enzankamihagihara, Kaminichikawa Pass; 35.73161°N, 138.83208°E; alt. 1580 m; 8 Jul. 2014; D. Kato leg.; BLKU. **Russia** • 1 ♂; Khabarovsk Krai, Khabarovsk City; 48.48022°N, 135.07191°E; alt. 80 m; 2 Jun. 2014 – 6 Jun. 2014; N.E. Vikhrev leg.; ZIN. • 1 ♂, 1 ♀; Primorsky Krai, Khasansky District, Primorsky Settlement, Zolotistyy [Golden] Stream; 43.10075°N, 131.54862°E; alt. 62 m; 13 Jun. 2007; N.M. Paramonov leg.; CKLP. • 1 ♂; Primorsky Krai, Kedrovaya Pad Nature Reserve; 43.10075°N, 131.54862°E; alt. 62 m; 7 Jul. 1940; A.S. Monchadskij leg. • 1 ♂; same locality; 12 Jun. 1962; E.P. Narchuk leg.; • 1 ♂; same locality; 2 Jul. 1962; E.P. Narchuk leg.; ZIN. • 1 ♂; Primorsky Krai, Kedrovaya Pad Nature Reserve, bog near Kedrovka River; 43.10075°N, 131.54862°E; alt. 62 m; 16 Jun. 2007; • 1 ♂; same locality; 1 Jun. 2007 – 11 Jun. 2007; N.M. Paramonov leg.; ZIN. • Primorsky Krai, Kedrovaya Pad Nature Reserve, Zolotistyy [Golden] Stream; 43.1007°N, 131.5486°E; alt. 62 m; 2007.06.13, 1 ♂, N.M. Paramonov leg.; ZIN. • 1 ♂; Primorsky Krai, Terney District, Terney Urban-type Settlement, Lower Serebryanka [Sanhobe] River Valley; 45.09314°N, 136.5852°E; alt. 60 m; 18 Jun. 1937; K.J. Grunin leg.; ZIN. • 5 ♂; Sakhalin Oblast, Yuzhno-Kurilsk Urban Settlement, Kuril Islands, Kunashir Island, near Lagunnoe Lake; 44.062°N, 145.759°E; alt. 20 m; 11 Jul. 1954; N.A. Violovich

leg.; ZIN. • 2 ♂; Sakhalin Oblast, Kunashir Island, lower course of the Saratovskaja River; 44.26042°N, 146.09912°E; alt. 16 m; 3 Jul. 2014 – 6 Jul. 2014; Y.N. Sundukov leg.; ZIN. • 1 ♂; Sakhalin Oblast, Kunashir Island, lower course of the Filatova River; 44.19078°N, 146.02006°E; alt. 60 m; 27 Jun. 2013 – 28 Jun. 2013; Y.N. Sundukov leg.; ZIN. • 1 ♂; Sakhalin Oblast, Kunashir Island, Alekhino Settlement [uninhabited]; 43.918°N, 145.529°E; alt. 5 m; 29 Jun. 1962; G.O. Krivoluckaja leg.; ZIN. • 1 ♀; Sakhalin Oblast, Sakhalin Island, Yuzhno-Sakhalinsk City; 46.959°N, 142.738°E; alt. 50 m; 22 Jun. 1956; • 1 ♂, 1 ♀; same locality; 27 Jun. 1956; N.A. Violovich leg.; ZIN.

Redescription. Head. Black with weak greyish pubescence (Fig. 28C, D). Rostrum short without nasus, but with few hairs (Fig. 28B, E); rostrum and mouthparts brown to black (Fig. 28B, E). Palpus brown to black, five-segmented; first two segments sometimes darker than the rest; last segment 1.3–1.8 × longer than penultimate. Scape cylindrical 1.5–2 × longer than pedicel (Fig. 4F); pedicel ovate; pedicel and scape same coloured or scape slightly darker, yellowish brown to brown; flagellum 14 segmented, monochrome dark brown to black; flagellar segments greatly expanded ventrally in male, last flagellomere cylindrical (Figs 4F, 28D). Flagellomeres 2–6 or 7 extended in female, remaining segments cylindrical (Figs 4F, 28E). Extended flagellomeres covered with dense whitish sensilla; 2–4 long verticels on dorsal surface, two verticels in lateral surface, two shorter on ventral side; first flagellomere always bearing additional verticels (Fig. 4F).

Thorax. Uniformly black with very weak greyish pubescence (Fig. 28B, C). Pleural area, base of wing, and base of halter yellowish or greyish white (Fig. 28B). Scatter, pale, short hairs present on mesonotum, forming two barely visible lines. Ventral part of thorax generally dark brown to uniformly black. Anterior half or more of mediotergite and almost all pleurotergite rugose (Fig. 28B). Trochanter yellow to pale brown; femur gradually darkening, basal part yellowish, apically dark brown; tibia gradually darkening distally, pale brown to dark brownish black; tarsus uniformly black (Fig. 28A). Wing hyaline, tinged with yellowish brown (typical "*serraticornis*" form) or infuscated ("*fuscipennis*" form); pterostigma pale brown to black; veins dark brown; three branches of M reaching wing margin; M_1 at same level as M_{1+2}, cell a_2 less than 6 × longer than wide (Fig. 5F); membrane with interference patterns, visible with dark background (Fig. 28A). Halter monochrome, yellowish brown to black (Fig. 28A).

Abdomen. Black, without any clear patterns (Fig. 28A).

Male terminalia: Relatively small, uniformly black or ventral parts of gonocoxite paler; directed caudally (Fig. 28A). Tergite 9 fused with gonocoxite (Fig. 29C); proximal margin with two obtuse triangular lobes, which bent back under tergite 9 (Fig. 29A). Sternite 9 fully membranous (Fig. 29B). Gonocoxite large, 1.7–1.8 × longer than tergite 9; with long ventral lobe, tip covered by pale, short spine-like setae (Fig. 29B, C); inner surface of gonocoxite sclerotised, forming dorsal plate with conspicuous edge next to tergite 9 (Fig. 29A). Gonostylus simple, tapering to tip (Fig. 29A–C). Aedeagus complex large, 1.2–1.3 × longer than gonocoxite. Ejaculator apodeme and sperm pump large, together half of length of aedeagal complex (Fig. 29D–F); not covered by parameres (Fig. 29F); interbase spoon-like with small notch apically in lateral view

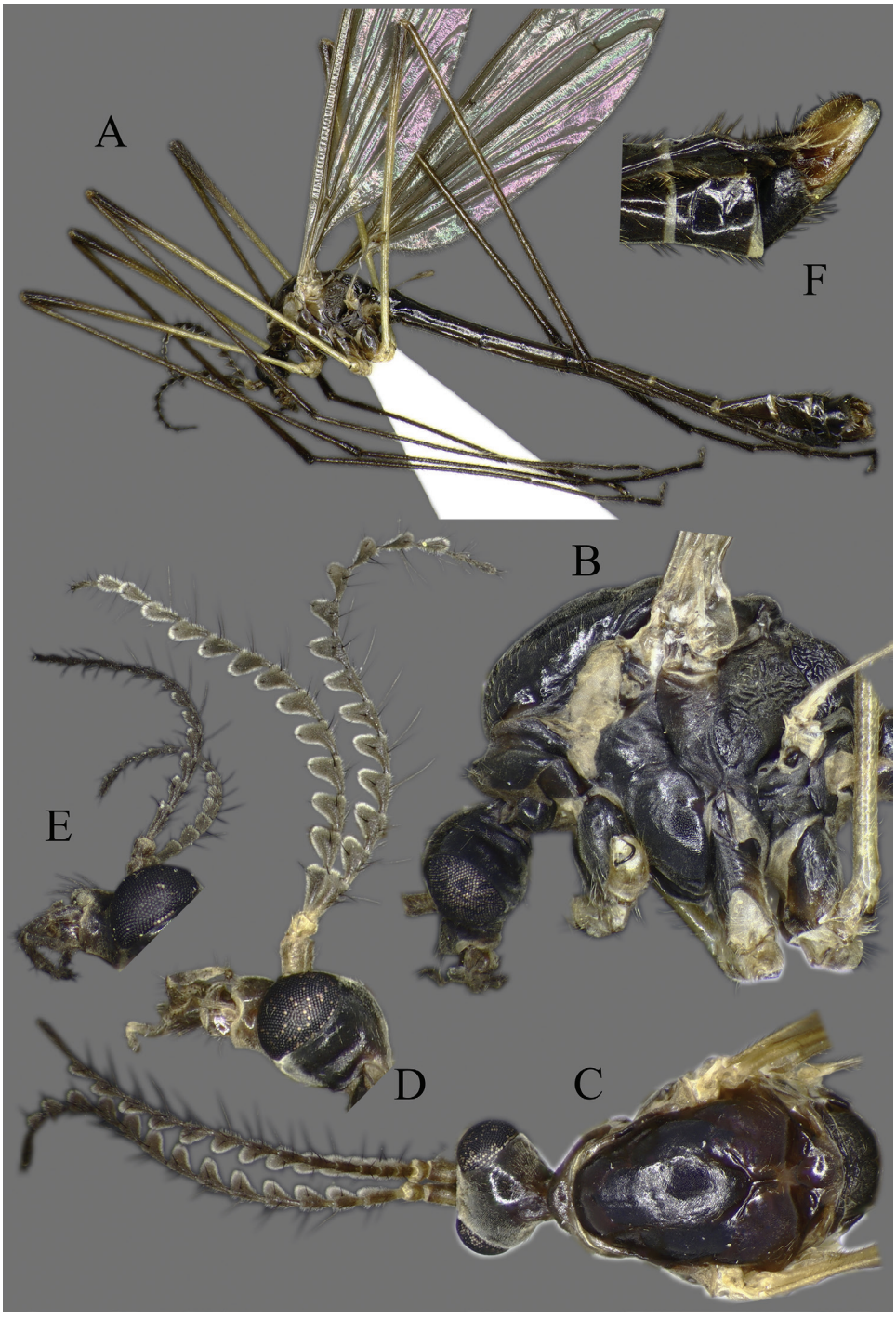

Figure 28. *Liogma serraticornis* Alexander, 1919 **A** habitus of male, lateral view (colouration of wings is artefact) **B** head and thorax, lateral view **C** head and thorax of male, dorsal view **D** head of male, lateral view **E** head of female, lateral view **F** female terminalia lateral view.

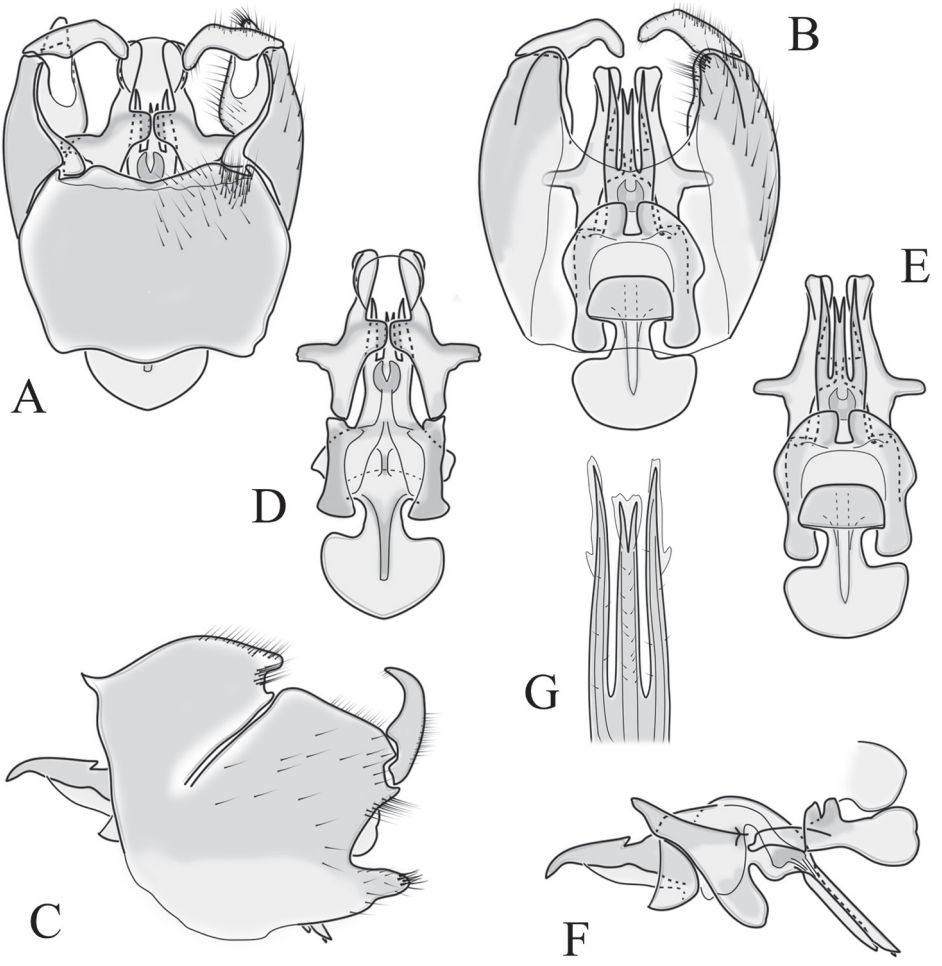

Figure 29. Male genital structures of *Liogma serraticornis* Alexander, 1919 **A** terminalia, dorsal view **B** Terminalia, ventral view **C** terminalia, lateral view **D** aedeagus complex, dorsal view **E** aedeagus complex, ventral view **F** aedeagus complex, lateral view **G** tip of the aedeagus.

(Fig. 29F); dorsal lobe of interbase small, directed inward in dorsal view (Fig. 29D); dorsal lobe between interbases large, globular and semi-transparent, as wide as tip of interbase in lateral view (Fig. 29F). Aedeagus straight, directed ventrally in 45°; sperm ducts branching from elongated portion of sperm pump, base of branches darkened (Fig. 29D, F); middle branch of aedeagus shorter than lateral branches; each with small spines ventrally; apical end of branches with hyaline membranous tissue (Fig. 29G).

Female terminalia: Brown to black, end of cercus and hypogynial valve yellowish (Fig. 28F). Tergite 8 > 2 × wider than tergite 9 in lateral view (Fig. 30B); not divided medially in dorsal view (Fig. 30A). Tergite 9 widening ventrally in lateral view, with small notch at posterior corner (Fig. 30B). Tergite 10 with triangular sclerite small-

er, ~ 1/3 of length of tergite 10; sclerite separated from tergite 10 (Fig. 30B); lateral lobe relatively long, at least 2 × longer than wide (Fig. 30B). Cercus oval; hypogynial valve elongated, blade-shaped. Cercus on dorsal surface close to apical end weakly, but clearly rugose, serrate (Fig. 30B); ventral margin of cercus without notch, evenly curved (Fig. 30B). Common spermathecal duct, short, indistinct; spermathecal ducts with extended parts, golf-tees-like (Fig. 30C); three round, spermathecae present, duct curved or straight (Fig. 30D).

Distribution. Japan (Hokkaido I, Honshu I, Shikoku I, and Kyushu I) and Russia (Primorsky Krai, Sakhalin Oblast (incl. Kuril I) (Oosterbroek 2021). First record from Khabarovsk Krai, Russia (Fig. 31A).

Comments. The morphological comparison of this species with *L. brevipecten* is discussed under that species. Colouration is variable within specimens of *Liogma serraticornis*. Usually, colouration is black with a paler pleural area, and the wing membrane is almost transparent, tinged with pale yellowish brown. In darker specimens,

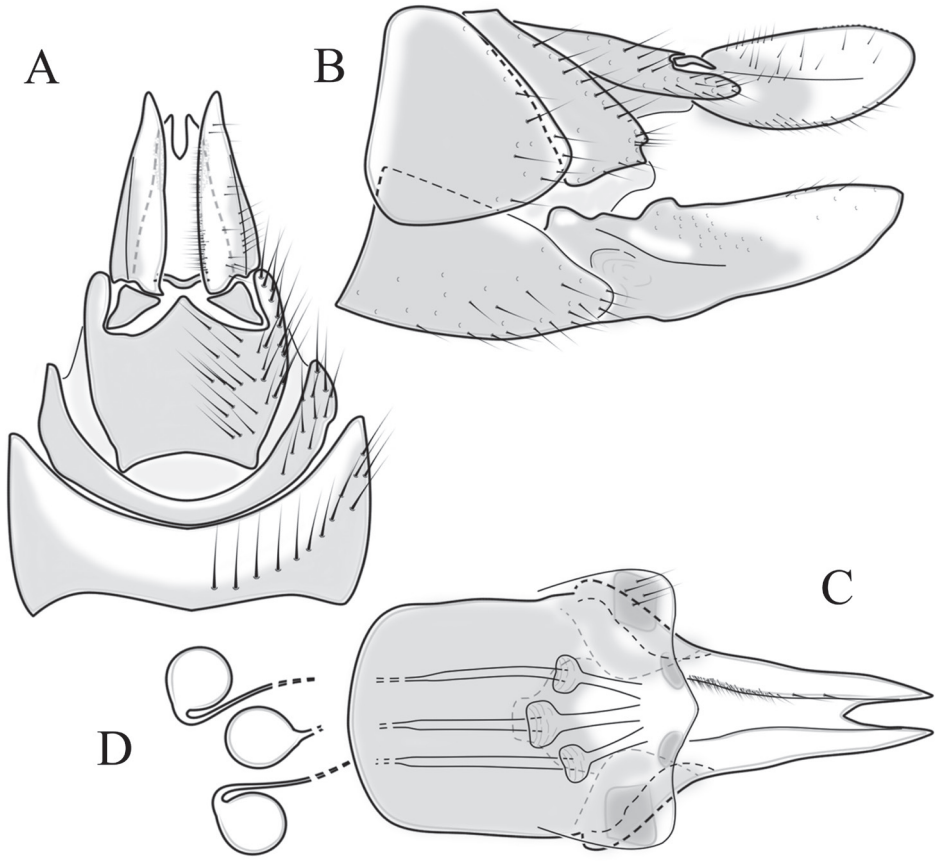

Figure 30. Female genital structures of *Liogma serraticornis* Alexander, 1919 **A** terminalia, dorsal view **B** terminalia, lateral view **C** sternite 8, hypogynial valve, genital fork, and sperm ducts, inner dorsal view **D** spermathecae.

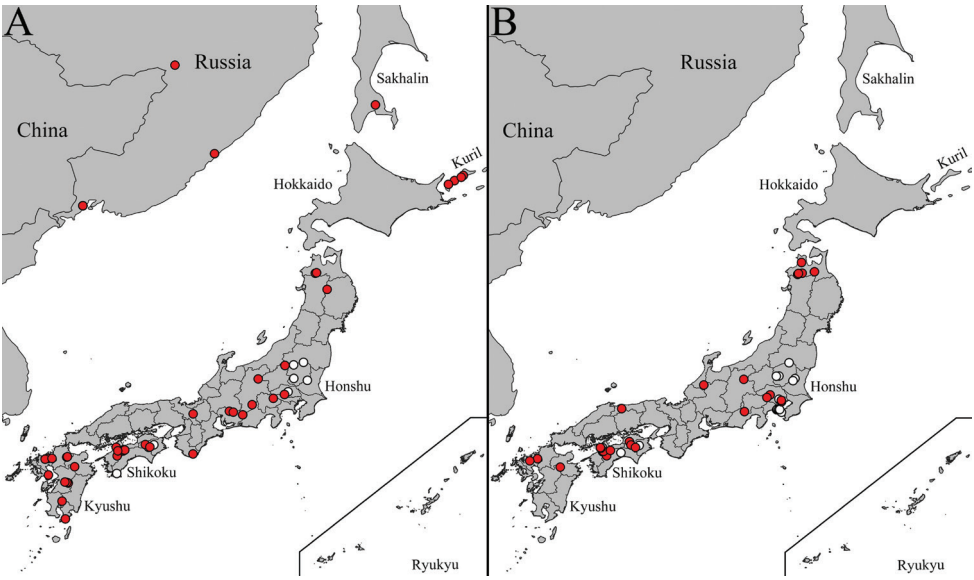

Figure 31. Occurrence data in Japan and surrounding areas of **A** *Liogma serraticornis* Alexander, 1919 **B** *Triogma kuwanai* (Alexander, 1913). Red dots indicate locations of investigated specimens, white dots indicate approximate locations of literature data.

the pleural area and wing membrane is infuscated. This darker form was described as a separate species, *Liogma fuscipennis* Alexander, 1932, but was later synonymised with *L. serraticornis* (Alexander 1953). No genital and genetic difference between the paler and darker specimens were found during our study.

Phalacrocera replicata (Linnaeus, 1758)

Figs 32, 33

Phalacrocera nudicornis (Schummel, 1829)
Phalacrocera brevirostris (Zetterstedt, 1838)
Phalacrocera diversa (Walker, 1856)
Phalacrocera neoxena Alexander, 1914.

Non-type material examined. **Canada** • 2 ♂, 1 ♀; Ontario, Ottawa, Stony Swamp; 45.3°N, 75.83° W; alt. 115 m; 10 May. 2017; F. Brodo leg.; CKLP. **Finland** • 2 ♂, 1 ♀; Kirkkonummi, Stormossen. 60.07901°N, 24.57980°E; alt. 7 m; 2 Jun. 2016; E. Viitanen leg.; CKLP. • 1 ♂, 2 ♀; Kaarina, Jarvela; 60.46157°N, 22.37418°E; alt. 38 m; 18 May. 2016 – 1 Jun. 2016; E. Viitanen leg.; Malaise trap; CKLP. • 1 ♂; Tervola, Karhakkamaanjanka; 66.19764°N, 25.12660°E; alt. 58 m; 25 May. 2004 – 28 Jun. 2004; J. Salmela leg.; CKLP. **Russia** • 1 ♂; Krasnoyarsk Krai, Turukhansky District, Igarka City, within the settlement, swampy lake shore in the

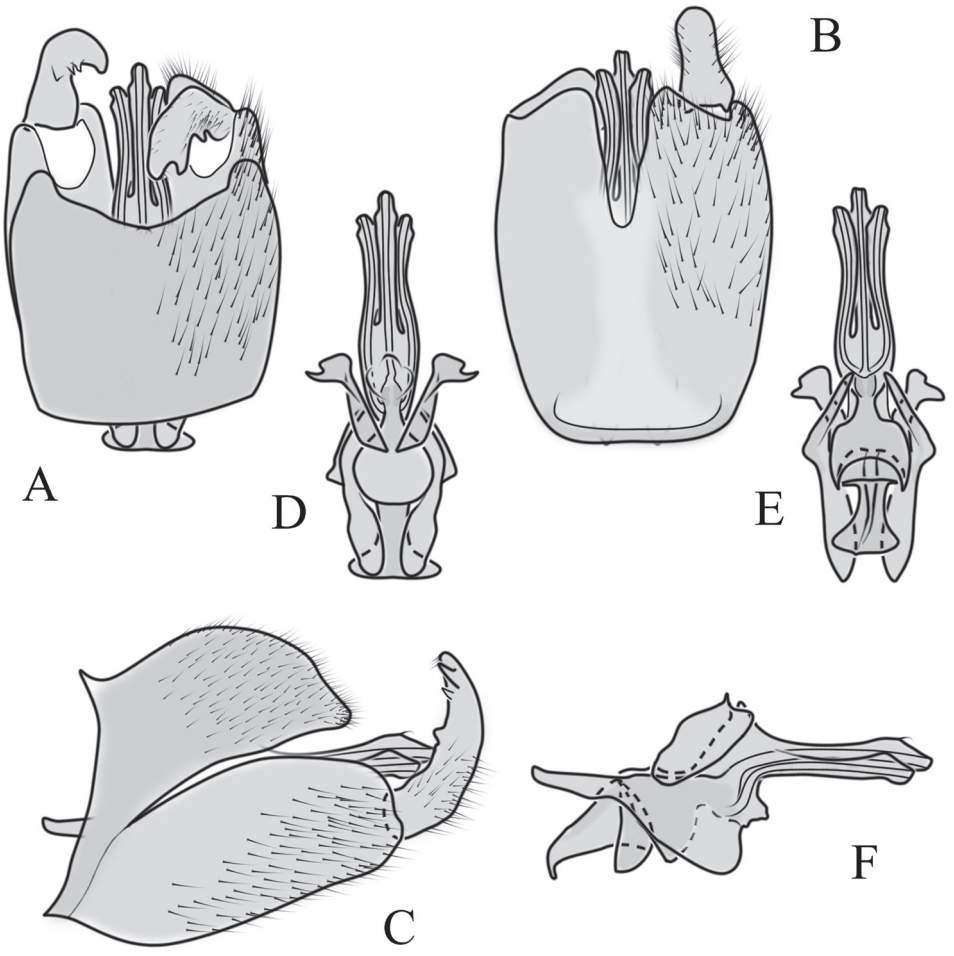

Figure 32. Male genital structures of *Phalacrocera replicata* (Linnaeus, 1758) **A** terminalia, dorsal view **B** terminalia, ventral view; **C** Terminalia, lateral view **D** aedeagus complex, dorsal view **E** aedeagus complex, ventral view **F** aedeagus complex, lateral view.

city; 67.466°N, 86.581°E; alt. 23 m; 30 Jun. 1967; K.B. Gorodkov leg.; CKLP. • 1 ♀; Krasnoyarsk Krai, Igarka City, within the settlement, sedge swamp; 67.466°N, 86.581°E; alt. 23 m; 1 Jul. 1967; K.B. Gorodkov leg.; CKLP. **USA** • 2 ♂; Michigan, Cheboygan, hard wood swamp; 45.29277°N, 84.42805° W, alt. 280 m; 20 May. 2015; F. Brodo leg.; CKLP.

Supplementary description. Male terminalia directed dorsally. Tergite 9 fused with gonocoxite and sternite 9 (Fig. 32C); caudal margin of tergite 9 with small, rounded lateral lobe both ventral and lateral view (Fig. 32A, C); posterior margin U- or V-shaped. Sternite 9 reduced to narrow band (Fig. 32B, C). Gonocoxite 1.2–1.3 × longer than tergite 9; ventral lobe relatively small, rounded (in dry specimen looks

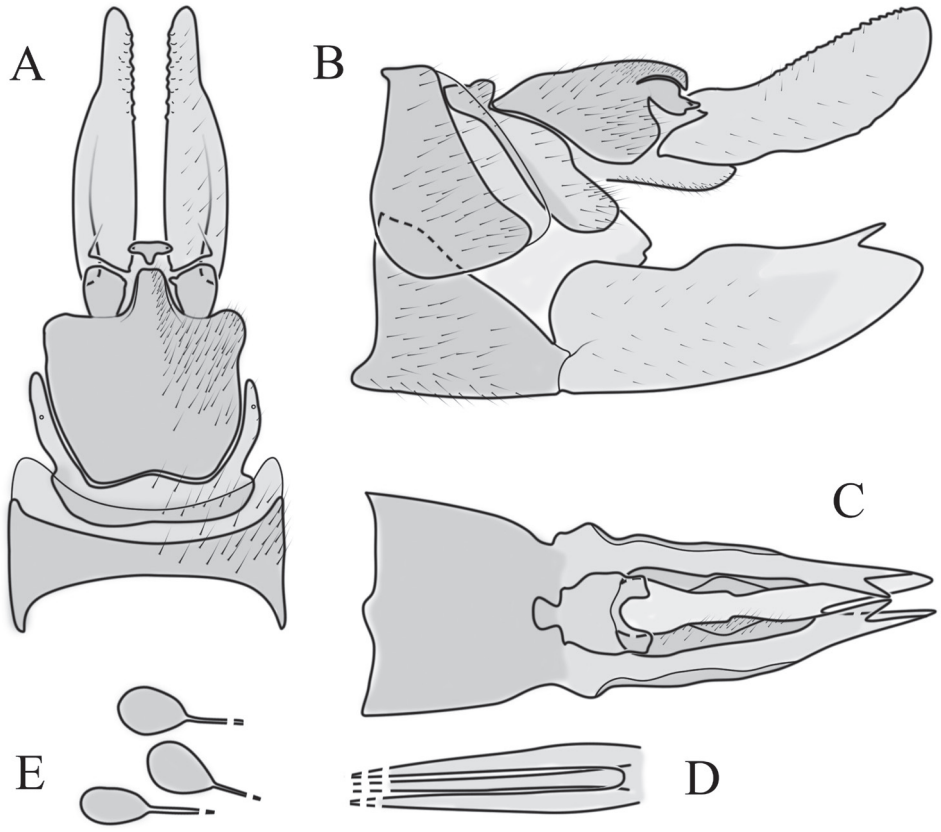

Figure 33. Female genital structures of *Phalacrocera replicata* (Linnaeus, 1758) **A** terminalia, dorsal view **B** terminalia, lateral view **C** sternite 8, hypogynial valve, and genital fork, inner dorsal view **D** sperm ducts **E** spermathecae.

more finger-like) (Fig. 32B); apical lobe indistinct; inner surface of gonocoxite sclerotised, with few hairs, without evident modifications. Gonostylus comparable large and complex, with a subapical tooth on outer margin; additional two or three smaller teeth basally (Fig. 32A, C). Aedeagus complex 1.2–1.3 × longer than gonocoxite in lateral view (Fig. 32C); ejaculator apodeme large, not covered by paramere in lateral view (Fig. 32F); interbase seems flat and wide, with a small dorsal tooth in lateral view (Fig. 32F); interbase directed dorso-laterally, with a deep notch on tip in dorsal view (Fig. 32D, E); dorsal lobe between interbases indistinct or absent (Fig. 32D); aedeagus half as long as entry aedeagus complex; aedeagus trifid, straight; median branch longer than lateral branches (Fig. 32D–F), with a triangular dorsal outgrowth; tip slightly bifid or trifid, depend on angle (Fig. 32A); lateral branches slightly curved laterally in dorsal and ventral view (Fig. 32D, E); tips of branch widened dorsally; sperm ducts branching from short elongation of sperm pump; branching area dark (Fig. 32D–F).

Female terminalia: Tergite 8 posterior part membranous, with few hairs, but not divided medially (Fig. 33A); wider than tergite 9 in lateral view (Fig. 33B). Tergite 10 with small, slightly separated median lobe in middle of posterior margin (Fig. 33A, B); covered with short hairs. Triangular sclerite widely fused with tip of tergite 10; tergite 10 without lateral lobe (Fig. 33B). Cercus elongated blade, with dorsal margin with weakly serrate margin (Fig. 33B). Hypogynial valve wide and long, dorsal margin close to tip with tooth-like lobe, directed caudally (Fig. 33B, C). Common spermathecal duct short or indistinct; sperm ducts simple, without distinct pattern, tapering proximally (Fig. 33D); three spermathecae elongated, with straight duct (Fig. 33E).

Distribution. Widely distributed in Holarctic. It has been reported from the Nearctic: Canada and USA from Ontario and Quebec, south to Michigan, Pennsylvania and Massachusetts. Palearctic: Austria, Belarus, Belgium, China (Heilongjiang), Czech Republic, Denmark, Estonia, Finland, France, Germany, Great Britain, Ireland, Italy (north), Lithuania, Mongolia, Netherlands, Norway, Poland, Russia: North European Russia, Central European Russia, East Siberia (Irkutsk Oblast), Far East (Republic of Sakha (Yakutia), Spain (Zamoro), Sweden, Switzerland, Ukraine (Oosterbroek 2021, Paramonov and Pilipenko 2021).. Here we record the species for the first time from Krasnoyarsk Krai, East Siberia, Russia.

Phalacrocera tipulina Osten Sacken, 1865

Figs 34, 35

Non-type material examined. Canada • 1 ♂; Quebec, Schefferville, Lac Le Jeune; 54.83006°N, 66.82436° W; alt. 500 m; 13 Jul 1981; F. Brodo leg.; CKLP. • 1 ♂; Quebec, Schefferville, Ashtray lake, 26 km SE from Schefferville; 54.66656°N, 66.65095° W; alt. 500 m; 15 Jul. 1981; F. Brodo leg.; CKLP. • 1 ♂; Quebec, Schefferville, Iron Arm, 18 km SE from Schefferville; 54.70211°N, 66.7630° W; alt. 530 m; 18 Jul. 1981; F. Brodo leg.; CKLP. **Usa** • 3 ♂, 2 ♀; Maine, Jonesport, Rogue Island, Bonney Point fen near coast; 44.57845°N, 67.52928° W; alt. 20 m; 2 Jun. 2011; F. Brodo leg.; CKLP. • 1 ♂, 1 ♀; Virginia, Pearisburg, Mountain Lake; 37.36106°N, 80.53231° W; alt. 1190 m; 25 Feb. 2018; Y. Imada leg.; CKLP.

Supplementary description. Male terminalia directed dorsally. Tergite 9 fused with gonocoxite and sternite 9 (Fig. 34C); caudal margin of tergite 9 medially with small, darker, outgrowths and with deep U-shaped notch between them (Fig. 34A); tip of median lobes rounded in dorsal view (Fig. 34A), triangular in in lateral view (Fig. 34C); tergite 9 without lateral lobes. Sternite 9 reduced to narrow band (Fig. 34B). Gonocoxite 1.2–1.3 × longer than tergite 9; ventral lobe very small membranous and indistinct (Fig. 34B, C); apical lobe indistinct; inner surface of gonocoxite sclerotised, with few hairs, forming a triangular sclerite. Gonostylus simple, tapering distally (Fig. 34A–C). Aedeagus complex 1.1–1.2 × longer than gonocoxite in lateral view (Fig. 34C); ejaculator apodeme medium sized, not covered by paramere in lateral view (Fig. 34F); interbase seems flat and wide, both dorsal and lateral view (Fig. 34D, F); interbase

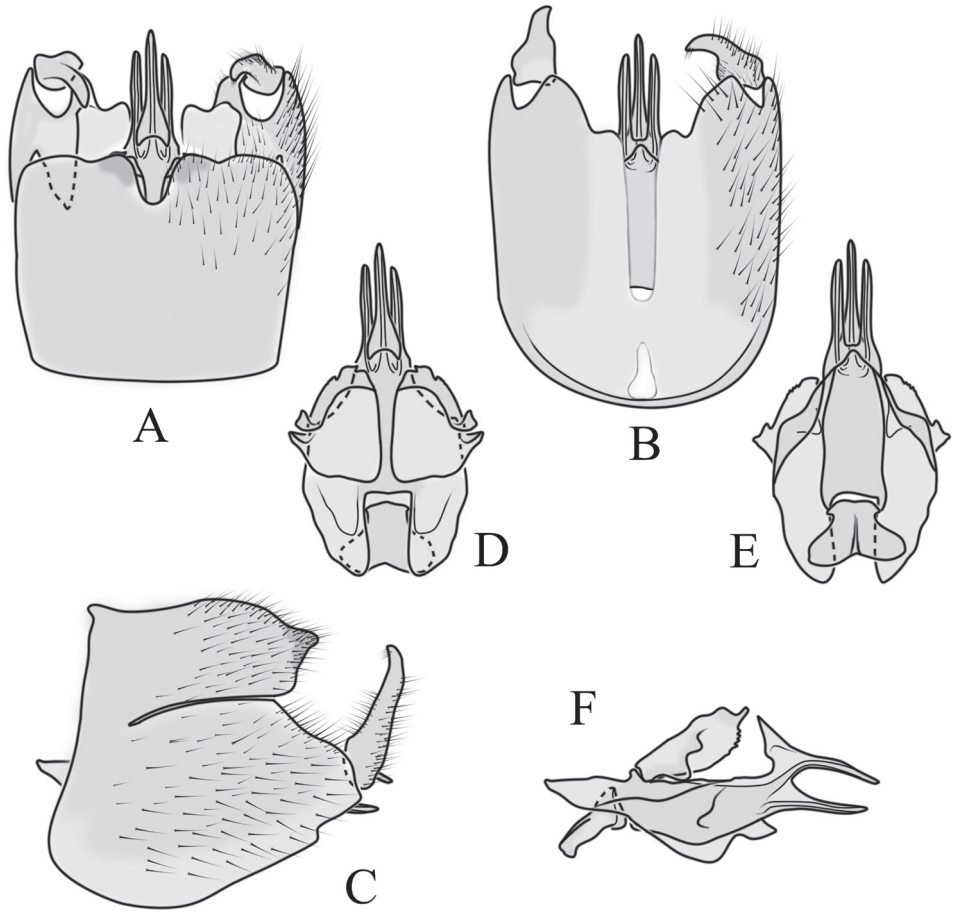

Figure 34. Male genital structures of *Phalacrocera tipulina* Osten Sacken, 1865 **A** terminalia, dorsal view **B** terminalia, ventral view **C** terminalia, lateral view **D** aedeagus complex, dorsal view **E** aedeagus complex, ventral view **F** aedeagus complex, lateral view.

with small tooth apically, directed inward in dorsal view; caudal margin with additional notches, which seems teeth in lateral view; median lobe between interbases absent or indistinct; parameres fused ventrally, and forming wide plate, as wide as interbases together (Fig. 34D, E); aedeagus trifid, lateral branches straight, shorten than median tube (Fig. 34D–F); median branch longer than lateral branches, situated dorsally to lateral branches, with a bifid (visible dorsally or caudally), prominent outgrowth; directed dorsally, slightly backward (Fig. 34F); tips of branch tapering distally; sperm ducts branching from wide elongation of sperm pump; branching area slightly dark (Fig. 34D–F).

Female terminalia: Tergite 8 posterior part membranous, with few hairs, but not divided medially (Fig. 35A); wider than tergite 9 in lateral view (Fig. 35B). Tergite 9 directed caudally, lateral corner triangular. Triangular sclerite large, fused with ter-

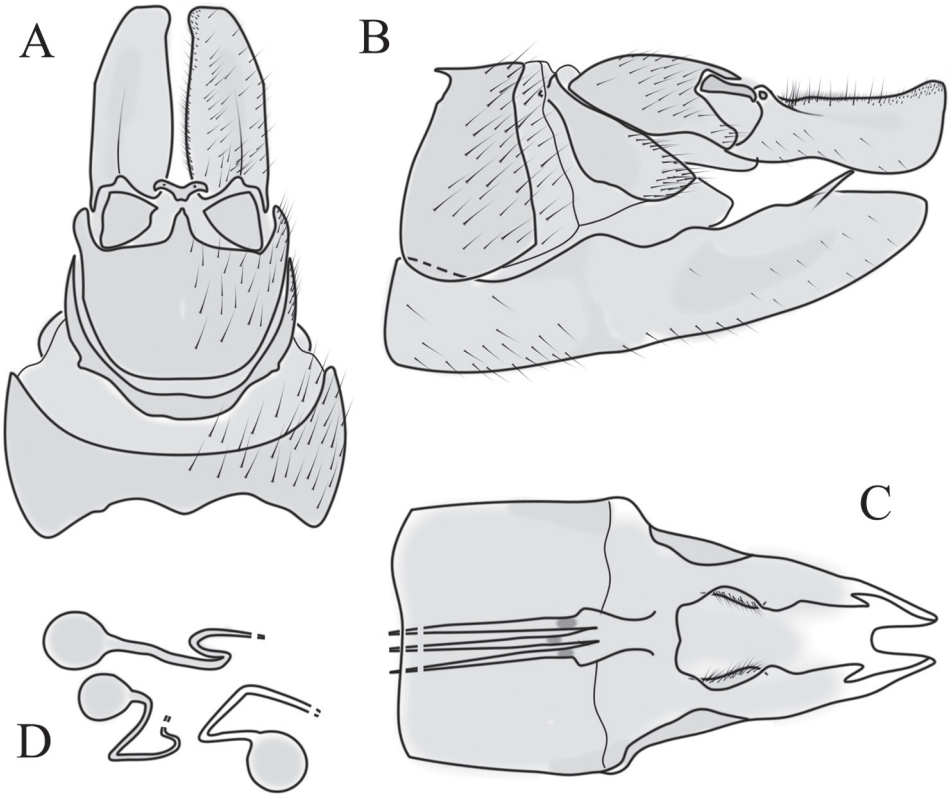

Figure 35. Female genital structures of *Phalacrocera tipulina* Osten Sacken, 1865 **A** terminalia, dorsal view **B** terminalia, lateral view **C** sternite 8, hypogynial valve, and sperm ducts, inner dorsal view **D** spermathecae.

gite 10 uncertain; tergite 10 with small, less separated lateral lobe (Fig. 35B). Cercus short, widening apically, with blunt tip; dorsal margin with rugged margin, formed by small outgrowths (Fig. 35A, B). Sternite 8 and hypogynial valve wide and long, dorsal margin close to tip with tooth-like lobe, directed caudally (Fig. 35B, C). Common spermathecal duct present; sperm ducts simple, with distinct darkened area after branching, evenly tapering proximally (Fig. 35C); three spermathecae rounded, with very long and irregularly curved duct (Fig. 35D).

Distribution. Canada, USA (Wisconsin to Ontario and Newfoundland, south to Virginia) (Oosterbroek 2021).

***Triogma kuwanai* (Alexander, 1913)**
Figs 4G, 5G, H, 31B, 36, 37, 38

Triogma kuwanai limbinervis Alexander, 1953, syn. nov.

Triogma nimbipennis Alexander, 1941, syn. nov.

Liogma kuwanai in Alexander 1913: 294–295, 321–322: illustration, original description; Alexander 1920: 15–16: female description.

Triogma kuwanai in Alexander 1928: 12: distribution, illustrations, comb. nov.; Esaki 1950: illustration; Alexander 1953a: 56: faunistic records; in Takahashi 1960: 81: distribution; Nakamura 2001: 23–29: identification key, illustration, distribution, faunistic records; Nakamura 2005: 685: illustration; Oosterbroek 2020 (since 2018): taxonomic status. Imada 2020: biology and ecology of larvae.

Triogma kuwanai kuwanai in Ishida 1955: 76–77: distribution; Sidorenko 1999: 68–70: identification key, illustration, distribution; Paramonov 2006: 888–889: identification key, illustration, distribution; Nakamura 2014: 54: distribution; Kato and Suzuki 2017: 16: faunistic records, distribution.

Triogma kuwanai limbinervis ssp. n. in Alexander 1953a: 56–57: original description, illustration; Alexander, 1953b: 77: distribution; Takahashi 1960: 82: distribution; Sidorenko 1999: 68–70: identification key, illustration, distribution; Paramonov 2006: 888–889: identification key, distribution; Nakamura 2014: 54: distribution.

Triogma limbinervis in Oosterbroek 2020 (since 2018): taxonomic status.

Triogma nimbipennis in Alexander 1941: 407–408: original description, illustration, comparison; Yang 1991: information about type material; Sinclair and Dorchin 2010: 80: information about type material; Alexander and Alexander 1973: 69: catalogue, distribution; Oosterbroek 2020: taxonomic status.

Type material examined. *Triogma kuwanai limbinervis* Alexander, 1953: ***Paratype***: **Japan** • ♀; Kochi, Tosa, Nisikawa, Mt. Yanase; alt. 800 m; 4 May. 1951; R. Takahashi leg.; USNM.

Triogma nimbipennis Alexander, 1941: ***Paratypes*: China** • ♂; Kuatun (Guadun), Fukien (Fukijen); 2500–3000 m; 23 Apr. 1938; • 2 ♀; same locality; 27 Apr. 1938 – 28 Apr. 1938; • 1 ♀; same locality; 27 Apr. 1938; Klapperich leg.; ZFMK.

Non-type material examined. *Triogma kuwanai kuwanai* (Alexander, 1913): **Japan** • 1 ♂; Aomori, Hirosaki, Koguriyama, Inekari River; 40.53658°N, 140.48701°E; alt. 170 m; 24 May. 2013; • 1 ♂; same locality; 25 May. 2013; • 1 ♀; same locality; 28 May. 2013; D. Kato leg.; BLKU. • 2 ♂; Aomori, Nakadomari, Osawanai, Osawanai Pond; 40.94641°N, 140.46231°E; alt. 35 m; 15 May. 2014; D. Kato leg.; BLKU. • 1 ♂; Aomori, Nishimeyamura, Hirasawa River; 40.48729°N, 140.31335°E; alt. 710 m; 4 Jun. 2013; D. Kato leg.; BLKU. • 1 ♂; Aomori, Towada, Okuse, Tsutanuma Path; 40.59084°N, 140.95705°E; alt. 468 m; 23 May. 2014; D. Kato leg.; BLKU. • 1 ♂; Ehime, Iyo, Mt. Saragamine; 33.72°N, 132.89°E, 8 May. 1949; M. Miyatake leg.; EUMJ. • 1 ♀; Ehime, Komi, Yanadani; 33.55°N, 133.01°E; 6 May. 1994 – 8 May. 1994; Ohbayashi, Nishino, Okada le.; EUMJ. • 1 ♀; Ehime, Matsuyama, Misaka-toge; 33.71°N, 132.85°E; 3 May. 1951; Yano T. leg.; EUMJ. • 1, sex unknown; Ehime, Matsuyama, Sugitate; 33.84°N, 132.79°E; 8 Ap. 1950; M. Miyatake leg.; EUMJ. • 1 ♀; Ehime, ?Matsuyama, Shichidori; 33.84°N, 132.79°E; 3 May. 1952; Ide leg.; EUMJ. • 1 ♂; Ehime, Saijo, spring and moss-

es rocks; 33.75504°N, 133.15377°E; alt. 1480 m; 5 Jun. 2019; L.-P. Kolcsár leg.; CKLP. • 1 ♂; Fukuoka, Fukuoka, Sawara-ku, Itaya, Mt. Sefuri; 33.43811°N, 130.36673°E; alt. 970 m; 2 May. 2015; D. Kato leg.; BLKU. • 1 ♂; Ishikawa, Hakusan, near to Hakusan National Park; 36.25869°N, 136.72558°E; 678 m; 27 May. 2015; M. Kato leg.; CYI. • 1 ♂, 1 ♀; Nagano, Ueda, Sanada-machi, Irikaruizawa; 36.47441°N, 138.25481°E; alt. 777 m; 16 May. 2012; D. Kato leg.; BLKU. • 1 ♂; Oita, Kokonoe, Tano; 33.11621°N, 131.23541°E; alt. 1150 m; 7 May. 2016; D. Kato leg.; BLKU. • 1 ♂; Okayama, Maniwa, Hiruzen-Kamifukuda, Nawashirodani-gawa River; 34.08837°N, 133.87994°E; alt. 600 m; 30 Apr. 2016; D. Kato leg.; BLKU. • 2 ♂, 1 ♀; Saga, Karatsu, Kyuragi-Hirano, Mt. Sakurei; 33.35701°N, 130.07038°E; alt. 862 m; 26 Apr. 2015; D. Kato leg.; BLKU. • 1 ♀; Saitama, Saitama; 35.88°N, 139.26°E; 29 May. 1919; R. Takahashi leg.; USNM. • 2 ♂, 1 ♀; Shizuoka, Shizuoka, Ikawa-touge; 35.24094°N, 138.28156°E; alt. 1471 m; 10 May. 2015; M. Kato leg.; •1 ♂; same locality; 18 May. 2016; Y. Imada leg.; CYI. • 1 ♂; Tokushima, Awa, Mt. Tsurugi; 33.87°N, 134.11°E; 31 May. 1950; Issiki-Ito leg.; USNM. • 2 ♂; Tokushima, Higashimiyoshi, Higashiyama, Ogawadani River; 34.08837°N, 133.87994°E; alt. 340 m; 21 Apr. 2014; D. Kato leg.; BLKU. • 1 ♂; Tokushima, Miyoshi, Higashiiya-Ochiai, around Matsuogawa Dam; 33.96478°N, 133.93908°E; alt. 900 m; 30 Apr. 2016; D. Kato leg.; BLKU. • 1, sex unknown; Tokyo, Meguro; 35.62°N, 139.7°E; 8 Apr. 1919; R. Takahashi leg.; USNM. • 1 ♂; Tokyo, Mt. Mitake; 35.78°N, 139.14°E; 10 May. 1931; B. Oda leg.; USNM. • 1, sex unknown; Tokyo, Tokyo; 35.67°N, 139.69°E; 8 Apr. 1930; R. Takahashi leg.; USNM. • 1 ♂; Tottori, Kurayoshi, Sekigane-cho-Nozoe, Mt. Karasuga; 35.35352°N, 133.58577°E; alt. 1000 m; 17 May. 2015; D. Kato leg.; BLKU.

Triogma kuwanai limbinervis Alexander: **Japan** • 7 ♂ 1 ♀; Ehime, Matsuyama, small ruderal streem; 33.86328°N, 132.77157°E; alt. 125 m; 31 Mar. 2019; L.-P. Kolcsár leg.; CKLP. • 2 ♀; Ehime, Matsuyama, ruderal forest and orange plantation; 33.86041°N, 132.76552°E; alt. 84 m; 6 Apr. 2019; L.-P. Kolcsár leg.; CKLP.

Redescription. Head. Rugose; ground colouration dark brown to black, with very intense greyish pubescence (Fig. 36B, C). Rostrum moderately long, with few short hairs; palpus greyish black, five segmented; last segment 1.4–1.6 × longer than penultimate in male, 1.2–1.3 × in female. Scape cylindrical, rugose, ~ 2 × as long as pedicel; pedicel ovate; flagellum 14 segmented monochrome greyish black (Figs 4G, 36B, D). Male flagellomeres, except ultimate, expanded ventrally, covered with dense whitish grey sensilla, denser ventrally; ultimate flagellomere cylindrical, with several sensilla (Figs 4G, 36B); female flagellomeres 1–5 or 6 extended ventrally, remaining flagellomeres fusiform to cylindrical; flagellomeres 1–10 or 11 bearing sparse whitish grey sensilla mostly on ventral side (Figs 4G, 36E). Flagellomere with two long verticels on dorsal surface, two short on lateral face, and two short on ventral side; first flagellomere always bearing additional 1–4 verticels.

Thorax. Ground colouration dark brown to black, with very dense and intensive grey pruinosity, thorax appearing grey (Fig. 36A–C). Pleural area, wing base, and halter yellow to yellowish brown (Fig. 36B). Anterior part of mesonotum with rugose sutures (Fig. 36C); lateral margin of scutum rugose (Fig. 36A, B). Ante-

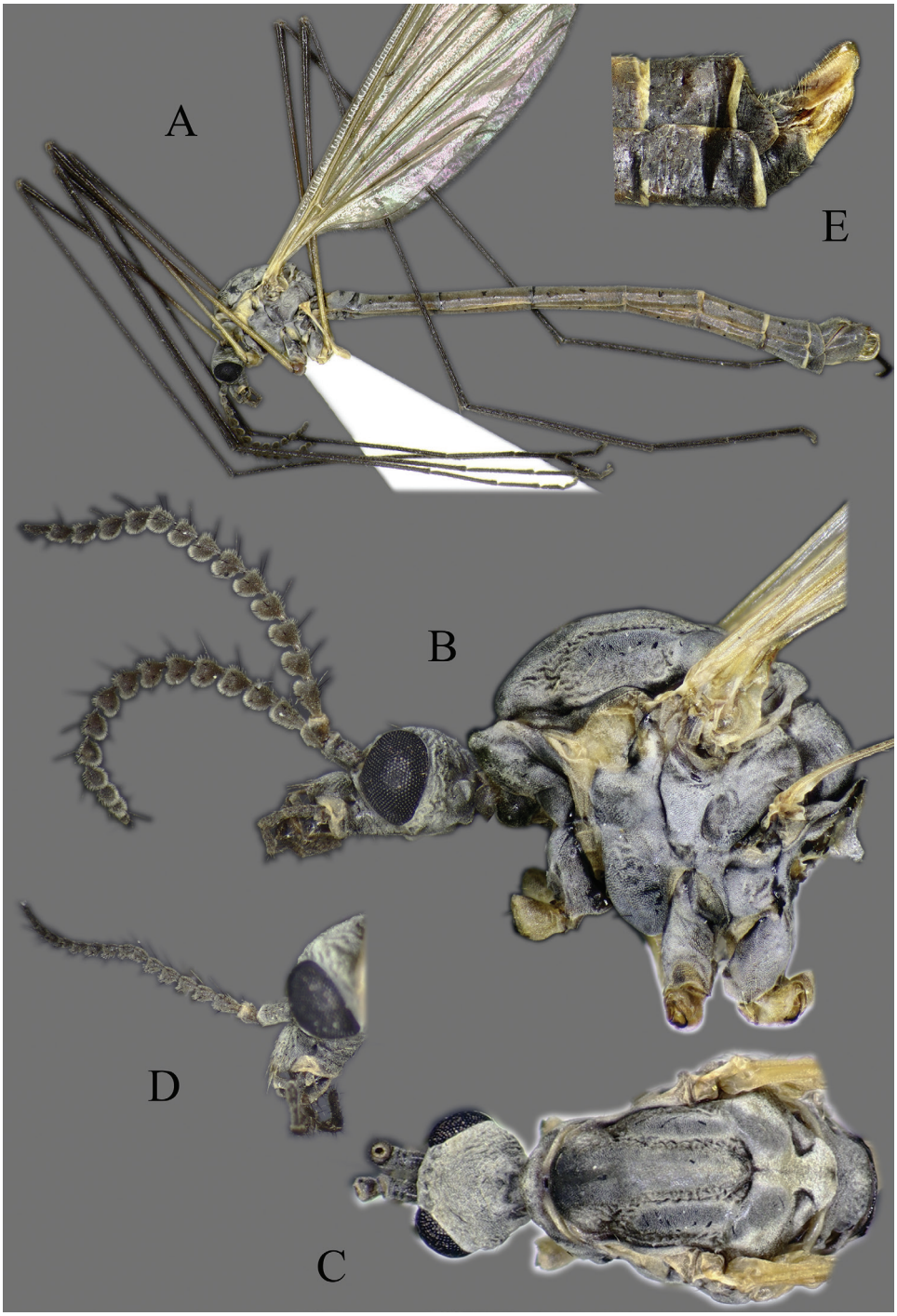

Figure 36. *Triogma kuwanai* (Alexander, 1913) **A** habitus of male, lateral view (colouration of wings is artefact) **B** head and thorax of male, lateral view **C** head and thorax, dorsal view **D** head of female, lateral view **E** female terminalia, lateral view.

rior half of mediotergite rugose (Fig. 36B). Katepisternum and metakatepisternum weakly rugose (Fig. 36B). Trochanter yellow to pale brown; femur gradually darkening apically, basally yellowish, apically black; tibia and tarsus uniformly black (Fig. 36A). Wing hyaline, tinged with pale brown; membrane with interference patterns, visible with dark background (Fig. 36A); pterostigma brown; veins yellow at base of wing, apically brownish; three branches of M reaching wing margin; M_1 at same level as M_{1+2}, cell a2 less than 6 × longer than wide (Fig. 5G, H); small, weakly infuscate areas around base and fork of Rs, at crossvein r-m (if present), at base of M_{1+2}, at crossvein m-cu, M_2, and crossvein m-m. Note: the early spring specimens from Shikoku Island have more intensive wing pattern (Fig. 5H), than the later spring specimens, or specimens collected in the other part of Japan (Fig. 5G). The pattern is more intensive in the living specimens, less prominent in the dead ones, and became paler after time.

Abdomen. Grey with reddish tinge, caudal half of tergites and sternites 8 and 9 darker. Abdominal plaques (external remnants of attachment sites of muscles in the pupa) shiny, punctuated (Fig. 36A).

Male terminalia: Reddish grey, directed caudally (Fig. 36A). Tergite 9 fused with gonocoxite at base, fusion suture present (Fig. 37C); tergite 9 with laterally directed, ear-like lobes in dorsal view (Fig. 37A), triangular or bird-head-shaped laterally (Fig. 37C); additional two very small, triangular lobe on posterior margin of tergite 9. Sternite 9 fully membranous (Fig. 37B). Gonocoxite large 1.5–1.6 × longer than tergite 9, without evident ventral lobe (Fig. 37B, C), small protuberance on ventral margin of gonocoxite in some specimen rarely present (Fig. 37C see arrow). Gonostylus simple, generally tapering to distal end (Fig. 37A, C). Aedeagus complex very large, 1.5–1.7 × longer than gonocoxite (Fig. 37D–F); ejaculatory apodeme and sperm pump large, not covered by paramere in lateral view (Fig. 37D–F); interbase simple, tip rounded or sharp, with small lobe dorsally in lateral view (Fig. 37F); dorsal lobe between interbases, membranous, bubble-like; sperm ducts branching from elongation of sperm pump, area darkened (Fig. 37F); aedeagus 2 × as wide as interbase in lateral view; directed ventrally then turned dorsally, almost turning back anteriorly (Fig. 37F); trifid, medial branch shorter than lateral branches (Fig. 37D–E); tips of branches widened and flattened (Fig. 37D–F).

Female terminalia: Cercus and hypopygial valve pale brown (Fig. 36E). Tergite 8, ~ 1.5 × larger than tergite 9 in lateral view (Fig. 38B); very broad in dorsal view, not divided medially (Fig. 38A). Tergite 9 triangular in lateral view, with a small round lobe at middle, with few longer setae (Fig. 38A). Triangular sclerites of tergite 10 variable in size (Fig. 38A), in some specimens partly fused with tergite 10. Cercus simple, tip rounded or weakly pointed; dorsal margin weakly rugged, formed by small pyramidal teeth (Fig. 38A, B). Hypogynial valve long, blade-like, longer than cercus; with pit at base, holding lateral lobes of male tergite 9 during copulation (Fig. 38B). Common spermathecal duct short; spermathecal ducts wide, carrot-shaped, suddenly narrow; inner wall rugged (Fig. 38C); three round spermathecae, with very narrow duct (Fig. 38D).

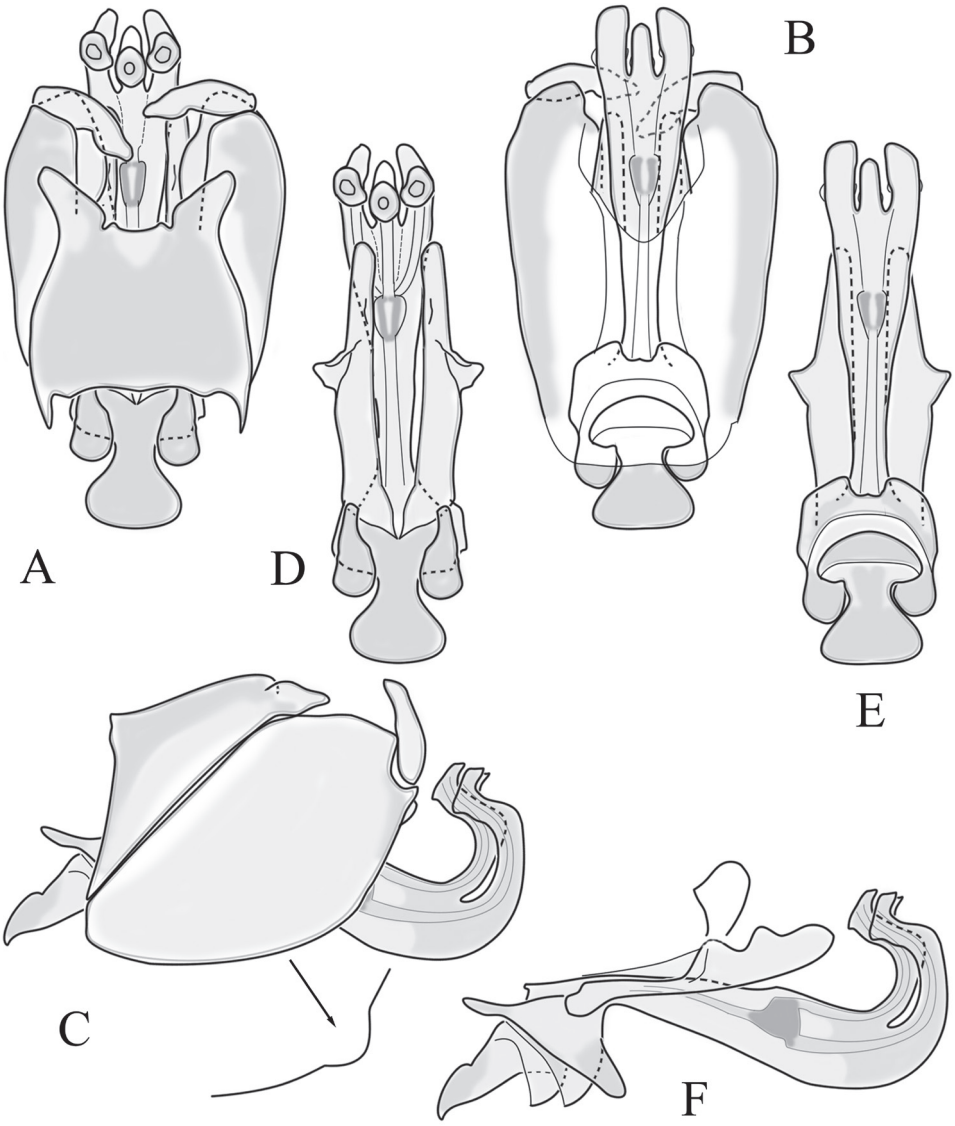

Figure 37. Male genital structures of *Triogma kuwanai* (Alexander, 1913) **A** terminalia, dorsal view **B** terminalia, ventral view **C** terminalia, lateral view, arrow indicating shape variability of gonocoxite margin **D** aedeagus complex, dorsal view **E** aedeagus complex, ventral view **F** aedeagus complex, lateral view.

Distribution. Japan (Fig. 31B) (Hokkaido I, Honshu I, Shikoku I, and Kyushu I) (Oosterbroek 2021). Distribution records of *Triogma kuwanai limbinervis* (Shikoku I) and *T. nimbipennis* transferred to *Triogma kuwanai* (China: Zhejiang and Fujian).

Comments. Alexander (1953a) described the subspecies, *Triogma kuwanai limbinervis*, from Shikoku Island, of which wing markings in some individuals

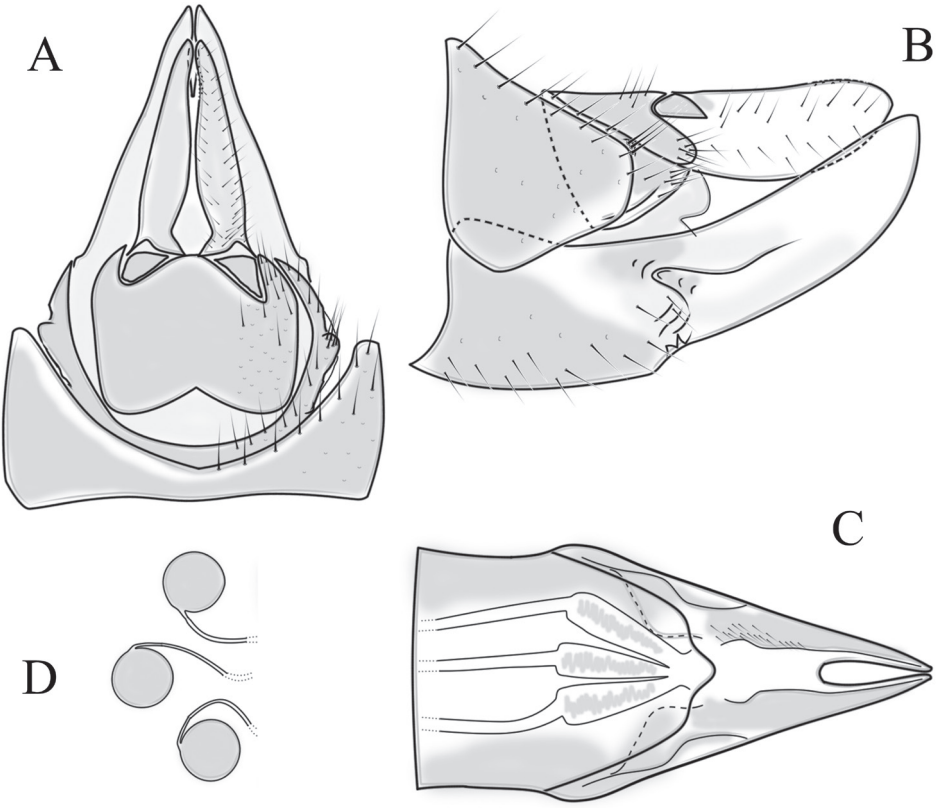

Figure 38. Female genital structures of *Triogma kuwanai* (Alexander, 1913) **A** terminalia, dorsal view **B** terminalia, lateral view **C** sternite 8, hypogynial valve, genital fork, and sperm ducts, inner dorsal view **D** spermathecae.

are more conspicuous than those of *T. k. kuwanai*. In the original description, Alexander noted, "there is evidence of mergence with the typical form – *Triogma kuwanai kuwanai* –, where the wings are unpatterned or virtually so" (Alexander 1953a). *Triogma k. limbinervis* has been referred to as the *T. limbinervis* in the CCW (since 2018) due to its sympatric occurrence with *Triogma kuwanai* in Shikoku Island. This study suggests that wing markings, the diagnostic character of *T. k. limbinervis* (Fig. 5H), appear only in early spring specimens from Shikoku and Kyushu Islands, but do not after early spring in later specimens. It is also observed that wing marking turns paler over time. Some specimens from northern Honshu occasionally have pale wing markings, as well, suggesting variation. These two subspecies do not significantly differ in terms of male and female terminalia, and were not distinguished as different by the barcode sequences. *Triogma k. limbinervis* syn. nov. is therefore synonymised with *Triogma kuwanai*. Another closely related species *T. nimbipennis* Alexander, 1941, was described from China (Zhejiang and Fujian) (Alexander 1941). This species is quite similar to *T. kuwanai*, and shows

a subtle difference in the colour tint: particularly, the wings of *T. nimbipennis* are darker than those of *T. kuwanai*. Alexander (1941) mentioned that *T. nimbipennis* can be considered as a subspecies of *T. kuwanai*. After the morphological comparison of the type specimens of *T. nimbipennis* with *T. kuwanai*, the two species were found not to differ in genital structure, and so *T. nimbipennis* syn. nov. is proposed as a junior synonym of *Triogma kuwanai*.

***Triogma trisulcata* (Schummel, 1829)**
Figs 39, 40

Triogma pulla (Meigen, 1830)

Non-type material examined. **Russia** • 1 ♂, 1 ♀; Leningrad Oblast, Luzhsky District, around Luga City; 58.74°N, 29.85°E; alt. 40 m; 5 Jun. 1954; A.A. Stackelberg leg.; CKLP. **United Kingdom** • 2 ♂; Birmingham, Sutton Park, Longmoor Valley; 52.5635°N, 1.8633° W; alt. 125 m; 30 Apr. 2019; P. Boardman leg.; CKLP.

Supplementary description. Male terminalia. Directed caudally. Tergite 9 fused with gonocoxites at base (Fig. 39C). Tergite 9 lateral parts weakly produced, triangular (Fig. 39A, C); posterior margin bent back under tergite 9, forming W-shaped plate (Fig. 39A). Sternite 9 fully membranous (Fig. 39B). Gonocoxite large ~ 1.5–1.6 × longer than tergite 9, without evident ventral or apical lobe (Fig. 39B, C); inner surface hairy. Gonostylus simple, narrowing to end (Fig. 39A, C). Aedeagus complex 1.4 × longer than gonocoxite (Fig. 39C); ejaculatory apodeme medium size, not covered by paramere in lateral view (Fig. 39F); interbase weakly curve dorsally, with small notch at tip in lateral view (Fig. 39F); dorsal lobe between interbases, membranous, bubble-like; sperm ducts branching from elongation of sperm pump, branching area darker (Fig. 39E, F); aedeagus trifid, as wide as interbase at mid-length in lateral view, aedeagus directed ventrally, just tip turning back dorsally (Fig. 39F); medial branch shorter than lateral branches (Fig. 39D–F).

Female terminalia: Tergite 8, ~ 2 × wider than tergite 9 in lateral view (Fig. 40B); not divided medially, posterior part partly membranous with a few hairs (Fig. 40A). Tergite 9 rectangular in lateral view (Fig. 40B). Triangular of tergite 10 large, fused with tergite 10 (Fig. 40A). Cercus simple, with distinct rugged area at tip; formed by short pyramid teeth (Fig. 40A, B); ventral margin with small, rounded notch at 1/3 of length. Hypogynial valve long, blade-like, shorter than cercus; with transverse ditch at base, holding lateral lobes of male tergite 9 during copulation (Fig. 40B). Common spermathecal duct short; spermathecal ducts carrot-shaped, without clear pattern; suddenly narrow (Fig. 40C); three spermathecae large, irregularly spherical, with comparably long and curved duct (Fig. 40D).

Distribution. Palearctic species, with a wide distribution range in Europe, except the southern parts. Previously reported from Austria, Belgium, Czech Re-

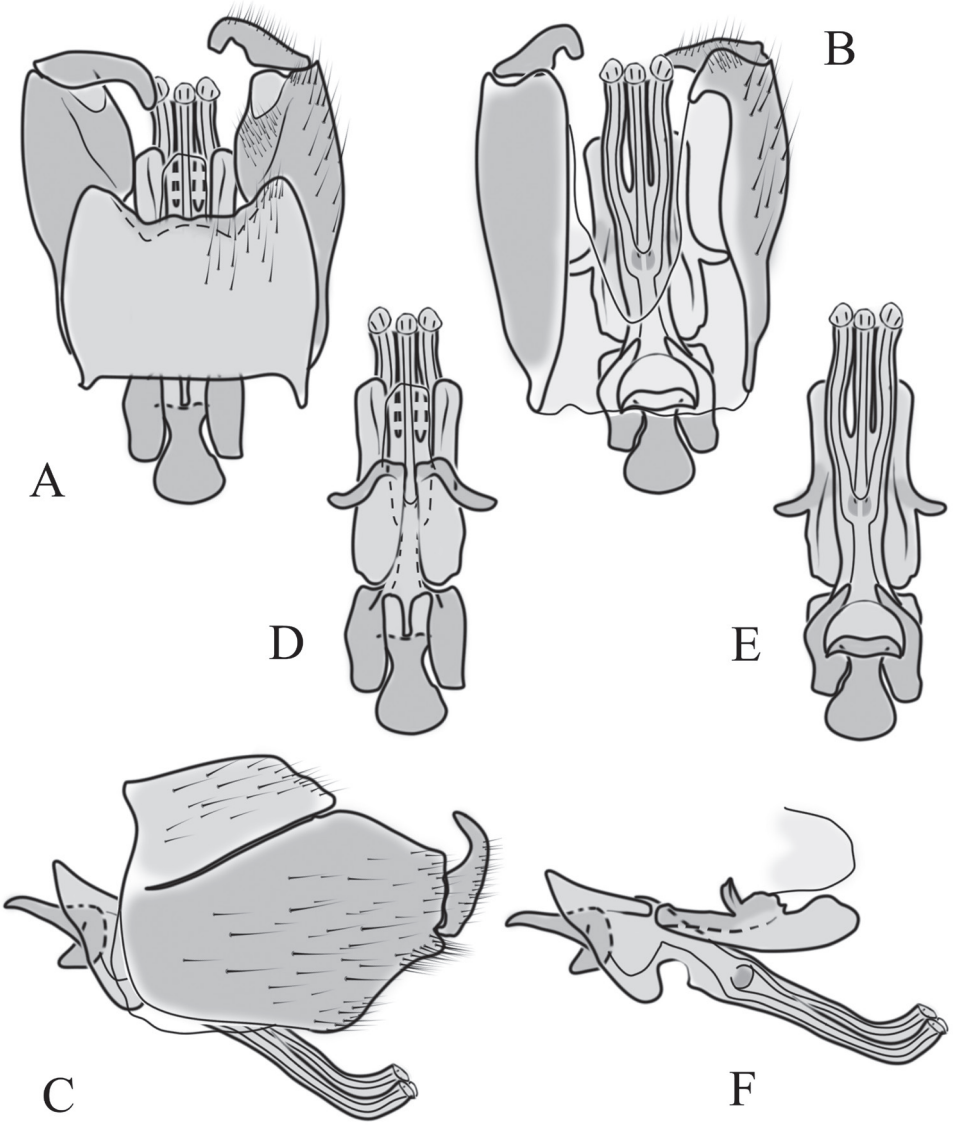

Figure 39. Male genital structures of *Triogma trisulcata* (Schummel, 1829) **A** terminalia, dorsal view **B** terminalia, ventral view **C** terminalia, lateral view **D** aedeagus complex, dorsal view **E** aedeagus complex, ventral view **F** aedeagus complex, lateral view.

public, Denmark, Estonia, Finland, France, Germany, Great Britain, Hungary, Italy, Latvia, Lithuania, Netherlands, Norway, Poland, Romania, Russia (North and Central European Russia), Slovakia, Sweden, and Switzerland. It was reported from Eastern Palearctic, but so far only from East Siberia (Irkutsk Oblast), Russia (Oosterbroek 2021).

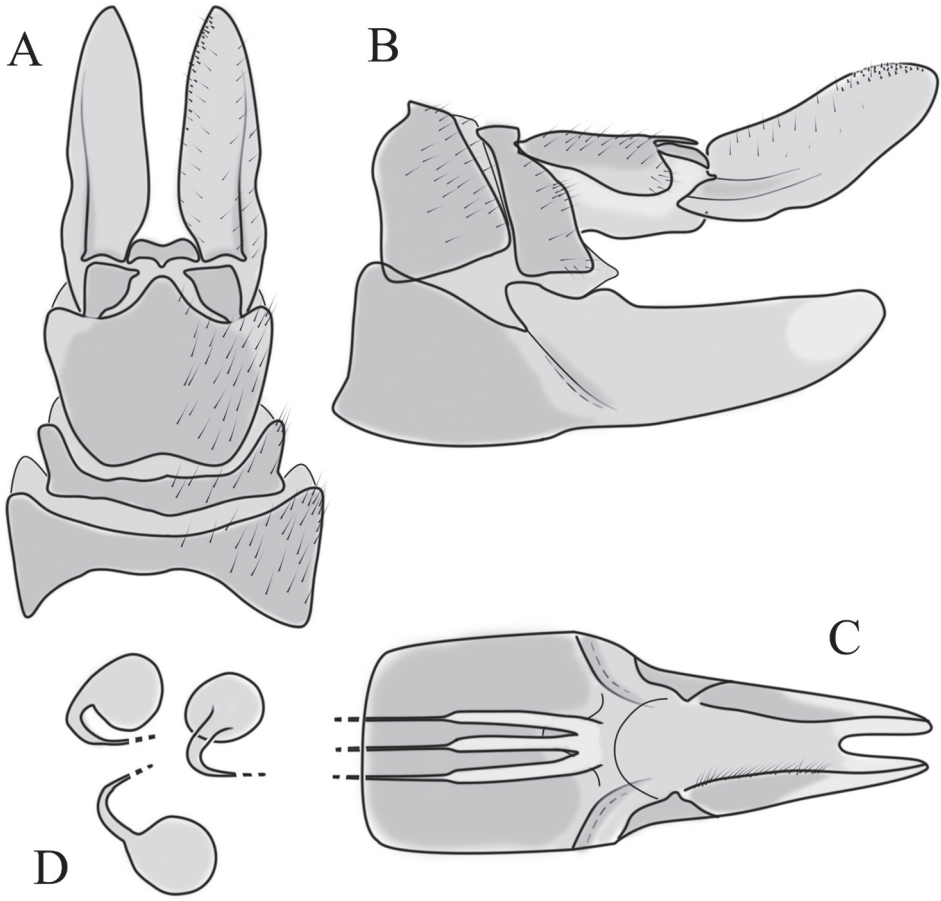

Figure 40. Female genital structures of *Triogma trisulcata* (Schummel, 1829) **A** terminalia, dorsal view **B** terminalia, lateral view **C** sternite 8, hypogynial valve, and sperm ducts, inner dorsal view **D** spermathecae.

Acknowledgements

We greatly appreciate Dr. Fenja Brodo (Ottawa, Canada), Dr. Jukka Salmela (Regional Museum of Lapland, Rovaniemi, Finland), Esko Viitanen (Espoo, Finland), and Pete Boardman (Natural England, Telford, United Kingdom) for providing some important materials for examination, and to all other contributors who provided us the cylindrotomine specimens examined herein. We thank Dr. Toshiharu Mita (Kyushu University, Fukuoka, Japan) for loaning the type specimen of *Diogma caudata* and Dr. Ximo Mengual (Zoological Research Museum Alexander Koenig, Bonn, Germany) for providing information about type specimens of *Triogma nimbipennis*.

This study was supported by the International Research Fellow of the Japan Society for the Promotion of Science, Grant Numbers: PE18038, P21094 to L.-P. Kolcsár, and also by Yoshida Scholarship Foundation, a research grant for Environmental Field Re-

search by the Asahi Glass Foundation, and JSPS KAKENHI Grant Numbers 14J00160, 18H06077, and 20K15852 to Y. Imada.

References

Alexander CP (1913) Report on a collection of Japanese crane-flies (Tipulidae), with a key to the species of *Ptychoptera*. Canadian Entomologist 45: 285–295, 313–322. https://doi.org/10.4039/Ent45197-7

Alexander CP (1919) Undescribed species of Japanese crane-flies (Tipulidae, Diptera). Annals of the Entomological Society of America 12: 327–348. https://doi.org/10.1093/aesa/12.4.327

Alexander CP (1920a) The crane-flies of New York. Part II. Biology and phylogeny. Memoirs, Cornell University Agricultural Experiment Station 38: 691–1133. https://doi.org/10.5962/bhl.title.33641

Alexander CP (1920b) New or little-known crane-flies from Japan (Tipulidae, Diptera). Transactions of the American Entomological Society 46: 1–26.

Alexander CP (1924) New or little-known crane flies from northern Japan (Tipulidae, Diptera). Philippine Journal of Science 24: 531–611.

Alexander CP (1928) Diptera. Family Tipulidae, Subfam. Cylindrotominae. Genera Insectorum 187: 1–16.

Alexander CP (1931) New or little-known Tipulidae from eastern Asia (Diptera). IX. Philippine Journal of Science 44: 339–368.

Alexander CP (1932) New or little-known Tipulidae from eastern Asia (Diptera). X. Philippine Journal of Science 49: 105–136.

Alexander CP (1941) New or little-known Tipulidae from eastern Asia (Diptera). XLIII. Philippine Journal of Science 73: 375–420.

Alexander CP (1949) New or little-known Tipulidae (Diptera). LXXXIII. Oriental-Australasian species. Annals and Magazine of Natural History 12(2): 178–205. https://doi.org/10.1080/00222935308654479

Alexander CP (1953a) Records and descriptions of Japanese Tipulidae (Diptera). Part I. The crane-flies of Shikoku. I. Philippine Journal of Science 82: 21–75.

Alexander CP (1953b) The insect fauna of Mt. Ishizuchi and Omogo Valley, Iyo, Japan. The Tipulidae (Diptera). Transactions of the Shikoku Entomological Society 3: 71–83.

Alexander CP (1966) The crane-fly fauna of the southern Kuriles (Tipulidae, Diptera). Mushi 39: 119–126.

Alexander CP, Alexander MM (1973) Tipulidae. In: Delfinado MD, Hardy DE (Eds) Catalog of the Diptera of the Oriental Region I, University Press of Hawaii, Honolulu, 10–224.

Bartsch H, Cederberg B, Engelmark R, Hedmark K, Viklund B (2005) Diptera. In: Gardenfors U (Ed.) The 2005 red list of Swedish species. Swedish Species Information Centre, Uppsala, 325–337.

Boldgiv B (2006) Spatial and genetic patterns of crane flies (Diptera, Tipuloidea) from Lake Hovsgol region, Mongolia. PhD Thesis; Faculties of the University of Pennsylvania, USA. https://repository.upenn.edu/dissertations/AAI3246143

Brodo F (1967) A review of the subfamily Cylindrotominae in North America (Diptera, Tipulidae). The University of Kansas Science Bulletin 47: 71–115.

Cumming JM, Wood DM (2017) Adult morphology and terminology. In: Kirk-Spriggs AH, Sinclair BJ (Eds) Manual of Afrotropical Diptera. Volume 1. Introductory chapters and keys to Diptera famlies. Suricata 4. South African National Biodiversity Institute, Pretoria, 107–151.

Edwards FW (1938) British short-palped craneflies. Taxonomy of adults. Transactions of the Society for British Entomology 5: 1–168.

Esaki T (1950) Diptera. Iconographia Insectorum Japonicorum, Ed. 2. Hokuryukan Ltd, Tokyo, 1500 pp.

Devyatkov VI (2021) Data on the crane fly fauna of the families Cylindrotomidae, Ptychopteridae and Tanyderidae (Diptera) of eastern and northeastern Kazakhstan. Euroasian Entomological Journal 20: 49–51. https://doi.org/10.15298/euroasentj.20.1.07

Folmer O, Black M, Hoeh W, Lutz R, Vrijenhoek R (1994) DNA primers for amplification of mitochondrial cytochrome c oxidase subunit I from diverse metazoan invertebrates. Molecular Marine Biology and Biotechnology 3: 294–297.

Gelhaus JK, Podenas S, Oyunchuluun Y, Podeniene V (2007) The crane fly family Cylindrotomidae (Diptera), newly recorded for Mongolia. Proceedings of the Academy of Natural Sciences of Philadelphia 156: 59–69. https://doi.org/10.1635/0097-3157(2007)156[59:TCFFCD]2.0.CO;2

Greenwalt DE, Bickel DJ, Kerr PH, Curler GR, Brown B, de Jong H, Fitzgerald SJ, Dikow T, Tkoc M, Kehlmaier C, Amorim DDS (2019) Diptera of the middle Eocene Kishenehn Formation. I. Documentation of diversity at the family level. Palaeontologia Eletronica 22(2): 1–56. https://doi.org/10.26879/891

Guindon S, Gascuel O (2003) PhyML, A simple, fast and accurate algorithm to estimate large phylogenies by maximum likelihood. Systematics Biology 52: 696–704. https://doi.org/10.1080/10635150390235520

Imada Y (2020) Moss mimesis *par excellence*: integrating previous and new data on the life history and larval ecomorphology of long-bodied craneflies (Diptera: Cylindrotomidae: Cylindrotominae). Zoological Journal of the Linnean Society 193(4): 1156-1204 https://doi.org/10.1093/zoolinnean/zlaa177

Ishida H (1955) The catalogue of the Japanese Tipulidae, with the keys to the genera and subgenera. II. *Tipula* (part) and Cylindrotominae. Annual Report of the Hyogo Agricultural College (Kenkyu Shuroku, 1955) 5: 59–77.

Kania-Kłosok I, Nel A, Szwedo J, Jordan-Stasiło W, Krzemiński W (2021) Phylogeny and Biogeography of the Enigmatic Ghost Lineage Cylindrotomidae (Diptera: Nematocera). Scientific Reports 11: e13916. https://doi.org/10.1038/s41598-021-91719-w

Kato D, Suzuki Y (2017) A revised list of the crane flies of Kanagawa, Japan, with newly recorded species (Diptera, Tipuloidea). Makunagi/Acta Dipterologica 28: 7–24.

Kim J, Bae YJ (2020) First Record of the Genus *Liogma* (Diptera: Cylindrotomidae) in Korea. Entomological Research Bulletin 36(2): 89–91.

Kolcsár LP, Török E, Keresztes L (2018) First record of *Cylindrotoma distinctissima* (Meigen, 1818) from Serbia and new data on the occurrence of Cylindrotomidae (Diptera) in Bul-

garia and Romania. Fragmenta Faunistica 60: 107–112. https://doi.org/10.3161/00159301FF2017.60.2.107

Krzemiński W, Blagoderov V, Dany AZAR, Lukashevich E, Szadziewski R, Wedmann S, André NEL, Collomb FM, Waller A, Nicholson DB (2019) True flies (Insecta: Diptera) from the late Eocene insect limestone (Bembridge Marls) of the Isle of Wight, England, UK. Earth and Environmental Science Transactions of the Royal Society of Edinburgh: 110(3–4): 495–554. https://doi.org/10.1017/S1755691018000464

Librado P, Rozas J (2009) DnaSP v5, a software for comprehensive analysis of DNA polymorphism data. Bioinformatics 25: 1451–1452. https://doi.org/10.1093/bioinformatics/btp187

Mukkala VM, Haarto A, Koponen S, Mukkala L, Rinne V, Salmela J (2005) On insects, arachnids and other invertebrates in Kivistönmäki, Ilmajoki. W-album 2: 1–34. https://doi.org/10.13140/RG.2.1.1584.4320

Nakamura T (2001) Cylindrotomidae of Tochigi Prefecture, Japan (Diptera, Tipulidae). Bulletin of the Tochigi Prefectural Museum 18: 23–30.

Nakamura T (2005) Tipulidae. In: Kawai T, Tanida T (Eds) Aquatic insects of Japan, Manual with keys and illustrations. Tokai University Press, Kanawaga, 671–716.

Nakamura T (2014) Cylindrotomidae. In: Nakamura T, Saigusa T, Suwa M (Eds) Catalogue of the insects of Japan, Volume 8 Diptera (Part 1 Nematocera - Brachycera Aschiza), Touka Shobo, Fukuoka, 54.

Oosterbroek P, Dufour C, Pilipenko VE (2001) On the presence of *Dolichopeza* (subgenus *Oropeza*) in the westpalaearctic (Diptera, Tipulidae). Bulletin de la Societe Neuchateloise des Sciences Naturelles 124: 119–123.

Oosterbroek P (2021) Catalogue of the Crane flies of the World (Insecta, Diptera, Nematocera, Tipuloidea). https://ccw.naturalis.nl/index.php [2021.09.07]

Paramonov NM (2004a) *Diogma caudata* Takahashi, 1960 new to the fauna of Russia (Diptera, Cylindrotomidae). Zoosystematica Rossica 12: e258.

Paramonov NM (2004b) To the fauna Cylindrotomidae (Diptera, Nematocera) of the Asian part of Russia. Tomsk State University Journal of Biology 11: 69.

Paramonov NM (2005) *Diogma dmitrii* sp. n., a new species of cylindrotomid crane-flies (Diptera, Cylindrotomidae) from the Caucasus. Entomologicheskoe Obozrenie 84: 215–218.

Paramonov NM (2006) Cylindrotomidae. In: Leley AS (Ed.) Key to the Insects of Russian Far East. 6. Diptera and Siphonaptera. 4. Supplement. Dalnauka, Vladivostok, 887–889.

Paramonov NM (2019) Superfamily Tipuloidea (Diptera), new taxon for Jewish Autonomous Region of Russia. Amurian Zoological Journal 11: 119–125. https://doi.org/10.33910/2686-9519-2019-11-2-119-125

Paramonov NM, Lobkova LE (2013) New host plants for larvae of *Cylindrotoma distinctissima distinctissima* (Meigen, 1818) (Diptera: Cylindrotomidae). Far Eastern Entomologist 258: 6–8.

Paramonov NM, Pilipenko VE (2021) New synonym and new records of craneflies (Diptera: Tipuloidea) in China. Russian Entomological Journal 30(2): 182–188. https://doi.org/10.15298/rusentj.30.2.13

Peus F (1952) Cylindrotomidae. In: Lindner E (Ed.) Die Fliegen der palaearktischen Region, 3, Lief, 1–80.

Pilipenko VE, Sidorenko VS (2004) International biodiversity observation year (IBOY), Crane flies (Diptera, Tipulidae, Cylindrotomidae) of the forest ecosystems of Primorye. Far Eastern Entomologist 136: 11–12.

Polevoi AV (2006) New data on the Diptera fauna of Kivach Nature Reserve. Trudy Karelskogo Nauchnogo Tsentra RAN (Transactions of the Karelian Research Centre of the Russian Academy of Science) 2006: 95–104.

Posada D, Crandall KA (1998) Modeltest, testing the model of DNA substitution. Bioinformatics 14: 817–818. https://doi.org/10.1093/bioinformatics/14.9.817

Ribeiro GC (2009) The Neotropical genus *Stibadocerina* Alexander and its phylogenetic relationship to other Stibadocerinae genera, further evidence of an ancestral trans-Pacific biota (Diptera, Cylindrotomidae). Systematic Entomology 24: 324–333. https://doi.org/10.1111/j.1365-3113.2008.00454.x

Sandström J (2008) ArtDatabanken: Faktablad, *Diogma caudata* – nordlig strimharkrank. https://www.artdatabanken.se/ [2020-09-01]

Salmela J (2008) Semiaquatic fly (Diptera, Nematocera) fauna of fens, springs, headwater streams and alpine wetlands in the northern boreal ecoregion, Finland. *W-album* 6: 1–63.

Salmela J (2012a) Annotated list of Finnish crane flies (Diptera, Tipulidae, Limoniidae, Pediciidae, Cylindrotomidae). Entomologica Fennica 22: 219–242. https://doi.org/10.33338/ef.5002

Salmela J (2012b) Biogeographic patterns of Finnish crane flies (Diptera, Tipuloidea). Psyche 2012: 1–19. https://doi.org/10.1155/2012/913710

Salmela J, Petrašiūnas A (2014) Checklist of the infraorder Tipulomorpha (Trichoceridae, Tipuloidea) (Diptera) of Finland. ZooKeys 441: 21–36. https://doi.org/10.3897/zookeys.441.7533

Sasakawa M (2008) A list of the Dipterous specimens (Insecta) deposited in the Osaka Museum of Natural History. Shi Zenshi Kenkyu. Occasional from the Osaka Museum of Natural History 3(8): 127–136.

Sidorenko VS (1999) Cylindrotomidae. In: Ler PA (Ed.) Key to the insects of Russian Far East. Vol. VI. Diptera and Siphonaptera. Part 1. Dalnauka, Vladivostok, 68–70.

Siitonen O (1984) *Diogma caudata* Takahashi, 1960 Suomella uusi vaaksiainen (Cylindrotomidae). Notulae entomologica 64(4): 203.

Sinclair BJ, Dorchin N (2010) Isoptera, Embioptera, Neuroptera, Mecoptera, Raphidioptera and Diptera types in ZFMK. Bonn Zoological Bulletin 58: 49–88.

Soós A, Oosterbroek P (1992) Family Cylindrotomidae. In: Soós A, Papp L, Oosterbroek P (Eds) Catalogue of Palaearctic Diptera 1. Hungarian Natural History Museum, Budapest, 179–182.

Takahashi M (1960) A revision of Japanese Cylindrotominae (Diptera, Tipulidae). Transactions of the Shikoku Entomological Society 6: 81–91.

Thompson JD, Higgins DG, Gibson TJ (1994) ClustalW, improving the sensitivity of progressive multiple sequence alignment through sequence weighting, position-specific gap penalties and weight matrix choice. Nucleic Acids Research 22: 4673–4680. https://doi.org/10.1093/nar/22.22.4673

Ujvárosi L, Kolcsár LP, Vaida R (2011) Additions to the Cylindrotomidae (Insecta, Diptera) fauna of Bulgaria and Romania. Entomologica Romanica 16: 47–50.

Yang X (1991) Catalogue of the insect type specimens preserved in the insect collections of the Institute of Zoology, Academia Sinica. China agricultural press, Beijing, 163 pp.

ZooKeys 1083: 89–107 (2022)
doi: 10.3897/zookeys.1083.76887
https://zookeys.pensoft.net

RESEARCH ARTICLE

A peer-reviewed open-access journal
ZooKeys
Launched to accelerate biodiversity research

Comparative analysis of the mitogenomes of two *Corydoras* (Siluriformes, Loricarioidei) with nine known *Corydoras*, and a phylogenetic analysis of Loricarioidei

Cheng-He Sun[1,2], Qi Huang[1], Xiao-Shu Zeng[1], Sha Li[3,4], Xiao-Li Zhang[1], Ya-Nan Zhang[1], Jian Liao[1], Chang-Hu Lu[2], Bo-Ping Han[1], Qun Zhang[1]

1 *Department of Ecology and Institute of Hydrobiology, Jinan University, Guangzhou 510632, China* **2** *College of Biology and the Environment, Nanjing Forestry University, Nanjing 210037, China* **3** *Chinese Sturgeon Research Institute, China Three Gorges Corporation, Yichang 443100, Hubei, China* **4** *Hubei Key Laboratory of Three Gorges Project for Conservation of Fishes, Yichang 443100, Hubei, China*

Corresponding author: Qun Zhang (tqzhang@jnu.edu.cn)

Academic editor: Tihomir Stefanov | Received 22 October 2021 | Accepted 6 January 2022 | Published 24 January 2022

http://zoobank.org/7B1D7ADC-5E9D-4387-9EB8-4C1A6081E6A3

Citation: Sun C-H, Huang Q, Zeng X-S, Li S, Zhang X-L, Zhang Y-N, Liao J, Lu C-H, Han B-P, Zhang Q (2022) Comparative analysis of the mitogenomes of two *Corydoras* (Siluriformes, Loricarioidei) with nine known *Corydoras*, and a phylogenetic analysis of Loricarioidei. ZooKeys 1083: 89–107. https://doi.org/10.3897/zookeys.1083.76887

Abstract

Corydoras is a speciose catfish genus from South America with widely investigated phylogenetic and evolutionary relationships. The complete mitogenomes of *C. aeneus* and *C. paleatus* were sequenced, assembled, and annotated using next-generation sequencing. The genome arrangements, gene contents, genome structures, base compositions, evolutionary features, codon usage, and tRNA structures of the two mitogenomes were compared and analyzed with nine published mitogenomes of *Corydoras*. Phylogenetic analysis was performed using concatenated nucleotide sequences with 13 protein-coding genes and two rRNAs with 44 mitogenomes of Siluriformes. These results provide information on the mitogenomes of eleven *Corydoras* species and evolutionary relationships within the suborder Loricarioidei, which may be applicable for further phylogenetic and taxonomic studies on Siluriformes and Loricarioidei.

Keywords

Corydoras aeneus, *Corydoras paleatus*, genome sequencing, mitochondrial DNA, Phylogenetic tree

Introduction

Fish mitochondrial DNA shares characteristics with other vertebrate mitochondrial DNA (Anderson et al. 1981; Manchado et al. 2007; Xu et al. 2011), e.g., small molecular weight, simple structure, and compact arrangement. It exists in the form of a covalently closed circular supercoil structure and contains heavy and light chains. The genetic material can be replicated, transcribed, and translated independently from the nuclear DNA in the cell. With few exceptions, fish mitochondrial DNA comprises 13 protein-coding genes (PCGs), 22 transfer RNA genes, two ribosomal RNA genes, original region of light-strand replication, and control region (D-loop) (Ojala et al. 1981; Gadaleta et al. 1989; Wolstenholme 1992 Simon et al. 1994; De Rijk et al. 1995). The mitochondrial DNA mutates rapidly, nearly 10-fold faster than the nuclear DNA, and the fragment length and evolution rate differ for each gene, providing molecular evidence for studying different species (Brown et al. 1979; Pesole et al. 1999). In addition, mitochondrial DNA is highly heterogeneous and harbors the genetic characteristics associated with maternal traits (O'Brien 1971; Michot et al. 1990; Bartlett and Davidson 1991; Meyer 1993; Beheregaray and Sunnucks 2001; Liu et al. 2002; Yoshizawa and Johnson 2003). Hence, mitochondrial DNA can be used to identify fish groups at the molecular level and explore geographic distribution, species origin, and species differentiation (Avise et al. 1987; Kai et al. 2002; Hrbek et al. 2007). As fish are a large group with a complex origin in the vertebrate subphylum, studies on their phylogenetic and evolutionary relationships performed using traditional morphological methods often provide limited information. With advances in biotechnology, complete mitochondrial genome sequences have been determined as a useful tool to study the phylogeny and phylogeography of fish (Bermingham and Avise 1986; Xu et al. 2020).

Corydoras Lacépède, 1803, belongs to the order Siluriformes, suborder Loricarioidei, family Callichthyidae. *Corydoras* contains 175 valid species, which makes it the most species-rich genus of the family Callichthyidae (Lima and Britto 2020; Tencatt et al. 2021). The body of these fish is covered with bone plates, and the pectoral and dorsal fins have hard spines that can be used for protection. In addition, *Corydoras* can use the back end of their intestines, which is rich in blood vessels, to obtain oxygen from air taken in at the water surface, enabling survival under environmental stress, such as drought or insufficient dissolved oxygen content in water. *Corydoras* catfish are benthic omnivorous fish (Moreira et al. 2016b, 2017; Liu et al. 2019b, 2019c; Saitoh et al. 2003). Typically, *Corydoras* is active only during feeding, and otherwise hide while resting. *Corydoras* is primarily distributed in South America. Most species of *Corydoras* gather in the middle and lower reaches of the river where the current is relatively gentle, whereas a few live in the upper reaches of the river in rapids (Saitoh et al. 2003; Liu et al. 2019c). *Corydoras* is also valuable as an ornamental fish. Some phylogenetic relationships in *Corydoras* remain unclear. The number of species reported in relevant articles is small, which is not sufficient to reflect the phylogenetic variety of the genus *Corydoras* (Alexandrou et al. 2011; Lujan et al. 2015; Roxo et al. 2019). Therefore, a comprehensive understanding of the relationships between different species of *Corydoras* is essential.

In this study, the complete mitogenomes of two species of *Corydoras* (Bronze corydoras *C. aeneus* Gill, 1858 and peppered corydoras *C. paleatus* Jenyns, 1842) were sequenced, assembled, and annotated. The genome organization, gene contents, repeat sequences, and tRNA structures of the eleven mitogenomes were compared and analyzed in combination with nine published mitogenomes of *Corydoras* (Saitoh et al. 2003; Moreira et al. 2016a, 2017; Liu et al. 2019a, b, c, d; Chen et al. 2020; Lv et al. 2020). Determining the similarities and differences in gene orders, genetic structures, base compositions, evolutionary features, and codon usage can provide molecular insights into the taxonomic and phylogenetic characteristics of the order Siluriformes. Based on these data, and those obtained from the NCBI database, we examined the phylogenetic relationships among species in the suborder Loricarioidei. We also evaluated the mitogenomes of eleven species of *Corydoras* and evolutionary relationships within the suborder Loricarioidei, thereby providing a valuable basis for further evolutionary studies on Siluriformes and Loricarioidei.

Materials and methods

Sample collection and identification

Single specimens of *C. aeneus* and *C. paleatus* were collected from the temple of Confucius flower and wood fish market, Nanjing city, Jiangsu province, China (32°0'27.1"N, 118°50'11.5"E) in June 2020 and identified based on their morphological characteristics, according to the latest taxonomic classification of fish (Popazoglo and Boeger 2000; Huysentruyt and Adriaens 2005a, b). Their geographic data and specific origins were unknown. All fresh tissues were immediately stored at -80 °C in 95% ethanol until DNA extraction. Total DNA was extracted from the muscle tissue using a TIANamp Marine Animals DNA Kit DP324 (Tiangen Biotech Co., Ltd., Beijing, China) according to the manufacturer's instructions. DNA integrity and purity were evaluated by 1% agarose gel electrophoresis, and DNA purity was determined with a NanoDrop 2000 (NanoDrop Technologies, Wilmington, DE, USA). DNA concentrations were quantified using a Qubit^{R} 2.0 Fluorometer (Life Technologies, Carlsbad, CA, USA). To ensure the accuracy of morphological identification, COI primers were designed based on the latest DNA barcoding database (NCBI and FishBase) and were amplified, sequenced, and compared. The COI sequences are provided in the Suppl. material 1. The results of the sequence alignment verify the accuracy of the morphological identification.

Genome sequencing and assembly

Next-generation sequencing was performed to determine the complete mitogenome sequence of the two species of *Corydoras*. The DNA libraries were sequenced on an Illumina sequencing platform by Novogene Co., Ltd. (Beijing, China). Briefly, the total DNA genome was quantified and fragmented into 250-base pair (bp) fragments using a Covaris M220 ultrasonic crushing system (Woburn, MA, USA) followed by whole-

genome shotgun sequencing. According to the manufacturer's instructions, a library was constructed based on two indices using an Illumina TruSeq DNA PCR-Free HT kit (San Diego, CA, USA). An Illumina Novaseq 6000 platform was used for sequencing of 150 paired-end reads approximately 4 Gb in size. Clean reads were generated as previously described, and the remaining high-quality reads were assembled using SPADES V3.15.2 (Bankevich et al. 2012) (http://cab.spbu.ru/software/spades/) and SOAPDENOVO2 V2.01 (Luo et al. 2012) software. The preliminary assembly results were compared with the NT database, and looped sequences annotated as mitochondrial genomes were screened. CAP3 was used to merge the splicing results from the two software programs, and the assembly results were compared with those of related species using MUMMER v3.23 (Delcher et al. 2003). The mitogenome composition was confirmed, and a complete, high-quality map of the mitochondrial genome was obtained.

Genome annotation and analysis

The tRNA genes were verified using tRNASCAN-SE V1.3.1 (Lowe and Eddy 1997) with default settings for the vertebrate mitochondrial genetic code. The software, which integrates multiple analysis tools, can identify 99% of the tRNA genes with a very low number of false positives and predict the secondary structure of tRNAs. Protein-coding regions were re-identified using GLIMMER V3.0 (Ingram et al. 2009), and manual comparisons were performed using the SEQMAN program of LASERGENE V7.1 (Burland 2000) (DNAStar, Inc., Madison, WI, USA) based on the PCGs of nine species of *Corydoras* and translated into putative proteins via GenBank. The non-coding RNAs were verified using RFAM V12.0 (Griffiths-Jones et al. 2003) and INFERNAL V1.1 (Nawrocki and Eddy 2013). The rRNA genes were assumed to extend to the boundaries of flanking genes, similar to the homologous regions of other published mitogenomes of *Corydoras* in GenBank. The MITOS WebServer (http://mitos2.bioinf.uni-leipzig.de/index.py) and MitoFish (Iwasaki et al. 2013) (http://mitofish.aori.u-tokyo.ac.jp/) online tools were used for the final annotation of the entire mitogenome sequence of the two species of *Corydoras*, and the annotated mitogenomes were compared with nine published mitogenomes of *Corydoras*. Base compositions, genetic distances, and relative synonymous codon usage values were determined using MEGA V7.0 (Kumar et al. 1994). A graph comparing the relative synonymous codon usage was drawn using PHYLOSUITE V1.2.2 (Zhang et al. 2020). Strand asymmetry was analyzed using the formula: AT-skew = (A – T)/(A + T). The numbers of non-synonymous (Ka) and synonymous (Ks) substitutions and the ratio of Ka/Ks and nucleotide diversity for the nine species of *Corydoras* were calculated using DNASP 5.1 (Librado and Rozas 2009). The MitoFish (http://mitofish.aori.u-tokyo.ac.jp/) online tool was used to generate circular mitogenome maps.

Phylogenetic analysis

Phylogenetic trees for the eleven mitogenomes of *Corydoras* within the family Callichthyidae and Suborder Loricarioidei were constructed by aligning 13 PCGs and two

rRNA sequences with those of 42 species of Loricarioidei, 29 species from Loricariidae, and one species from Trichomycteridae (Table 1). The mitogenomes of *Pterocryptis cochinchinensis* (Resende et al. 2016) and *Silurus asotus* (Nakatani et al. 2011) (accession no. NC_027107.1 and NC_015806.1, respectively, suborder Siluroidei) were included as outgroups to root the Loricarioidei tree. All operations were performed in PHYLOSUITE V1.2.2 (Zhang et al. 2020) software package. The nucleotide sequences of 13 PCGs from 44 mitogenomes were aligned in batches with MAFFT V7.313 (Katoh and Standley 2013) (https://mafft.cbrc.jp/alignment/server/) using the

Table 1. Information on 44 Siluriformes species evaluated in the study.

No.	Suborder	Family	Taxa	GenBank accession no.	Length (bp)	Location/Reference
1	Loricarioidei	Callichthyidae	*Corydoras aeneus*	MZ571336	16604	This study
2			*Corydoras agassizii*	MN641875.1	16538	Lv et al. 2020
3			*Corydoras arcuatus*	NC_049096.1	16177	Liu et al. 2019d
4			*Corydoras duplicareus*	NC_049095.1	16632	Liu et al. 2019a
5			*Corydoras nattereri*	KT239008.1	16557	Moreira et al. 2016a
6			*Corydoras paleatus*	MZ571337	16320	This study
7			*Corydoras panda*	NC_049097.1	16398	Liu et al. 2019b
8			*Corydoras rabauti*	NC_004698.1	16711	Saitoh et al. 2003
9			*Corydoras schwartzi*	KT239007.1	15671	Moreira et al. 2017
10			*Corydoras sterbai*	NC_048967.1	16520	Liu et al. 2019c
11			*Corydoras trilineatus*	NC_049098.1	15359	Chen et al. 2020
12			*Hoplosternum littorale*	KX087170.1	16262	Parente et al. 2018
13		Loricariidae	*Ancistomus snethlageae*	KX087166.1	16464	Moreira et al. 2017
14			*Ancistrus cryptophthalmus*	MF804392.1	16333	Lv et al. 2020
15			*Ancistrus multispinis*	KT239006.1	16539	Moreira 2018
16			*Ancistrus temminckii*	NC_051963.1	16439	Meng et al. 2021
17			*Aphanotorulus emarginatus*	KT239019.1	16597	Moreira et al. 2017
18			*Baryancistrus xanthellus*	KX087167.1	16167	Moreira et al. 2017
19			*Dekeyseria amazonica*	KX087168.1	16409	Moreira 2018
20			*Hemipsilichthys nimius*	KT239011.1	16477	Moreira et al. 2017
21			*Hisonotus thayeri*	KX087173.1	16269	Moreira et al. 2017
22			*Hypancistrus zebra*	KX611143.1	16202	Magalhães et al. 2017
23			*Hypoptopoma incognitum*	NC_028072.1	16313	Moreira et al. 2016b
24			*Hypostomus affinis*	KT239013.1	16330	Moreira et al. 2017
25			*Hypostomus ancistroides*	NC_052710.1	16422	Rocha-Reis et al. 2020
26			*Hypostomus francisci*	NC_045188.1	16916	Pereira et al. 2019
27			*Hypostomus plecostomus*	NC_025584.1	16562	Liu et al. 2016
28			*Kronichthys heylandi*	KT239014.1	16632	Moreira et al. 2017
29			*Loricaria cataphracta*	KX087174.1	16831	Moreira et al. 2017
30			*Loricariichthys castaneus*	KT239015.1	16521	Moreira et al. 2017
31			*Loricariichthys platymetopon*	KT239018.1	16521	Moreira et al. 2017
32			*Neoplecostomus microps*	KX087175.1	16523	Moreira et al. 2017
33			*Otocinclus affinis*	MT323116.1	16501	Zhang et al. 2021
34			*Pareiorhaphis garbei*	KX087178.1	16630	Moreira et al. 2017
35			*Parotocinclus maculicauda*	KX087179.1	16541	Moreira et al. 2017
36			*Peckoltia furcata*	KX087180.1	16497	Moreira et al. 2017
37			*Pterygoplichthys anisitsi*	KT239003.1	16636	Parente et al. 2017
38			*Pterygoplichthys disjunctivus*	NC_015747.1	16667	Nakatani et al. 2011
39			*Pterygoplichthys pardalis*	KT239016.1	16822	Moreira et al. 2017
40			*Schizolecis guntheri*	KT239017.1	16611	Moreira et al. 2017
41			*Sturisomatichthys panamensis*	NC_045877.1	16526	Ren et al. 2019
42		Trichomycteridae	*Trichomycterus areolatus*	AP012026.1	16657	Nakatani et al. 2011
43	Siluroidei	Siluridae	*Pterocryptis cochinchinensis*	NC_027107.1	16826	Resende et al. 2016
44			*Silurus asotus*	NC_015806.1	16593	Nakatani et al. 2011

codon alignment mode. The results were optimized using MACSE V2.03 (Ranwez et al. 2018). The nucleotide sequences of two rRNAs were aligned using the online tool MAFFT with default settings. Ambiguously aligned regions were removed via GBLOCKS 0.91 b with default settings. The resulting alignments were concatenated into a single dataset with PHYLOSUITE. The best partition schemes and optimal substitution models were selected by MODELFINDER (Kalyaanamoorthy et al. 2017) with the greedy algorithm and Bayesian information criterion (Watanabe 2013). The best substitution models applied to each partition are listed in Suppl. material 1: Table S1. Phylogenetic trees were constructed using two inference methods: maximum likelihood (ML) and Bayesian inference (BI). ML analyses were performed with IQ-TREE V1.6.8 with the models selected for each partition, and 1,000 bootstrap replicates were used to estimate node reliability. Bayesian analyses were performed using MRBAYES V3.2.6 (Huelsenbeck and Ronquist 2001). One million generations of two independent runs were performed with four chains and sampling trees every 100 generations. The initial 25% of trees generated prior to reaching stable log-likelihood values were discarded as burn-in. The remaining trees were used to calculate the Bayesian posterior probabilities. The resulting phylogenetic trees and gene orders were visualized and edited using iTOL (Letunic and Bork 2016).

Results and discussion

Genome structure and organization

The complete mitogenomes of *C. aeneus* and *C. paleatus* comprising 16,604 and 16,593 bp, respectively, were submitted to GenBank (accession nos. MZ571336 and MZ571337, respectively) (Fig. 1, Table 2). The two mitogenomes were circular and contained 37 mitochondrial genes (13 PCGs, 22 tRNA genes, and two rRNA genes)

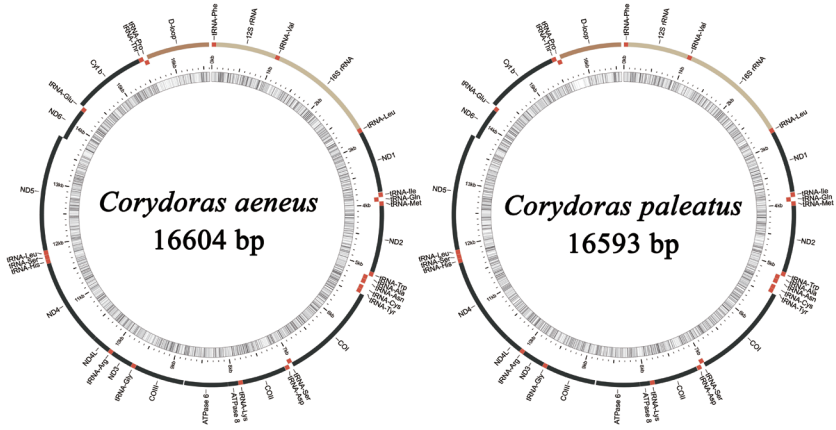

Figure 1. Gene maps of the two newly sequenced *Corydoras* species.

Table 2. Characteristic features of *Corydoras aeneus* and *Corydoras paleatus* mitogenomes (+ denotes heavy strand; - denotes light strand).

Feature	Position				Length (bp)		Start codons		Stop codons		Anticodon	Strand	Intergenic nucleotides	
	C. aeneus		*C. paleatus*		*C. aeneus*	*C. paleatus*	*C. a*	*C. p*	*C. a*	*C. p*				
	From	to	From	to									*C. a*	*C. p*
tRNA-Phe	1	68	1	68	68	68					GAA	+	0	0
12S rRNA	69	1014	69	1013	946	945						+	0	0
tRNA-Val	1015	1086	1014	1085	72	72					TAC	+	0	0
16S rRNA	1087	2757	1086	2753	1671	1668						+	0	0
tRNA-Leu	2758	2832	2754	2828	75	75					TAA	+	0	0
ND1	2833	3804	2829	3800	972	972	ATG	ATG	TAG	TAG		+	8	8
tRNA-Ile	3813	3884	3809	3880	72	72					GAT	+	-2	-2
tRNA-Gln	3883	3953	3879	3949	71	71					TTG	-	-1	-1
tRNA-Met	3953	4022	3949	4018	70	70					CAT	+	0	0
ND2	4023	5067	4019	5063	1045	1045	ATG	ATG	T	T		+	0	0
tRNA-Trp	5068	5139	5064	5134	72	71					TCA	+	1	1
tRNA-Ala	5141	5209	5136	5204	69	69					TGC	-	1	1
tRNA-Asn	5211	5283	5206	5278	73	73					GTT	-	30	31
tRNA-Cys	5314	5380	5310	5377	67	68					GCA	-	-1	-1
tRNA-Tyr	5380	5449	5377	5446	70	70					GTA	-	1	1
COI	5451	7010	5448	7007	1560	1560	GTG	GTG	AGG	AGG		+	-13	-13
tRNA-Ser	6998	7068	6995	7065	71	71					TGA	-	4	4
tRNA-Asp	7073	7141	7070	7138	69	69					GTC	+	4	6
COII	7146	7836	7145	7835	691	691	ATG	ATG	T	T		+	0	0
tRNA-Lys	7837	7910	7836	7909	74	74					TTT	+	1	1
ATPase 8	7912	8079	7911	8078	168	168	ATG	ATG	TAA	TAA		+	-10	-10
ATPase 6	8070	8753	8069	8752	684	684	ATG	ATG	TAA	TAA		+	17	21
COIII	8771	9554	8774	9557	784	784	ATG	ATG	T	T		+	0	0
tRNA-Gly	9555	9626	9558	9629	72	72					TCC	+	0	0
ND3	9627	9975	9630	9978	349	349	ATG	ATG	T	T		+	0	0
tRNA-Arg	9976	10045	9979	10048	70	70					TCG	+	0	0
ND4L	10046	10342	10049	10345	297	297	ATG	ATG	TAA	TAA		+	-7	-7
ND4	10336	11716	10339	11719	1381	1381	ATG	ATG	T	T		+	0	0
tRNA-His	11717	11786	11720	11789	70	70					GTG	+	0	0
tRNA-Ser	11787	11853	11790	11856	67	67					GCT	+	1	1
tRNA-Leu	11855	11927	11858	11930	73	73					TAG	+	0	0
ND5	11928	13754	11931	13757	1827	1827	ATG	ATG	TAA	TAA		+	-4	-4
ND6	13751	14266	13754	14269	516	516	ATG	ATG	TAA	TAA		-	0	0
tRNA-Glu	14267	14335	14270	14337	69	68					TTC	-	2	3
Cyt b	14338	15475	14341	15478	1138	1138	ATG	ATG	T	T		+	0	0
tRNA-Thr	15476	15548	15479	15550	73	72					TGT	+	-2	-2
tRNA-Pro	15547	15616	15549	15618	70	70					TGG	-	0	0
D-loop	15617	16604	15619	16593	988	975							0	0

and one D-loop. The position of each gene in the mitogenome was identical to that in other species of *Corydoras* (Saitoh et al. 2003; Moreira et al. 2016a, 2017; Liu et al. 2019a, b, c, d; Chen et al. 2020; Lv et al. 2020). One of the 13 PCGs (ND6) and eight tRNAs (tRNA-Ala, tRNA-Cys, tRNA-Glu, tRNA-Asn, tRNA-Pro, tRNA-Gln, tRNA-Ser(TGA), and tRNA-Tyr) were encoded by the light chain (-), whereas the other 28 genes, including 12 PCGs, 14 tRNAs, two rRNAs, and one D-loop, were encoded by the heavy chain (+) (Fig. 1, Table 2). The 44 mitogenomes of Siluriformes (Nakatani et al. 2011; Liu et al. 2016; Moreira et al. 2016b, 2018; Resende et al. 2016;

Magalhães et al. 2017; Parente et al. 2017; Parente et al. 2018; Pereira et al. 2019; Ren et al. 2019; Rocha-Reis et al. 2020; Meng et al. 2021; Zhang et al. 2021) used in this study were compared, and the gene composition and order were consistent (Suppl. material 1: Fig. S1). The nucleotide composition of the two entire mitogenomes was as follows: *C. aeneus* A = 5417 (32.63%), T = 4299 (25.89%), G = 2451 (14.76%), C = 4437 (26.72%) and *C. paleatus* A = 5380 (32.42%), T = 4282 (25.81%), G = 2481 (14.95%), C = 4450 (26.82%). The two mitogenomes (values for *C. aeneus* followed by values for *C. paleatus*) had high A+T contents of 58.52% and 58.23% (Suppl. material 1: Table S2), including 58.08% and 57.67% in PCGs, 56.97% and 57.04% in tRNA genes, 59.70% and 59.10% in 16S rRNA, 55.30% in 12S rRNA, and 67.51% and 68.21% in the D-loop, respectively, which agrees with the typical base bias of fish mitogenomes (Gadaleta et al. 1989; Manchado et al. 2007; Xu et al. 2011). The overall AT and GC skew values in the entire mitogenome of *C. aeneus* were 0.115 and -0.288 and in *C. paleatus* were 0.114 and -0.284, respectively. The GC skew value of the eleven mitogenomes of *Corydoras*, except for tRNA, was slightly negative (-0.014 to -0.288), showing a higher occurrence of C than of G. In contrast, AT skew value, except for the second codon position, was slightly positive (0.028 to 0.379), showing a higher content of A than of T. The K2P genetic distances of the eleven mitogenomes of *Corydoras* were all less than 0.12 (Suppl. material 1: Table S3). *C. nattereri* and *C. sterbai* and *C. nattereri* and *C. trilineatus* showed the largest K2P genetic distances among the eleven species of *Corydoras*.

Protein-coding genes

The 13 PCGs of the two new mitogenomes and those of the previously published nine mitogenomes of *Corydoras* contained COI–COIII, ND1–ND6, ND4L, two ATPases, and one Cyt-b, similar to that in other Siluriformes (Nakatani et al. 2011; Liu et al. 2016; Moreira et al. 2016b; Resende et al. 2016; Magalhães et al. 2017; Parente et al. 2017; Moreira 2018; Parente et al. 2018; Pereira et al. 2019; Ren et al. 2019; Rocha-Reis et al. 2020; Meng et al. 2021; Zhang et al. 2021). The total lengths of PCGs in the eleven mitogenomes of *Corydoras* were 11,400–11,414 bp, accounting for 67.84–69.24% of the entire mitogenome. Similar to the mitogenomes of other species of Loricarioidei, ND5 and ATPase 8 were largest (1,827 bp) and smallest (168 bp), respectively. Most PCGs stringently start with an ATG start codon, except for all COIs, which start with GTG, *C. nattereri* COIII (Moreira et al. 2016a) which starts with GCA, and *C. schwartzi* COII (Moreira et al. 2017), which starts with CCA (Suppl. material 1: Table S4). Most PCGs are stringently terminated by the stop codon TAR (TAA/TAG) or an incomplete stop codon T, except for all COIs, which terminate with AGG and *C. schwartzi* ATPase 6 and *C. nattereri* ND3, which terminate with TA. The presence of a truncated stop codon is common among vertebrate mitochondrial genes and is thought to be introduced by posttranscriptional poly-adenylation.

Similar to most previously sequenced members of Loricarioidei, the AT-skews (0.033 to 0.052) and GC-skews (-0.268 to -0.299) of the PCGs were similar among

the eleven species of *Corydoras* (Suppl. material 1: Table S2). Summaries of the relative synonymous codon usage and the number of amino acids in the annotated PCGs are presented in Suppl. material 1: Figs S2, S3. The PCGs of the eleven mitogenomes of *Corydoras* (Saitoh et al. 2003; Moreira et al. 2016a, 2017; Liu et al. 2019a, b, c, d; Chen et al. 2020; Lv et al. 2020) translate into 3,798–3,802 codons and showed very similar codon usage, excluding the stop codons (26–28 bp). Ile (310.82 ± 2.69 codons), Thr (312.64 ± 2.27 codons), Ala (312.73 ± 3.08 codons), and Leu1 (CUN) (475.45 ± 12.89 codons) were the four most predominant codon families and may be associated with the coding function of the chondriosome. In contrast, Cys (24.91 ± 0.79 codons) and Ser1 (AGN) (52.18 ± 0.83 codons) had the smallest number of codons. A/T rather than G/C bias was observed in the third position, as almost all frequently used codons ended with A/T. The synonymous codon preferences for the eleven species of *Corydoras* were conserved, possibly because of the close relationships among members of this genus.

To reveal the evolutionary pattern of the PCGs, the Ka/Ks, nucleotide diversity, and K2P genetic distance across all mitogenomes of *Corydoras* were calculated for each aligned PCG. The K2P genetic distances of 13 PCGs were all less than 0.12 (Fig. 2a). Among the PCGs detected, ND4 and ATPase 8 showed the largest K2P genetic distance among the eleven species of *Corydoras*, followed by ND2 and ND3. The nucleotide diversity of the 13 PCGs was less than 0.11 (Fig. 2b). ND4 showed the highest nucleotide diversity, whereas COII showed the lowest diversity. To investigate the selective pressure across species of *Corydoras*, the Ka/Ks ratios of the PCGs of each mitogenome were estimated (Fig. 2c). The Ka/Ks value was highest for ND6, followed by ND2; the lowest values were observed for COI, COIII, ND1, and ND4L. All 13 PCGs showed Ka/Ks << 1, suggesting that all PCGs of *Corydoras* evolved under purifying selection.

tRNAs, ribosomal RNAs, and control region

The total lengths of the 22 tRNA genes ranged from 1,438 (*C. schwartzi*) to 1,561 bp (*C. arcuatus* and *C. panda*), whereas individual tRNA genes typically ranged from 58 to 75 bp. All tRNA genes displayed the expected cloverleaf secondary structures with normal base pairing, except for tRNA-Ser(GCT), which lacked the DHU stem (Suppl. material 1: Fig. S4), forming a loop commonly found in other vertebrates (Ojala et al. 1981; Gadaleta et al. 1989; Wolstenholme 1992). The A+T contents of these tRNAs were 56.55–57.58%. All AT-skew and GC-skew values were slightly positive, indicating a slight bias toward the use of A and G in the tRNAs (Suppl. material 1: Table S2). These rRNA genes are between tRNA-Phe and tRNA-Leu(TAA) and are separated by tRNA-Val. The average total size of the two rRNAs was 2,614 bp, and the average A+T content was 57.89%. Like the tRNAs, all AT-skew values were positive, whereas all GC-skew values were negative, indicating that rRNAs favor C compared to tRNAs in *Corydoras*.

The control region (D-loop), also known as the A+T rich region that contains hypervariable non-coding sequences and regulates the replication and transcription of mitochondrial DNA, is the largest non-coding region and is located between tRNA-

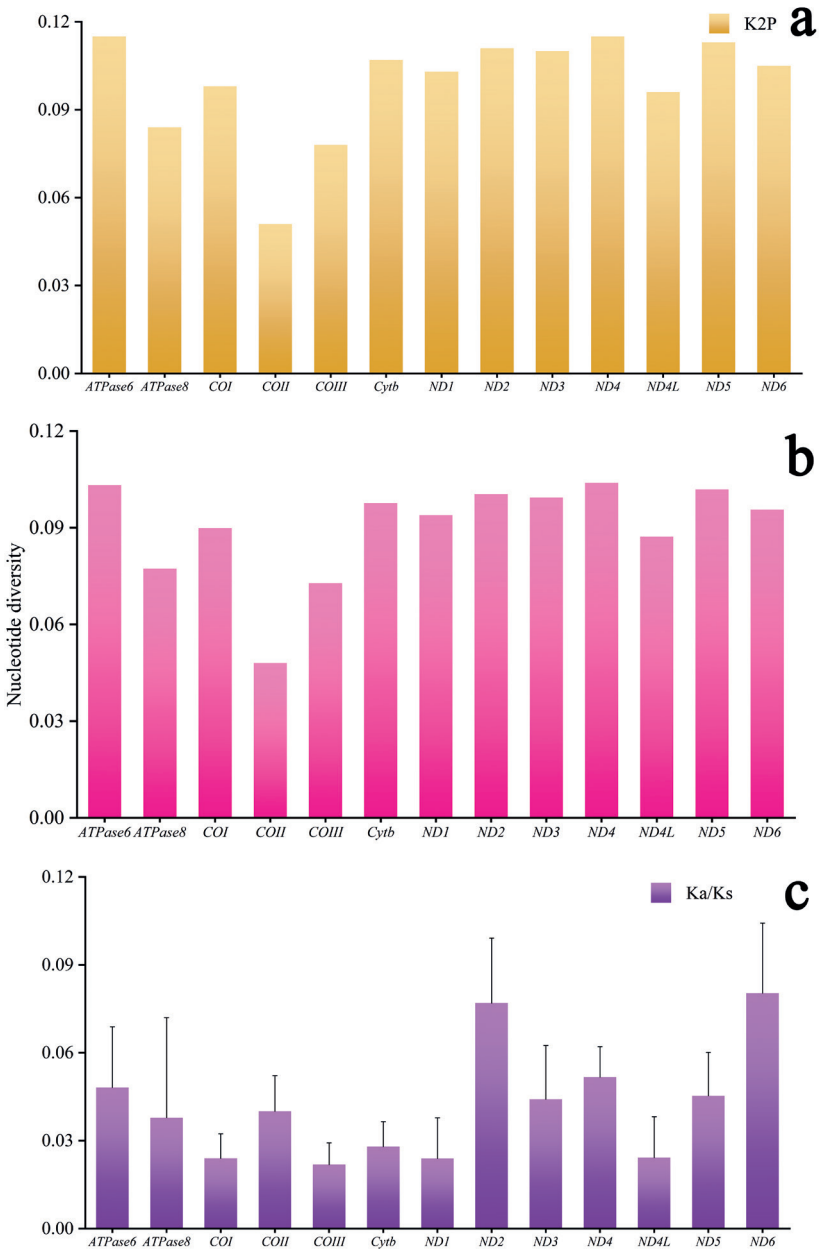

Figure 2. K2P genetic distance **a** nucleotide diversity **b** Ka/Ks ratio **c** analyses of protein-coding genes among the eleven *Corydoras* mitogenomes.

Pro and tRNA-Phe in these mitogenomes. Compared with PCGs, the D-loop displayed a higher mutation rate and the highest variation throughout the mitogenome; thus, this region is dominant and can be used to evaluate intraspecies variations. The

D-loops in the eleven species of *Corydoras* were 718−1,218 bp. Compared with the other four regions (entire genome, PCGs, tRNAs, and rRNAs), the control region showed the highest A+T content, ranging from 66.77% to 71.87%. Like the rRNAs, all AT-skew values were positive, and all GC-skew values were negative.

Phylogenetic analysis

To determine the phylogenetic relationships within the suborder Loricarioidei and family Callichthyidae, we obtained the concatenated nucleotide sequences of 13 PCGs and two rRNAs from 42 species of Loricarioidei. Phylogenetic analyses based on both ML and BI methods revealed same topologies, which also generally agreed with those presented in previous studies (Alexandrou et al. 2011; Lujan et al. 2015; Moreira et al. 2017; Roxo et al. 2019) (Figs 3, 4). These analyses confirmed that the genus *Corydoras* was part of the monophyletic family Callichthyidae.

Both Callichthyidae and Loricariidae were recovered as monophyletic with very high support values (BI posterior probabilities, PP = 1; ML bootstrap, BS = 100). The 44 species of Siluriformes were divided into four major clades corresponding to the families Siluridae Callichthyidae, Trichomycteridae, and Loricariidae. The target

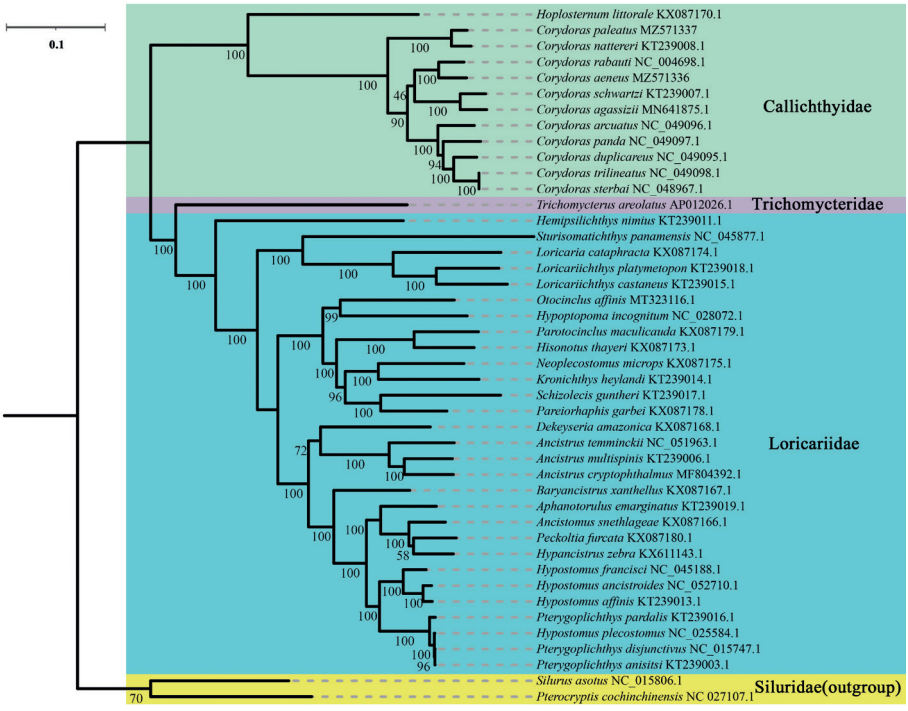

Figure 3. Phylogenetic trees of 44 Siluriformes species using concatenated nucleotide sequences of 13 protein-coding genes and two rRNAs using the maximum likelihood method. Numbers in the ML tree represent SH-aLRT support/ultrafast bootstrap support values.

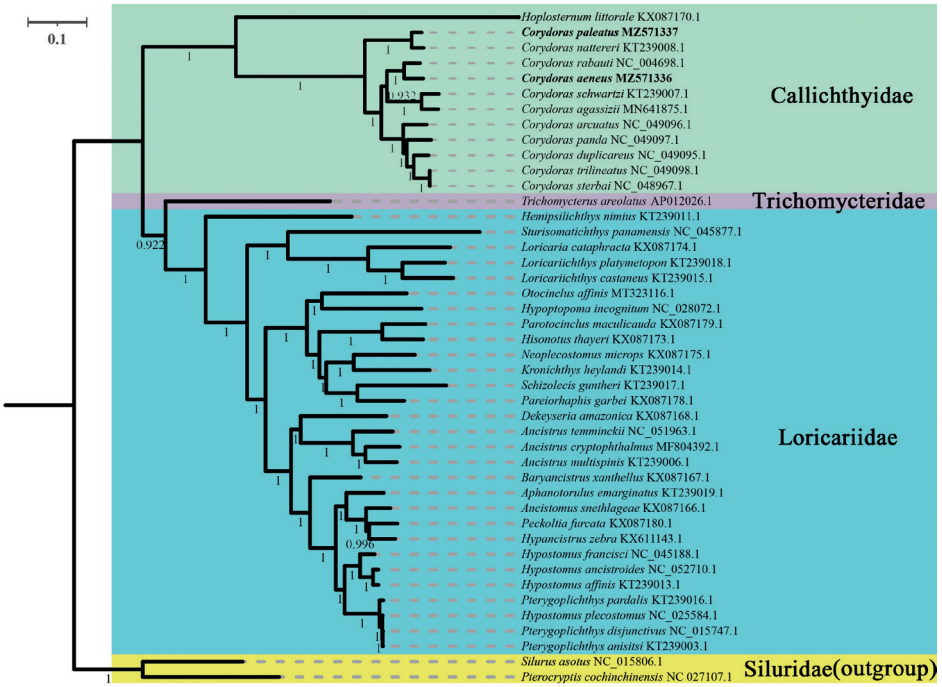

Figure 4. Phylogenetic tree of 44 Siluriformes species using concatenated nucleotide sequences of 13 protein-coding genes and two rRNAs via the Bayesian interference method. Applicable posterior probability values are shown.

species *C. aeneus* and *C. paleatus* were clustered into two clades (*C. aeneus* + *C. rabauti*) and (*C. paleatus* + *C. nattereri*) with a high nodal support value (PP = 1; BS = 100). The eleven species of the genus *Corydoras* clustered together quite well [((*C. aeneus* + *C. rabauti*) + (*C. schwartzi* + *C. agassizii*)) + (*C. arcuatus* + (*C. panda* + (*C. duplicareus* + (*C. sterbai* + *C. trilineatus*))))] + [(*C. paleatus* + *C. nattereri*)]. *Corydoras trilineatus* and *C. sterbai* have short, almost non-existent branch lengths; thus, they are likely the same species. The K2P genetic distances of these two species are 0.000 (Suppl. material 1: Table S3), which verifies that they are the same species. This may be caused by incorrect identification, taxonomic problems (these two species are, in fact, synonymous), and/or introgressive hybridization. Moreover, in the family Loricariidae, the genera *Ancistrus* and *Loricariichthys* were clustered into monophyletic clades [(*A. cryptophthalmus* + *A. multispinis*) + *A. temminckii*] and (*L. castaneus* + *L. platymetopon*) with a high nodal support value (PP = 1; BS = 100). There was a paraphyletic relationship between the genera *Hypostomus* and *Pterygoplichthys*, [*H. francisci* + (*H. ancistroides* + *H. affinis*), *P. pardalis* + (*H. plecostomus* + (*P. anisitsi* + *P. disjunctivus*))]. Our results demonstrate that the concatenated nucleotide sequences of the 13 PCGs and two rRNAs were useful for determining the phylogenetic relationships of the order Siluriformes. These results can be used to improve classification of the families Callichthyidae and Loricariidae.

Conclusions

Using next-generation sequencing methods, the complete mitogenomes of the bronze *C. aeneus* and peppered *C. paleatus* were analyzed and compared with those of nine members of *Corydoras*. The complete mitogenomes of *C. aeneus* and *C. paleatus* comprised 16,604 and 16,593 bp, respectively. The two mitogenomes had high A+T contents (58.52% in *C. aeneus* and 58.23% in *C. paleatus*), a phenomenon that agrees with the typical base bias of ichthyic mitogenomes. Our results indicate that the mitogenome features, including genome size, gene content, and gene arrangement, in *Corydoras* are highly conserved. Phylogenetic analysis was performed with 42 species of Loricarioidei and two outgroup species. These analyses confirmed the occurrence of the genus *Corydoras* within the monophyletic family Callichthyidae. The complete mitogenome information, including the gene content, gene orders, genome structure, base compositions, evolutionary features, codon usage, gene arrangement, and phylogenetic analyses, provides a basis for future studies on the population genetic and evolution of *Corydoras* and related groups.

Acknowledgements

This work was supported by the National Key R&D Program of China (Grant number 2018YFD0900802); Director's Fund of the Hubei Key Laboratory of Three Gorges Project for Conservation of Fishes, China Three Gorges Corporation (0704157); Outstanding Innovative Talents Cultivation Funded Programs for Doctoral Students of Jinan University (Project No: 2021CXB022) and Priority Academic Program Development of Jiangsu Higher Education Institutions (PAPD). We gratefully acknowledge two reviewers for their constructive comments and would like to thank Editage (www.editage.com) for their support with language editing.

References

Alexandrou MA, Oliveira C, Maillard M, McGill RA, Newton J, Creer S, Taylor MI (2011) Competition and phylogeny determine community structure in Müllerian co-mimics. Nature 469: 84–88. https://doi.org/10.1038/nature09660

Anderson S, Bankier AT, Barrell BG, de Bruijn MH, Coulson AR, Drouin J, Eperon IC, Nierlich DP, Roe BA, Sanger F, Schreier PH, Smith AJ, Staden R, Young IG (1981) Sequence and organization of the human mitochondrial genome. Nature 290: 457–465. https://doi.org/10.1038/290457a0

Avise JC, Arnold J, Ball RM, Bermingham E, Lamb T, Neigel JE, Reeb CA, Saunders NC (1987) Intraspecific phylogeography: The mitochondrial DNA bridge between population genetics and systematics. Annual Review of Ecology and Systematics 18: 489–522. https://doi.org/10.1146/annurev.es.18.110187.002421

Bankevich A, Nurk S, Antipov D, Gurevich AA, Dvorkin M, Kulikov AS, Lesin VM, Nikolenko SI, Pham S, Prjibelski AD, Pyshkin AV, Sirotkin AV, Vyahhi N, Tesler G, Alekseyev MA, Pevzner PA (2012) SPAdes: A new genome assembly algorithm and its applications to single-cell sequencing. Journal of Computational Biology 19: 455–477. https://doi.org/10.1089/cmb.2012.0021

Bartlett SE, Davidson WS (1991) Identification of *Thunnus* tuna species by the polymerase chain reaction and direct sequence analysis of their mitochondrial cytochrome b genes. Canadian Journal of Fisheries and Aquatic Sciences 48: 309–317. https://doi.org/10.1139/f91-043

Beheregaray LB, Sunnucks P (2001) Fine-scale genetic structure, estuarine colonization and incipient speciation in the marine silverside fish *Odontesthes argentinensis*. Molecular Ecology 10: 2849–2866. https://doi.org/10.1046/j.1365-294X.2001.t01-1-01406.x

Bermingham E, Avise JC (1986) Molecular zoogeography of freshwater fishes in the southeastern United States. Genetics 113: 939–965. https://doi.org/10.1007/BF00123216

Brown WM, George M, Wilson AC (1979) Rapid evolution of animal mitochondrial DNA. Proceedings of the National Academy of Sciences 76: 1967–1971. https://doi.org/10.1073/pnas.76.4.1967

Burland TG (2000) DNASTAR's Lasergene sequence analysis software. In: Misener S, Krawetz SA (Eds) Bioinformatics Methods and Protocols. Methods in Molecular Biology, vol. 132. Humana Press, Totowa, 71–91. https://doi.org/10.1385/1-59259-192-2:71

Chen L, Xu B, Xiao T, Liu Q (2020) Characterization and phylogenetic analysis of Using MUMmer to identify similar regions in large sequence sets *Corydoras trilineatus* mitochondrial genome. Mitochondrial DNA Part B Resources 5: 3017–3018. https://doi.org/10.1080/23802359.2020.1797551

Delcher AL, Salzberg SL, Phillippy AM (2003) Using MUMmer to identify similar regions in large sequence sets. Current Protocols in Bioinformatics 00: 10.3.1–10.3.18. https://doi.org/10.1002/0471250953.bi1003s00

De Rijk P, Van de Peer Y, Van den Broeck I, De Wachter R (1995) Evolution according to large ribosomal subunit RNA. Journal of Molecular Evolution 41: 366–375. https://doi.org/10.1007/BF01215184

Gadaleta G, Pepe G, De Candia G, Quagliariello C, Sbisà E, Saccone C (1989) The complete nucleotide sequence of the *Rattus norvegicus* mitochondrial genome: Cryptic signals revealed by comparative analysis between vertebrates. Journal of Molecular Evolution 28: 497–516. https://doi.org/10.1007/BF02602930

Griffiths-Jones S, Bateman A, Marshall M, Khanna A, Eddy SR (2003) Rfam: An RNA family database. Nucleic Acids Research 31: 439–441. https://doi.org/10.1093/nar/gkg006

Hrbek T, Seckinger J, Meyer A (2007) A phylogenetic and biogeographic perspective on the evolution of poeciliid fishes. Molecular Phylogenetics and Evolution 43: 986–998. https://doi.org/10.1016/j.ympev.2006.06.009

Huelsenbeck JP, Ronquist F (2001) MRBAYES: Bayesian inference of phylogenetic trees. Bioinformatics 17: 754–755. https://doi.org/10.1093/bioinformatics/17.8.754

Huysentruyt F, Adriaens D (2005a) Descriptive osteology of *Corydoras aeneus* (Siluriformes: Callichthyidae). Cybium 29: 261–73.

Huysentruyt F, Adriaens D (2005b) Adhesive structures in the eggs of *Corydoras aeneus* (Gill 1858; Callichthyidae). Journal of Fish Biology 66: 871–876. https://doi.org/10.1111/j.0022-1112.2005.00647.x

Ingram S, Munzner T, Olano M (2009) Glimmer: Multilevel MDS on the GPU. IEEE Transactions on Visualization and Computer Graphics 15: 249–261. https://doi.org/10.1109/TVCG.2008.85

Iwasaki W, Fukunaga T, Isagozawa R, Yamada K, Maeda Y, Satoh TP, Sado T, Mabuchi K, Takeshima H, Miya M, Nishida M (2013) MitoFish and MitoAnnotator: A mitochondrial genome database of fish with an accurate and automatic annotation pipeline. Molecular Biology Evolution 30: 2531–2540. https://doi.org/10.1093/molbev/mst141

Kai Y, Nakayama K, Nakabo T (2002) Genetic differences among three colour morphotypes of the black rockfish, *Sebastes inermis*, inferred from mtDNA and AFLP analyses. Molecular Ecology 11: 2591–2598. https://doi.org/10.1046/j.1365-294X.2002.01628.x

Kalyaanamoorthy S, Minh BQ, Wong TKF, von Haeseler A, Jermiin LS (2017) ModelFinder: Fast model selection for accurate phylogenetic estimates. Nature Methods 14: 587–589. https://doi.org/10.1038/nmeth.4285

Katoh K, Standley DM (2013) MAFFT multiple sequence alignment software version 7: Improvements in performance and usability. Molecular Biology Evolution 30: 772–780. https://doi.org/10.1093/molbev/mst010

Kumar S, Tamura K, Nei M (1994) MEGA: Molecular evolutionary genetics analysis software for microcomputers. Computer Applications in the Biosciences 10: 189–191. https://doi.org/10.1093/bioinformatics/10.2.189

Letunic I, Bork P (2016) Interactive tree of life (iTOL) v3: An online tool for the display and annotation of phylogenetic and other trees. Nucleic Acids Research 44: W242–W245. https://doi.org/10.1093/nar/gkw290

Librado P, Rozas J (2009) DnaSP v5: A software for comprehensive analysis of DNA polymorphism data. Bioinformatics 25: 1451–1452. https://doi.org/10.1093/bioinformatics/btp187

Lima FCT, Britto MR (2020) A new *Corydoras* (Ostariophysi: Siluriformes: Callichthyidae) with an unusual sexual dimorphism from the Rio Juruena basin, Brazil. Zootaxa 4742: 518–530. https://doi.org/10.11646/zootaxa.4742.3.6

Liu H, Tzeng CS, Teng HY (2002) Sequence variations in the mitochondrial DNA control region and their implications for the phylogeny of the Cypriniformes. Canadian Journal of Zoology 80: 569–581. https://doi.org/10.1139/z02-035

Liu Q, Liu Y, Xiao T, Xu B (2019a) Complete mitochondrial genome of *Corydoras panda* (Teleostei, Siluriformes, Callichthyidae, Corydoradinae). Mitochondrial DNA Part B Resources 4: 2878–2879. https://doi.org/10.1080/23802359.2019.1660253

Liu Q, Liu Y, Xu B, Xiao T (2019b) Next-generation sequencing yields the complete mitochondrial genome of *Corydoras sterbai* (Teleostei, Siluriformes, Callichthyidae, Corydoradinae). Mitochondrial DNA Part B Resources 4: 2880–2881. https://doi.org/10.1080/23802359.2019.1660255

Liu Q, Xu B, Xiao T (2019c) Complete mitochondrial genome of *Corydoras duplicareus* (Teleostei, Siluriformes, Callichthyidae). Mitochondrial DNA Part B Resources 4: 1832–1833. https://doi.org/10.1080/23802359.2019.1612714

Liu S, Zhang J, Yao J, Liu Z (2016) The complete mitochondrial genome of the armored catfish, *Hypostomus plecostomus* (Siluriformes: Loricariidae). Mitochondrial DNA Part A DNA Mapping, Sequencing, and Analysis 27: 1908–1909. https://doi.org/10.3109/19401736.2014.971281

Liu Y, Xu B, Xiao T, Liu Q (2019d) Characterization and phylogenetic analysis of *Corydoras arcuatus* mitochondrial genome. Mitochondrial DNA Part B Resources 4: 2876–2877. https://doi.org/10.1080/23802359.2019.1660251

Lowe TM, Eddy SR (1997) TRNAscan-SE: A program for improved detection of transfer RNA genes in genomic sequence. Nucleic Acids Research 25: 955–964. https://doi.org/10.1093/nar/25.5.955

Lujan NK, Armbruster JW, Lovejoy NR, López-Fernández H (2015) Multilocus molecular phylogeny of the suckermouth armored catfishes (Siluriformes: Loricariidae) with a focus on subfamily Hypostominae. Molecular phylogenetics and evolution 82: 269–288. https://doi.org/10.1016/j.ympev.2014.08.020

Luo R, Liu B, Xie Y, Li Z, Huang W, Yuan J, He G, Chen Y, Pan Q, Liu Y, Tang J, Wu G, Zhang H, Shi Y, Liu Y, Yu C, Wang B, Lu Y, Han C, Wang J (2012) SOAPdenovo2: An empirically improved memory-efficient short-read de novo assembler. GigaScience 1: 18. https://doi.org/10.1186/2047-217X-1-18

Lv L, Su H, Xu B, Liu Q, Xiao T (2020) Complete mitochondrial genome of *Corydoras agassizii*. Mitochondrial DNA Part B Resources 5: 727–728. https://doi.org/10.1080/23802359.2020.1715277

Magalhães MGP, Moreira DA, Furtado C, Parente TE (2017) The mitochondrial genome of *Hypancistrus zebra* (Isbrücker Nijssen 1991) (Siluriformes: Loricariidae), an endangered ornamental fish from the Brazilian Amazon. Conservation Genetics Resources 9: 319–324. https://doi.org/10.1007/s12686-016-0645-5

Manchado M, Catanese G, Ponce M, Funes V, Infante C (2007) The complete mitochondrial genome of the Senegal sole, *Solea senegalensis* Kaup. Comparative analysis of tandem repeats in the control region among soles. DNA Sequence 18: 169–175. https://doi.org/10.1080/10425170701308956

Meng F, Yin X, Zhang T, Zhao C, Xue X, Xia X, Zhu X, Duan Z, Liu B, Liu Y (2021) The first determination and analysis of the complete mitochondrial genome of *Ancistrus temmincki* (Siluriformes: Loricariidae). Mitochondrial DNA Part B Resources 6: 1583–1585. https://doi.org/10.1080/23802359.2020.1866446

Meyer A (1993) Evolution of mitochondrial DNA in fishes. In: Hochachka PW, Mommsen TP (Eds) Biochemistry and Molecular Biology of Fishes. Elsevier Press, [xxxx,] 1–38.

Michot B, Qu LH, Bachellerie JP (1990) Evolution of large-subunit rRNA structure: The diversification of divergent D3 domain among major phylogenetic groups. European Journal of Biochemistry 188: 219–229. https://doi.org/10.1111/j.1432-1033.1990.tb15393.x

Moreira DA (2018) O que Dados transcriptômicos revelam sobre a biodiversidade e evolução de Loricarioidei (Siluriformes) [Doctoral Dissertation, Instituto Oswaldo Cruz, Fundação Oswaldo Cruz, Rio de Janeiro].

Moreira DA, Buckup PA, Britto MR, Magalhães MGP, de Andrade PCC Furtado C, Parente TE (2016a) The complete mitochondrial genome of *Corydoras nattereri* (Callichthyidae: Cory-

doradinae). Neotropical Ichthyology 14(01): e1501670. https://doi.org/10.1590/1982-0224-20150167

Moreira DA, Buckup PA, Furtado C, Val AL., Schama R, Parente TE (2017) Reducing the information gap on Loricarioidei (Siluriformes) mitochondrial genomics. BMC Genomics 18: 1–13. https://doi.org/10.1186/s12864-017-3709-3

Moreira DA, Magalhães MGP, de Andrade PCC, Furtado C, Val AL, Parente TE (2016b) An RNA-based approach to sequence the mitogenome of *Hypoptopoma incognitum* (Siluriformes: Loricariidae). Mitochondrial DNA Part A DNA Mapping, Sequencing, and Analysis 27: 3784–3786. https://doi.org/10.3109/19401736.2015.1079903

Nakatani M, Miya M, Mabuchi K, Saitoh K, Nishida M (2011) Evolutionary history of Otophysi (Teleostei), a major clade of the modern freshwater fishes: Pangaean origin and Mesozoic radiation. BMC Evolutionary Biology 11: 177. https://doi.org/10.1186/1471-2148-11-177

Nawrocki EP, Eddy SR (2013) Infernal 1.1: 100-Fold faster RNA homology searches. Bioinformatics 29: 2933–2935. https://doi.org/10.1093/bioinformatics/btt509

O'Brien TW (1971) The general occurrence of 55 S ribosomes in mammalian liver mitochondria. Journal of Biological Chemistry 246: 3409–3417. https://doi.org/10.1016/S0021-9258(18)62239-2

Ojala D, Montoya J, Attardi G (1981) tRNA punctuation model of RNA processing in human mitochondria. Nature 290: 470–474. https://doi.org/10.1038/290470a0

Parente TE, Moreira DA, Buckup PA, de Andrade PCC, Magalhães MGP, Furtado C, Britto MR, Val AL (2018) Remarkable genetic homogeneity supports a single widespread species of *Hoplosternum littorale* (Siluriformes, Callichthyidae) in South America. Conservation Genetics Resources 10: 563–569. https://doi.org/10.1007/s12686-017-0831-0

Parente TE, Moreira DA, Magalhães MGP, de Andrade PCC, Furtado C, Haas BJ, Stegeman JJ, Hahn ME (2017) The liver transcriptome of suckermouth armoured catfish (*Pterygoplichthys anisitsi*, Loricariidae): Identification of expansions in defensome gene families. Marine Pollution Bulletin 115: 352–361. https://doi.org/10.1016/j.marpolbul.2016.12.012

Pereira AH, Facchin S, Oliveira do Carmo A, Núñez Rodriguez D, Cardoso Resende LC, Kalapothakis Y, Brandão Dias Ferreira Pinto P, Mascarenhas Alves CB, Henrique Zawadzki C, Kalapothakis E (2019) Complete mitochondrial genome sequence of *Hypostomus francisci* (Siluriformes: Loricariidae). Mitochondrial DNA Part B Resources 4: 155–157. https://doi.org/10.1080/23802359.2018.1544860

Pesole G, Gissi C, De Chirico A, Saccone C (1999) Nucleotide substitution rate of mammalian mitochondrial genomes. Journal of molecular evolution 48: 427–434. https://doi.org/10.1007/PL00006487

Popazoglo F, Boeger WA (2000) Neotropical Monogenoidea 37. Redescription of Gyrodactylus superbus (Szidat 1973) comb. n. and description of two new species of *Gyrodactylus* (Gyrodactylidea: Gyrodactylidae) from *Corydoras paleatus* and *C. ehrhardti* (Teleostei: Siluriformes: Callichthyidae) of southern Brazil. Folia Parasitologica 47(2): 105–110. https://doi.org/10.14411/fp.2000.022

Ranwez V, Douzery EJP, Cambon C, Chantret N, Delsuc F (2018) MACSE v2: toolkit for the alignment of coding sequences accounting for frameshifts and stop codons. Molecular Biology Evolution 35: 2582–2584. https://doi.org/10.1093/molbev/msy159

Ren F, Chen D, Ma X (2019) The complete mitochondrial genome of *Sturisomatichthys panamense* (Siluriformes: Loricariidae) analysed by next-generation sequencing and phylogeny of the catfish subfamily Loricariinae (Siluriformes: Loricariidae). Biologia 75: 1365–1372. https://doi.org/10.2478/s11756-019-00389-7

Resende LC, Carmo AOd, Núñez-Rodriguez D, Pimentel JdSM, Bedore AG, Leal HG, Kalapothakis E (2016) *Pimelodus maculatus* (Siluriformes, Pimelodidae): Complete mtDNA sequence of an economically important fish from the São Francisco river basin. Mitochondrial DNA Part B Resources 1: 806–808. https://doi.org/10.1080/23802359.2016.1219646

Rocha-Reis DA, Pasa R, Menegidio FB, Heslop-Harrison JS, Schwarzacher T, Kavalco KF (2020) The complete mitochondrial genome of two armored catfish populations of the genus *Hypostomus* (Siluriformes, Loricariidae, Hypostominae). Frontiers in Ecology and Evolution 8: e579965. https://doi.org/10.3389/fevo.2020.579965

Roxo FF, Ochoa LE, Sabaj MH, Lujan NK, Covain R, Silva GS, Oliveira C (2019) Phylogenomic reappraisal of the Neotropical catfish family Loricariidae (Teleostei: Siluriformes) using ultraconserved elements. Molecular Phylogenetics and Evolution 135: 148–165. https://doi.org/10.1016/j.ympev.2019.02.017

Saitoh K, Miya M, Inoue JG, Ishiguro NB, Nishida M (2003) Mitochondrial genomics of ostariophysan fishes: Perspectives on phylogeny and biogeography. Journal of Molecular Evolution 56: 464–472. https://doi.org/10.1007/s00239-002-2417-y

Simon C, Frati F, Beckenbach A, Crespi B, Liu H, Flook P (1994) Evolution, weighting, and phylogenetic utility of mitochondrial gene sequences and a compilation of conserved polymerase chain reaction primers. Annals of the Entomological Society of America 87: 651–701. https://doi.org/10.1093/aesa/87.6.651

Tencatt LFC, Dos Santos SA, Evers HG, Britto MR (2021) *Corydoras fulleri* (Siluriformes: Callichthyidae), a new catfish species from the Rio Madeira basin, Peru. Journal of Fish Biology 99(2): 614–628. https://doi.org/10.1111/jfb.14750

Watanabe S (2013) A widely applicable Bayesian information criterion. Journal of Machine Learning Research 14: 867–897.

Wolstenholme DR (1992) Animal mitochondrial DNA: Structure and evolution. International Review of Cytology 141: 173–216. https://doi.org/10.1016/S0074-7696(08)62066-5

Xu B, Su H, Liu Q, Lv L, Chen K, Xiao T (2020) Complete mitochondrial genome of *Brochis multiradiatus*. Mitochondrial DNA Part B Resources 5: 646–647. https://doi.org/10.1080/23802359.2019.1711227

Xu TJ, Cheng YZ, XZ, Liu GS, Wang RX (2011) The complete mitochondrial genome of the marbled rockfish *Sebastiscus marmoratus* (Scorpaeniformes, Scorpaenidae): Genome characterization and phylogenetic considerations. Molekulyarnaya Biologiya (Mosk) 45: 392–403. https://doi.org/10.1134/S0026893311020191

Yoshizawa K, Johnson KP (2003) Phylogenetic position of *Phthiraptera* (Insecta: Paraneoptera) and elevated rate of evolution in mitochondrial 12S and 16S rDNA. Molecular Phylogenetics and Evolution 29: 102–114. https://doi.org/10.1016/S1055-7903(03)00073-3

Zhang D, Gao F, Jakovlić I, Zou H, Zhang J, Li WX, Wang GT (2020) PhyloSuite: An integrated and scalable desktop platform for streamlined molecular sequence data manage-

ment and evolutionary phylogenetics studies. Molecular Ecology Resources 20: 348–355. https://doi.org/10.1111/1755-0998.13096

Zhang K, Liu Y, Chen J, Zhang H, Gong L, Jiang L, Liu L, Lü Z, Liu B (2021) Characterization of the complete mitochondrial genome of *Macrotocinclus affinis* (Siluriformes; Loricariidae) and phylogenetic studies of Siluriformes. Molecular Biology Reports 48: 677–689. https://doi.org/10.1007/s11033-020-06120-z

Supplementary material 1

COI sequences of *Corydoras aeneus* and *C. paleatus* Tables S1–S4, Figs S1–S4

Authors: Cheng-He Sun, Qi Huang, Xiao-Shu Zeng, Sha Li, Xiao-Li Zhang, Ya-Nan Zhang, Jian Liao, Chang-Hu Lu, Bo-Ping Han, Qun Zhang

Data type: docx file

Explanation note: COI sequences of *Corydoras aeneus* and *C. paleatus*. Table S1. Best substitution models for Bayesian inference (BI) and maximum-likelihood (ML) analyses. Table S2. Summarized mitogenomic characteristics of the eleven *Corydoras* species investigated in this study. Table S3. The K2P genetic distances of the eleven mitogenomes of *Corydoras*. Table S4. Start and stop codons of protein-coding genes in the eleven *Corydoras* mitogenomes. Figure S1. Gene orders of mitogenomes of the studied species. Figure S2. Relative synonymous codon usage of 13 protein-coding genes in the mitogenomes of eleven *Corydoras* species. Figure S3. Codon usage patterns of eleven *Corydoras* mitogenomes. Figure S4. Secondary structures of tRNA-Ser(GCT) in the two newly sequenced *Corydoras* species.

Link: https://doi.org/10.3897/zookeys.1083.76887.suppl1

ZooKeys 1083: 109–128 (2022)
doi: 10.3897/zookeys.1083.69047
https://zookeys.pensoft.net

RESEARCH ARTICLE

A peer-reviewed open-access journal
ZooKeys
Launched to accelerate biodiversity research

Ex situ population of the Harpy Eagle and its potential for integrated conservation

Marcos José de Oliveira[1], Francisca Helena Aguiar-Silva[2,3], Wanderlei de Moraes[4], Tânia Margarete Sanaiotti[3,5], Aureo Banhos[3,6], Nei Moreira[7]

1 *Itaipu Binacional, Av. Tancredo Neves, 6731, Itaipu "A", 85856–970, Foz do Iguaçu, Paraná, Brazil* **2** *Universidade de São Paulo – USP, Centro de Energia Nuclear na Agricultura – CENA, Av. Centenário, 303, São Dimas, 13400–970, Piracicaba, Brazil* **3** *Projeto Harpia (Harpy Eagle Project), Av. André Araújo, 2936, Aleixo, 69067–375, Manaus, Amazonas, Brazil* **4** *Médico veterinário autônomo – Rua do Angico, 186, Itaipu B, 85867–100, Foz do Iguaçu, Paraná, Brazil* **5** *Instituto Nacional de Pesquisas da Amazônia – INPA, Coordenação de Biodiversidade, Av. André Araújo, 2936, Aleixo, 69067–375, Manaus, Amazonas, Brazil* **6** *Universidade Federal do Espírito Santo – UFES, Departamento de Biologia, Centro de Ciências Exatas, Naturais e da Saúde, Alto Universitário, s/n°, Guararema, 29500–000, Alegre, Espírito Santo, Brazil* **7** *Universidade Federal do Paraná – UFPR, Programa de Pós-Graduação em Zoologia, Departamento de Biociências, Rua Pioneiro, 2153, Jardim Dallas, 85950–000, Palotina, Paraná, Brazil*

Corresponding author: Marcos José de Oliveira (marcosjo.oliveira@gmail.com)

Academic editor: Knud Jønsson | Received 24 May 2021 | Accepted 20 December 2021 | Published 25 January 2022

http://zoobank.org/9E2B157F-B04B-4228-B7BA-E8C08B239CF8

Citation: de Oliveira MJ, Aguiar-Silva FH, de Moraes W, Sanaiotti TM, Banhos A, Moreira N (2022) Ex situ population of the Harpy Eagle and its potential for integrated conservation. ZooKeys 1083: 109–128. https://doi.org/10.3897/zookeys.1083.69047

Abstract

A main priority in conservation is the protection of species in their natural habitat. However, ex situ management of threatened species is a recognised strategy of conservation. Harpy Eagles (*Harpia harpyja*) are removed from the wild due to illegal capture, nest tree destruction, or other conflict sources. This study presents a review of the current ex situ Harpy Eagle populations in Brazil and worldwide, including information on the origin, sex, and year of entrance or year of birth under human care. Worldwide, until 2020 there were 205 Harpy Eagles in 77 different facilities in 16 countries, with 40 institutions in Brazil and 37 in other countries. The largest ex situ Harpy Eagle population is maintained in Brazil, with 139 individuals (75 females and 64 males) in 40 institutions. Of these institutions, there were 24 zoos, seven conservation breeding centres, six commercial breeders, two wildlife shelters, and one wildlife sorting centre. In Brazil, 62% (n = 86) of the individuals were hatched in the wild and 38% (n = 53) were bred in captivity under human care; for the wild individuals, only 73% (n = 64) have a known state of origin,

with the majority from Pará state. This investigation provided relevant information to establish an ex situ demographic database. These individuals may potentially constitute a genetically and demographically viable safety population for future conservation strategies, as well as a source for research and education applied to Harpy Eagle integrated conservation.

Keywords
Birds of prey, captive breeding, *Harpia harpyja*, threatened species

Introduction

Conservation actions for endangered bird populations involve the maintenance of the natural habitat, with protection of the nests and offspring until they are mature enough to disperse (Butchart et al. 2006; Pacifico et al. 2014). The Harpy Eagle (*Harpia harpyja* Linnaeus, 1758) is a bird of prey and a top predator with a large carrying capacity (Voous 1969). With a low population density and slow reproductive rate in nature, the Harpy Eagle relies on conservation action plans and is the subject of extensive research projects (Soares et al. 2008; Brasil 2014b; Aguiar-Silva et al. 2015; Sanaiotti et al. 2015; Watson et al. 2016; Oliveira 2018).

The Harpy Eagle is globally classified as a Vulnerable species (Bird Life International 2021) and is listed in Appendix I of CITES (2017). In Brazil, which has the largest population, it has been classified as Vulnerable to extinction since 2014 due to the loss of habitat and removal of individuals from nature (Brasil 2014a; Banhos et al. 2018). However, in the evaluation of the Brazilian Atlantic Forest states, the population status of the Harpy Eagle is more concerning categories, being considered Endangered in Rio de Janeiro state (Alves et al. 2000), Critically Endangered in São Paulo, Paraná (Silveira et al. 2009) and Espírito Santo states (Duca et al. 2019), and probably Extinct in Rio Grande do Sul state (Bencke et al. 2003). However, in the far South of Brazil, there were recently documented records of an adult and a juvenile eagle in the region of Turvo State Park (Meller and Guadagnin 2016; Kuhn 2018). The first Harpy Eagles in the care of a zoo in Brazil were reported during the 1890's (Sanjad et al. 2012; Pais 2013), but in the last few decades, they have been frequently removed from nature by anthropogenic actions (Trinca et al. 2008; DeLuca 2012; Silva et al. 2013; Freitas et al. 2014; Gusmão et al. 2016; Gusmão et al. 2020), and many have been destined for zoos (This study, Table 1).

The Convention on Biological Diversity (CDB 1993) and International Union for the Conservation of Nature (IUCN/SSC 2014) recognised that in situ conservation actions, such as captive breeding in zoos, will need to be combined with ex situ approaches. Some National Actions Plans for Species Conservation (hereafter PAN-Plano de Ação Nacional) that involve the Harpy Eagle have been implemented in many regions for which there are records of occurrence for this species in Brazil (Soares et al. 2008; Brasil 2012, 2014b, c, 2017). PAN for Birds of Prey Conservation (Soares et al. 2008) included, among the goals for the birds of prey captive population management,

Table 1. Harpy Eagle (*Harpia harpyja*) ex situ population in Brazil in 2020. Regions: N–North, NE–Northeast, MW–Midwest, SE–Southeast, and S–South. Management category: Zoo, ConsBr–Conservationist Breeder, ComBr–Commercial Breeder, WSC–Wildlife Sorting Centre, WS–Wildlife Shelter. IBAMA–Brazilian Institute of Environment and Renewable Natural Resources (Instituto Brasileiro do Meio Ambiente e dos Recursos Naturais Renováveis). For state acronyms, see Materials and methods.

#	Institution keeper	Region	State	City	Administration Type	Management Category	Origin of Birth				Breeding Period	Replied Survey
							Wild		Bred in Captivity			
							♂	♀	♂	♀		
1	Parque Zoobotânico Getúlio Vargas	NE	BA	Salvador	State	Zoo	0	1	0	1	2017	Yes
2	Criadouro Comercial Haras Claro	NE	CE	Caucaia	Private	ComBr	1	1	0	0	–	Yes
3	Criadouro Comercial Sítio Tibagi	NE	CE	Guaramiranga	Private	ComBr	1	1	0	0	2006–2018	Yes
4	Criadouro Conservacionista Ararajuba do Ipê – Gilrassic Park	NE	MA	Santa Inês	Private	ConsBr	0	3	0	0	–	–
5	Parque Estadual Dois Irmãos	NE	PE	Recife	State	Zoo	0	1	0	0	–	Yes
6	Parque Estadual Zoobotânico de Piauí	NE	PI	Teresina	State	Zoo	0	1	0	0	–	Yes
7	Parque dos Falcões	NE	SE	Itabaiana	Private	ConsBr	1	1	0	0	–	No
8	Centro de Triagem de Fauna Silvestre- IBAMA	N	AC	Rio Branco	Federal	WSC	0	2	0	0	–	–
9	Parque Urbano Estadual Chico Mendes	N	AC	Rio Branco	State	Zoo	0	1	0	0	–	Yes
10	Zoológico do Centro de Instrução de Guerra na Selva	N	AM	Manaus	Federal	Zoo	0	2	0	0	–	Yes
11	RPPN Revecom	N	AP	Santana	Private	WS	0	1	0	0	–	Yes
12	Criadouro Fazenda Paricuiã	N	PA	Terra Alta	Private	ConsBr	1	0	0	0	–	–
13	Fundação Zoobotânica de Marabá	N	PA	Marabá	Private	Zoo	1	1	0	0	–	No
14	Mantenedouro de Fauna Silvestre Santo Antonio	N	PA	Ananindeua	Private	WS	0	1	0	0	–	–
15	Parque Zoobotânico Emilio Goeldi	N	PA	Belém	Federal	Zoo	0	1	0	0	–	Yes
16	Parque Zoobotânico Vale	N	PA	Carajás	Private	Zoo	1	0	0	0	2015	Yes
17	Zoológico Faculdade da Amazônia – UNAMA	N	PA	Santarém	Private	Zoo	1	1	0	0	–	No
18	Criadouro Conservacionista Spazen	MW	DF	Brasília	Private	ConsBr	1	0	1	0	–	Yes
19	Fundação Jardim Zoológico de Brasília	MW	DF	Brasília	Foundation	Zoo	1	1	0	0	–	Yes
20	Criadouro Científico Instituto Onça Pintada	MW	GO	Mineiros	Private	ConsBR	0	0	1	2	–	Yes
21	Zoológico de Goiânia	MW	GO	Goiânia	County	Zoo	0	1	0	0	–	No
22	Zoopark da Montanha	SE	ES	Marechal Floriano	Private	Zoo	0	1	0	1	–	No
23	CRAX Sociedade de Pesquisa de Fauna Silvestre	SE	MG	Contagem	Private	ConsBr	3	6	9	3	1999–2005	No
24	Centro de Reprodução de Falconiformes e Falcoaria Ltda-Criadouro Cerefalco	SE	MG	Patrocínio	Private	ComBr	1	0	1	2	–	Yes
25	Criadouro Científico de Aves de Rapina Pró-Raptors	SE	MG	Brumadinho	Private	ConsBr	4	3	0	0	–	Yes
26	Criadouro Global Falcons	SE	MG	Sete Lagoas	Private	ComBr	0	1	0	0	–	Yes
27	Fundação Zoobotânica de Belo Horizonte	SE	MG	Belo Horizonte	Foundation	Zoo	2	1	0	0	–	Yes
28	Zoológico Vale Verde	SE	MG	Betim	Private	Zoo	0	0	1	0	–	No

#	Institution keeper	Region	State	City	Administration Type	Management Category	Origin of Birth				Breeding Period	Replied Survey
							Wild		Bred in Captivity			
							♂	♀	♂	♀		
29	Jardim Zoológico do Rio de Janeiro	SE	RJ	Rio de Janeiro	County/ Concession	Zoo	1	1	0	0	–	Yes
30	Fazenda Itaoca	SE	SP	Indaiatuba	Private	ComBr	1	1	0	3	2007–2009	Yes
31	Fundação Parque Zoológico de São Paulo	SE	SP	São Paulo	Foundation	Zoo	2	2	0	0	–	Yes
32	Parque Ecológico de São Carlos	SE	SP	São Carlos	County	Zoo	1	1	0	0	–	Yes
33	Parque Ecológico Municipal Eng. Cid Almeida Franco	SE	SP	Americana	County	Zoo	1	1	0	0	–	Yes
34	Parque Zoológico Municipal Quinzinho de Barros	SE	SP	Sorocaba	County	Zoo	1	1	0	0	–	Yes
35	Zooparque de Itatiba	SE	SP	Itatiba	Private	Zoo	2	2	1	0	2012	Yes
36	Criadouro Onça Pintada	S	PR	Curitiba	Private	Zoo	1	0	0	1	–	Yes
37	Parque das Aves	S	PR	Foz do Iguaçu	Private	Zoo	1	1	0	0	–	Yes
38	Zoológico Municipal de Curitiba	S	PR	Curitiba	County	Zoo	0	1	1	1	–	Yes
39	Zoológico Roberto Ribas Lange – Itaipu Binacional	S	PR	Foz do Iguaçu	Private	Zoo	4	5	14	10	2006–2020	Yes
40	Hayabusa Falcoaria e Consultoria Ambiental	S	RS	São Francisco de Paula	Private	ComBr	1	2	0	0	–	Yes
						Total	35	51	29	24	–	–

the identification of the number of individuals in Brazil and abroad, including information about the sex, individual identification (rings and microchips), time under human care, and origin. PAN of Amazonian Birds recommended integrated in situ and ex situ conservation programs (Brasil 2014b), as was stated in the IUCN guidelines about the use of ex situ management for species conservation (IUCN/SSC 2014). Seen in these terms, this article presents a revision of the Harpy Eagle ex situ population worldwide with a focus on Brazil.

Materials and methods

'Ex situ' was used here as defined by the IUCN ex situ Guidelines, as conditions under which individuals are spatially restricted with respect to their natural spatial patterns or those of their progeny, are removed from many of their natural ecological processes, and are managed on some level by humans (IUCN/SSC 2014).

Some information about the ex situ population of Harpy Eagle was gathered from previous data available in environmental institutions, such as wildlife raptor centres, wildlife centres, the environmental police, animal institution keepers, and breeding centres, hereafter called ex situ facilities. Three methods were used to gather data.

Available information and published data

A literature review took place to gather data about the ex situ facilities with records of Harpy Eagles under human care in Brazil and other countries. Moreover, three data sources were updated with information from researchers that work with this species in Brazil and had previously gathered data: Azeredo (2002, 2005), Banhos (2009), Banhos et al. (2016), and the Harpy Eagle Project database. The latter were collected from 2001 to 2020 during visits to Brazilian institutions keeping Harpy Eagles when personal communication, transcription from files, and interviews with employees took place. The Brazilian Institute of Environment and Renewable Natural Resources (**IBAMA**; Brazil 2019) database was also consulted using the Citizen Information Service Electronic System. Historic files were rare, although records from the early 1960's were obtained. The results were compiled in two groups: before 1983 with the law legalising zoos in Brazil (Brasil 1983) and after 1984.

Survey

A survey form was applied to 36 institutions keeping Harpy Eagles in Brazil (Suppl. material 1: Table S1). The queries included the number of individuals, gender, place of origin, and details in cases of rescued animals, including origin (from wild or bred in captivity under human care) and mating, with data up to 2020. The acronym names for all states that received the forms are as follows:

AC	Acre;	**MG**	Minas Gerais;
AM	Amazonas;	**PA**	Pará;
AP	Amapá;	**PE**	Pernambuco;
BA	Bahia;	**PI**	Piauí;
CE	Ceará;	**PR**	Paraná;
DF	Distrito Federal;	**RJ**	Rio de Janeiro;
ES	Espírito Santo;	**RS**	Rio Grande do Sul;
GO	Goiás;	**SE**	Sergipe;
MA	Maranhão;	**SP**	São Paulo.

There were another five institutions keeping Harpy Eagles that were contacted after the surveys were finished. They did not receive the survey form, but their information was included in the results.

Zoological Information Management Software database

The Species360 Zoological Information Management Software (**ZIMS**) database (ZIMS 2020) was consulted. Additionally, experts in birds of prey were asked to identify institutions that had ex situ populations of Harpy Eagles outside Brazil, and the Harpy Eagle Project collection database was referred to for visits to institutions outside Brazil, in Panama, Ecuador, Argentina, and French Guiana (2014–2018).

Results

Ex situ Harpy Eagle population in Brazil

Survey form

Twenty-nine (72.5%) institutions keeping Harpy Eagles ex situ answered the survey form, which provided institutional results to be combined with the information from other sources. Seven (17.5%) institutions do not return the survey answered (Table 1), with exception of the Crax Sociedade de Pesquisa de Fauna Silvestre, all other facilities have one individual or a pair.

Entrance of Harpy Eagles to ex situ facilities

Harpy Eagles from the wild

Thirteen records came from documented reports from 1963 to 1983 (20-years period), referring to one individual in 1966, 1972, and 1980 and two individuals in 1963, 1973, 1975, and four individuals 1979. Of those 13 individuals, only one was still alive in 2020. In the last 37 years (1984 to 2020), it was possible to document a

minimum of 122 wild Harpy Eagle entrances to facilities in Brazil, with an average of 3.2 individuals/year. The highest entrance rate was nine individuals in 2004 and 2007 (Fig. 1). Of those 122 wild individuals, 35 died before the initiation of this study.

Harpy Eagles bred in captivity under human care

The first record of Harpy Eagle breeding under human care in Brazil was in 1995 by the former conservation breeder Erico Albuquerque de Abreu e Lima; however, the chick did not survive (Azeredo 2005; Fig. 1). In 1988, one Harpy Eagle hatched and was bred in captivity under human care in Germany. In 1996, it was sent to Brazil to the care of the Society of Research and Wildlife – CRAX (R Azeredo pers. comm.; Globo Rural 2012; Fig. 1). The first successful captive breeding in Brazil occurred in 1999 by CRAX (Azeredo 2005). Sixty-two individuals hatched under human care in the period 1999–2020 (Fig. 1). Of those 62 individuals, six died and four were sent to institutions in Europe.

Harpy Eagle ex situ population in 2020

In 2020, the Harpy Eagle ex situ population in Brazil comprised 139 individuals kept in 40 institutions (Table 1), of which 86 (62%) were taken from the wild (35 males and 51 females), while 53 (38%) hatched and were bred in captivity under human care

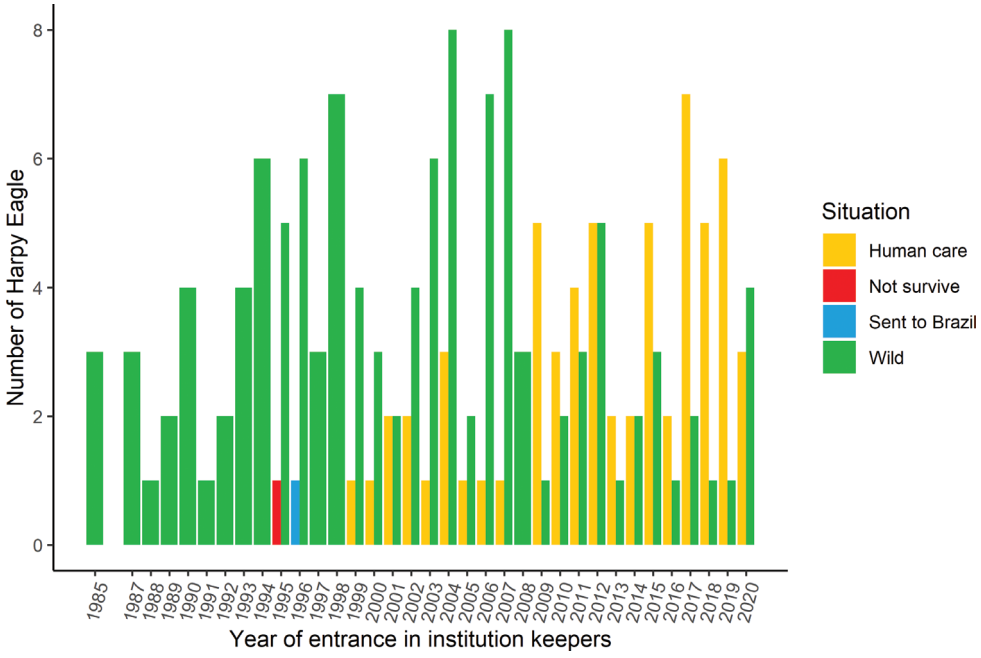

Figure 1. Number of Harpy Eagles (*Harpia harpyja*) yearly entrance to Brazilian institutions between 1984 and 2020.

(29 males and 24 females; Table 1). On average (±SD), the institutions kept 2.2 ± 1.4 Harpy Eagles, not including two institutions, CRAX Society of Research and Wildlife and Roberto Ribas Lange Zoo, that kept 21 and 33 individuals, respectively (Table 1).

Wild Harpy Eagle locality of origin

Of the 86 wild Harpy Eagles, 64 (74%) individuals had a known state of origin, and 22 (26%) individuals were of unknown origin. Most Harpy Eagles came from the Amazon biome, Pará state (*n* = 31; 35%), followed by Rondônia state (*n* = 10; 11%) and Amazonas state (*n* = 8; 9%), Mato Grosso state (*n* = 4; 5%), Acre state (*n* = 2; 2%), and Amapá state (*n* = 2; 2%). In addition to the Amazon biome, other biomes were also the source of wild Harpy Eagles, including the Brazilian Atlantic Forest, Bahia state (*n* = 4; 4%) and Paraná state (*n* = 1; 1%). The Cerrado had two (2%) individuals from Goiás state (Fig. 2).

Type of entrance from nature to the first facility

The source of their entrance to the first facility was possible to determine for 53 (60%) individuals only due to the lack of information. Records were classified as wildlife catching (33%), wildlife rescue (17%), and voluntary handover (10%). Females were the majority in all categories (Fig. 3).

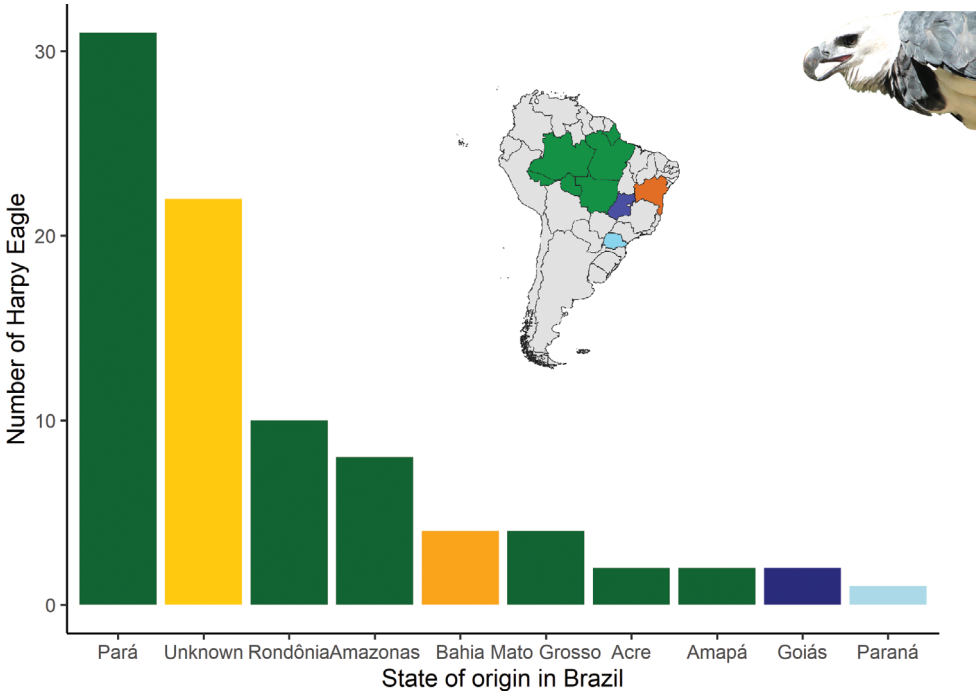

Figure 2. Origin of wild Harpy Eagles (*Harpia harpyja*) by state and biome kept in Brazilian ex situ facilities in 2020.

Location, management category, and administration type of the institution

Geographic locations for the 40 Harpy Eagle facilities in Brazil were mainly in the Southeast (n = 14) and North regions (n = 10), with seven in the northeast, five in the south, and four in the midwest (Table 1). Of the facilities, 60% were under private administration, followed by state (40%), county (15%), federal (7.5%), and foundation administration (7.5%; Table 1). The majority of these ex situ facilities were registered in the management category as zoos (n = 24; 60%), followed by conservation breeders (n = 7; 17.5%), commercial breeders (n = 6; 15%), wildlife shelters (n = 2; 5%), and wildlife sorting centre (n = 1; 2.5%; Table 1).

Among those institutions, 23 kept one Harpy Eagle pair or more individuals, while other 17 institutions kept only single. Within the institutions with one gender, there were ten zoos (11 females and 2 males), one commercial breeder (1 female), three conservation breeding (3 females and 3 males), two wildlife shelters (2 females), and one wildlife sorting centre (IBAMA; 2 females; Table 1).

Harpy Eagle breeding records under human care

Based only on the survey information, seven institutions had some attempt or success of captive breeding from 1999 to 2020 (Table 1). Three other ex situ facilities that no longer exist had breeding success: the conservation breeder Tropicus in the Rio de Janeiro municipality (2001), the conservation breeder Erico Albuquerque de Abreu e

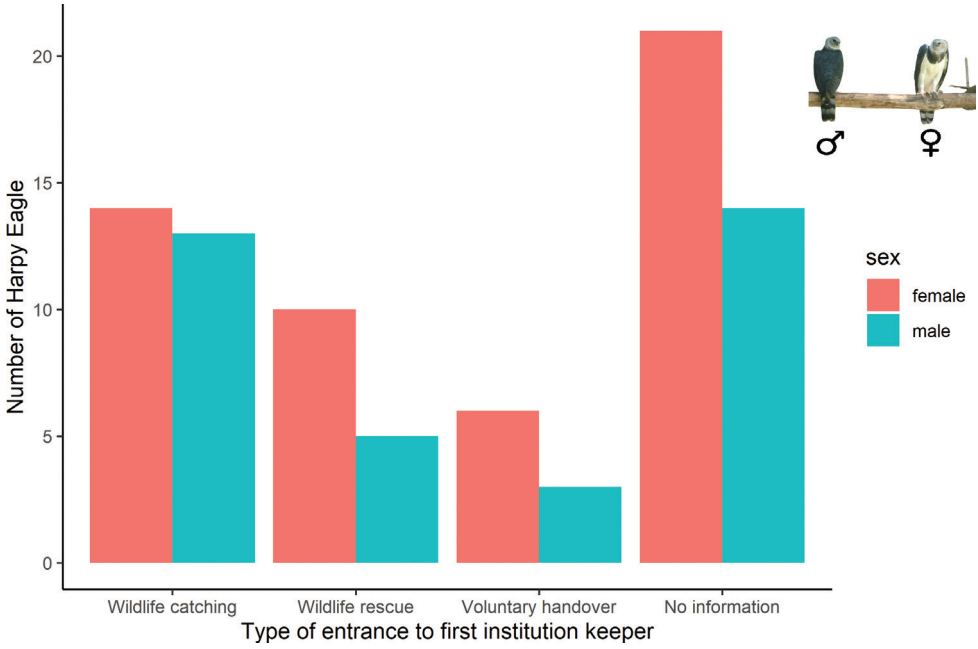

Figure 3. Type of entrance of wild Harpy Eagles (*Harpia harpyja*) to their first ex situ facility in Brazil.

Lima in the Distrito Federal municipality (2005), and the breeder Parque da Varginha in the Tocantins municipality (2010). The three individuals kept in these institutions were transferred to active ex situ facilities.

Ex situ Harpy Eagle population outside Brazil

In 2020, there were 66 Harpy Eagles kept in 37 facilities outside Brazil, distributed among 15 countries, representing 32% of the entire ex-situ population (68% were in Brazil) and 48% of all ex situ facilities (52% were in Brazil; Fig. 4). The United States, Germany, Peru, Ecuador, and Colombia had the largest number of individuals (Fig. 4). Of those 66 Harpy Eagles, 36 were males and 29 were females, and in one, the sex was unknown. In South America, 26 came from the wild (13 males and 13 females), one male was bred in captivity under human care, and eight were of unknown origin. In Central America, two females came from the wild and one male was bred in captivity under human care. In North America, two males came from the wild, 14 were bred in captivity under human care (7 males and 7 females). In Europe, 11 were bred in captivity under human care (7 males and 4 females), and one was of unknown origin (Suppl. material 2: Table S2).

Discussion

Lack of data regarding the capture method and place of origin (locality) of the Harpy Eagles imposed a challenge to information collection in this study. In most cases, there was a lack of data on the records of wildlife catching and rescue centres, contributing to a high number of unknown origin localities. Additionally, much information was lost when Harpy Eagles were transferred between institutions.

The first Harpy Eagle reported in the care of a zoo in Brazil was in 1895, at the Parque Zoobotânico do Museo Goeldi, in the state of Pará, one of the oldest zoos in the country (Sanjad et al. 2012). This same zoo received a second individual in 1901 (Sanjad et al. 2012). The voucher specimen MPEG3445 conserved by taxidermy from the "Fernando Novaes" bird collection at Museo Paraense Emílio Goeldi, dated from 1904, probably belonged to one of those birds. A small private zoo, Jardim Zoológico Vila Isabel in Rio de Janeiro, also held a Harpy Eagle, which died sometime between 1890 and 1899 and was donated to the Museo Nacional (Pais 2013). Of the three oldest recorded individuals, two of them entered the Zoológico de Goiânia in 1963; both came from Roraima state (José Hidasi, pers. comm). One of these birds was taxidermically conserved (skin voucher N.13.268) in the bird collection at Fundação Museo de Ornitologia. The third Harpy Eagle entered the Zoológico de Brasília in 1966 but died in 1969 with no further information.

The compilation from 1963 to 1983 did not reflect a precise quantity due to the lack of recorded files at the majority of institutions, which were our information sources. However, the compilation from 1984 to 2020 was well recorded and revealed

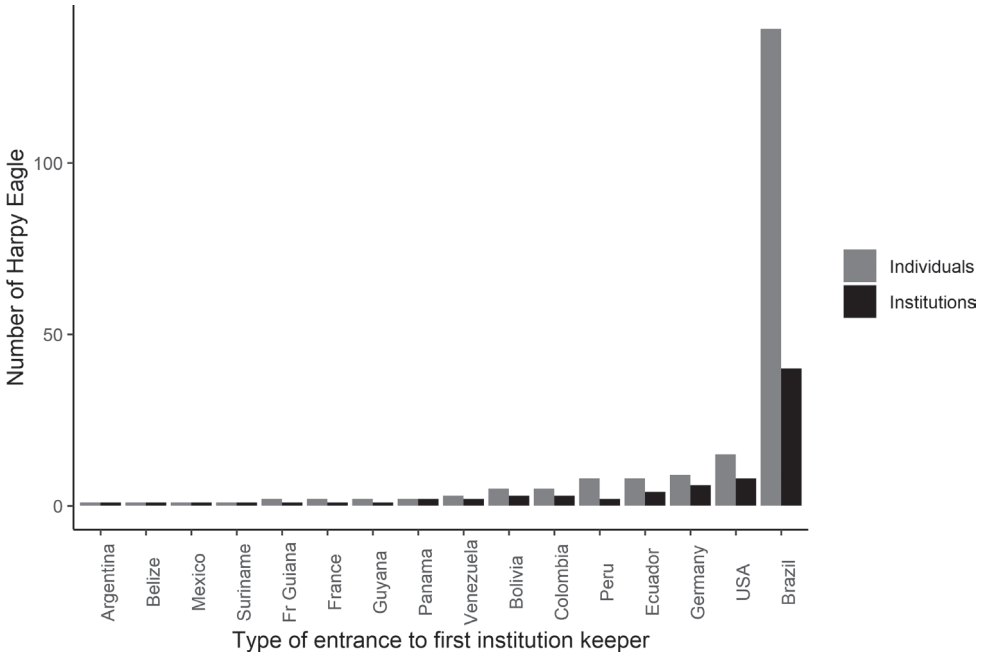

Figure 4. Harpy Eagles (*Harpia harpyja*) ex situ population worldwide in 2020.

a high rate of individuals removed from nature (3.2 individuals/year), including bird victims from conflict between birds and humans in Brazil. In 2020, four Harpy Eagles entered Brazilian ex situ facilities; this number is four times greater than the previous two years, and it was the highest number since 2012 (Fig. 1). Notably, in 2020, the global COVID-19 pandemic began and had strong impacts on people's health and activities; however, it also impacted biodiversity due to the reduction in protection and inspection of natural habitats (Bang and Khadakkar 2020; Corlett et al. 2020), and apparently the Harpy Eagle was not exempt from this effect. Although the type of conflicts involved has not been documented for the majority of cases, in general, individuals removed from nature and sent to these ex situ facilities were attained after suffering from collision traumas with vehicles, falling from tree-nests, being injured by gunshot, receiving wounds of uncertain origin and being kept in captivity illegally by people (Soares et al. 2008; Amorim et al. 2010; Silva et al. 2010). The retention of Harpy Eagle individuals that were alive but could not return to the wild, in addition to the number that were killed by hunters (Trinca et al. 2008; Giraldo-Amaya et al. 2021) and other sources of human-animal conflict (Gusmão et al. 2020), most likely contributed to the populational decline of the Harpy Eagle in the wild. Harpy Eagles transferred from the wild into zoos were mainly females (59%), which may have impacted the demography of the wild Harpy Eagle population.

The Amazon has been the major source of Harpy Eagles that have been removed from nature, and the states of origin within the region are mainly Para, Rondônia,

Amazonas, and Mato Grosso, which have experienced the world's highest absolute rate of forest destruction (Soares-Filho et al. 2006; Silva Junior et al. 2021). Likewise, the Brazilian Atlantic Forest was reduced and fragmented (Ribeiro et al. 2009), and there have been few records about free-ranging Harpy Eagles (Aguiar-Silva et al. 2012; Meller and Guadagnin 2016). The Brazilian Atlantic forests have still been subject to Harpy Eagle removal from nature, with five individuals taken from Bahia state in the northeast region (Table 1). One individual was removed from the Biome Cerrado. In this biome, Harpy Eagle records have been always rare and this corresponds to this comparably low number. However, there were more records available in gallery forests and in the transition into the Amazonia (Pinheiro and Dornas 2009; Silva et al. 2013; Pascoal et al. 2014) and the Atlantic Forest (Oliveira and Silva 2006; Pereira and Salzo 2006).

For Harpy Eagle conservation, the return of all captured Harpy Eagles in adequate health conditions back to nature, re-establishing these individuals into the natural population, is a complex process but one that is necessary for a health and functional ecosystem. There exists a decision tree to assist the assessment of birds in Brazil at stages of the process after a rescue of injured individuals or from trades and from illegal traffic or captivity (Efe et al. 2006). In 2018, the Harpy Eagle Project in Brazil (Projeto Harpia) began a national network to rehabilitate those Harpy Eagles; however, rehabilitation through the network has not yet been possible; in most cases, this was declared to be due to lack of funds, staff, and specific infrastructure, although the Project has succeeded with a number of individuals in the past for specific regions in the country. The idea of this network is to use the zoo's support during the rehabilitation of the individuals. If rehabilitation is not possible, individuals may be allocated to an ex situ conservation program. An integrated in situ and ex situ conservation program, involving the rehabilitation of animals removed from nature seems necessary. There is an increasing need for a 'one plan approach' to develop multi-disciplinary conservation strategies that include the integration of in situ and ex situ management processes (Byers et al. 2013).

Captive breeding can play a crucial role in the recovery of some species for which effective alternatives are unavailable in the short term, while protecting species habitats and ecosystems (Collar and Butchart 2014; Fleming et al. 2011; Snyder et al. 1996). Breeding under human care has the potential to maintain targeted populations as an 'insurance policy' against threats until reintroduction into the wild is possible (Conde et al. 2011). Breeding aimed at the restoration of populations in danger of extinction must not be replaced with breeding for other goals such as exposition, conservationist education, or research (Snyder et al. 1996). However, zoos have played an important role in the conservation of endangered species by promoting and supporting environmental awareness, providing professional qualifications, and facilitating research and in situ conservation programs to support environmental recovery projects (Snyder et al. 1996; Conde et al. 2011). Moreover, zoos contributed to species conservation and increased interest and public affection by reporting the success of captive breeding and by educating the public about the importance of a high biodiversity (Gusset and Dick 2010;

Zimmermann 2010). In Brazil, for example, the Roberto Ribas Lange Zoo, in a five-year period (2012 to 2017), was visited by 146,633 visitors (Cubas et al. 2017). Zoos worldwide are providing conservation funds, investing millions in ex situ and in situ wildlife activities (Gusset and Dicke 2010; Zimmermann 2010; Fa et al. 2014). Assisted reproduction may be of high future for ex situ conservation and should be considered in future as part of a multidisciplinary one-plan approach for the conservation of Harpy Eagles (Blanco et al. 2002a, b; Gee et al. 2004; Fischer et al. 2014).

Harpy Eagle ex situ populations outside Brazil consisted of 35 wild individuals, most in South America. An important step is to understand their characteristics as a source of genetic diversity. Currently, some of those zoos in Europe that have Harpy Eagle individuals hatched in captivity are contributing to ex situ and in situ conservation of Harpy Eagles by promoting funds for research, for example, ZooParc de Beauval (France) and Tiergarten Nürnberg (Germany).

To reach the ex situ conservation goals as required by article 9 of the CBD (Glowka et al. 1994; Conde et al. 2011), future conservation activities should be focused on joining forces and acting in an integrated manner for handling. The establishment of a structured ex situ Harpy Eagle program and an international Harpy Eagle studbook seems to be required. The potential roles of a species conservation program must be clearly defined and should include the maintenance of a healthy and genetically diverse ex situ backup population, measures to rescue and rehabilitate wild individuals, population restoration, research, training, and education in accordance with the IUCN guidelines (McGowan et al. 2017).

Conclusions

Brazil maintains the largest ex situ Harpy Eagle population in the world. Brazilian institutions played an important role in breeding for ex situ conservation of the Harpy Eagle. A great number of institutions in South and Central America keep wild individuals, while North America and Europe mainly keep individuals bred in captivity under human care. Information about ex situ individuals must be incorporated into a studbook for Harpy Eagle population management. These individuals may potentially constitute a genetically and demographically viable backup population for future conservation attempts, as well as a source of research and education applied to Harpy Eagle conservation. The Harpy Eagle ex situ population must be used in integrated planning to support in situ population conservation.

Acknowledgements

We thank the Binational Itaipu for support. Funding support was obtained from the Cleveland Zoo, Fundação O Boticário de Proteção à Natureza, Conselho Nacional de Desenvolvimento Científico e Tecnológico (CNPq), Fundação de Amparo à Pesquisa

e Inovação do Espírito Santo (FAPES), Beauval Nature, Tiergarten Nürnberg, Instituto Internacional de Educação do Brasil (IEB), Instituto Nacional de Pesquisas da Amazônia (INPA), and Projeto Harpia. An FHAS post-doc Grant was obtained from CNPq-PDJ152371/2019–2. We thank the Harpy Project Ex Situ Coordinator Yara Barros for her technical support. Additionally, we thank the institutions that shelter and/or breed Harpy Eagle in Brazil for their participation by providing answers to the survey and/or receiving the Projeto Harpia team at their facilities between 2001 and 2020, as listed in table 1. We also thank the institutions that are no longer Harpy Eagle keepers but received the Projeto Harpia team: CRAS – Campo Grande – MS; Criadouro Erico A de Abreu e Lima-DF; Criadouro Tropicus; Parque Zoológico Sapucaia do Sul-RS; Parque Zoobotânico Gavião-real (Capitão Poço); Zoológico de São José do Rio Preto – SP; Zoológico da UFMT-Cuiabá; Fundação Museo de Ornitologia and IBAMA – Cetas (Manaus e Parintins-AM, Guarantã do Norte-MT, Macapá-AP, Goiânia-GO, Belém-PA); Cetas UHE Santo Antonio-RO; and Cetas UHE Belo Monte – PA. A number of researchers and experts helped to complete the database for this study: from **South America**, José Hidasi, Nicolas Neumann, Andrea Mabel Morales Vargas, Mario Daniel Zambrana Lopez, Raul Rojas, Claudia Venegas, Alex Ospina, Sandy Zangen, Joep Hendrix, Ruth Muniz López, Olivier Bongard, José Antonio Otero, Tatiana Rivarola, Jorge Mauricio De la O Castro, Antonio Fernandini Guerrero, Pilar Alexander Blanco, and Andrea Echeverry; from **Central America**, Karla Aparicio and Angel Muela; from **North America**, Eduardo Alvarez-Cordero, Alan Monroy Oyeda, and Frank Camacho; from **Europe**, Lorenzo Von Fersen. This is publication #13 of the Harpy Eagle Project (Projeto Harpia). This study is part of MJO's Master's degree at the Universidade Federal do Paraná (UFPR). We are grateful to Israel Schneiberg for the updates to the figures. The images of harpies in Figs. 2 and 3 are from the MJO's collection.

References

Aguiar-Silva FH, Sanaiotti TM, Jaudoin O, Srbek-Araujo AC, Siqueira G, Banhos A (2012) Harpy Eagle sightings, traces and nesting records at the" Reserva Natural Vale", a Brazilian Atlantic Forest remnant in Espírito Santo, Brazil. Revista Brasileira de Ornitologia 20(2): 148–155.

Aguiar-Silva FH, Junqueira TG, Sanaiotti TM, Guimarães VY, Mathias PVC, Mendonça CV (2015) Resource availability and diet in Harpy Eagle breeding territories on the Xingu River, Brazilian Amazon. Brazilian Journal of Biology 75(3, suppl.): S181–S189. https://doi.org/10.1590/1519-6984.00914BM

Alves MAS, Pacheco JF, Gonzaga LAP, Cavalcanti RB, Raposo MA, Yamashita C, Maciel NC, Castanheira M (2000) Aves. In: Bergallo HG, Rocha CFD, Alves MAS, Sluys MV na (Eds) A fauna ameaçada de extinção do Estado do Rio de Janeiro. Editora da Universidade Estadual do Rio de Janeiro, Rio de Janeiro, 113–124.

Amorim PRN, Silva RR, Lemos M, Barreto ML (2010) Recuperação de um uiraçu (*Harpia harpyja*) na Reserva Particular do Patrimônio Natural REVECOM. Spizaetus 10: 16–22.

Azeredo R (2002) Reproducción y manejo del Harpía en cautiverio. Neotropical Raptor Conference and Harpy Eagle Symposium. Panama, 24–27.

Azeredo R (2005) Reprodução de *Harpia harpyja* em cativeiro. Rapina 1(1): 6–13.

Bang A, Khadakkar S (2020) Opinion: Biodiversity conservation during a global crisis: Consequences and the way forward. Proceedings of the National Academy of Sciences 117(48): 29995–29999. https://doi.org/10.1073/pnas.2021460117

Banhos A (2009) Genética, distribuição e conservação do gavião-real (*Harpia harpyja*) no Brasil. PhD. Thesis. INPA/UFAM, Manaus, AM, 163 pp.

Banhos A, Hrbek T, Sanaiotti TM, Farias IP (2016) Reduction of Genetic Diversity of the Harpy Eagle in Brazilian Tropical Forests. PLoS ONE 11(2): e0148902.

Banhos A, Sanaiotti TM, Aguiar-Silva FH, Martins FD, Luz BB, Carvalho AS, Ruiz CM (2018) *Harpia harpyja* (Linnaeus, 1758), Livro Vermelho da Fauna Brasileira Ameaçada de Extinção: Volume III – Aves ICMBio/MMA, Brasília, 124–128.

Bencke GA, Fontana CS, Dias RA, Maurício GN, Mähler Jr JK (2003) Aves. In: Fontana CS, Bencke GA, Reis RE (Eds) Livro Vermelho da Fauna Ameaçada de Extinção no Rio Grande do Sul. EdiPUCRS, Porto Alegre, 40 pp.

Birdlife International (2021) Harpia harpyja. The IUCN RedList of Threatened Species 2021: e.T22695998A197957213.

Blanco J, Wildt D, Hofle U, Voelker W, Donoghue A (2009) Implementing artificial insemination as an effective tool for ex situ conservation of endangered avian species. Theriogenology 71: 200–213. https://doi.org/10.1016/j.theriogenology.2008.09.019

Blanco JM, Gee GF, Wildt DE, Donoghue AM (2002a) Producing progeny from endangered birds of prey, urine contamination, intramagnal insemination. Journal of Zoo and Wildlife Medicine 33: 1–7. https://doi.org/10.1638/1042-7260(2002)033[0001:PPFEBO]2.0.CO;2

Blanco JM, Wildt DE, Monfort SL, Gee GF, Donoghue AM (2002b) Developing assisted reproductive technologies to promote ex situ raptor conservation. In: The Second International Symposium on Assisted Reproductive Technology (ART) for the Conservation and Genetic Management of Wildlife, Omaha, Nebraska, USA, 264 pp.

Brasil (1983) Lei n° 7.173, de 14 de dezembro de 1983. Dispõe sobre o estabelecimento e funcionamento de jardins zoológicos e dá outras providências. Diário Oficial da União, Brasília, DF, 15 de dezembro de 1983. http://www.planalto.gov.br/ccivil_03/Leis/1980-1988/L7173.html [accessed 12 Dec 2020]

Brasil (2008) Ministério de Meio Ambiente. Instituto Chico Mendes de Conservação da Biodiversidade. Instrução Normativa 169, de 20 de fevereiro de 2008. www.icmbio.gov.br/sisbio/legislacao-especifica.html [accessed 06 June 2018]

Brasil (2012) Ministério do Meio Ambiente, Instituto Chico Mendes de Conservação da Biodiversidade. Plano de ação nacional para a conservação das espécies endêmicas e ameaçadas de extinção da fauna da região do Baixo e Médio Xingu – PAN Baixo e Médio Xingu. Portaria N° 16, 17 de fevereiro de 2012. Ministério do Meio Ambiente, Brasília, 19 pp.

Brasil (2014a) Ministério do Meio Ambiente, Instituto Chico Mendes de Conservação da Biodiversidade. Lista nacional das espécies da fauna Brasileira ameaçadas de extinção. Portaria n° 444, 17 de dezembro de 2014. MMA/ICMBio, Brasília, Brasil, 1–13.

Brasil (2014b) Ministério do Meio Ambiente, Instituto Chico Mendes de Conservação da Biodiversidade. Plano de Ação Nacional para Conservação das Aves da Amazônia ameaçadas de extinção, PAN – Aves da Amazônia. Portaria n° 35, 27 de março de 2014. Ministério do Meio Ambiente, Brasília.

Brasil (2017) Ministério do Meio Ambiente, Instituto Chico Mendes de Conservação da Biodiversidade. Plano de Ação Nacional para a Conservação das Aves da Mata Atlântica. Portaria N° 34, 24 de janeiro de 2017. Ministério do Meio Ambiente, Brasília.

Brasil (2018) Ministério do Meio Ambiente, Instituto Chico Mendes de Conservação da Biodiversidade. Plano de Ação Nacional para a Conservação das Aves de Rapina. www.icmbio.gov.br/portal/faunabrasileira/plano-de-acao-nacional-lista

Brasil (2019) Ministério do Meio Ambiente, Instituto Brasileiro do Meio Ambiente e dos Recursos Naturais Renováveis. Serviço de Informação ao Cidadão por formulário eletrônico via Internet- e-SIC. Protocolo n° 01390000628201940, 22/04/2019.

Butchart SHM, Satterfield AJ, Collar NJ (2006). How many bird extinctions have we prevented? Oryx 40(3): 266–278. https://doi.org/10.1017/S0030605306000950

Byers O, Lees C, Wilcken J, Schwitzer C (2013) The One Plan Approach: The philosophy and implementation of CBSG's approach to integrated species conservation planning. WAZA Magazine 14: 2–5.

Cerri C (1996) Senhora dos Ares. Globo Rural 129: 38–45. https://doi.org/10.3406/etnor.1996.2238

CITES (2019) Convention on International Trade in Endangered Species of Wild Fauna and Flora. Appendices I, II and III. www.cites.org/eng/app/index [accessed 06/2019]

Collar NJ, Butchart SHM (2014) Conservation breeding and avian diversity: chances and challenges. International Zoo Yearbook 48: 7–28. https://doi.org/10.1111/izy.12039

Conde DA, Flesness N, Colchero F, Jones OR, Scheuerlein A (2011) An emerging role of zoos to conserve biodiversity. Science 331(6023): 1390–1391. https://doi.org/10.1126/science.1200674

Corlett RT, Primack RB, Devictor V, Maas B, Goswami VR, Bates AE, Koh LP, Regan TJ, Loyola R, Pakeman RJ, Cumming GS, Pidgeon A, Johns D, Roth R (2020) Impacts of the coronavirus pandemic on biodiversity conservation. Biological Conservation 246: e108571. https://doi.org/10.1016/j.biocon.2020.108571

Curti M, Valdez U (2009) Incorporating community education in the strategy for Harpy Eagle conservation in Panama. Journal of Environmental Education 40: 3–16. https://doi.org/10.3200/JOEE.40.4.3-16

Deluca JJ (2012) Birds of conservation concern in eastern Acre, Brazil: distributional records, occupancy estimates, human-caused mortality, and opportunities for ecotourism. Tropical Conservation Science 5: 301–319. https://doi.org/10.1177/194008291200500306

Efe MA, Martins-Ferreira C, Olmos F, Mohr LV, Silveira LF (2006) Diretrizes da Sociedade Brasileira de Ornitologia para a destinação de aves silvestres provenientes do tráfico e cativeiro. Revista Brasileira de Ornitologia 14(1): 67–72.

Fa JE, Gusset M, Flesness N, Conde DA (2014) Zoos have yet to unveil their full conservation potential. Animal Conservation 17: 97–100. https://doi.org/10.1111/acv.12115

Fischer D, Neumann D, Purchase C, Bouts T, Meinecke-Tillmann S, Wehrend A, Lierz M (2014) The use of semen evaluation and assisted reproduction in Spix's macaws in terms of species conservation. Zoo Biol 33(3): 234–244. https://doi.org/10.1002/zoo.21129

Fleming LV, Douse AF, Williams NP (2011) Captive breeding of peregrine and other falcons in Great Britain and implications for conservation of wild populations. Endangered Species Research. 14: 243–257. https://doi.org/10.3354/esr00352

Freitas MA, Lima DM, Gomes FBR (2014) Registro de abate de gaviões-reais *Harpia harpyja* (Accipitridae) para consumo humano no Maranhão, Brasil. Atualidades Ornitológicas 178: 12–15.

Gee GF, Bertschinger H, Donoghue AM, Blanco J, Soley J (2004) Reproduction in Nondomestic Birds: Physiology, Semen Collection, Artificial Insemination and Cryopreservation. Avain and Poultry Biology Reviews. 15: 47–101. https://doi.org/10.3184/147020604783637435

Giraldo-Amaya M, Aguiar-Silva FH, Aparicio-U KM, Zuluaga S (2021) Human persecution of the Harpy Eagle: a widespread threat? Journal of Raptor Research 55(2): 281–286. https://doi.org/10.3356/0892-1016-55.2.281

GLOBO RURAL (2012) 'Doutor harpia' cria aves silvestres para a reintrodução na natureza. http://g1.globo.com/natureza/noticia/2012/01/doutor-harpia-cria-animais-silvestres-para-reintroducao-na-natureza.html [accessed 13 apr 2021]

Glowka L, Burhenne-Guilmin F, Synge H (1994) A guide to the Convention on Biological Diversity. IUCN, Gland and Cambridge, [xii +] 161pp.

Gusmão AC, Banhos A, Aguiar-Silva FH, Souza LS, Sanaiotti TM, Silva AM, Costa TM, Oliveira LE, Morais WG, Ferrari SF (2016) Records of the occurrence, nesting, and hunting of the Harpy Eagle (*Harpia harpyja*) (Aves: Accipitridae) in Rondônia, Southwestern Brazilian Amazonia. Atualidades Ornitológicas 190: 18–23.

Gusmão AC, Degra D, Silva ODD, Souza LSD, Frota AVBD, Tuyama CA, Tuyama MC, Costa TMD, Dalbem AP, Barnett AA, Aguiar-Silva FH, Santos Filho MD (2020) Power lines as a threat to a canopy predator: electrocuted Harpy Eagle in southwestern Brazilian Amazon. Journal of Threatened Taxa 12(13): 16904–16908. https://doi.org/10.11609/jott.6198.12.13.16904-16908

Gusset M, Dick G (2010) 'Building a Future for Wildlife'? Evaluating the contribution of the world zoo and aquarium community to in situ conservation. International Zoo Yearbook 44: 183–191. https://doi.org/10.1111/j.1748-1090.2009.00101.x

IUCN/SSC (2014) Guidelines on the use of ex situ management for species conservation. Version 2.0. Gland, Switzerland: IUCN Species Survival Commission.

Kuhn CN (2018) [WA2997981, *Harpia harpyja* (Linnaeus, 1758)]. Wiki Aves – A Enciclopédia das Aves do Brasil. http://www.wikiaves.com/2997981 [accessed 04 April 2019]

Lerner HRL, Johnson JA, Lindsay AR, Kiff LF, Mindell DP (2009) It is not too late for the Harpy Eagle (*Harpia harpyja*): High levels of genetic diversity and differentiation can fuel conservation programs. PLoS ONE 4(10): e10. https://doi.org/10.1371/journal.pone.0007336

McGowan PJ, Traylor-Holzer K, Leus K (2017) IUCN guidelines for determining when and how ex situ management should be used in species conservation. Conservation Letters 10(3): 361–366. https://doi.org/10.1111/conl.12285

Meller DA, Guadagnin DL (2016) Rediscovery of the Harpy Eagle *Harpia harpyja* (Accipitriformes: Accipitridae) for Rio Grande do Sul state, Brazil. Revista Brasileira de Ornitologia 24(1): 53–57. https://doi.org/10.1007/BF03544329

Oliveira ALD, Silva RSE (2006) Registro de Harpia (*Harpia harpyja*) no cerrado de Tapira, Minas Gerais, Brasil. Revista Brasileira de Ornitologia 14(4) 433–434.

Oliveira MJ (2018) Manejo Reprodutivo de Harpia em cativeiro no Brasil. Master Dissertation. Universidade Federal do Paraná, Curitiba, 137 pp.

Pacifico EC, Barbosa EA, Filadelfo T, Oliveira KG, Silveira LF, Tella JL (2014) Breeding to non-breeding population ratio and breeding performance of the globally Endangered Lear's Macaw *Anodorhynchus leari*: conservation and monitoring implications. Bird Conservation International 24(4): 466–476. https://doi.org/10.1017/S095927091300049X

Pais JA (2013) Jardim Zoológico: Desafios para a aplicação do conceito de Museo aos espaços de exposição de organismos vivos. Master Thesis. Universidade Federal do Estado do Rio de Janeiro – UNIRIO / Museo de Astronomia e Ciências Afins -MAST, Rio de Janeiro, 379 pp.

Pascoal W, Souza LBE, Teixeira DR, Paula MJD, Crozariol MA, Dornas T (2014) Registro do gavião-real, *Harpia harpyja* (Accipitriformes, Accipitridae) em área urbana no bioma Cerrado. Atualidades Ornitológicas 177: 13–15.

Pereira AMM, Salzo I (2006) Primeiro registro de nidificação de Harpia harpyja (Falconiformes, Accipitridae) na Serra da Bodoquena (Mato Grosso do Sul, Brasil). Revista Brasileira de Ornitologia 14(2): 157–160.

Pinheiro RT, Dornas T (2009) Distribuição e conservação das aves na região do Cantão, Tocantins: ecótono Amazônia/Cerrado. Biota Neotropical 9(1): 187–205. https://doi.org/10.1590/S1676-06032009000100019

Ribeiro MC, Metzger JP, Martensen AC, Ponzoni FJ, Hirota MM (2009) The Brazilian Atlantic Forest: How much is left, and how is the remaining forest distributed? Implications for conservation. Biological Conservation 142(6): 1141–1153. https://doi.org/10.1016/j.biocon.2009.02.021

Sanaiotti TM, Junqueira TG, Palhares V, Aguiar-Silva FH, Henriques LMP, Oliveira, G, Guimarães VY, Castro V, Mota D, Trombin DF, Villar DNA, Lara KM, Fernandes D, Castilho L, Yosheno E, Alencar RM, Cesca L, Dantas SM, Laranjeiras TO, Mathias PC, Mendonça CV (2015) Abundance of Harpy and Crested Eagles from a reservoir-impact area in the Low- and Mid-Xingu River Sanaiotti. Brazilian Journal of Biology 75(3 suppl.): S190–S204. https://doi.org/10.1590/1519-6984.00614BM

Sanjad N, Oren DC, e Silva JdeS Jr, Hoogmoed MS, Higuchi H (2012) Documentos para a história do mais antigo jardim zoológico do Brasil: o Parque Zoobotânico do Museo Goeldi. Boletim do Museo Paraense Emílio Goeldi. Ciências Humanas 7(1): 197–258. https://doi.org/10.1590/S1981-81222012000100013

Seddon PJ, Griffiths CJ, Soorae PS, Armstrong DP (2014) Reversing defaunation: Restoring species in a changing world. Science 345(6195): 406–412. https://doi.org/10.1126/science.1251818

Silva DA, Melo FR, Guimarães Jr IG (2013) Historical and recent records of the Harpy Eagle (*Harpia harpyja*) in the Cerrado biome of the state of Goiás, Brazil. Revista Brasileira de Ornitologia 21(4): 260–263.

Silva AG, Knoechelmann CM, Mororó DI, Lisbôa FM, Araújo Jr LM (2010) Manejo de animais silvestres conservados na Fundação Zoobotânica de Marabá, Pará, Brasil. Enciclopédia Biosfera, Centro Científico Conhecer 6(10): 1–10.

Silva Junior CHL, Pessôa ACM, Carvalho NS, Reis JBC, Anderson LO, Aragão LEOC (2021) The Brazilian Amazon deforestation rate in 2020 is the greatest of the decade. Nature Ecology & Evolution 5: 144–145. https://doi.org/10.1038/s41559-020-01368-x

Silveira LF, Benedicto GA, Schunck F, Sugieda AM (2009) Aves. In: Bressan PM, Kierulff MCM, Sugieda AM (Eds) Fauna ameaçada de extinção no Estado de São Paulo: Vertebrados. Governo do Estado de São Paulo/Secretaria do Meio Ambiente/Fundação Parque Zoológico de São Paulo, São Paulo, 87–100.

Snyder NF, Derrickson SR, Beissinger SR, Wiley JW, Smith TB, Toone WD, Miller B (1996) Limitations of captive breeding in endangered species recovery. Conservation Biology 10(2): 338–348. https://doi.org/10.1046/j.1523-1739.1996.10020338.x

Soares ES, Amaral FSR, Carvalho-Filho EPM, Granzinolli MA, Albuquerque MJLB, Lisboa JS, Azevedo MAG, Moraes W, Sanaiotti TM, Guimarães G (2008) Plano de Ação Nacional para a Conservação de Aves de Rapina. Instituto Chico Mendes de Conservação da Biodiversidade, Brasília, 136 pp.

Soares-Filho BS, Nepstad DC, Curran LM, Cerqueira GC, Garcia RA, Ramos CA, Voli E, McDonald A, Lefebvre P, Schlesinger P (2006) Modelling conservation in the Amazon basin. Nature 440(7083): 520–523. https://doi.org/10.1038/nature04389

Todd FS (1972) Captive breeding of Harpy Eagles. Journal of Raptor Research 6(4): 137–143.

Todd FS, Meachan T (1974) Breeding of the Harpy Eagle at the Los Angeles Zoo. International Zoo Yearbook 14: 90–94. https://doi.org/10.1111/j.1748-1090.1974.tb00775.x

Trinca CT, Ferrari SF, Lees A (2008) Curiosity killed the bird: arbitrary hunting of Harpy Eagles *Harpia harpyja* on an agricultural frontier in southern Brazilian Amazonia. Cotinga 30: 12–15.

Vargas FC, Faria PJ, Guedes NMR (2001) Incubação artificial, translocação e reintrodução de ninhegos de arara-azul (*Anodorhynchus hyacinthinus*) no Pantanal de Miranda, MS. In: Straube FC (Ed.) Ornitologia sem Fronteiras e Resumos IX Congresso Brasileiro de Ornitologia, Pontifícia Universidade Católica do Paraná, Curitiba, PR, 385–386.

Voous KH (1969) Predation potential in birds of prey from Surinam. Ardea 57: 119–148.

Watson RT, Mcclure CJW, Vargas FH, Jenny JP (2016) Trial restoration of the Harpy Eagle, a large, long-lived, tropical forest raptor, in Panama and Belize. Journal of Raptor Research 50(1): 3–22. https://doi.org/10.3356/rapt-50-01-3-22.1

Zimmermann A (2010) The role of zoos in contributing to in situ conservation. In: Kleiman DG, Thompson KV, Baer CK (Eds) Wild Mammals in Captivity: Principles and Techniques for Zoo Management. The University of Chicago Press 23: 281–287.

ZIMS (2020) Zoological Information Management System. Taxon Report *Harpia harpyja*. zims. https://www.species360.org/ [accessed 05 May 2020]

Supplementary material 1

Table S1

Authors: Marcos José de Oliveira, Francisca Helena Aguiar-Silva, Wanderlei de Moraes, Tânia Margarete Sanaiotti, Aureo Banhos, Nei Moreira

Data type: docx. file

Explanation note: Survey form sent to 40 Harpy Eagles (Harpia harpyja) ex situ facilities in Brazil.

Link: https://doi.org/10.3897/zookeys.1083.69047.suppl1

Supplementary material 2

Table S2

Authors: Marcos José de Oliveira, Francisca Helena Aguiar-Silva, Wanderlei de Moraes, Tânia Margarete Sanaiotti, Aureo Banhos, Nei Moreira

Data type: docx. file

Explanation note: Harpy Eagle (Harpia harpyja) ex situ population outside Brazil in 2020. SAm-South America, CAm-Central America, NAm-North America, EU-Europe.

Link: https://doi.org/10.3897/zookeys.1083.69047.suppl2

ZooKeys 1083: 129–146 (2022)
doi: 10.3897/zookeys.1083.78233
https://zookeys.pensoft.net

RESEARCH ARTICLE

A peer-reviewed open-access journal
ZooKeys
Launched to accelerate biodiversity research

A new species of Asiatic shrew of the genus *Chodsigoa* (Soricidae, Eulipotyphla, Mammalia) from the Dabie Mountains, Anhui Province, eastern China

Zhongzheng Chen[1*], Tingli Hu[2*], Xiaoxin Pei[1], Guangdao Yang[3], Fan Yong[4], Zhen Xu[2], Weiying Qu[1], Kenneth O. Onditi[5], Baowei Zhang[1,2,3]

1 *Collaborative Innovation Center of Recovery and Reconstruction of Degraded Ecosystem in Wanjiang Basin Co-founded by Anhui Province and Ministry of Education, School of Ecology and Environment, Anhui Normal University, Wuhu, Anhui 241002, China* **2** *School of Life Sciences, Anhui University, Hefei, Anhui 230601, China* **3** *Forestry Investigation and Planning Institute of Anhui Province, Hefei, 230001, Anhui, China* **4** *Research Center for Nature Conservation and Biodiversity, Nanjing Institute of Environmental Sciences, Ministry of Ecology and Environment, Nanjing, Jiangsu, 210042, China* **5** *Kunming Institute of Zoology, Chinese Academy of Sciences, Kunming, Yunnan 650204, China*

Corresponding author: Baowei Zhang (zhangbw@ahu.edu.cn)

Academic editor: Nedko Nedyalkov | Received 20 November 2021 | Accepted 8 January 2022 | Published 25 January 2022

http://zoobank.org/0BB575E8-AF6A-4FEB-A41A-D3FFD27B01FC

Citation: Chen Z, Hu T, Pei X, Yang G, Yong F, Xu Z, Qu W, Onditi KO, Zhang B (2022) A new species of Asiatic shrew of the genus *Chodsigoa* (Soricidae, Eulipotyphla, Mammalia) from the Dabie Mountains, Anhui Province, eastern China. ZooKeys 1083: 129–146. https://doi.org/10.3897/zookeys.1083.78233

Abstract

Asiatic shrews of the genus *Chodsigoa* (Soricidae, Eulipotyphla) currently comprise nine species, mostly occurring in southwest China. From May 2017 to August 2020, 11 specimens of *Chodsigoa* were collected from the Dabie Mountains in Anhui Province, eastern China. Their morphology was compared with other species within the genus and one mitochondrial (cytochrome b) and two nuclear (apolipoprotein B and breast cancer 1) genes were sequenced to estimate the phylogenetic relationships of these specimens. Based on morphological and molecular evidence, these specimens are recognized as a distinct species, *Chodsigoa dabieshanensis* **sp. nov.**, which is formally described here. Morphologically, the new species is most similar to *Chodsigoa hypsibia*, but it is distinguishable from all known congeners by the combination of dark brownish pelage, small size, and relatively short tail. Phylogenetic analyses revealed that *C. dabieshanensis* **sp. nov.** forms a phylogenetic lineage sister to the clade containing *C. parva* + *C. hypsibia*. The-Kimura 2-parameter

* These authors contributed equally.

genetic distances of the cytochrome b (CYT B) gene between the new species and other nominal *Chodsigoa* species ranged between 8.6 and 17.6%. The new species is distributed at elevations from 750 to 1250 m in the Dabie Mountains and is geographically distant from other species in the genus.

Keywords
Chodsigoa dabieshanensis, molecular analysis, morphology, new species, taxonomy

Introduction

Asiatic shrews of the genus *Chodsigoa* Kastchenko, 1907 are mainly distributed in southwest China, adjacent Myanmar, Vietnam, and Thailand, and have also been recorded in central and eastern China and Taiwan (Hoffmann and Lunde 2008; Wilson and Mittermeier 2018). Animals in this genus are small in size (< 15 g) and mainly occur in mid-to high-montane forests, making them one of the least studied taxa among mammals. The genera *Chodsigoa* and *Episoriculus* were regarded as a subgenus of *Soriculus* (Hoffmann 1985) until recently, when Hutterer (2005) promoted them to full genus status. The most distinctive morphological characters distinguishing *Chodsigoa* from *Soriculus*/*Episoriculus* is the number of upper unicuspids. *Chodsigoa* has three upper unicuspids while *Soriculus*/*Episoriculus* has four. Nine species are currently recognized in *Chodsigoa*: *C. caovansunga* Lunde, Musser & Son, 2003, *C. furva* Anthony, 1941, *C. hoffmanni* Chen, He, Huang, Wan, Lin, Liu & Jiang, 2017, *C. hypsibia* (De Winton in De Winton and Styan 1899), *C. parca* Allen, 1923, *C. parva* Allen, 1923, *C. salenskii* (Kastschenko 1907), *C. smithii* Thomas, 1911 (Thomas 1911a), and *C. sodalis* Thomas, 1913.

The De Winton's shrew (*C. hypsibia*) is endemic to China and is the most widely distributed species (Jiang and Hoffmann 2005). This gray, long-tailed shrew was first described by De Winton (1989) based on specimens from Yangliu-pa (= Yangliu ba), Pingwu, in Sichuan province. It contains two subspecies: *C. h. hypsibia*, recorded in Qinghai, Sichuan, Shaanxi, Tibet, Yunnan, Anhui, and Henan provinces (Zhang et al. 2018; Zhou et al. 2020) and *C. h. larvarum* Thomas, 1911 (Thomas 1911b), recorded in Beijing, Hebei, and Shanxi provinces (Liu et al. 2011). Zhang et al. (2018) reported the first record of *C. hypsibia* in Anhui province based on a specimen collected from Yaoluoping National Nature Reserve, Dabie Mountains. However, the collection site is distant from the known distribution of *C. hypsibia*, and the genetic distance of the CYT B gene between the specimen and *C. hypsibia* from Sichuan and Shaanxi (near the type locality in Pingwu, Sichuan) is relatively high (8.4–8.5%), and the two populations form deeply diverged clades in the Bayesian tree (posterior probabilities = 1.00; Zhang et al. 2018). These results suggest that additional studies with more specimens were necessary to confirm the taxonomic status of the population from the Dabie Mountains.

For three years, we conducted extensive field surveys in the Dabie Mountains, during which we collected 11 specimens of *Chodsigoa*. Based on morphological and molecular phylogenetic analysis, we recognize the population from the Dabie Mountains as distinct from *C. hypsibia* and other known *Chodsigoa* species, representing a new species *Chodsigoa dabieshanensis* sp. nov., which we describe herein.

Materials and methods

A total of 11 *Chodsigoa* specimens were collected from May 2017 to August 2020 from Yaoluoping National Nature Reserve (*n* = 1), Bancang Natural Reserve (*n* = 4), and Foziling Natural Reserve (*n* = 6), all located in the Dabie Mountains, Anhui province, eastern China (Fig. 1). Shrews were sampled using the pitfalls (plastic buckets 15 cm in diameter and 28 cm in depth). Specimens were euthanized and liver or muscle tissues were extracted and preserved in pure ethanol. Skulls were also extracted and cleaned. Specimens and tissues were deposited at the Biological Museum of Anhui University (**BMAHU**). Animals were handled consistent with the animal care and use guidelines of the American Society of Mammologists (Sikes et al. 2016), and also following the guidelines and regulations approved by the internal review board of Anhui Normal University, and with the permissions of local authorities.

External measurements including head and body length (**HB**), tail length (**TL**), hindfoot length (**HF**), ear length (**EL**) were taken in the field with a ruler to the nearest 0.1 mm. The body weight (**W**) of each specimen was weighed to the nearest 0.01 g using an electronic scale. All craniodental measurements were taken by CZZ using digital calipers graduated to the nearest 0.01 mm following Heaney and Timm (1983), Woodman and Timm (1993), and Chen et al. (2017). The following 19 measurements were taken:

CIL condyloincisive length;
IOB interorbital breadth;
CB cranial breadth;
CH cranial height;
RL rostral length;
PRL postrostral length;
PIL palatoincisive length;
PPL postpalatal length;
UTL upper toothrow length;
M^2–M^2 maximum width across the upper second molars;
P^4–M^3 distance from the upper fourth premolar to the upper third molar;
PPD postpalatal depth;
BMF foramen magnum breadth;
ML mandibular length;
LTR lower toothrow length;
LLI length of lower incisor;
HCP height of coronoid process;
HCV height of coronoid valley;
HAC height of articular condyle.

Comparative morphological data of another 149 *Chodsigoa* specimens were obtained from our previous study (Chen et al. 2017), including *C. caovansunga* (3), *C. furva* (5), *C. hoffmanni* (14), *C. hypsibia* (64), *C. parca* (19), *C. parva* (31), *C. smithii* (11), and *C. sodalis* (2).

To evaluate the morphological variation among populations of *Chodsigoa*, we performed a principal component analysis (**PCA**) in SPSS 19.0 (SPSS Inc., USA) using the $\log_{10}$-transformed craniodental measurements. We compared the morphology of the putative new species with other *Chodsigoa* species stored in Kunming Institute of Zoology (**KIZ**), the Sichuan Academy of Forestry (**SAF**), the Museum of Comparative Zoology, Harvard University (**MCZ**), and the American National Museum of Natural

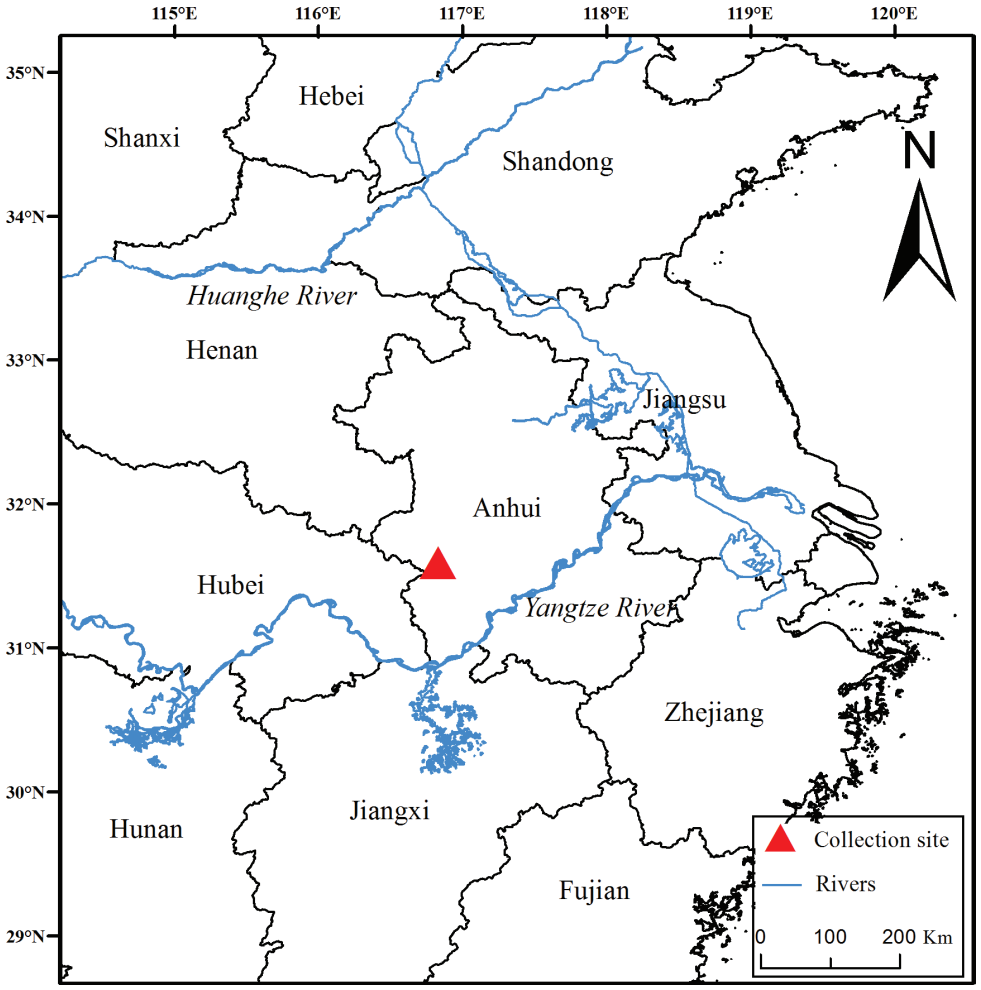

Figure 1. Map showing the collection site of *Chodsigoa dabieshanensis* sp. nov. in the Dabie Mountains, Anhui Province, eastern China.

History (**AMNH**). The terminology for morphological descriptions followed Hoffman (1985), Lunde et al. (2003), and Chen et al. (2017).

Total genomic DNA of 10 *C. dabieshanensis* specimens were extracted using a DNA extraction kit (Qiagen DNeasy Blood and Tissue Kit, China). The complete CYT B gene and two nuclear gene segments [apolipoprotein B (APOB) and breast cancer 1 (BRCA1)] were amplified using primers and PCR conditions from Chen et al. (2021). The PCR products were purified and sequenced in both directions using the BigDye Terminator Cycle kit v. 3.1 (Invitrogen, USA) on an ABI 3730xl sequencer (Applied Biosystems, USA). Corresponding sequences of other *Chodsigoa* species were downloaded from GenBank (Table 1) and aligned with our new sequences using MUSCLE (Edgar 2004) and then checked manually by eye. Sequences of *Episoriculus caudatus* (Horsfield, 1851) and *Neomys fodiens* (Pennant, 1771) were included in the

Table 1. Samples and sequences used for molecular analyses. New sequences generated in this study are shown in bold.

Species	Museum code	Collecting site	CYT B	BRCA1	APOB
Chodsigoa dabieshanensis	AHUDBS017001	China: Anhui	MG462711	**OM200122**	**OM200113**
Chodsigoa dabieshanensis	AHUDBS017002	China: Anhui	**OM200132**	**OM200123**	**OM200115**
Chodsigoa dabieshanensis	AHUDBS017003	China: Anhui	**OM200131**	**OM200124**	**OM200114**
Chodsigoa dabieshanensis	AHUDBS017004	China: Anhui	**OM200130**	**OM200125**	**OM200116**
Chodsigoa dabieshanensis	AHU2008FZL001	China: Anhui	**OM200133**	**OM200121**	**OM200112**
Chodsigoa dabieshanensis	AHU2008FZL002	China: Anhui	**OM200129**	**OM200120**	N.A.
Chodsigoa dabieshanensis	AHU2008FZL003	China: Anhui	**OM200127**	**OM200119**	**OM200111**
Chodsigoa dabieshanensis	AHU2008FZL004	China: Anhui	**OM200128**	N.A	**OM200110**
Chodsigoa dabieshanensis	AHU2008FZL005	China: Anhui	**OM200126**	**OM200118**	**OM200109**
Chodsigoa dabieshanensis	AHU2008FZL006	China: Anhui	N.A.	**OM200117**	**OM200108**
Chodsigoa caovansunga	KIZ:027112	China: Yunnan	JX508288	KX765593	KX765546
Chodsigoa caovansunga	AMNH:101500	Viet Nam: Ha Giang	AB175103	DQ630263	DQ630182
Chodsigoa caovansunga	AMNH:101520	Viet Nam: Ha Giang	AB175104	DQ630265	DQ630184
Chodsigoa furva	KIZ:032216	China: Yunnan	KX765525	KX765617	KX765571
Chodsigoa furva	KIZ:032217	China: Yunnan	KX765526	KX765618	KX765572
Chodsigoa hypsibia	KIZ:021075	China: Yunnan	KX765534	KX765625	KX765581
Chodsigoa hypsibia	KIZ:021483	China: Yunnan	KX765536	KX765626	KX765583
Chodsigoa hypsibia	KIZ:021485	China: Yunnan	KX765535	KX765627	KX765582
Chodsigoa hypsibia	KIZ:032302	China: Sichuan	KX765527	KX765637	KX765575
Chodsigoa hypsibia	KIZ:032250	China: Qinghai	KX765528	KX765624	KX765574
Chodsigoa hypsibia	KIZ:032251	China: Qinghai	KX765529	KX765630	KX765577
Chodsigoa parca	KIZ:032246	China: Yunnan	KX765502	KX765600	KX765551
Chodsigoa parca	KIZ:032239	China: Yunnan	KX765504	KX765607	KX765549
Chodsigoa parca	KIZ:032243	China: Yunnan	GU981265	KX765602	KX765550
Chodsigoa parva	KIZ:032235	China: Yunnan	KX765539	KX765631	KX765586
Chodsigoa parva	KIZ:022222	China: Yunnan	KX765542	KX765632	KX765591
Chodsigoa parva	KIZ:020265	China: Yunnan	KX765543	KX765633	KX765589
Chodsigoa smithii	SAF: BLG012	China: Sichuan	KX765521	KX765609	KX765567
Chodsigoa smithii	SAF: BLG144	China: Sichuan	KX765522	KX765610	KX765568
Chodsigoa smithii	SAF: JJSA616	China: Sichuan	KX765524	KX765612	KX765562
Chodsigoa sodalis	JUM016	China: Taiwan	AB175102	DQ630274	DQ630194
Chodsigoa sodalis	T0497	China: Taiwan	AB127978	DQ630271	DQ630191
Chodsigoa sodalis	THUB-S-00007	China: Taiwan	GU981270	GU981191	GU981116
Chodsigoa hoffmanni	KIZ:019442	China: Yunnan	KX765509	KX765594	KX765555
Chodsigoa hoffmanni	KIZ:019458	China: Yunnan	KX765510	KX765595	KX765558
Chodsigoa hoffmanni	KIZ:019459	China: Yunnan	KX765512	KX765596	KX765559
Episoriculus caudatus	19716	China: Yunnan	GU981272	GU981193	GU981118
Neomys fodiens	65298	Germany	GU981295	GU981205	GU981130

alignments as outgroup taxa. The Kimura-2-parameter (K2P) distances of the CYT B gene between species were calculated in MEGA 7 (Kumar et al. 2016).

Three datasets were used for the phylogenetic analyses: CYT B gene, concatenated nuclear genes, and concatenated mitochondrial and nuclear genes (Table 1). Maximum likelihood (**ML**) and Bayesian inference (**BI**) analyses were performed to reconstruct the phylogenetic relationships in PhyloSuite (Zhang et al. 2020) based on the best-fit partitioning schemes estimated using PartitionFinder v. 2.0 (Lanfear et al. 2012). The ultrafast bootstrap values (UFBoot) ≥ 95 and posterior probabilities (PP) ≥ 0.95 were considered as strong supports (Huelsenbeck and Rannala 2004; Minh et al. 2018).

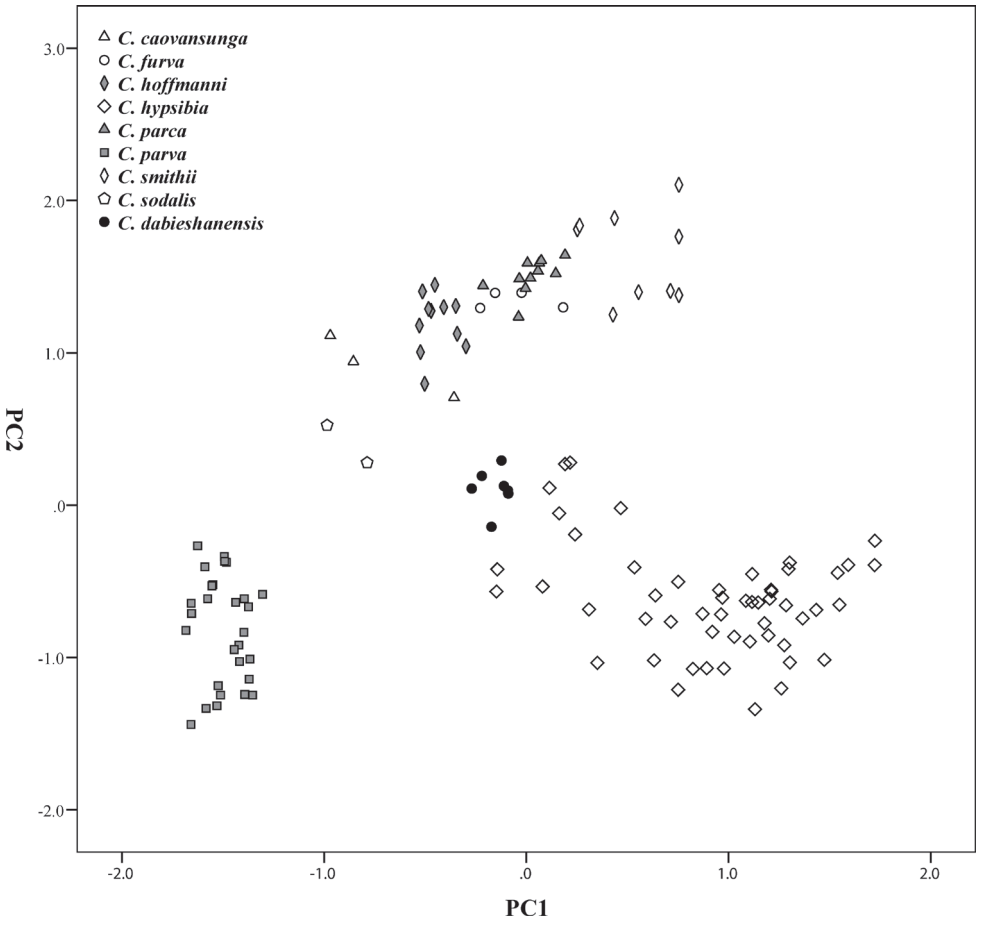

Figure 2. Results of principal component analysis of *Chodsigoa* based on the 19 $\log_{10}$-transformed craniodental measurements.

Results

External and cranial measurements are summarized in Table 2. The PCA based on 128 intact skulls produced two axes with eigenvalues exceeding 1.0, which explained 94.2% of the variation (Table 3). The first axes (PC1) explained 86.2% of the variation and was strongly positively correlated with all variables, indicating it represented the overall skull size (Table 3). The second axis (PC2) explained 8.0% of the variation and was highly positively correlated with CH and BMF (loading > 0.67). A plot of PC1 and PC2 (Fig. 2) showing that *C. dabieshanensis* are separated well from all named species. This new species occurs in the center of the morphospace, indicating its medium size in the genus. Morphologically, it is most similar to *C. hypsibia*, with which it occupies the upper left corner morphospace without overlap (Fig. 2), indicating its generally smaller size, larger BMF, and higher CH (Table 2).

Table 2. External and craniomandibular measurements (mm), including mean values, standard deviations, ranges, and sample sizes of *Chodsigoa* species. The measurements were obtained from Chen et al. (2017), except for *C. dabieshanensis* sp. nov.

Variable	*C. dabieshanensis* sp. nov.	*C. caovansunga*	*C. furva*	*C. hypsibia*	*C. parca*	*C. hoffmanni*	*C. parva*	*C. smithii*	*C. sodalis*
	***N* = 11**	***N* = 3**	***N* = 5**	***N* = 58**	***N* = 16**	***N* = 14**	***N* = 31**	***N* = 11**	***N* = 2**
W	5.24±0.36 4.67–5.89; 9	6.20; 1	6.05±0.64 5.60–6.50; 2	10.40±1.61 6.40–14.00; 30	9.35±1.09 7.90–11.90; 13	7.54±0.80 7.00–9.60; 12	3.59±0.56 2.60–5.20; 29	9.69±1.46 7.00–12.00; 10	
HB	67.22±3.23 62.00–73.00; 9	74.00; 1	71.67±3.06 69.00–75.00; 3	75.48±5.75 62.00–86.00; 52	70.30±4.40 62.00–77.00; 14	66.75±5.15 58.00–75.00; 12	56.66±4.33 47.00–64.00; 29	79.70±2.71 76.00–84.00; 10	55.50±2.12 54.00–57.00; 2
TL	59.67±3.28 54.00–64.00; 9	83.00; 1	86.00±1.73 84.00–87.00; 3	65.69±4.01 56.00–73.00; 52	90.60±5.70 77.00–99.00; 14	81.67±4.21 74.00–88.00; 12	44.90±8.23 4.60–52.00; 29	98.90±5.28 93.00–110.00; 10	57.50±3.54 55.00–60.00; 2
HF	13.44±0.53 13.00–14.00; 9	15.00; 1	17.33±1.15 16.00–18.00; 3	15.35±1.17 13.00–18.00; 53	16.50±0.90 15.00–18.00; 15	15.50±0.80 14.00–17.00; 12	10.81±0.51 10.00–12.00; 29	17.90±1.13 16.00–20.00; 10	13.00±0.00 13.00–13.00; 2
EL	8.22±0.44 8.00–9.00; 9	9.00; 1	8.00±0.00 8.00–8.00; 2	7.04±1.12 5.00–9.50; 37	8.89±1.24 7.00–11.50; 14	8.83±1.11 7.00–11.00; 12	6.93±0.54 5.00–8.00; 28	8.89±1.96 6.00–12.00; 9	8.50±0.71 8.00–9.00; 2
CIL	19.08±0.22 18.65–19.26; 8	17.96±0.74 17.38–18.80; 3	20.63±0.39 20.16–21.06; 4	20.66±0.89 19.03–22.62; 46	20.37±0.29 20.08–20.88; 8	19.13±0.39 18.31–19.57; 12	15.79±0.27 15.08–16.17; 29	22.23±0.54 21.50–23.05; 9	17.97±0.12 17.88–18.05; 2
IOB	4.52±0.07 4.41–4.62; 8	4.30±0.06 4.23–4.35; 3	4.96±0.10 4.85–5.05; 4	5.04±0.33 3.99–5.56; 51	4.77±0.11 4.60–4.99; 10	4.40±0.13 4.14–4.58; 12	3.55±0.15 3.25–3.85; 29	5.23±0.21 4.86–5.48; 9	4.10±0.15 3.99–4.20; 2
CB	9.01±0.18 8.81–9.37; 9	8.78±0.08 8.71–8.87; 3	9.38±0.34 9.10–9.84; 4	9.42±0.40 8.38–10.34; 49	9.57±0.14 9.33–9.82; 10	9.06±0.25 8.45–9.39; 12	7.30±0.22 6.93–7.73; 29	9.95±0.25 9.67–10.45; 9	8.14±0.45 7.82–8.46; 2
CH	4.96±0.18 4.67–5.23; 9	5.24±0.28 5.05–5.57; 3	5.67±0.29 5.45–6.09; 4	4.57±0.28 4.05–5.10; 47	5.95±0.15 5.71–6.19; 10	5.61±0.16 5.30–5.87; 12	4.02±0.19 3.71–4.32; 29	6.09±0.16 5.87–6.30; 9	4.74±0.14 4.64–4.84; 2
RL	6.61±0.11 6.48–6.81; 8	6.43±0.58 6.04–7.10; 3	7.76±0.17 7.57–7.91; 4	7.72±0.46 6.93–9.00; 52	7.83±0.15 7.55–7.98; 9	7.29±0.19 6.78–7.56; 12	5.63±0.16 5.33–6.07; 29	8.78±0.35 8.14–9.18; 9	6.70±0.01 6.69–6.70; 2
PRL	11.84±0.18 11.56–12.04; 8	10.86±0.67 10.09–11.27; 3	12.35±0.48 11.93–12.84; 4	12.97±0.61 11.55–14.23; 46	12.24±0.18 12.06–12.55; 9	11.57±0.28 11.02–11.96; 12	9.87±0.18 9.32–10.14; 29	13.29±0.29 12.93–13.80; 9	10.79±0.15 10.68–10.89; 2
PIL	8.36±0.16 8.08–8.49; 8	7.96±0.30 7.76–8.31; 3	8.97±0.24 8.76–9.30; 4	9.17±0.51 8.05–10.37; 52	9.08±0.14 8.90–9.28; 9	8.43±0.18 8.06–8.75; 12	6.61±0.13 6.38–6.85; 29	9.92±0.37 9.40–10.50; 9	7.95±0.06 7.91–7.99; 2
PPL	8.85±0.12 8.63–8.97; 8	8.11±0.43 7.80–8.60; 3	9.28±0.34 8.89–9.59; 4	9.55±0.41 8.87–10.78; 46	9.11±0.19 8.77–9.35; 10	8.79±0.18 8.57–9.11; 12	7.60±0.19 7.10–7.90; 29	10.03±0.36 9.67–10.84; 9	8.15±0.01 8.14–8.15; 2
UTL	8.05±0.11 7.85–8.19; 8	7.76±0.25 7.58–8.05; 3	8.86±0.25 8.57–9.18; 4	8.50±0.38 7.88–9.42; 52	8.85±0.12 8.59–9.02; 9	8.11±0.16 7.68–8.31; 12	6.44±0.14 6.11–6.67; 29	9.70±0.38 9.01–10.20; 9	7.73±0.06 7.69–7.77; 2

Variable	*C. dabieshanensis* sp. nov.	*C. caovansunga*	*C. furva*	*C. hypsibia*	*C. parca*	*C. hoffmanni*	*C. parva*	*C. smithii*	*C. sodalis*
	***N* = 11**	***N* = 3**	***N* = 5**	***N* = 58**	***N* = 16**	***N* = 14**	***N* = 31**	***N* = 11**	***N* = 2**
M^2–M^2	5.56±0.09	5.13±0.11	5.58±0.16	6.04±0.34	5.36±0.09	5.22±0.08	4.24±0.19	5.92±0.15 5.75–	4.49±0.18
	5.42–5.66; 8	5.06–5.26; 3	5.39–5.75; 4	5.34–6.74; 52	5.26–5.51; 10	5.12–5.36; 12	3.92–4.53; 29	6.24; 9	4.36–4.62; 2
P^4–M^3	4.89±0.05	4.65±0.10	5.39±0.22	5.27±0.26	5.71±0.09	4.82±0.11	3.94±0.12	5.78±0.24 5.47–	4.85±0.04
	4.82–4.95; 8	4.57–4.77; 3	5.07–5.56; 4	4.66–5.86; 52	5.57–5.84; 10	4.59–5.03; 12	3.57–4.12; 29	6.10; 9	4.82–4.88; 2
PPD	2.81±0.10	3.25±0.08	3.50±0.09	3.07±0.19	3.90±0.09	3.50±0.14	2.47±0.13	3.84±0.21 3.50–	3.05±0.08
	2.64–2.95; 8	3.18–3.34; 3	3.40–3.59; 4	2.66–3.37; 51	3.72–3.98; 10	3.11–3.65; 12	2.20–2.69; 29	4.12; 9	2.99–3.11; 2
BMF	3.20±0.11	3.17±0.07	3.57±0.13	2.76±0.14	3.32±0.13	3.26±0.09	2.57±0.17	3.71±0.24 3.40–	2.99±0.01
	3.07–3.43; 9	3.11–3.24; 3	3.38–3.65; 4	2.53–3.21; 51	3.18–3.55; 9	3.12–3.44; 12	2.22–2.86; 29	4.20; 9	2.98–2.99; 2
ML	10.05±0.17	10.06±0.33	11.07±0.29	10.94±0.51	11.45±0.17	10.60±0.19	8.33±0.18	12.20±0.42	9.66±0.32
	9.74–10.29; 9	9.79–10.43; 3	10.79–11.35; 4	10.18–12.37; 54	11.13–11.72; 10	10.31–10.96; 12	7.97–8.76; 28	11.70–12.90; 9	9.43–9.88; 2
LTR	7.41±0.25	7.25±0.14	8.06±0.20	8.10±0.42	8.15±0.13	7.50±0.14	5.95±0.13	8.78±0.34 8.30–	6.95±0.35
	7.21–8.09; 9	7.12–7.39; 3	7.88–8.26; 4	7.31–9.12; 53	7.96–8.34; 10	7.19–7.67; 12	5.70–6.23; 28	9.20; 9	6.70–7.20; 2
LLI	3.27±0.06	3.19±0.15	3.17±0.20	3.67±0.30	3.42±0.16	3.23±0.09	2.53±0.15	3.65±0.19 3.25–	2.71±0.21
	3.22–3.42; 9	3.06–3.36; 3	2.89–3.35; 4	2.70–4.25; 53	3.07–3.62; 10	3.08–3.37; 12	2.25–2.78; 28	3.90; 9	2.56–2.86; 2
HCP	3.94±0.12	4.00±0.06	3.98±0.12	4.35±0.30	4.64±0.11	4.06±0.15	2.96±0.17	4.37±0.29 3.90–	3.43±0.03
	3.71–4.09; 9	3.93–4.05; 3	3.88–4.12; 4	3.85–5.09; 54	4.52–4.81; 10	3.70–4.36; 12	2.63–3.31; 28	4.72; 9	3.41–3.45; 2
HCV	2.34±0.08	2.61±0.01	2.65±0.09	2.71±0.26	3.01±0.10	2.66±0.07	1.96±0.10	2.95±0.15 2.80–	2.33±0.01
	2.21–2.46; 9	2.60–2.62; 3	2.56–2.77; 4	2.20–3.32; 54	2.87–3.26; 10	2.56–2.80; 12	1.77–2.19; 28	3.20; 9	2.32–2.33; 2
HAC	2.85±0.10	3.31±0.02	3.45±0.11	3.43±0.27	3.67±0.06	3.45±0.13	2.48±0.12	3.78±0.15 3.60–	2.92±0.10
	2.70–2.98; 9	3.30–3.34; 3	3.31–3.57; 4	2.87–4.02; 46	3.59–3.79; 10	3.24–3.66; 12	2.18–2.68; 28	4.00; 9	2.85–2.99; 2

Table 3. Character loadings, eigenvalues, and proportion of variance explained by the first two axes (PC1 and PC2) of a principal component analysis using the $\log_{10}$-transformed measurements of *Chodsigoa*. The meanings of variable abbreviations are given in the Materials and methods section.

Variables	Principal component	
	1	2
ML	0.991	0.047
PIL	0.990	–0.085
LTR	0.988	–-0.073
CIL	0.987	–0.107
UTL	0.986	0.060
P^4–M^3	0.982	–0.057
CB	0.977	–0.009
RL	0.972	–0.030
HCP	0.961	–0.052
IOB	0.955	–0.200
PRL	0.949	–0.262
HCV	0.940	0.078
HAC	0.939	0.075
PPL	0.937	–0.221
M^2–M^2	0.932	–0.259
LLI	0.910	–0.269
PPD	0.841	0.464
CH	0.692	0.670
BMF	0.610	0.713
Eigenvalue	16.385	1.519
Variance explained	86.235	7.993

Nine CYT B (1140 bp), nine APOB (513 bp), and nine BRCA1 (768 bp) sequences of *C. dabieshanensis* were obtained (GenBank accession numbers: OM200108–OM200133; Table 1). The ML and BI trees recovered very similar topologies, and therefore, only the ML gene trees are shown (Fig. 3). The phylogenetic analyses of all three datasets supported *Chodsigoa* clustered into two major clades (UFboot > 99, PP = 1.00). One clade was composed of *C. parva*, *C. hypsibia*, and *C. dabieshanensis* (Clade I), and the other clade was composed of *C. caovansunga*, *C. furva*, *C. hoffmanni*, *C. parca*, *C. salenskii*, *C. smithii*, and *C. sodalis* (Clade II). The *C. dabieshanensis* clade was strongly supported as a monophyletic lineage, sister to the clade containing *C. parva* and *C. hypsibia* (UFboot > 98, PP = 1.00). The K2P genetic distances of the CYT B gene between *C. dabieshanensis* and other nominal *Chodsigoa* species ranged from 8.6% (with *C. hypsibia*) to 17.6% (with *C. sodalis*) (Table 4).

Based on the morphological, morphometric, and molecular evidence and the modern phylogenetic species concept (phylogenetic species concept based on both diagnosability and monophyly as operational criteria) (Mayden 1997; Gutierrez and Garbino 2018), we recognize the population from the Dabie Mountains as a new species of *Chodsigoa*, which is formally described below.

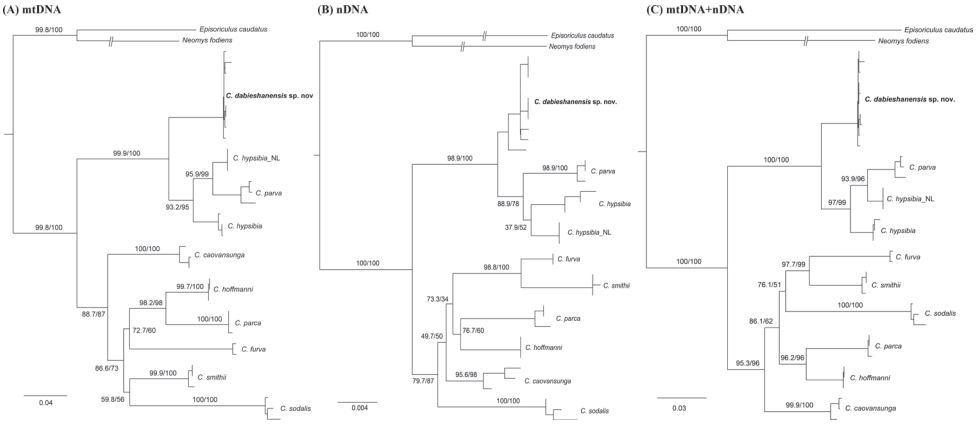

Figure 3. Maximum likelihood phylogenetic trees derived from **A** the CYT B gene **B** the concatenated nuclear genes **C** the concatenated mitochondrial-nuclear trees. Branch labels indicate Bayesian posterior probabilities (PP) and ultrafast bootstrap supports (UFBoot). Scale bars represent substitutions per site.

Table 4. The Kimura-2-parameter distances between *Chodsigoa* species based on the CYT B gene.

	***C. dabieshanensis* sp. nov.**	***C. caovansunga***	***C. furva***	***C. hoffmanni***	***C. hypsibia***	***C. parca***	***C. parva***	***C. smithii***
C. dabieshanensis sp. nov.	–	–	–	–	–	–	–	–
C. caovansunga	0.147	–	–	–	–	–	–	–
C. furva	0.151	0.131	–	–	–	–	–	–
C. hoffmanni	0.147	0.116	0.132	–	–	–	–	–
C. hypsibia	0.086	0.144	0.155	0.146	–	–	–	–
C. parca	0.152	0.128	0.131	0.082	0.152	–	–	–
C. parva	0.102	0.154	0.162	0.154	0.058	0.160	–	–
C. smithii	0.163	0.112	0.119	0.104	0.153	0.122	0.164	–
C. sodalis	0.176	0.144	0.155	0.136	0.162	0.140	0.162	0.131

Taxonomic account

***Chodsigoa dabieshanensis* sp. nov.**
http://zoobank.org/A2EF195A-A19C-43CD-A774-A06218E96EE9
Figures 4, 5, Table 2

Suggested common name. Dabieshan long-tailed shrew; 大别山缺齿鼩 (Dabieshan Quechiqu)

Holotype. AHU2008FZL005, an adult female collected by Zhen Xu and Ruolei Sun in August 2020, at Foziling natural reserve (31°07'07"N, 116°14'41"E, 1187 m a.s.l.), the north slope of the Dabie Mountains, Huoshan County, Luan City, Anhui province, China. Cleaned skulls and remaining carcasses frozen at –20 °C deposited in the Biological Museum of Anhui University (BMAHU).

Paratypes. AHUDBS017001-005; AHU2008FZL001-004, 006. Ten specimens collected between May 2017 and August 2020 from the Dabie Mountains, Anhui

province, China. All specimens are deposited in the Biological Museum of Anhui University (BMAHU).

Etymology. The specific name *dabieshanensis* is derived from the Dabie Mountains, the type locality of the new species: *-shan* means mountain in Chinese, and the Latin adjectival suffix *-ensis* means "belonging to".

Diagnosis. The new species is assigned to the genus *Chodsigoa* for having three upper unicuspid teeth, with the tips of the teeth lightly pigmented (Fig. 4). *Chodsigoa dabieshanensis* sp. nov. can be distinguished from the other known species of *Chodsigoa* by the following combination of characters: small to medium in size (HB = 67.22 mm; CIL = 19.08 mm), dark brownish pelage; tail shorter than the HB, nearly similar ventral and dorsal pelage color, a small tuft of longer hairs at the tip of the tail (Fig. 5); markedly flattened braincase; and the foramen magnum is relatively wider than *C. hypsibia*. Phylogenetic analyses show that the new species is monotypic, sister to *C. hypsibia* and *C. parva* (Fig. 3).

Description. A small to medium-sized shrew (W = 5.24±0.36 g, range 4.67–5.89 g; HB = 67.22±3.23 mm, range 62.00–73.00 mm, Table 2) with dark brown dorsal pelage and slightly paler ventral pelage (Fig. 5). Tail is short (TL = 59.67±3.28 mm), about 90% of the head and body length, brown above, slightly paler below, and with a small tuft of longer hairs at the tip. External ears are prominent, rounded, and covered with very short dark hairs. Eyes are very small. The dorsal surfaces of hands and hind feet are covered with short brown hair, lighter at the margin. The thenar and hypothenar pads at the soles of the hindfeet are well separated.

The skull of *C. dabieshanensis* sp. nov. is short and broad, and the braincase is markedly flattened (Fig. 4). The skull is similar to *C. hypsibia*, but much shorter and broader. The rostrum is short, and the interorbital region is wide. From the ventral view, the rostrum gradually narrows in the premaxillary region. The palate is short, with an abrupt posterior edge. The basisoccipital is developed and the ridges are approximately parallel. The dentition is the same for the genus: 3.1.1.3/2.0.1.3 = 28. The first incisor is long, falciform; the apex straight downwards; the talon much lower than U^1, approximately equal to U^3. Three upper unicuspids are present. All unicuspids are crowded and overlap slightly at the base. U^1–U^3 gradually decrease in size; U^3 is about half as high as U^1, and in contact with P^4, which is large and triangular in outline. The posterior borders of P^4 and M^1 are deeply excavated, appearing crescent, while the posterior borders of M^2 are much shallower. M^3 is reduced and much narrower with a single lobe. The tips of the anterior teeth have a lightly pigmented chestnut color except the molars.

The mandible is slender. The coronoid process is tall and squared, rising straight upward from the posterior of the toothrow. The condyloid process is weak and bi-faceted, forming an angle at approximately 45° with the coronoid process. The angular process is long, straight, and very thin. The first lower incisor is long, with only a single basal cusplet. The incisor is slightly curved upwards, forming a hook at the tip. The first lower unicuspid is small and procumbent, crowded with a large incisor and the following premolar. The premolar has one forward-leaning cusp. The molar gradually decreases in size from M^1 to M^3. Only the tips of I_1, U_1, P_1, and M_1 are chestnut-pigmented but not those of M_2 and M_3.

Figure 4. Dorsal, ventral, and lateral views of the skull and lateral views of the mandible of the holotype of *Chodsigoa dabieshanensis* sp. nov. (AHU2008FZL004; left) and *Chodsigoa hypsibia* (KIZ 016077; right). Scale bar: 10 mm.

Comparison. Among the species in the genus *Chodsigoa*, *C. dabieshanensis* sp. nov. is morphologically similar to the widely distributed *C. hypsibia*. However, the new species can be distinguished from *C. hypsibia* by many characters. In terms of body size, *C. dabieshanensis* sp. nov. is much smaller than *C. hypsibia* for most external and craniomandibular measurements (Table 2). In particular, the range of weight (4.67–5.89 g vs 6.40–14.00 g) and rostral length (6.48–6.81 mm vs 6.93–9.00 mm) between the two species does not overlap. The overall pelage of *C. dabieshanensis* sp. nov. is dark brown, almost black, which differs from the gray pelage of *C. hypsibia.* The skull of *C. dabieshanensis* sp. nov. is relatively shorter and broader than *C. hypsibia*,

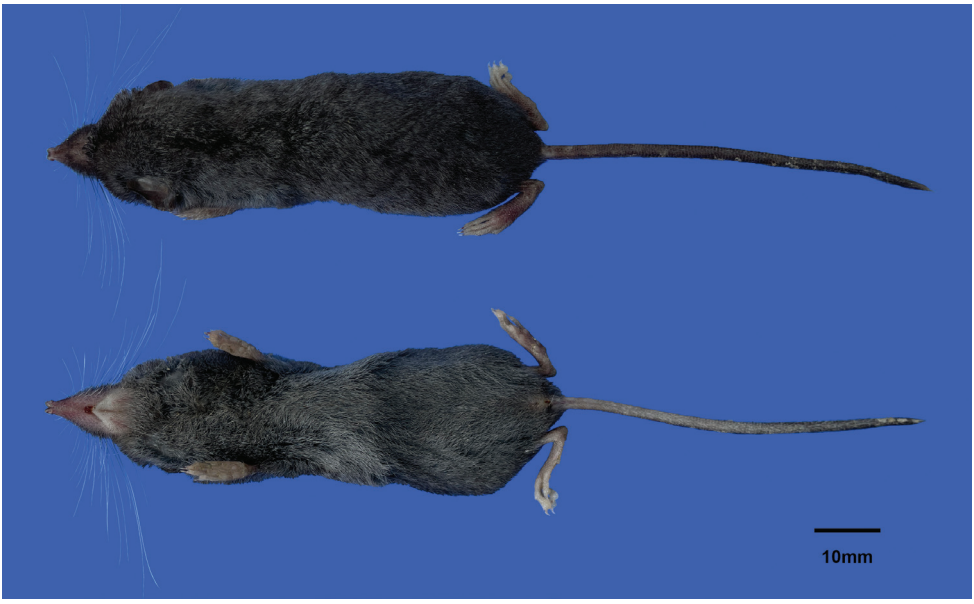

Figure 5. Dorsal and ventral view of *Chodsigoa dabieshanensis* sp. nov.

especially in the interorbital region, which appears much flatter (Fig. 4). The foramen magnum breadth is relatively larger than *C. hypsibia.* The posterior borders of M_2 in *C. hypsibia* are much more deeply excavated than in *C. dabieshanensis* sp. nov.. In *C. dabieshanensis* sp. nov., the basioccipital is well developed and the ridges are approximately parallel. By contrast, the basioccipital of *C. hypsibia* is narrow, so the ridges are nearly confluent in the middle.

Chodsigoa dabieshanensis sp. nov. (CIL = 19.08±0.22 mm) can be easily distinguished from *C. parva* (CIL = 15.79±0.27 mm) by its much larger size and the ranges of most of their external and cranial measurements do not overlap (Table 2). Furthermore, the tail of *C. dabieshanensis* sp. nov. (TL/HB = 80%) is relatively longer than *C. parva* (TL/HB = 88%). If the mean condyloincisive length is used as an indicator of overall size, *C. dabieshanensis* sp. nov. (CIL = 19.08±0.22 mm) is larger than *C. sodalis* (CIL = 17.97±0.12 mm), but smaller than *C. furva* (CIL = 20.63±0.39 mm), *C. parca* (CIL = 20.37±0.29 mm), and *C. smithii* (CIL = 22.23±0.54 mm) (Table 2). The markedly flattened cranium of *C. dabieshanensis* sp. nov. is clearly distinguished from all other species in the genus, including *C. caovansunga*, *C. furva*, *C. hoffmanni*, *C. parca*, *C. salenskii*, *C. smithii*, and *C. sodalis.* The tail of *C. dabieshanensis* sp. nov. is shorter than head and body length, and it differs from *C. sodalis* (TL/HB ≈ 100%) and all other *Chodsigoa* species (TL/HB > 100%). The new species has a tuft of longer hair at the tip of the tail, in contrast to *C. caovansunga*, *C. furva*, and *C. smithii*. The thenar and hypothenar pads at the soles of the hindfeet are well separated and distinguishable from *C. caovansunga*, whose thenar and hypothenar pads of hindfeet are close together.

Distribution and habits. *Chodsigoa dabieshanensis* sp. nov. is currently known from Yaoleping National Nature Reserve, Bancang Natural Reserve, and Foziling Natural Reserve, all located in the Dabie Mountains, Anhui province, eastern China. Most specimens were collected from deciduous broad-leaf forests at 750–1250 m a.s.l.

Discussion

Prior to this study, nine species were recognized in the genus *Chodsigoa* (Chen et al. 2017; Wilson and Mittermeier 2018). Our morphological and molecular results support that the specimens from the Dabie Mountains represent a new species of *Chodsigoa*, C. *dabieshanensis* sp. nov., based on the diagnosis-and-monophyly-based phylogenetic species concept (Mayden 1997; Gutierrez and Garbino 2018). *Chodsigoa dabieshanensis* sp. nov. is morphologically closely related to *C. hypsibia* and was previously considered as a marginal population of that taxon (Zhang et al. 2018). However, it can be distinguished from *C. hypsibia* by its dark brownish pelage and smaller size (Table 2). The large genetic distance (8.6% by the CYT B gene) and phylogenetic analysis also strongly support they are two distinct species (UFboot > 98, PP = 1.00). As *Chodsigoa* are mainly distributed in southwest China and adjacent areas (Wilson and Mittermeier 2018), the distribution area of *C. dabieshanensis* sp. nov. is marginal. It is the only known species of *Chodsigoa* recorded in Anhui province, separated by at least 500 km from any other member of the genus, i.e., C. *hypsibia* from Luanxian, Henan Province (Zhou et al. 2020). The new species has no known congeners in Anhui Province; there are only two other soricid taxa recorded, *Chimarrogale lender* Tomas, 1902 and *Crocidura* spp. (Wang 1990; Jiang et al. 2015). The former is a large aquatic shrew (W > 20 g), and the latter has white, unpigmented dentition; these taxa are easily distinguishable from the new species.

The new species brings the number of *Chodsigoa* species to 10, sorted into two major clades; one including *C. parva* + *C. hypsibia* + *C. dabieshanensis* sp. nov. (Clade I), and the other (Clade II) comprised of the remaining species (Fig. 3). These results are also supported by morphology. Compared with the species in Clade II, the cranium of Clade I species is markedly flatter, and the tail of Clade I is relatively shorter (Clade I: TL/HB < 100%; Clade II: TL/HB ≥ 100%). All our gene trees showed *C. dabieshanensis* sp. nov. forms a subclade inside the main Clade I as the sister group of the subclade *C. parva* + *C. hypsibia* (UFboot > 98, PP = 1.00, Fig. 3).

As the most easterly distributed species of *Chodsigoa*, the discovery of *C. dabieshanensis* sp. nov. from the Dabie Mountains is important in understanding the macroevolution of the genus. Previous studies suggested that the tribe Nectogalini originated from Europe and migrated eastward to western Siberia and southward along northern China to southwest China (He et al. 2010). While the Hengduan Mountains are considered to serve as an important route for the southward migration (Zhang 2002; He et al. 2010), we have no knowledge of how this group migrated eastward. The oldest fossils of *Chodsigoa* are from the Early Pliocene in Gansu Provence,

northern China (Zhang and Zheng 2001). Fossils of *C.* cf. *hypsibia* and *C.* cf. *parva* were discovered from the Early Pleistocene in Jianshi, Hubei and Wuhu, Anhui, both in eastern China, and more fossils were found in Wushan, Chongqing, southwest China in the Late Pleistocene (Qiu and Li 2005). These fossil records, together with our finding of *C. dabieshanensis* sp. nov., diverged earlier than *C. hypsibia* and *C. parva*, which suggests that the ancestor of Clade I arrived early in eastern China. Due to the present lack of broad geographic sampling, how the genus migrated to eastern China is still an open question. The Dabie Mountains are an extension of the Qinling fold belt and gradually stabilized by the end of the Tertiary (Feng 1976). Considering that the montane archipelagos always act as refugia and corridors to facilitate the dispersal of terrestrial small mammals (Chen et al. 2015; He and Jiang 2014; He et al. 2019), a parsimonious biogeographic scenario of the migration is via the Qinling and Dabie mountains. The ancestor of new species then became isolated due to climate change and following habitat turnover, resulting in a new species. Finer taxon sampling with additional sequence data is warranted to illustrate the migration patterns of the genus.

Acknowledgements

The study was supported by the National Natural Science Foundation of China (no. 31900318), National Science & Technology Fundamental Resources Investigation Program of China (grant no. 2019FY101800), the Anhui Provincial Natural Science Foundation (2008085QC106), and the University Synergy Innovation Program of Anhui province (GXXT-2020-075).

References

Allen GM, Andrews RC, Heller E (1923) New Chinese insectivores. American Museum Novitates 100: 1–11. http://hdl.handle.net/2246/4530

Anthony HE (1941) Mammals collected by the Vernay-Cutting Burma Expedition. Field Museum of Natural History, Chicago 27: 37–123.

Chen SD, Sun ZY, He K, Jiang XL, Liu Y, Koju NP, Zhang XY, Tu FY, Fan ZX, Liu SY (2015) Molecular phylogenetics and phylogeographic structure of *Sorex bedfordiae* based on mitochondrial and nuclear DNA sequences. Molecular Phylogenetics and Evolution 84: 245–253. https://doi.org/10.1016/j.ympev.2014.12.016

Chen ZZ, He K, Huang C, Wan T, Lin LK, Liu SY, Jiang XL (2017) Integrative systematic analyses of the genus *Chodsigoa* (Mammalia: Eulipotyphla: Soricidae), with descriptions of new species. Zoological Journal of the Linnean Society 180: 694–713. https://doi.org/10.1093/zoolinnean/zlw017

Chen ZZ, He SW, Hu WH, Song WY, Onditi OK, Li XY, Jiang XL (2021) Morphology and phylogeny of scalopine moles (Eulipotyphla: Talpidae: Scalopini) from the eastern

Himalayas, with descriptions of a new genus and species. Zoological Journal of the Linnean Society 193: 432–444. https://doi.org/10.1093/zoolinnean/zlaa172

De Winton W, Styan F (1899) On Chinese mammals, principally from western Sechuen, with notes on Chinese squirrels. Proceedings of Zoological Society 67: 572–578. https://doi.org/10.1111/j.1469-7998.1899.tb06875.x

Feng WK (1976) Geomorphotectonic features of the Dabieshan area, China. Chinese Journal of Geology 11(3): 266–276. http://en.dzkx.org/article/id/geology_8690

Gutierrez EE, Garbino GST (2018) Species delimitation based on diagnosis and monophyly, and its importance for advancing mammalian taxonomy. Zoological Research 39(5): 301–308. https://doi.org/10.24272/j.issn.2095-8137.2018.037

He K, Gutiérrez EE, Heming NM, Koepfli KP, Wan T, He SW, Jin W, Liu SY, Jiang XL (2019) Cryptic phylogeographic history sheds light on the generation of species diversity in sky-island mountains. Journal of Biogeography 46(10): 2232–2247. https://doi.org/10.1111/jbi.13664

He K, Jiang XL (2014) Sky islands of southwest China. I: an overview of phylogeographic patterns. Chinese Science Bulletin 59: 585–597. https://link.springer.com/article/10.1007/s11434-013-0089-1

He K, Li YJ, Brandley MC, Lin LK, Wang YX, Zhang YP, Jiang XL (2010) A multi-locus phylogeny of Nectogalini shrews and influences of the paleoclimate on speciation and evolution. Molecular Phylogenetics and Evolution 56: 734–746. https://doi.org/10.1016/j.ympev.2010.03.039

Heaney LR, Timm RM (1983) Systematics and distribution of shrews of the genus *Crocidura* (Mammalia: Insectivora) in Vietnam. Proceedings of the Biological Society of Washington 96: 115–120. https://kuscholarworks.ku.edu/handle/1808/5903

Hoffmann RS (1985) A review of the genus *Soriculus* (Mammalia: Insectivora). Journal of the Bombay Natural History Society 82: 459–481.

Hoffmann RS, Lunde D (2008) Soricomorpha. In: Smith AT, Xie Y (Eds) A Guide to the Mammals of China. Princeton University Press, Princeton, 297–327.

Horsfield T (1851) A catalogue of the Mammalia in the Museum of the Hon. East-India Company. W. H. Allen and Company, London, 226 pp.

Huelsenbeck JP, Rannala B (2004) Frequentist properties of Bayesian posterior probabilities of phylogenetic trees under simple and complex substitution models. Systematic Biology 53: 904–913. https://doi.org/10.1080/10635150490522629

Hutterer R (2005) Order Soricomorpha. In: Wilson DE, Reeder DA (Eds) Mammal Species of the World: a Taxonomic and Geographic Reference. 3rd edn. John Hopkins University Press, Baltimore, 220–311.

Jiang XL, Hoffman RS (2005) Geographic variation and biogeography of De Winton's shrew *Chodsigoa hypsibia* (Insectivora: Soricidae). In: Merritt JF, Churchfield S, Hutterer R, Sheftel BI (Eds) Advances in the Biology of Shrews II. International Society of Shrew Biologists, New York, 71–85.

Kastschenko N (1907) *Chodsigoa* subgen. nov. (gen. *Soriculus*, fam. Soricidae). Annuaire du Musée zoologique de l'Académie de Sciences de St. Pétersbourg 10: 251–254.

Kumar S, Stecher G, Tamura K (2016) MEGA7: Molecular Evolutionary Genetics Analysis version 7.0 for bigger datasets. Molecular Biology and Evolution 33: 1870–1874. https://doi.org/10.1093/molbev/msw054

Lanfear R, Calcott B, Ho SY, Guindon S (2012) PartitionFinder: combined selection of partitioning schemes and substitution models for phylogenetic analyses. Molecular Biology and Evolution 29: 1695–1701. https://doi.org/10.1093/molbev/mss020

Lehmann EV (1955) Die Säugetiere aus Fukien (SO-China) im Museum A. Koenig, Bonn. Bonner Zoologische Beiträge 6: 147–170.

Liu Y, Liu S, Sun Z, Tang M, Hou Q, Liao R (2011) New record of *Chodsigoa hypsibia* in Shanxi Province. Sichuan Journal of Zoology 30: 967–968.

Lunde DP, Musser GG, Son NT (2003) A survey of small mammals from Mt. Tay Con Linh II, Vietnam, with the description of a new species of *Chodsigoa* (Insectivora: Soricidae). Mammal Study 28: 31–46. https://doi.org/10.3106/mammalstudy.28.31

Mayden RL (1997) A hierarchy of species concepts: the denouement in the saga of the species problem. In: Claridge MF, Dawah HA, Wilson MR (Eds) Species: the Units of Biodiversity. Chapman & Hall, London, 381–423.

Minh BQ, Trifinopoulos J, Schrempf D, Schmidt HA (2018) IQ-TREE version 1.6.8: Tutorials and Manual. Phylogenomic software by maximum likelihood. http://www.iqtree.org

Pennant T (1771) Synopsis of Quadrupeds. J. Monk, Chester.Qiu Z, Storch G (2005) The fossil record of the Eurasian Neogene insectivores (Erinaceomorpha, Soricomorpha, Mammalia), Part I: China. Scripta Geologica Special Issue 5: 37–50. https://repository.naturalis.nl/pub/215573/SGSI05_037-050.pdf

Sikes RS, Gannon WL, Animal Care and Use Committee of the American Society of Mammalogists (2016) Guidelines of the American Society of Mammalogists for the use of wild mammals in research and education. Journal of Mammalogy 97: 663–688. https://doi.org/10.1093/jmammal/gyw078

Thomas O (1902) On two new mammals from China. Annals and Magazine of Natural History (Series 7) 10(56): 163–166. https://doi.org/10.1080/00222930208678653

Thomas O (1911a) Mammals collected in the provinces of Kan-su and Sze-chwan, western China, by Mr. Malcolm Anderson, for the Duke of Bedford's exploration of Eastern Asia. Abstracts of the Proceedings of the Zoological Society of London 90: 3–5.

Thomas O (1911b) On mammals collected in the provinces of Szechwan and Yunnan, W. China, by Malcolm Anderson, for the Duke of Bedford's Exploration. Abstracts of the Proceedings of the Zoological Society of London 100: 48–50.

Thomas O (1913) Four new shrews. Annals and Magazine of Natural History (Series 8) 11: 214–218. https://doi.org/10.1080/00222931308693310

Wilson DE, Mittermeier RA (2018) Handbook of the Mammals of the World: Insectivores, Sloths and Colugos. Lynx Edicions, Barcelona, 710 pp.

Woodman N, Timm RM (1993) Intraspecific and interspecific variation in the *Cryptotis nigrescens* species complex of small-eared shrews (Insectivora: Soricidae), with the description of a new species from Colombia. Fieldiana Zoology 74: 1–30. https://doi.org/10.5962/bhl.title.3574

Zhang D, Gao F, Jakovlić I, Zou H, Zhang J, Li WX, Wang GT (2020) PhyloSuite: an integrated and scalable desktop platform for streamlined molecular sequence data management and evolutionary phylogenetics studies. Molecular Ecology Resources 20: 348–355. https://doi.org/10.1111/1755-0998.13096

Zhang H, Qian LF, Zhou L, Wang CC, Liu Y, Tan K, Zhan HS, Zhao K, Zhang BW (2018) Discovery of De Winton's Shrew (*Chodsigoa hypsibia*) in Dabie Mountains, Anhui Province. Chinese Journal of Zoology 53(1): 40–45. http://www.cqvip.com/qk/94741x/201801/674422007.html

Zhang RZ (2002) Geological events and mammalian distribution in China. Acta Zoologica Sinica 48(2): 141–153. http://sourcedb.igsnrr.cas.cn/zw/lw/200906/P020090625724045637685.PDF

Zhang ZQ, Zheng SH (2001) Late Miocene-Pliocene biostratigraphy of Xiaoshigou section, Lingtai, Gansu. Vertebrata PalAsiatica 39: 62–69. https://en.cnki.com.cn/Article_en/CJFDTotal-GJZD200101006.htm

Zheng SH (2004) Jianshi Hominid Site. Science Press, Beijing.

Zhou YY, Ke JZ, Su LF, Lu JQ, Tian JD (2020) A new record of insectivorous species in Henan Province, China – *Chodsigoa hypsibia* de Winton, 1899. Acta Theriologica Sinica 40(6): 646–650. http://www.mammal.cn/EN/10.16829/j.slxb.150405

ZooKeys 1083: 147–168 (2022)
doi: 10.3897/zookeys.1083.76651
https://zookeys.pensoft.net

RESEARCH ARTICLE

A peer-reviewed open-access journal
ZooKeys
Launched to accelerate biodiversity research

DNA barcoding of the leaf-miner flies (Diptera, Agromyzidae) of Mitaraka, French Guiana

Stéphanie Boucher[1], Jade Savage[2]

1 *Department of Natural Resource Sciences, McGill University, Macdonald Campus, Ste-Anne-de-Bellevue, H9X 3V9, Quebec, Canada* **2** *Bishop's University, Sherbrooke, J1M 1Z7, Quebec, Canada*

Corresponding author: Stéphanie Boucher (stephanie.boucher@mcgill.ca)

Academic editor: O. Lonsdale | Received 16 October 2021 | Accepted 5 January 2022 | Published 25 January 2022

http://zoobank.org/2CA481C1-57B7-4C64-84FD-33BDF381997E

Citation: Boucher S, Savage J (2022) DNA barcoding of the leaf-miner flies (Diptera, Agromyzidae) of Mitaraka, French Guiana. ZooKeys 1083: 147–168. https://doi.org/10.3897/zookeys.1083.76651

Abstract

Species level identification of Agromyzidae based on morphology is often challenging due to their small size and morphological homogeneity. DNA barcoding has been used regularly to assist with the identification of economically important species of Agromyzidae, but rarely as a tool for species delineation or identification in biodiversity surveys. The main objective of this study was to investigate whether DNA barcoding and the BIN (Barcoding Index) system could assist with species identification, species delineation, male/ female association, and diversity assessment of Agromyzidae material previously determined to morphospecies from Mitaraka, French Guiana. Amplification success was low, with sequences over 400 bp recovered for only 24 (48%) of the selected specimens. Sequences assigned to 17 morphospecies formed 16 distinct branches or clusters separated by very high (minimum of 10%) sequence divergence. Following the reassessment and subsequent reassignment of one specimen, congruence between morphology and DNA barcodes was high with a single instance of two morphospecies sharing identical sequences. While DNA barcoding did not assist with identification (none of our sequences matched those of named taxa in BOLD or GenBank), it did provide support for most of our morphospecies concepts, including male/female associations. The BIN system also provided access to information about the distribution and habitat preferences of several taxa. We conclude that DNA barcoding was a useful approach to study the species diversity of our samples but that much work remains to be done before it can be used as an identification tool for the Agromyzidae fauna of Mitaraka and the rest of the Neotropical region.

Keywords

Agromyzidae, Barcode Index Number (BIN), CO1, DNA barcoding, French Guiana, Neotropical

Introduction

The Agromyzidae is a family of small flies, measuring on average 2–4 mm in wing length, although they can be smaller than 1 mm or measure up to 6.5 mm. Their coloration is variable, from yellow and/or black, brown, or grey, sometimes with metallic greenish, bluish, or coppery coloration. Most have clear wings, but they may be patterned or infuscated in a few tropical species. The family contains approximately 3200 described species found worldwide (von Tschirnhaus 2021). The larvae of all species feed internally on living plant tissues, with most species with known biology developing inside leaves, hence their common name of leaf-miner flies. The family includes some important pest species of agricultural and ornamental plants, including three well known species occurring in many parts of the world, including South America: *Liriomyza huidobrensis* (Blanchard), *Liriomyza trifolii* (Burgess), *Liromyza sativae* Blanchard. Agromyzidae species identification based on morphology alone is a difficult task due to their small size and morphological homogeneity, but also due to their high diversity, presence of numerous undescribed species and lack of recent identification keys for many countries (Benavent-Corai et al. 2005; Boucher 2010; Boucher and Pollet 2021). Misidentification has happened repeatedly in the literature even when identification was performed by specialists (Scheffer and Winkler 2008). Examination of male genitalia through dissection is often required to confirm species identity, or to support morphospecies delineation in biodiversity surveys (Boucher and Pollet 2021), but this is not an easy process requiring laborious preparation and expertise. In addition to these challenges, species descriptions are often based on one sex only (more commonly males), making male/ female association difficult, especially when sexually dimorphic species are involved.

DNA barcoding, the sequencing of a short fragment of DNA sequence of the mitochondrial cytochrome c oxidase 1 (CO1) gene, is being increasingly used as an identification tool, especially for very diverse and/or morphologically difficult taxa. DNA barcoding was initially proposed as a tool for the identification of animal species (Hebert et al. 2003), but later found to be useful for many other applications in taxonomy and biodiversity studies including species delineation and biodiversity assessment (Hebert et al. 2016), the discovery of cryptic species, female identification, and male/female association (Janzen et al. 2009; Ekrem et al. 2010; Renaud et al. 2012; DeSalle and Goldstein 2019). The Barcode Index Number (BIN) system (Ratnasingham and Hebert 2013) implemented in the Barcode of Life Data System (BOLD) (Ratnasingham and Hebert 2007) is used to group similar COI sequences into genetic clusters (Molecular Operational Taxonomic Units: MOTUs) that can be used as proxy for species. These genetic clusters are assigned unique identifiers (BINs) and include any barcoded specimens on BOLD (even from unrelated projects) with similar sequences, sometimes providing useful metadata such as locality, elevation, habitat type, sex, picture of the specimen, collection date, sampling technique, and taxonomic assignment if named reference sequences are included in the BIN. This could provide

important information for biodiversity inventories and revisionary taxonomic studies (Telfer et al. 2005; Ratnasingham and Hebert 2013).

In the family Agromyzidae, the use of the CO1 gene has been used mainly as a tool to differentiate and identify economically important and invasive species (e.g., Scheffer et al. 2006; Bhuiya et al. 2011; Blacket et al. 2015; Czepak et al. 2018; Firake et al. 2018; Xu et al. 2021), to uncover and identify cryptic species (e.g., Scheffer and Lewis 2006; Scheffer et al. 2014; Weintraub et al. 2017; Mlynarek and Heard 2018), to discover new species (e.g., Scheffer and Wiegmann 2000) and to elucidate Agromyzidae phylogenetic relationships (e.g., Scheffer and Wiegmann 2000; Scheffer et al. 2007; Winkler et al. 2009).

DNA barcoding has rarely been used as a tool for Agromyzidae species identification, morphospecies delineation or gender association in biodiversity surveys, although its use could provide faster and more accurate identification results. Two large biotic surveys occurring in Ontario have used barcoding to provide species identification of thousands of taxa including 21 species (Telfer et al. 2005) and 13 species (deWaard et al. 2018) of Agromyzidae without the expertise of an agromyzid specialist.

A recent and relatively short biotic survey conducted in 2015 at the Mitaraka massif, a mostly unexplored region of French Guiana (Touroult et al. 2018), resulted in 138 agromyzid specimens (43 males; 95 females), delineated into 50 morphospecies (Boucher and Pollet 2021). Based on a combination of external and genitalic characters, male specimens could be delineated into 23 morphospecies, but 69% of the specimens collected were females and morphospecies delineation and male/ female association were highly challenging due to the lack of external diagnostic characters. This problem was especially noticeable for the genera *Melanagromyza* and *Ophiomyia*, the two most abundant and diverse agromyzid genera at Mitaraka (Boucher and Pollet 2021).

Prior to the 2015 Mitaraka expedition, approximately 500 agromyzid species were recorded in the Neotropical region including only four species in French Guiana (*Liriomyza huidobrensis* (Blanchard), *Liriomyza trifolii* (Burgess), *Liromyza sativae* Blanchard, *Nemorimyza maculosa* (Malloch)) (EPPO 2021)). Morphological examination indicated that the Mitaraka agromyzids did not correspond to any of the named species previously recorded for French Guiana (Boucher and Pollet 2021), but some questions remained related to species delineation and identification for the Mitaraka specimens.

The main objective of this study was to investigate whether DNA barcoding could assist with species identification, species delineation, male/ female association, and diversity assessment of the Agromyzidae specimens collected from the Mitaraka Massif (French Guiana) and previously identified as morphospecies (Boucher and Pollet 2021). We also explored if the Barcode Index Number (BIN) system could provide information other than taxonomic assignment (e.g., distribution range, elevation, host plant, etc.) in a region where most of the Agromyzidae fauna is unknown and expected to be undescribed.

Materials and methods

Agromyzid specimens were collected in 2015 as part of the Mitaraka expedition, French Guiana (Touroult et al. 2018). The samples were stored in 70% ethanol and subsequently dried using hexamethyldisilazane (HMDS), mounted on cardboard points and identified to morphospecies. A total of 138 specimens representing ten genera and 50 morphospecies were recorded (Boucher and Pollet 2021). Of these, 54 specimens from 5 genera (*Melanagromyza*, *Ophiomyia*, *Nemorimyza*, *Liriomyza*, *Cerodontha*) representing 33 morphospecies of Agromyzidae were selected for DNA barcoding (Tables 1, 2). The selection included 29 specimens of *Melanagromyza* representing all 15 morphospecies, 17 specimens of *Ophiomyia* representing all 14 morphospecies, two specimens of *Nemorimyza*, representing the two morphospecies, five specimens of *Liriomyza* representing one morphospecies, and one specimen of *Cerodontha*, representing the single *Cerodontha* specimen collected from Mitaraka (Boucher and Pollet 2021). In addition to these Mitaraka specimens, one paratype specimen of *Cerodontha (Diz) nigrihalterata* Boucher (2005) from Costa Rica and housed at the Lyman Entomological Museum was also selected for barcoding for possible comparison with the only *Cerodontha* collected in Mitaraka. The specimens were chosen based on ambiguities and uncertainties that arose during the morphospecies determination (further details below).

DNA amplification and Sanger sequencing were performed at the Centre for Biodiversity Genomics (CBG) (previously known as the Canadian Centre for DNA Barcoding (CCDB)) except for specimens #24, 25, 26, 32–34, 51–54 (Tables 1, 2) that were processed through the LifeScanner barcoding service. Tissue samples for DNA extraction, consisting of one or two leg(s) from each specimen, were sent to these institutions following their submission protocols (CBG: http://ccdb.ca/resources/); LifeScanner: http://lifescanner.net/). Primers C_LepFolF/C_LepFolR (Hernández-Triana et al. 2014) were used for DNA amplification of most specimens except the two specimens of *Liriomyza* (#25–26, Table 1) for which primer set MLepF1/C_LepFolR (Hajibabaei et al. 2006) was used. All COI sequences over 400bp were aligned using the Barcode of Life Data System (BOLD) (Ratnasingham and Hebert 2007) and subsequently uploaded in MEGA X (Kumar et al. 2018), where a neighbor-joining (NJ) tree (Saitou and Nei 1987) was built from a distance matrix computed using the Kimura 2-parameter method (Kimura 1980). The NJ tree provides a graphic representation of genetic distance between sequences from a selected dataset. All sequences retrieved from the Mitaraka specimens were compared to the reference sequence libraries of BOLD (using BOLD identification system) and GenBank (using the Basic Local Alignment Search Tool (BLAST)) for a possible match to a named species. All CO1 sequences were deposited in GenBank with accession number listed in Table 1. Collection data, sequences, and specimen photographs are available on the Barcode of Life Data System (BOLD) (dx.doi.org/10.5883/DS-AGROMIT). Specimens from Mitaraka are presently housed in the Lyman Entomological Museum, Ste-Anne-de-Bellevue, QC (**LEMQ**) but will eventually be deposited in the Muséum national d'Histoire naturelle, Paris, France (**MNHN**).

Table 1. List of Mitaraka specimens sent for barcoding and for which a sequence was retrieved. Includes specimen number for in-text reference, morphospecies name (from Boucher and Pollet 2021), BOLD process ID, BIN assignment, sex, CO1 sequence length, and GenBank accession number. Color text is used when more than one Mitaraka specimen were clustering together in the same BIN (matching color is used in Fig. 1 for easy reference).

Specimen number	Morphospecies	BOLD process ID	BIN assignment (*added for new BIN)	Sex	CO1 Sequence length	GenBank number
1	*Melanagromyza* Mit-1	BUICD1529–19	BOLD:ADX5410*	M	613	OK623732
2	*Melanagromyza* Mit-2	BUICD1440–18	BOLD:ADR6853*	M	658	OK623717
3	*Melanagromyza* Mit-2	BUICD1441–18	BOLD:ADR6853*	M	658	OK623728
4	*Melanagromyza* Mit-2	BUICD1443–18	BOLD:ADR6853*	F	631	OK623740
5	*Melanagromyza* Mit-2	BUICD1444–18	BOLD:ADR6853*	F	658	OK623741
6	*Melanagromyza* Mit-3	BUICD1446–18	BOLD:ADR6852*	M	658	OK623742
7	*Melanagromyza* Mit-4 (previously identified as *M.* Mit-2)	BUICD1445–18	BOLD:ACJ8134	F	658	OK623727
8	*Melanagromyza* Mit-4	BUICD1532–19	BOLD:ACJ8134	F	549	OK623722
9	*Melanagromyza* Mit-4	BUICD1447–18	BOLD:ACJ8134	M	658	OK623729
10	*Melanagromyza* Mit-6	BUICD1534–19	BOLD:ADW8881*	F	602	OK623723
11	*Melanagromyza* Mit-7	BUICD1536–19	BOLD:ADW8881*	F	658	OK623726
12	*Melanagromyza* Mit-9	BUICD1538–19	BOLD:ADB0898	F	658	OK623739
13	*Melanagromyza* Mit-10	BUICD1539–19	BOLD:ADW8248*	F	571	OK623721
14	*Melanagromyza* Mit-10	BUICD1540–19	BOLD:ADW8248*	F	596	OK623733
15	*Melanagromyza* Mit-11	BUICD1541–19	BOLD:ADX5409*	F	555	OK623738
16	*Melanagromyza* Mit-12	BUICD1542–19	BOLD:ADW8247*	M	570	OK623737
17	*Melanagromyza* Mit-12	BUICD1543–19	BOLD:ADW8247*	F	570	OK623735
18	*Melanagromyza* Mit-13	BUICD1544–19	BOLD:ADX3977*	F	658	OK623724
19	*Melanagromyza* Mit-14	BUICD1545–19	BOLD:ADW2860*	F	658	OK623734
20	*Melanagromyza* Mit-15	BUICD1546–19	BOLD:ADX5411*	F	590	OK623736
21	*Ophiomyia* Mit-10	BUICD1558–19	BOLD:ADW4594*	F	564	OK623718
22	*Ophiomyia* Mit-12	BUICD1561–19	Not assigned	F	417	OK623725
23	*Nemorimyza* Mit-1	BUICD1564–19	BOLD:ADW8176*	F	590	OK623720
24	*Nemorimyza* Mit-2	MOBIL8769–18	BOLD:ADB9391	F	600	OK623730
25	*Liriomyza* Mit-1	MOBIL11198–20	Not assigned	F	356	OK623731
26	*Liriomyza* Mit-1	MOBIL11196–20	Not assigned	F	356	OK623719

Results

Amplification success was low (48%), with COI sequences recovered for only 26 of the 54 submitted specimens (Tables 1, 2). Twenty sequences were recovered from *Melanagromyza* specimens, two from *Ophiomyia*, two from *Nemorimyza*, and two short ones of 356 bp from *Liriomyza* (Table 1). None of the COI sequences retrieved from the Mitaraka specimens matched a named species in BOLD or GenBank. In the NJ tree (Fig. 1), the 24 sequences of at least 400 bp representing 17 morphospecies formed 16 distinct clusters with pairwise K2P distances between clusters ranging from 10.7% to 20.9%.

Following the reexamination and subsequent reassignment of specimen #7 (Table 1) to *Melanagromyza* sp. Mit-4, the congruence between morphology and clustering patterns of DNA barcodes was very high, with a single instance of two morphospecies (*Melanagromyza* Mit-6 and *M.* Mit-7) being assigned to the same BIN (BOLD:ADW8881). A total of 15 BINs were assigned to the Mitaraka dataset (Fig. 1, Table 1), all of which were newly created except for BOLD:ACJ8134,

Table 2. Specimens sent for barcoding for which no sequence was retrieved. Includes specimen number for in-text reference, morphospecies name (from Boucher and Pollet 2021), BOLD process ID and sex.

Specimen number	Morphospecies	BOLD process ID	Sex
27	*Melanagromyza* Mit-2	BUICD1442–18	F
28	*Melanagromyza* Mit-4	BUICD1530–19	F
29	*Melanagromyza* Mit-4	BUICD1531–19	F
30	*Melanagromyza* Mit-5	BUICD1533–19	M
31	*Melanagromyza* Mit-6	BUICD1535–19	F
32	*Melanagromyza* Mit-6	Lifescanner Vial ID: BOLD AT1	F
33	*Melanagromyza* Mit-6	Lifescanner Vial ID: BOLD DM0	F
34	*Melanagromyza* Mit-7	Lifescanner Vial ID: BOLD 8E4	F
35	*Melanagromyza* Mit-8	BUICD1537–19	F
36	*Ophiomyia* Mit-1	BUICD1547–19	M
37	*Ophiomyia* Mit-1	BUICD1548–19	M
38	*Ophiomyia* Mit-2	BUICD1549–19	M
39	*Ophiomyia* Mit-3	BUICD1550–19	M
40	*Ophiomyia* Mit-3	BUICD1551–19	F
41	*Ophiomyia* Mit-4	BUICD1552–19	M
42	*Ophiomyia* Mit-5	BUICD1553–19	M
43	*Ophiomyia* Mit 6	BUICD1554–19	F
44	*Ophiomyia* Mit-7	BUICD1555–19	M
45	*Ophiomyia* Mit-8	BUICD1556–19	F
46	*Ophiomyia* Mit-9	BUICD1557–19	F
47	*Ophiomyia* Mit-11	BUICD1559–19	M
48	*Ophiomyia* Mit-12	BUICD1560–19	F
49	*Ophiomyia* Mit-13	BUICD1562–19	F
50	*Ophiomyia* Mit-14	BUICD1563–19	M
51	*Liriomyza* Mit-1	BUICD1449–18	M
52	*Liriomyza* Mit-1	BUICD1448–18	M
53	*Liriomyza* Mit-1	Lifescanner Vial ID: BOLD 5K8	M
54	*Cerodontha* Mit-1	Lifescanner Vial ID BOLD NO6	M
55	*Cerodontha nigrihalterata*	Lifescanner Vial ID BOLD 1N9	F

BOLD:ADB0898 and BOLD:ADW8248 (Table 1). Even if none of these three BINs were associated to named species in BOLD the presence of sequences from specimens from other localities than Mitaraka provided information on the distribution range of *Melanagromyza* Mit-4, *M.* Mit-9, and *Nemorimyza* Mit-2 (Tables 3, Figs 19, 20).

Detailed results by genus are presented below.

Melanagromyza

Sequences more than 500 bp were successfully recovered for 20 specimens (69%) belonging to 13 morphospecies and distributed into 12 BINs (Table 1); no sequences were recovered for specimens assigned to *Melanagromyza* Mit-5 and *Melanagromyza* Mit-8 (Table 2).

Sequences from one specimen each of *Melanagromyza* Mit-6 and *Melanagromyza* Mit-7 displayed identical barcodes and were therefore assigned to the same BIN (BOLD:ADW8881) (Table 1; Fig. 1). *Melanagromyza* Mit-7 (2 females) was separated morphologically from *M.* Mit-6 (8 females) by the weaker metallic reflection of the

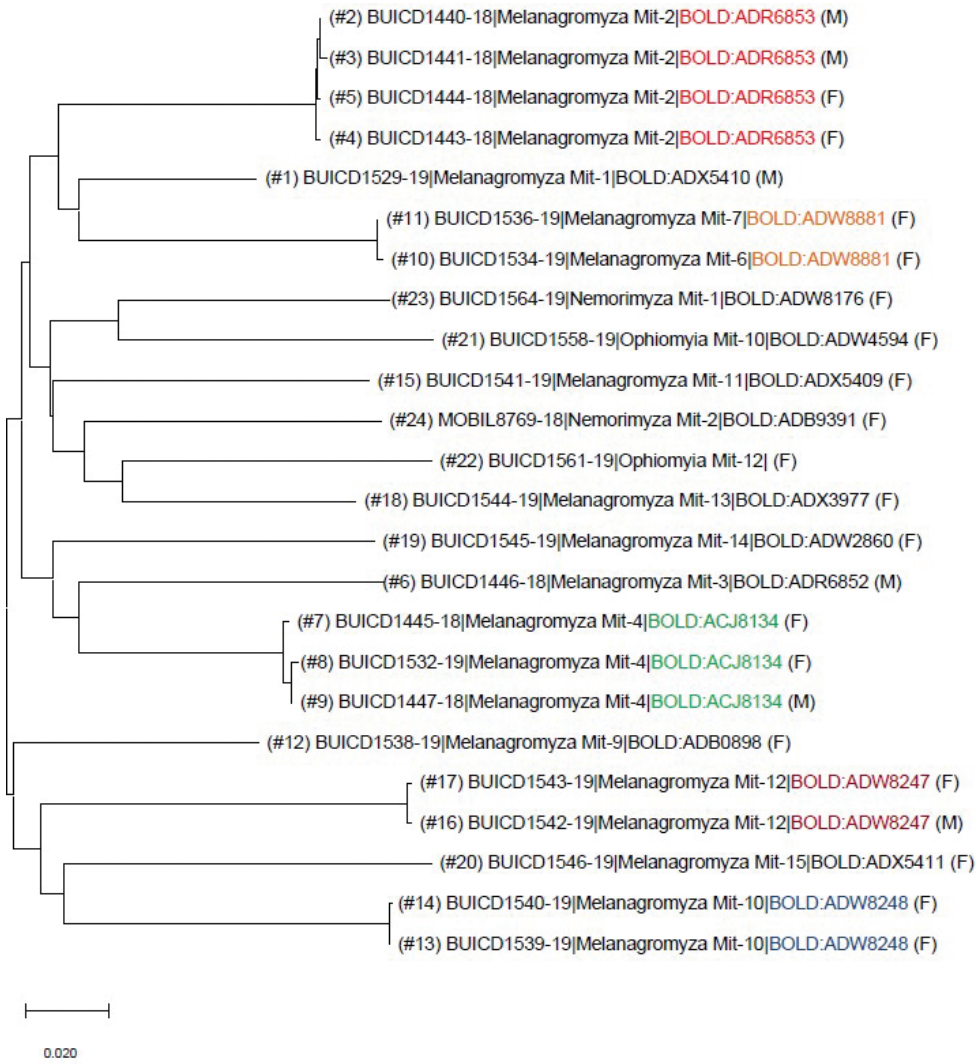

Figure 1. Neighbor-joining tree based on K2P-distance of the 24 specimens of Mitaraka Agromyzidae for which a sequence over 400 bp were retrieved. Information includes specimen number (from Table 1), BOLD process ID, morphospecies name, BIN number and sex. Color text is used when more than one Mitaraka specimen were clustering together in the same BIN.

abdomen, ocellar triangle more extended and not as well defined, and body paler. While a BIN merge for *M.* Mit-6 and *M.* Mit-7 could indicate that *Melanagromyza* Mit-6 and Mit-7 are conspecific, it could also represent a case of misidentification for one specimen. Unfortunately, *M.* Mit-6 (specimen #10, Table 1) was lost in the process of tissue sampling, thereby precluding any further morphological comparison with specimen *M.* Mit-7 (specimen #11, Table 1), and no sequences were recovered from the other specimens of *M.* Mit-6 (3 females) and *M.* Mit-7 (1 female) submitted for barcoding (Table 2).

Table 3. Specimen records (public) included in BIN(BOLD:ACJ8134) with associated specimen data.

BOLD identification	BOLD process ID	Sex	CO1 sequence length	Locality/ coordinate/ elevation	Habitat/collecting technique /sampling date
Melanagromyza Mit-4	BUICD1445–18	F	658	Mitaraka, French Guiana, 2.233, -54.463, 471m	Minor inselberg with savane-roche vegetation /6 m Malaise trap/August 2015
Melanagromyza Mit-4	BUICD1532–19	F	549	Mitaraka, French Guiana 2.233, -54.463, 471m	Minor inselberg with savane-roche vegetation /6 m Malaise trap/August 2015
Melanagromyza Mit-4	BUICD1447–18	M	658	Mitaraka, French Guiana 2.233, -54.463, 471m	Minor inselberg with savane-roche vegetation /6 m Malaise trap/August 2015
Agromyzidae	GMAFN352–15	?	633	Reserva El Bagual. Formosa, Argentina -26.3028, -58.815, 57m	Unknown/Malaise trap/November 2013
Agromyzidae	GMCRM972–13	F	658	Area de Conservacion Guanacaste. Guanacaste, Costa Rica 10.8438, -85.6138, 300m	Forest/Malaise trap/May 2012

Of the six specimens of *Melanagromyza* Mit-2 submitted for barcoding, only one (#27, Table 2) failed to produce a sequence. Four sequences (2 males and 2 females, #2–5, Table 1) clustered together in BOLD:ADR6853 but one (female #7, Table 1) clustered with material of *Melanagromyza* Mit-4 in BOLD:ACJ8134 (Fig. 1). *Melanagromyza* Mit-2 and *M*. Mit-4 are very similar (Figs 2, 3, 6, 7) except for the shorter pubescence on the arista of *Melanagromyza* Mit-2 (Fig. 4). After re-examination, it was found that specimen #7 (Table 1), previously identified as *Melanagromyza* Mit-2, had long pubescence on the arista matching that of specimens assigned to *Melanagromyza* Mit-4 (Fig. 5). The identification of specimen #7 was therefore updated to *Melanagromyza* Mit-4 (Table 1). *Melanagromyza* Mit-2 was the most common of the Mitaraka Agromyzidae (Boucher and Pollet 2021), but morphological differences were observed between males and some females, including abdomen coloration (Figs 8–10) and number of mid-tibial bristles (Figs 11, 12) which created some uncertainties in gender association. Having sequences from both male and female specimens clustering together in the same BIN (BOLD:ADR6853) with a low sequence divergence, ranging from 0.15 to 0.30% provided additional support for conspecificity.

Another case of uncertainty in morphospecies determination involved two female specimens (#13–14; Table 1) that were identified as *Melanagromyza* Mit-10 (Boucher and Pollet 2021), although they exhibited slight external differences (Figs 13, 14) including a paler reddish-brown gena, paler lunule and paler anterior orbit for specimen #14. Identical sequences were retrieved for the two specimens and these were assigned to BOLD:ADW8248 (Fig. 1).

Although agromyzid male genitalia are usually species-specific, providing useful characters for species differentiation, it was not the case for males of *Melanagromyza* Mit-3 and *M.* Mit-4 who exhibited very similar genitalia. They were assigned to separate morphospecies based on a few subtle external characters, including a smaller size for *M.* Mit-4 and, in spite of their morphological similarities, material from these morphospecies produced very distinct DNA barcodes with interspecific distances ranging from 11.99% to 12.60%.

When sequences were recovered for more than one specimen of a single morphospecies, as seen in *M.* Mit-2, *M.* Mit-4, *M.* Mit-10, and *M.* Mit-12, intraspecific divergences were low, with maximum intraspecific distance (0.37%) recorded in

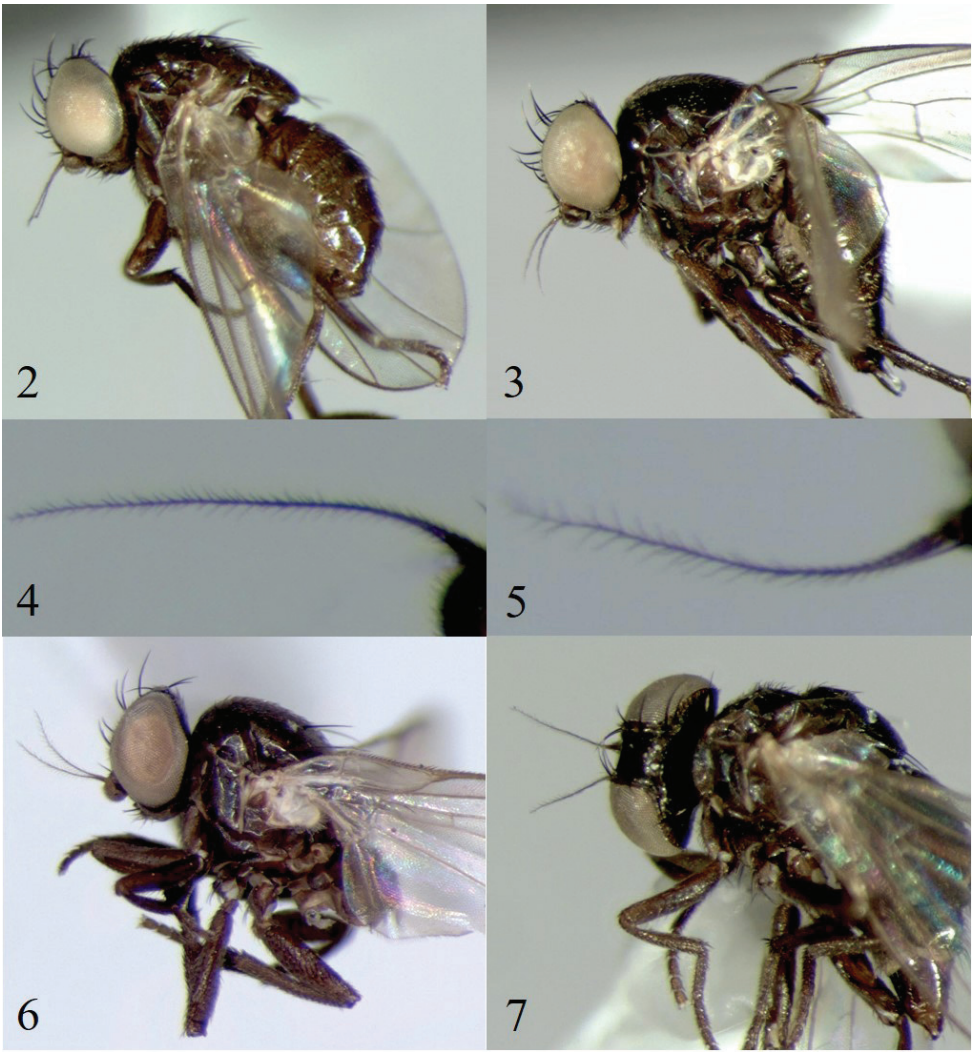

Figures 2–7. (**2–4**) *Melanagromyza* Mit-2. (**5–7**) *Melanagromyza* Mit-4. **2** specimen BUICD1441–18, lateral view **3** specimen BUICD1444–18, lateral view **4** Arista showing short pubescence **5** Arista showing long pubescence **6** specimen BUIC1447–18, lateral view **7** specimen BUIC1445–18, lateral view.

Melanagromyza Mit-4 (BIN (BOLD:ACJ8134) (Fig. 1). On the other hand, interspecific distances were high in this genus, ranging from 10.70% between *Melanagromyza* Mit-2 (specimen #4) and *M.* Mit-1 (specimen #1) and 20.90% between *Melanagromyza* Mit-15 (specimen #20) and *Melanagromyza* Mit-6 (specimen #10) (Fig. 1).

Of the 12 BINs assigned to the Mitaraka *Melanagromyza* specimens, most were new, except BOLD:ACJ8134 and BOLD:ADB0898 (Table 1) that were shared with specimens from other projects. BOLD:ACJ8134 included a total of ten specimens: three specimens from Mitaraka, French Guiana (*Melanagromyza* Mit-4) and seven specimens (two public and five private records) collected in Guanacaste, Costa Rica and Formosa,

Argentina (Table 3; Fig. 19). The other shared BIN: BOLD:ADB0898 included the single female specimen of *Melanagromyza* Mit-9 collected at Mitaraka and two specimens (one public record, one private) from Guanacaste, Costa Rica (Table 4; Fig. 20). Surprisingly, *Melanagromyza* Mit-2, the most commonly collected Agromyzidae at Mitaraka (Boucher and Pollet 2021) was attributed a new BIN (BOLD:ADR6853) (Table 1).

Ophiomyia

Amplification success for *Ophiomyia* material was very low, with sequences retrieved from only two of the 17 selected specimens (Tables 1, 2). These sequences (both from females), representing *Ophiomyia* Mit-10 and *Ophiomyia* Mit-12 (Table 1) were separated by an interspecific distance of 18.8% (Fig. 1). The short sequence for *Ophiomyia* Mit-12 (#22, Table 1) did not match an existing BIN and did not meet the 500 bp requirement for erecting a new BIN (Ratnasingham and Hebert 2013). *Ophiomyia* Mit-10 (BUICDIP1646) was assigned a new BIN (BOLD:ADW4594) (Table 1).

Nemorimyza

The five *Nemorimyza* specimens (one male, four females) collected in Mitaraka were originally treated as one morphospecies (*Nemorimyza* Mit-1), until subtle morphological differences were found in two females that were subsequently treated as a distinct morphospecies (*Nemorimyza* Mit-2) (Boucher and Pollet 2021). A sequence over 500 bp was successfully recovered for each of the *Nemorimyza* female specimens representing *Nemorimyza* Mit-1 and *N*. Mit-2 (Table 1). These were assigned to separate BINS, BOLD:ADW8176 and BOLD:ADB9391, and separated by a high interspecific distance

Table 4. Specimen records (public) included in BIN (BOLD:ADB0898) with associated specimen data.

BOLD identification	BOLD process ID	Sex	CO1 sequence length	Locality /coordinate/ elevation	Habitat /collecting technique /sampling date
Melanagromyza Mit-9	BUICD1538–19	F	658	Mitaraka, French Guiana 2.233, -54.463, 471m	Minor inselberg with savane-roche vegetation /6 m Malaise trap/August 2015
Agromyzidae	JICAZ278–16	F	543	Area de Conservacion Guanacaste. Guanacaste, Costa Rica 10.764, -85.335, 828m	Subtropical/tropical moist lowland forest/ Malaise trap/March 2014

Table 5. Specimen records (public) included in BIN (BOLD:ADB9391) with associated specimen data.

BOLD identification	BOLD process ID	Sex	CO1 sequence length	Locality /coordinate / elevation	Habitat /collecting technique /sampling date
Nemorimyza Mit-2	MOBIL8769–18	F	600	Mitaraka, French Guiana/ 2.233, -54.463/, 471m	Minor inselberg with savane-roche vegetation /6 m Malaise trap/August 2015
Agromyzidae	JCCCY4402–16	F	576	Area de Conservacion Guanacaste. Guanacaste, Costa Rica 10.763, -85.334, 820m	Subtropical/tropical moist lowland forest/ Malaise trap/ November 2014

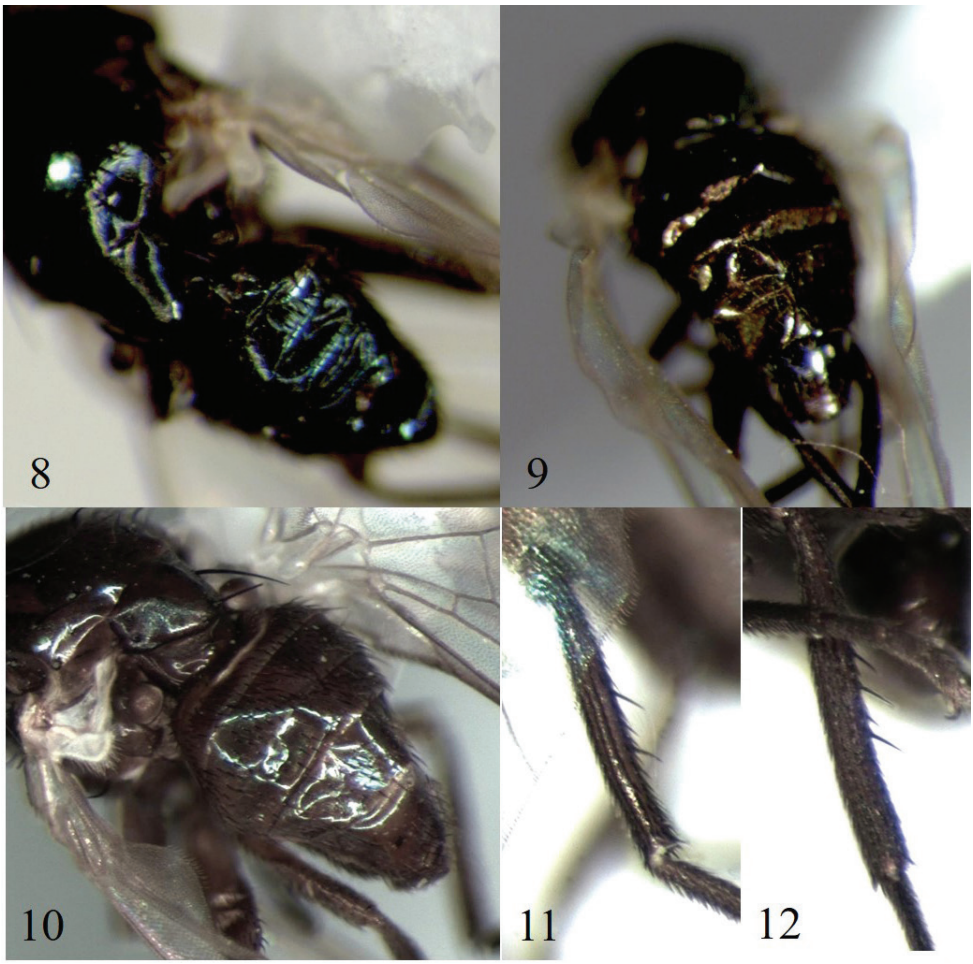

Figures 8–12. (**8–10**) abdomen (color variation) of *Melanagromyza* Mit-2. **8** specimen BUICD1440–18; **9** specimen BUICD1443–18 **10** specimen BUICD1441–18 (**11, 12**) midtibial bristles (number variation) of *Melanagromyza* Mit-2. **11** specimen BUICD1441–18 **12** specimen BUICD1444–18.

of 13.9%. *Nemorimyza* Mit-1 (#23) was assigned a new BIN (BOLD:ADW8176), while *Nemorimyza* Mit-2 (#24) was assigned to BOLD:ADB9391 (Table 1) already containing five other BOLD records (one public) from Guanacaste, Costa Rica (Table 5; Fig. 20).

Liriomyza Mik

One of the morphospecies (*Liriomyza* Mit-1) collected at Mitaraka was very similar to *Liriomyza sativae*, a species previously recorded in French Guiana, but was treated as distinct based on small male genitalic differences. Of the five male *L.* Mit-1 specimens selected for barcoding, only #25 and #26 produced short sequences of 356 bp (Table 1). These short identical sequences did not match any existing BINs or reference

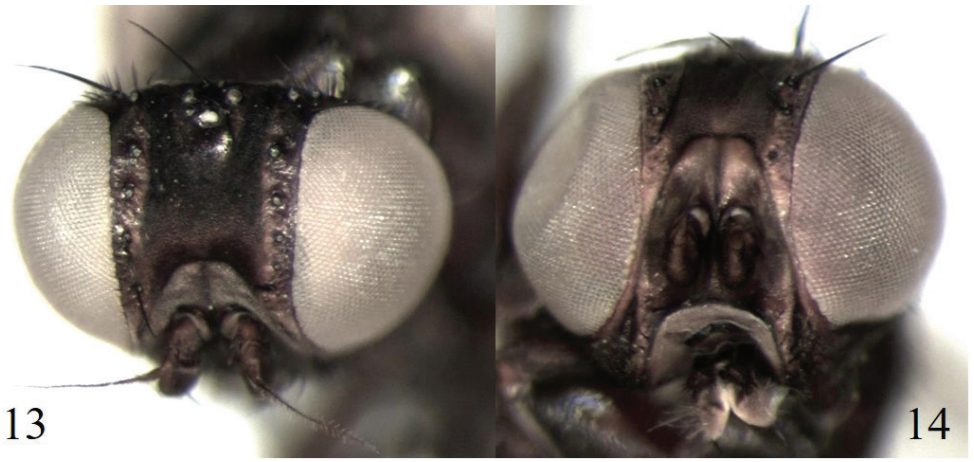

Figures 13, 14. *Melanagromyza* Mit-10. **13** specimen BUICD1539–19, head dorsal view **14** specimen BUICD1540–19, head antero-dorsal view.

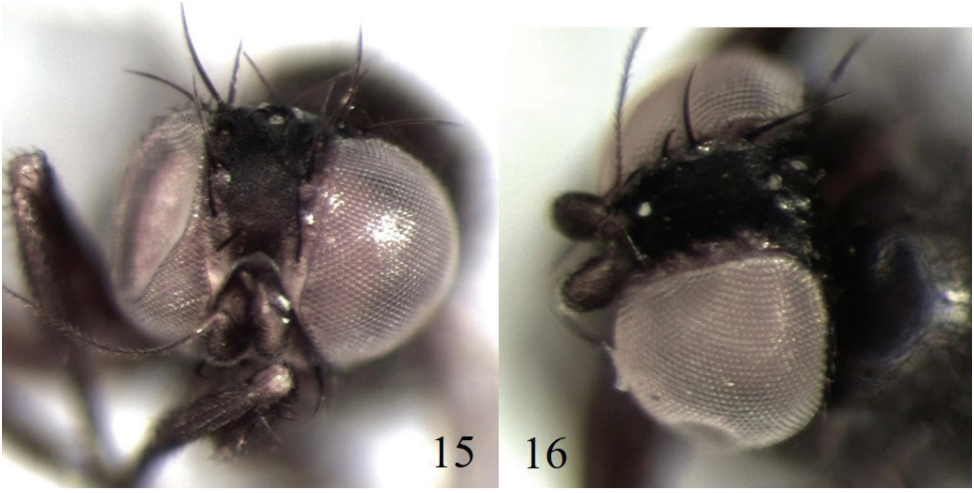

Figure 15–16. 15 *Nemorimyza* Mit-1 BUICD1564–19, head dorsal view **16** *Nemorimyza* Mit-2 MOBIL8769–18, head latero-dorsal view.

taxon in GenBank and did not meet the 500 bp requirement for erecting a new BIN (Ratnasingham and Hebert 2013). They also had more than 11% genetic distance with reference sequences of *Liriomyza sativae* found in BOLD and GenBank, supporting the assignment of the material to a separate morphospecies.

Cerodontha Rondani

One morphospecies (*Cerodontha* Mit-1) (Fig. 17) was very similar to *Cerodontha (Dizygomyza) nigrihalterata* (Fig. 18) a species previously recorded from Costa Rica (Boucher 2005). While a few external characters differentiated *C.* Mit-1 from

Figure 17–18. 17 *Cerodontha* Mit-1, lateral view **18** *Cerodontha nigrihalterata* Boucher, paratype, lateral view.

C. nigrihalterata, we could not investigate their genetic differences as no sequences were retrieved for either of the specimens representing these taxa (Table 2).

Discussion

There are several possible reasons explaining the low amplification success of the sampled specimens such as the fact that they were not freshly collected and had been kept in 70% ethanol before being dried and mounted, instead of 95% ethanol as recommended for DNA preservation (Nagy 2010). However, most of our specimens were very small (< 2.0 mm) and we suspect that the small amount of tissue submitted for DNA extraction (one or two legs per specimen) may not have been enough.

While DNA barcoding is regularly used as a method of identification for economically important species of Agromyzidae (see introduction), it was not helpful in providing species identification for any of the Mitaraka specimens. This is in part due to the fact that some (if not most) of our material belongs to undescribed taxa. This has been confirmed at least for *Nemorimyza*, where *Nemorimyza* Mit-1 and *N.* Mit-2 do not match any of the five described species (including *N. maculosa*, a species previously reported from French Guiana (EPPO 2021) and with reference sequences available on BOLD from the Nearctic region). Another likely explanation for the absence of a match between our material and reference sequences is the under-representation of identified Neotropical Agromyzidae in BOLD (Fig. 21) and GenBank, making a match unlikely. For example, as of September 2021, there were 540 public records for *Melanagromyza* in BOLD, representing 18 species. More than half (326) of these records (including 319 records from Pakistan) represent *Melanagromyza obtusa* (Malloch), a well-known economically important species recently reported in the Americas, including Colombia (Martinez-Alava et al. 2016). Of the remaining 17 species, only one, *Melanagromyza minimoides* Spencer is from the Neotropical region and none of the barcoded Mitaraka specimens matched that species.

Figure 19. Distribution map for BOLD records for BIN: BOLD:ACJ8134 (*Melanagromyza* Mit-4). Distribution data points include Guanacaste, Costa Rica; Formosa, Argentina and Mitaraka, French Guiana (created with SimpleMappr).

As for *Liriomyza*, most reference sequences in BOLD belong to economically important species and this barcode library is important to facilitate the identification of the most important agromyzid pests. As of September 2021, there were 3411 public records of *Liriomyza* in BOLD representing 49 species. More than half (1803) of these records belong to four agricultural pests: *L. sativae* (677 records); *L. trifolii* (668 records); *L. brassicae* (Riley) (339 records) and *L. huidobrensis* (119 records), all recorded from the Neotropical region. Other than these four species, no other named Neotropical species of *Liriomyza* have been barcoded, except for five specimens of *L. nigra* Spencer (with short sequences of 307 bp) belonging to a private project managed by the first author. The short sequence retrieved for *Liriomyza* Mit-1 did not match those of any *Liriomyza* species found in BOLD. Further investigation will be required to confirm the identity of *Liriomyza* Mit-1. The genus *Liriomyza* is the most diverse agromyzid genus in the Neotropical region with approximately 105 species known. Species level identification is difficult due to the lack of recent keys to the Neotropical species and the fact that some species that have been described based on female specimens only (e.g., *L. mikaniovora* Spencer from Venezuela; *L. pagana* (Malloch) from Argentina and *L. quiquevittata* Sasakawa from Chile).

Although DNA barcoding and the BIN system were not useful to assign names to any of our morphospecies, they did provide information relevant to the taxonomy

Figure 20. Distribution map for BOLD records for BIN: BOLD:ADB0898 (*Melanagromyza* Mit-9) and BIN (BOLD:ADB9391) (*Nemorimyza* Mit-2). Distribution data points include Guanacaste, Costa Rica and Mitaraka, French Guiana (created with SimpleMappr).

and diversity of the Mitaraka agromyzid fauna. They allowed us to flag and reassess the identification of some specimens (see results under *Melanagromyza*) and assisted with male/female associations. Due to the importance of male genitalic character for species recognition in agromyzids, females are often left unidentified in taxonomic and faunistic studies (Černý and Bächli 2018; Eiseman and Lonsdale 2018), excluded from type series because of uncertainties in gender association (eg: *Calycomyza addita* Spencer (1983)) or left undescribed or unnamed in the absence of conspecific male (e.g., *Liriomyza* sp. B (Boucher and Wheeler 2014); *Japanagromyza* "female 1" (Lonsdale 2013)). Females can be particularly abundant in biodiversity surveys, especially when Malaise traps are used (Scheirs et al. 1997). This was the case for the Mitaraka survey where 95 females and 43 males were collected (Boucher and Pollet 2021). In the present work, DNA barcoding supported the male/ female conspecificity of specimens assigned to three *Melanagromyza* morphospecies (*M*. Mit-2, *M*. Mit-4, *M.* Mit-12). Furthermore, the high sequence divergence measured between branches or clusters of barcoded morphospecies (Fig. 1) supported almost all the morphospecies assignments even when these were erected only based on female material. The sequencing of additional material will be needed to further investigate the grouping of *Melanagromyza* Mit-6 and *M.* Mit-7 in the same BIN (BOLD:ADW8881) due to the accidental destruction of the only specimen of *M.* Mit-6 with a DNA barcode.

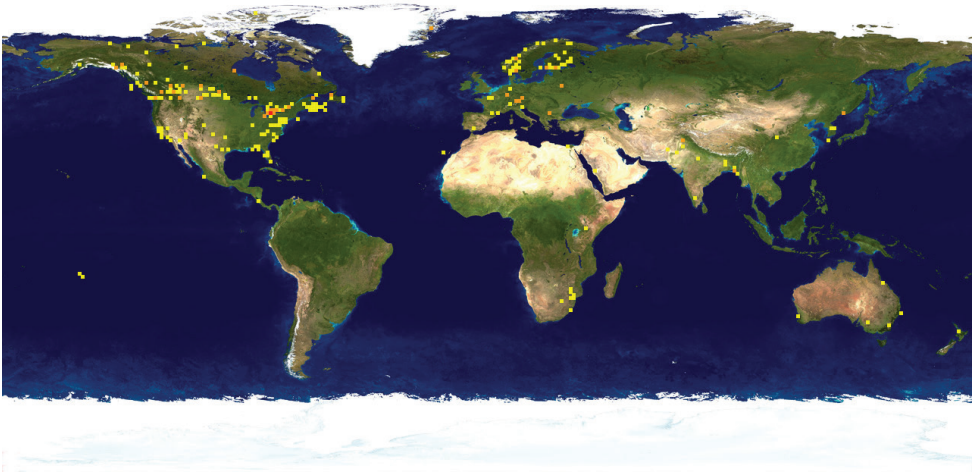

Figure 21. Map of Agromyzidae species occurrence on BOLD. Map generated by BOLD (September 2021).

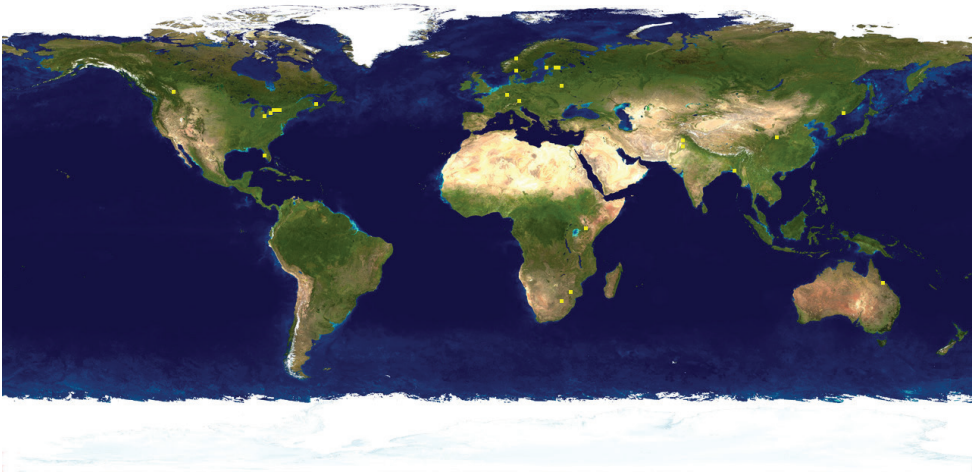

Figure 22. Map of *Melanagromyza* species occurrence on BOLD. Map generated by BOLD (September 2021).

Very little data was available on the agromyzid fauna of French Guiana before the 2015 Mitaraka survey. The high congruence between DNA barcodes/ BIN assignments and morphology presented here suggests that DNA barcoding is an effective approach to estimate the Agromyzidae species diversity of Mitaraka and beyond, especially when females are abundant in samples. Additional studies will be necessary to further evaluate the robustness of the approach since it is widely recognized that levels of congruence between species limits and DNA barcodes/ BINS vary according to the study group. While causes such as hybridization and incomplete lineage sorting (Funk and Omland 2003) are most commonly evoked, simple errors in morphology-based identification can also account for mismatches, especially in the case of morphologically challenging

taxa such as agromyzid flies. An approach combining multiple data sources such as morphology, DNA sequences, and life history traits such host plants should therefore be favored whenever possible.

The genus *Melanagromyza* was the most diverse at Mitaraka with 15 morphospecies (Boucher and Pollet 2021). This diversity resulting from a short survey in a single locality of French Guiana was surprisingly high when compared to known diversity of *Melanagromyza* in different Neotropical countries such as Brazil (19 species), Venezuela (20 species), or Colombia (14 species). The diversity of *Melanagromyza* from the Mitaraka survey could even be greater considering that 70% of the identified specimens were not sequenced and could include cryptic species that failed to be differentiated morphologically. We therefore suspect that much is left to be discovered about the agromyzid fauna of French Guiana and the Neotropical region in general.

We also found that the Barcode Index Number (BIN) system, along with the metadata associated with each barcoded specimen in BOLD, provided important insight into the distribution pattern, habitats, and elevation preference of some species (Tables 3–5), in addition to allowing researchers to locate material easily for revisionary taxonomic studies.

Considering the difficulty associated with species-level identification of Neotropical Agromyzidae and the risks associated with the postal transport of type material, a reference library of DNA barcodes for named species of Neotropical Agromyzidae (including sequences from type material whenever possible) would not only help with identification but also reduce taxonomic errors that may lead to long lists of synonyms such as seen for several species of economic importance such as *L. sativae* and *L. brassicae*.

This study has contributed a total of 23 new barcode-compliant CO1 sequences (more than 500 bp), of Neotropical Agromyzidae, distributed into 15 BINs (including 12 unique BINs). Although these sequences lack species-level determination, they set a stronger base for future taxonomic work and facilitate the discovery of conspecific supplementary material for morphological studies.

Acknowledgments

We would like to thank the LifeScanner team at the Centre for Biodiversity Genomics, in particular Megan Milton, Michelle Pyle, and Sujeevan Ratnasingham who provided helpful information and support for the barcoding results obtained through their barcoding service. We would also like to thank Valerie Levesque-Beaudin at the Centre for Biodiversity Genomics for her great assistance with BOLD, and Andréanne Lessard for the lab assistance at Bishop's University. Financial support for DNA barcoding was provided by Bishop's University to J. Savage. All the material for this study was collected during the *Our Planet Reviewed* Guyane-2015 expedition in the Mitaraka range, in the core area of the French Guiana Amazonian Park, organized by the MNHN and Pro-Natura international. The expedition was funded by the European Regional Development Fund (ERDF), the Conseil régional de Guyane, the Conseil général de

Guyane, the Direction de l'Environnement, de l'Aménagement et du Logement and by the Ministère de l'Éducation nationale, de l'Enseignement supérieur et de la Recherche. It was realized in collaboration with the Parc amazonien de Guyane and the Société Entomologique Antilles-Guyane (SEAG). We would also like to thank Marc Pollet for the invitation to SB for studying the Agromyzidae collecting during this project and for sending the specimens. Marc participated to this expedition as member of the first team (22 February-11 March 2015), hereby supported financially by MNHN and Pro-Natura international. We would also like to thank Pierre-Henri Dalens and his team for collecting the major part of the agromyzid material during the August mission.

References

Benavent-Corai J, Martinez M, Jiménez Peydró R (2005) Catalogue of the hosts-plants of the world Agromyzidae (Diptera). Bollettino Di Zoologia Agraria E Di Bachicoltura. Serie II. Vol 37. Supplementum, 1–97.

Bhuiya BA, Amin S, Mazumdar S (2011) First report of vegetable leafminer *Liriomyza sativae* Blanchard (Diptera: Agromyzidae) through DNA barcoding from Bangladesh. Journal of taxonomy and Biodiversity Research 5: 15–17.

Blacket MJ, Rice AD, Semeraro L, Malipatil MB (2015) DNA-based identifications reveal multiple introductions of the vegetable leafminer *Liriomyza sativae* (Diptera: Agromyzidae) into the Torres Strait Islands and Papua New Guinea. Bulletin of Entomological research 105(5): 533–544. https://doi.org/10.1017/S0007485315000383

Boucher S (2005) Description of an unusual new Costa Rican species of *Cerodontha (Dizygomyza)* with additional notes on Neotropical species of *Dizygomyza* (Diptera: Agromyzidae). Zootaxa 993: 1–8. https://doi.org/10.11646/zootaxa.993.1.1

Boucher S (2010) Family Agromyzidae (leaf-mining flies). In B.V. Brown, A. Borkent, J.M. Cumming, D.M. Wood, N.E. Woodley and M. Zumbado (Eds). Manual of Central American Diptera. Volume 2. National Research Council Press, Ottawa, 1057–1071.

Boucher S, Wheeler TA (2014) Neotropical Agromyzidae (Diptera) of the Mission Géodésique de l'Équateur: Becker (1920) revisited. Zootaxa 3779(2): 157–176. https://doi.org/10.11646/zootaxa.3779.2.3

Boucher S, Pollet M (2021) The leaf-miner flies (Diptera: Agromyzidae) of Mitaraka, French Guiana. Zoosystema 43(6): 113–125. https://doi.org/10.5252/zoosystema2021v43a6

Černý M, Bächli G (2018) New records of Agromyzidae (Diptera) from Switzerland and an updated checklist. Alpine entomology 2: 115–137. https://doi.org/10.3897/alpento.2.28973

Czepak C, Nunes M le S, Carvalhais T, Anjos MV dos, Silverio RF, de Oliveira Lima PBS, Godinho KCA, de Lima AM Junior, Coelho RMS, da Costa Gontijo P (2018) First record of the soybean stem fly *Melanagromyza sojae* (Diptera: Agromyzidae) in the Brazilian Savannah. Pesquisa Agropecuária Tropical 48(2): 200–203. https://doi.org/10.1590/1983-40632018v4853158

DeSalle R, Goldstein P (2019) Review and Interpretation of Trends in DNA Barcoding. Frontiers in Ecology and Evolution 7: 1–11. https://doi.org/10.3389/fevo.2019.00302

deWaard JR, Levesque-Beaudin V, deWaard SL, Ivanova NV, McKeown JTA, Miskie R, Naik S, Perez KHJ, Ratnasingham S, Sobel CN, Sones JE, Steinke C, Telfer AC, Young AD, Young MR, Zakharov EV, Hebert PDN (2018) Expedited assessment of terrestrial arthropod diversity by coupling Malaise traps with DNA barcoding, 1–11. https://doi.org/10.1139/gen-2018-0093

Eiseman CS, Lonsdale O (2018) New state and host records for Agromyzidae (Diptera) in the United States, with the description of thirty new species. Zootaxa 4479: 1–156. https://doi.org/10.11646/zootaxa.4479.1.1

Ekrem T, Stur E, Hebert PDN (2010) Females do count: Documenting Chironomidae (Diptera) species diversity using DNA barcoding. Organisms Diversity & Evolution 10: 397–408. https://doi.org/10.1007/s13127-010-0034-y

EPPO (2021) EPPO Global database. Paris, France. https://gd.eppo.int

Firake DM, Sankarganesh E, Sharma B, Firake PD, Behere GT (2018) DNA barcoding confirmed the occurrence of invasive vegetable leaf miner, *Liriomyza sativae* Blanchard (Diptera: Agromyzidae) in Northeast India. Journal of Asia-Pacific Biodiversity 11: 56–60. https://doi.org/10.1016/j.japb.2017.10.002

Funk DJ, Omland KE (2003) Species-level paraphyly and polyphyly: Frequency, causes, and consequences, with insights from animal mitochondrial DNA. Annual Review of Ecology, Evolution and Systematics 34: 397–423. https://doi.org/10.1146/annurev.ecolsys.34.011802.132421

Hajibabaei M, Janzen DH, Burns JM, Hallwachs W, Hebert PDN (2006) DNA barcodes distinguish species of tropical Lepidoptera. Proceedings of the National Academy of Sciences of the United States of America 103: 968–971. https://doi.org/10.1073/pnas.0510466103

Hebert PDN, Cywinska A, Ball SL, deWaard JR (2003) Biological identifications through DNA barcodes. Proceedings of the Royal Society of London B: Biological Sciences 270: 313–321. https://doi.org/10.1098/rspb.2002.2218

Hebert PDN, Ratnasingham S, Zakharov EV, Telfer AC, Levesque-Beaudin V, Milton MA, Pedersen S, Jannetta P, deWaard JR (2016) Counting animal species with DNA barcodes: Canadian insects. Philosophical Transactions of the Royal Society B 371: e20150333. http://doi.org/10.1098/rstb.2015.0333

Hernández-Triana LM, Prosser SW, Rodríguez-Perez MA, Chaverri LG, Hebert PDN, Gregory TR (2014) Recovery of DNA barcodes from blackfly museum specimens (Diptera: Simuliidae) using primer sets that target a variety of sequence lengths. Molecular Ecology Resource 14(3): 508–518. https://doi.org/10.1111/1755-0998.12208

Janzen DH, Hallwachs W, Blandin P, Burns JM, Cadiou J, Chacon I, Dapkey T, Deans AR, Epstein ME, Espinoza B, Franclemont JG, Haber WA, Hajibabaei M, Hall JPW, Hebert PDN, Gauld ID, Harvey DJ, Hausmann A, Kitching IJ, Lafontaine D, Landry J, Lemaire C, Miller JY, Miller JS, Miller L, Miller SE, Montero J, Munroe E, Green SR, Ratnasingham S, Rawlins JE, Robbins RK, Rodriguez JJ, Rougerie R, Sharkey MJ, Smith MA, Solis MA, Sullivan JB, Thiaucourt P, Wahl DB, Weller SJ, Whitfield JB, Willmott KR, Wood DM, Woodley NE, Wilson JJ (2009) Integration of DNA barcoding into an ongoing inventory of complex tropical biodiversity. Molecular Ecology Resources 9: 1-26. https://doi.org/10.1111/j.1755-0998.2009.02628.x

Kimura M (1980) A simple method for estimating evolutionary rate of base substitutions through comparative studies of nucleotide sequences. Journal of Molecular Evolution 16: 111–120. https://doi.org/10.1007/BF01731581

Kumar S, Stecher G, Li M, Knyaz C, Tamura K (2018) MEGA X: Molecular Evolutionary Genetics Analysis across computing platforms. Molecular Biology and Evolution 35: 1547–1549. https://doi.org/10.1093/molbev/msy096

Lonsdale O (2013) *Japanagromyza* Sasakawa (Diptera: Agromyzidae) of Africa. Zootaxa 3709: 445–460. https://doi.org/10.11646/zootaxa.3709.5.3

Martinez-Alava JO, Serna F, Pérez AL (2016) *Melanagromyza obtusa* (Diptera : Agromyzidae), a new record for Colombia. Agronomía Colombiana 34(2): 292–294. https://doi.org/10.15446/agron.colomb.v34n2.56958

Mlynarek JJ, Heard SB (2018) Strong and complex host- and habitat-associated genetic differentiation in an apparently polyphagous leaf mining insect. Biological Journal of the Linnean Society 125(4): 885–899. https://doi.org/10.1093/biolinnean/bly166

Nagy ZT (2010) A hands-on overview of tissue preservation methods for molecular genetic analyses. Organisms Diversity & Evolution 10: 91–105. https://doi.org/10.1007/s13127-010-0012-4

Ratnasingham S, Hebert PDN (2007) BOLD: The Barcode of Life Data System (www.barcodinglife.org). Molecular Ecology Notes 7: 355–364. https://doi.org/10.1111/j.1471-8286.2007.01678.x

Ratnasingham S, Hebert PDN (2013) A DNA-based registry for all animal species: the barcode index number (BIN) system. PLoS ONE 8(7): e66213. https://doi.org/10.1371/journal.pone.0066213

Renaud AK, Savage J, Adamowicz SJ (2012) DNA barcoding of Northern Nearctic Muscidae (Diptera) reveals high correspondence between morphological and molecular species limits. BMC Ecology 12: e24. https://doi.org/10.1186/1472-6785-12-24

Saitou N, Nei M (1987) The neighbor-joining method: A new method for reconstructing phylogenetic trees. Molecular Biology and Evolution 4: 406–425. https://doi.org/10.1093/oxfordjournals.molbev.a040454

Scheffer SJ, Wiegmann BM (2000) Molecular Phylogenetics of the Holly Leafminers (Diptera: Agromyzidae: *Phytomyza*): Species limits, Speciation, and Dietary Specialization. Molecular Phylogenetics and Evolution 17: 244–255. https://doi.org/10.1006/mpev.2000.0830

Scheffer SJ, Lewis ML (2006) Mitochondrial Phylogeography of the vegetable pest *Liriomyza trifolii* (Diptera: Agromyzidae): diverged clades and invasive populations. Annals of the entomological Society of America 99(6): 991–998. https://doi.org/10.1603/0013-8746(2006)99[991:MPOTVP]2.0.CO;2

Scheffer SJ, Lewis ML, Joshi RC (2006) DNA barcoding applied to invasive leafminers (Diptera: Agromyzidae) in the Philippines. Annals of the Entomological Society of America 99(2): 204–210. https://doi.org/10.1603/0013-8746(2006)099[0204:DBATIL]2.0.CO;2

Scheffer SJ, Winkler IS, Wiegmann BM (2007) Phylogenetic relationships within the leaf-mining flies (Diptera: Agromyzidae) inferred from sequence data from multiple genes. Molecular phylogenetics and evolution 42(3): 756–775. https://doi.org/10.1016/j.ympev.2006.12.018

Scheffer SJ, Winkler IS (2008) The first confirmed record of the leafminer *Phytomyza rufipes* in the United States. Proceedings of the Entomological Society of Washington 110(3): 674–678. https://doi.org/10.4289/07-057.1

Scheffer SJ, Lewis ML, Gaimari SD, Reitz SR (2014) Molecular survey for the invasive leafminer pest *Liriomyza huidobrensis* (Diptera: Agromyzidae) in California uncovers only the native pest *Liriomyza langei*. Journal of Economic Entomology 107(5): 1959–1964. https://doi.org/10.1603/EC13279

Scheirs J, De Bruyn L, von Tschirnhaus M (1997) Comparison of different trapping methods in Agromyzidae (Diptera). Journal of Applied Entomology 121: 429–433. https://doi.org/10.1111/j.1439-0418.1997.tb01430.x

Spencer KA (1983) Leaf mining Agromyzidae (Diptera) in Costa Rica. Revista de Biologia Tropical 31(1): 41–67.

Telfer A, Young M, Quinn J, Perez K, Sobel C, Sones J, Levesque-Beaudin V, Derbyshire R, Fernandez-Triana J, Rougerie R, Thevanayagam A, Boskovic A, Borisenko A, Cadel A, Brown A, Pages A, Castillo A, Nicolai A, Glenn Mockford B, Bukowski B, Wilson B, Trojahn B, Lacroix C, Brimblecombe C, Hay C, Ho C, Steinke C, Warne C, Garrido Cortes C, Engelking D, Wright D, Lijtmaer D, Gascoigne D, Hernandez Martich D, Morningstar D, Neumann D, Steinke D, Marco DeBruin D, Dobias D, Sears E, Richard E, Damstra E, Zakharov E, Laberge F, Collins G, Blagoev G, Grainge G, Ansell G, Meredith G, Hogg I, McKeown J, Topan J, Bracey J, Guenther J, Sills-Gilligan J, Addesi J, Persi J, Layton K, D'Souza K, Dorji K, Grundy K, Nghidinwa K, Ronnenberg K, Lee K, Xie L, Lu L, Penev L, Gonzalez M, Rosati M, Kekkonen M, Kuzmina M, Iskandar M, Mutanen M, Fatahi M, Pentinsaari M, Bauman M, Nikolova N, Ivanova N, Jones N, Weerasuriya N, Monkhouse N, Lavinia P, Jannetta P, Hanisch P, McMullin R, Ojeda Flores R, Mouttet R, Vender R, Labbee R, Forsyth R, Lauder R, Dickson R, Kroft R, Miller S, MacDonald S, Panthi S, Pedersen S, Sobek-Swant S, Naik S, Lipinskaya T, Eagalle T, Decaëns T, Kosuth T, Braukmann T, Woodcock T, Roslin T, Zammit T, Campbell V, Dinca V, Peneva V, Hebert P, deWaard J (2015) Biodiversity inventories in high gear: DNA barcoding facilitates a rapid biotic survey of a temperature nature reserve. Biodiversity data journal 3: e6313. https://doi.org/10.3897/BDJ.3.e6313

Touroult J, Pollet M, Pascal O (2018) Overview of Mitaraka survey: research frame, study site and field protocols. In Touroult J. (Ed.), "Our Planet Reviewed" 2015 large-scale biotic survey in Mitaraka, French Guiana. Zoosystema 40(13): 327–365. https://doi.org/10.5252/zoosystema2018v40a13

Von Tschirnhaus M (2021) Morphological arguments for the retainment of three long time established genera in Agromyzidae (Diptera): *Chromatomyia* Hardy, *Napomyza* Westwood, and *Ptochomyza* Hering. Dipterist Digest 28: 105–117.

Weintraub PG, Scheffer SJ, Visser D, Valladares G, Correa AS, Shepard BM, Rauf A, Murphy ST, Mujica N, MacVean C, Kroschel J, Kishinevsky M, Joshi RC, Johansen NS, Hallett RH, Civelek HS, Chen B, Metzler HB (2017) The invasive *Liriomyza huidobrensis* (Diptera: Agromyzidae): Understanding its pest status and management globally. Journal of Insect Science 17(1): 28: 1–27. https://doi.org/10.1093/jisesa/iew121

Winkler I, Scheffer SJ, Mitter C (2009) Molecular phylogeny and systematic of leaf-mining flies (Diptera: Agromyzidae): delimitation of *Phytomyza* Fallén sensu lato and included species groups, with new insights on morphological and host-use evolution. Systematic Entomology 34: 260–292. https://doi.org/10.1111/j.1365-3113.2008.00462.x

Xu X, Coquilleau MP, Ridland PM, Umina PA, Yang Q, Hoffmann AA (2021) Molecular identification of leafmining flies from Australia including new *Liriomyza* outbreaks. Journal of Economic Entomology 20(20): 1–8. https://doi.org/10.1093/jee/toab143

ZooKeys 1083: 169–210 (2022)
doi: 10.3897/zookeys.1083.72939
https://zookeys.pensoft.net

RESEARCH ARTICLE

A peer-reviewed open-access journal
ZooKeys
Launched to accelerate biodiversity research

Battle of the bands: systematics and phylogeny of the white *Goniobranchus* nudibranchs with marginal bands (Nudibranchia, Chromodorididae)

Giun Yee Soong[1], Lynn J. Bonomo[2], James D. Reimer[1,3], Terrence M. Gosliner[2]

1 *Molecular Invertebrate Systematics and Ecology Laboratory, Graduate School of Engineering and Science, University of the Ryukyus, Senbaru 1, Nishihara, Okinawa 903–0213, Japan* **2** *Department of Invertebrate Zoology & Geology, California Academy of Sciences, San Francisco, California 94118, USA* **3** *Tropical Biosphere Research Center, University of the Ryukyus, Senbaru 1, Nishihara, Okinawa 903–0213, Japan*

Corresponding author: Giun Yee Soong (giunyee@gmail.com)

Academic editor: Nathalie Yonow | Received 12 August 2021 | Accepted 2 December 2021 | Published 25 January 2021

http://zoobank.org/68368C58-5F54-4800-A2EB-5FEFFD2585B4

Citation: Soong GY, Bonomo LJ, Reimer JD, Gosliner TM (2021) Battle of the bands: systematics and phylogeny of the white *Goniobranchus* nudibranchs with marginal bands (Nudibranchia, Chromodorididae). ZooKeys 1083: 169–210. https://doi.org/10.3897/zookeys.1083.72939

Abstract

Species identities of *Goniobranchus* nudibranchs with white bodies and various marginal bands have long been problematic. In this study, specimens of these *Goniobranchus* nudibranchs from the Philippines, Peninsular Malaysia, Japan, Papua New Guinea, and Madagascar were analyzed and molecular data were obtained in order to re-examine the relationships between species within this "white *Goniobranchus* with marginal bands" group. The analyses clearly recovered six species groups corresponding to the described species *Goniobranchus albonares*, *G. preciosus*, *G. rubrocornutus*, *G. sinensis*, and *G. verrieri* as well as one new species, *G. fabulus* Soong & Gosliner, **sp. nov.** Notably, *G. preciosus*, *G. sinensis*, *G. rubrocornutus*, *G. verrieri*, and *G. fabulus* Soong & Gosliner, **sp. nov.** exhibit color variation and polymorphism, suggesting that some aspects of color patterns (e.g., presence or absence of dorsal spots) may not always be useful in the identification of species in the "white *Goniobranchus* with marginal bands" group, whereas other features such as gill and rhinophore colors and the arrangement and colors of the mantle marginal bands are more diagnostic for each species.

Keywords

Biodiversity, coral reefs, mtDNA, species delimitation, taxonomy

Introduction

Research focusing on the diversity within Nudibranchia through molecular work has increased in recent years (e.g., Epstein et al. 2019; Korshunova et al. 2020), and a better understanding of the phylogenetic relationships within the clade has been achieved via molecular phylogenetic analyses. These studies have also revealed new species, many of which have been cryptic or pseudocryptic species or members of species complexes (e.g., Layton et al. 2018; Matsuda and Gosliner 2018a; Epstein et al. 2019; Sørensen et al. 2020). The genus *Goniobranchus* was previously synonymized with the genus *Chromodoris*, but molecular analyses by Johnson and Gosliner (2012) revealed that *Chromodoris* was non-monophyletic. This resulted in the generic reinstatement of *Goniobranchus* for one of the distinct clades of *Chromodoris* (Johnson and Gosliner 2012), but morphological differences are not clear. *Goniobranchus* currently contains 57 described species (MolluscaBase 2021), and members of this genus can be identified for laying raised egg masses (i.e., one edge of the egg mass is attached to the substrate, while the other stands up in the water column).

Within *Goniobranchus* there are several species complexes, each containing similar species grouped together based on their external coloration and patterns, and many times involving cryptic or pseudocryptic species (Johnson and Gosliner 2012; Soong et al. 2020). One such group is the red-reticulate species complex with three described species and several synonymies that were summarized by Rudman (1973). A recent molecular phylogenetic examination revealed the presence of five potentially undescribed species within this species complex that are cryptic with the described species (Soong et al. 2020).

Another likely pseudocryptic *Goniobranchus* species complex contains species with white bodies and variously colored marginal bands. This group has not been thoroughly examined through molecular sequencing. Rudman (1985) provided the most recent taxonomic assessment on this species complex and placed *Goniobranchus preciosus* (Kelaart, 1858), *G. verrieri* (Crosse, 1875), *G. trimarginatus* (Winckworth, 1946), *G. sinensis* (Rudman, 1985), *G. rubrocornutus* (Rudman, 1985), and *G. galactos* (Rudman & Johnson, 1985) within the group. Gosliner et al. (2015) subsequently included *G. albonares* (Rudman 1990) in the complex due to a similarity in color patterns. Since all these species share similar colors and patterns on their bodies, and as the group has a large geographic range from the Indian Ocean to the Western Pacific Ocean (Debelius 1996; Debelius and Kuiter 2007; Coleman 2008; Gosliner et al. 2008, 2015, 2018), it has been postulated that undescribed, cryptic species may exist within this group (Rudman 1985; Gosliner et al. 2008, 2015, 2018). However, previous taxonomic studies on this group of *Goniobranchus* focused only on morphological analyses and most of the previous molecular sequences were by Johnson and Gosliner (2012) who included only a few representatives of this particular group, namely *G. sinensis*, *G. preciosus*, *G. verrieri*, and *G. daphne*; they recovered a monophyletic group of species with white bodies with variously colored marginal bands in their study. Here, we incorporate molecular data to re-examine the phylogenetic relationships between several putative

Goniobranchus species with white bodies and variously colored marginal bands and, as a result of our phylogenetic and morphological analyses, we formally describe one novel species. Specimens of two species that Rudman (1985) included in his study (*G. galactos* and *G. trimarginatus*) were not included in the present study, as no material appropriately fixed for molecular sequencing was available.

Materials and methods

Taxon sampling

A total of 35 *Goniobranchus* specimens with white mantles and various marginal bands was examined in this study (Table 1). The specimens were either deposited in the California Academy of Sciences Invertebrate Zoology collection or newly collected from Kagoshima and Okinawa in southern Japan by SCUBA diving (Table 1). Additionally, sequences from specimens of *Glossodoris* species (*G. bonwanga*, *G. andersonae*, *G. buko*, *G. cincta*, *G. pallida*, *G. acosti*, and *G. hikuerensis*) were used as the outgroup in our analyses, based on the most recently published family Chromodorididae phylogeny (Johnson and Gosliner 2012). Specimens were photographed in situ before collection and fixation, in either 95% or 99.5% ethanol for DNA molecular work or 10% formalin for morphological work. All specimens were preliminarily identified based on their external morphologies and subsequent identifications were made by the senior author.

DNA extraction, amplification, sequencing

DNA was extracted from the *Goniobranchus* specimen tissues using a Qiagen DNeasy Blood and Tissue Kit (Qiagen, Tokyo, Japan) either at the Molecular Invertebrate Systematics and Ecology (MISE) Laboratory (Okinawa, Japan) or at the California Academy of Sciences Center for Comparative Genomics (CCG; San Francisco, CA, USA). Polymerase chain reaction (PCR) amplifications for specimens deposited in the California Academy of Sciences Invertebrate Zoology were done following a protocol used by Bonomo and Gosliner (2020). PCR amplifications for the remaining specimens were performed at the Molecular Invertebrate Systematics and Ecology Laboratory using 20 µL reaction volume, consisting of 7 µL H2O, 10 µL Hot Start Taq Plus Master Mix Kit (Qiagen, Tokyo, Japan), 1 µL of each primer and 1 µL of genomic DNA. Two mitochondrial genes, cytochrome c oxidase subunit I (COI) and 16S ribosomal RNA (16S rDNA), were amplified. The universal primers used for COI were LCO1490 (5'-GGTCAACAAATCATAAAGATATTGG-3') and HCO2198 (5'-TAAACTTCAGGGTGACCAAAAAATCA-3') from Folmer et al. (1994). The universal primers used for 16S were 16Sar-L (5'-CGCCTGTTTATCAAAAACAT-3') by Palumbi et al. (1991) and 16SR (5'-CCGGTTTGAACTCAGATCATGT-3') from Palumbi (1996). The targeted fragment length for COI was 658 base pairs and for

Table 1. List of specimens used in this study. Asterisk indicates sequence acquired from GenBank. Institution and voucher codes: CASIZ (California Academy of Sciences Invertebrate Zoology), WAM (Western Australian Museum), SAM (South Australian Museum), UQ (University of Queensland), MISE (Molecular Invertebrate Systematics and Ecology), Okinawa, Japan.

Species name	Morpho–type	Voucher number	Location	Depth (m)	GenBank accession numbers	
					COI	16S
Outgroups						
Glossodoris acosti	–	CASIZ 175327*	Bohol Island, Philippines	1–5	KT600696	KT595626
Glossodoris andersonae	–	CASIZ 192288*	Abulad Islands, Saudi Arabia	7	KT600694	KT595623
Glossodoris bonwanga	–	CASIZ 194018*	South Madagascar, Madagascar	3–8	KT600695	KT595647
Glossodoris buko	–	CASIZ 177408*	Batangas Province, Philippines	21	KT600711	KT595638
Glossodoris cincta	–	CASIZ 177257*	Batangas Province, Philippines	14	KT600700	KT595627
Glossodoris hikuerensis	–	CASIZ 116935*	Kwajalein Atoll, Marshall Islands	16	KT600704	KT595632
Ingroups						
Goniobranchus albonares	–	CASIZ 191440	Madang Province, Papua New Guinea	–	OL685221	OL684806
Goniobranchus albonares	–	CASIZ 228939	Batangas Province, Philippines	5	OL685222	OL684786
Goniobranchus albonares	–	CASIZ 194037	South Madagascar, Madagascar	22	OL685223	OL684810
Goniobranchus albonares	–	N/A*	New South Wales, Australia	–	KJ001299	KJ018909
Goniobranchus albopunctatus	–	CASIZ 121268*	Western Australia, Australia	30	JQ727827	JQ727700
Goniobranchus albopustulosus	–	CASIZ 142953*	Maui, Hawai'i	7	JQ727828	JQ727701
Goniobranchus aureopurpureus	–	N/A*	–	–	EU512128	EU512055
Goniobranchus coi	–	CASIZ 158683*	Batangas Province, Philippines	20	EU982734	EU982785
Goniobranchus coi	–	N/A*	–	–	EU512144	EU512061
Goniobranchus collingwoodi	–	CASIZ 139597*	Bali, Indonesia	24	JQ727834	JQ727710.1
Goniobranchus cf. *collingwoodi*	–	CASIZ 159382*	Queensland, Australia	–	JQ727835	JQ727711
Goniobranchus daphne	–	UQ 802*	Tasmania, Australia	5	MH018004	MH017991
Goniobranchus daphne	–	N/A*	Queensland, Australia	–	KJ001297	KJ018921
Goniobranchus decorus	–	N/A*	–	–	EU512146	EU512068
Goniobranchus decorus	–	CASIZ 157025*	Batangas Province, Philippines	8	EU982735	EU982786
Goniobranchus epicurius	–	SAM D19285*	Tasmania, Australia	–	EF535114	AY458804
Goniobranchus fabulus	A	CASIZ 177517	Batangas Province, Philippines	–	OL685216	OL684785
Goniobranchus fabulus	A	CASIZ 201949	Batangas Province, Philippines	–	OL685224	OL684787
Goniobranchus fabulus	A	CASIZ 177685	Batangas Province, Philippines	15	OL685217	OL684807
Goniobranchus fabulus	B	CASIZ 191271	Madang Province, Papua New Guinea	–	OL685220	OL684804
Goniobranchus fabulus	B	CASIZ 191118	Madang Province, Papua New Guinea	3	OL685219	OL684805
Goniobranchus fidelis	–	CASIZ 175556*	Iles Radama, Madagascar	30	JQ727839	JQ727714
Goniobranchus fidelis	–	CASIZ 175426*	Batangas Province, Philippines	–	JQ727838	JQ727715
Goniobranchus geminus	–	CASIZ 173434*	Iles Radama, Madagascar	13–16	JQ727840	JQ727716
Goniobranchus geometricus	–	CASIZ 144023*	Queensland, Australia	11	JQ727841	JQ727718
Goniobranchus geometricus	–	CASIZ 177549*	Batangas Province, Philippines	22.7	JQ727842	JQ727717
Goniobranchus geometricus	–	MO6*	North Sulawesi, Indonesia	> 6	MK348906	MK322449
Goniobranchus geometricus	–	Goge 16S1*	North Sulawesi, Indonesia	6–19	MN339442	MN104715
Goniobranchus geometricus	–	Goge 16S2*	North Sulawesi, Indonesia	6–19	MN339443	MN104716
Goniobranchus geometricus	–	Goge 16S3*	North Sulawesi, Indonesia	6–19	MN339444	MN104717
Goniobranchus heatherae	–	CASIZ 175546*	Cape Peninsula, South Africa	–	JQ727844	JQ727720
Goniobranchus hintuanensis	–	CASIZ 158346*	Batangas Province, Philippines	10	JQ727845	JQ727721
Goniobranchus hunterae	–	UQ 915*	Tasmania, Australia	–	MH018008	MH017995
Goniobranchus hunterae	–	UQ 824*	Tasmania, Australia	–	MH018006	MH017993
Goniobranchus leopardus	–	CASIZ 159384*	Queensland, Australia	16	JQ727847	JQ727726

Species name	Morpho–type	Voucher number	Location	Depth (m)	GenBank accession numbers	
					COI	16S
Goniobranchus leopardus	–	SAM D 19288*	Queensland, Australia	–	EF535116	AY458808
Goniobranchus loringi	–	WAM S111031*	New South Wales, Australia	–	MH018013	MH018000
Goniobranchus preciosus	A	CASIZ 208420	Oriental Mindoro Province, Philippines	4–22	OL685227	OL684811
Goniobranchus preciosus	A	CASIZ 208415	Oriental Mindoro Province, Philippines	–	OL685226	OL684794
Goniobranchus preciosus	B	CASIZ 208574	Oriental Mindoro Province, Philippines	6–16	OL685230	OL684813
Goniobranchus preciosus	C	CASIZ 176752	Pulau Tioman, Peninsular Malaysia	13	OL685213	OL684815
Goniobranchus preciosus	D	CASIZ 176761	Pulau Tioman, Peninsular Malaysia	17	OL685215	OL684814
Goniobranchus cf. *roboi*	–	CASIZ 121275*	Rottnest Island, Australia	30	JQ727854	JQ727734
Goniobranchus rubrocornutus	A	CASIZ 203047	Batangas Province, Philippines	–	OL685225	OL684782
Goniobranchus rubrocornutus	B	CASIZ 208563	Oriental Mindoro Province, Philippines	18	OL685229	OL684783
Goniobranchus rufomaculatus	–	N/A*	–	–	EU512131	EU512057
Goniobranchus sinensis	A	CASIZ 176759	Pulau Tioman, Peninsular Malaysia	13	OL685214	OL684793
Goniobranchus sinensis	A	CASIZ 175727	Pulau Tioman, Peninsular Malaysia	13	OL685212	OL684792
Goniobranchus sinensis	A	CASIZ 189457	Pulau Tioman, Peninsular Malaysia	–	OL685218	OL684809
Goniobranchus sinensis	B	MISE–KS008–19	Okinawa, Japan	8	OL685232	OL684795
Goniobranchus sinensis	B	MISE–KS009–19	Okinawa, Japan	8	OL685233	OL684796
Goniobranchus sinensis	B	MISE–KS010–19	Okinawa, Japan	8	OL685234	OL684797
Goniobranchus sinensis	B	MISE–KS018–19	Okinawa, Japan	6	OL685235	OL684798
Goniobranchus sinensis	B	MISE–KS020–18	Okinawa, Japan	9	OL685236	OL684799
Goniobranchus sinensis	B	MISE–KS021–18	Okinawa, Japan	10	OL685237	OL684800
Goniobranchus sinensis	B	MISE–KS022–18	Okinawa, Japan	10	OL685238	OL684801
Goniobranchus sinensis	B	MISE–KS023–18	Okinawa, Japan	9	OL685239	OL684802
Goniobranchus sinensis	B	MISE–KS024–18	Okinawa, Japan	–	OL685240	OL684803
Goniobranchus sinensis	B	MISE–KS024–19	Okinawa, Japan	5	OL685241	OL684784
Goniobranchus sinensis	B	MISE–KS055–19	Okinawa, Japan	–	OL685245	OL684790
Goniobranchus sinensis	B	MISE–KS056–19	Okinawa, Japan	12	OL685246	OL684791
Goniobranchus sinensis	C	MISE–KS037–19	Kagoshima, Japan	–	OL685242	OL684788
Goniobranchus sinensis	C	MISE–KS039–19	Kagoshima, Japan	8	OL685243	OL684808
Goniobranchus sinensis	C	MISE–KS047–19	Kagoshima, Japan	–	OL685244	OL684789
Goniobranchus splendidus	–	CASIZ 146039*	Queensland, Australia	21	EU982738	EU982789
Goniobranchus splendidus	–	UQ 1102*	Queensland, Australia	–	MH018011	MH017998
Goniobranchus splendidus	–	SAM D19292*	Queensland, Australia	–	EF535115	AY458815
Goniobranchus tasmaniensis	–	UQ 892*	Tasmania, Australia	–	MH018007	MH017994
Goniobranchus tasmaniensis	–	SAM D19295*	Tasmania, Australia	–	EF535113	AY458817
Goniobranchus aff. *tinctorius*	–	WAM S71088*	Queensland, Australia	–	MH018010	MH017997
Goniobranchus aff. *tinctorius*	–	CASIZ 156921*	Batangas Province, Philippines	–	JQ727853	JQ727733
Goniobranchus aff. *tinctorius*	–	N/A*	Queensland, Australia	–	KJ001315	KJ018910
Goniobranchus aff. *tinctorius*	–	Gore 16Sa1*	North Sulawesi, Indonesia	6–9	MN339446	MN104719
Goniobranchus aff. *tinctorius*	–	Gore 16Sa2*	North Sulawesi, Indonesia	6–9	MN339447	MN104720
Goniobranchus verrieri	Unknown	CASIZ 158796*	Batangas Province, Philippines	–	JQ727858	JQ727740
Goniobranchus verrieri	A	CASIZ 203059	Batangas Province, Philippines	–	OL685231	OL684816
Goniobranchus verrieri	B	CASIZ 208442	Batangas Province, Philippines	3–30	OL685228	OL684812
Goniobranchus vibratus	–	CASIZ 175564*	Hawai'i, USA	–	JQ727859	JQ727741
Goniobranchus woodwardae	–	N/A*	–	–	EU512127	EU512103

16S was 560 base pairs. The COI amplification started with an initial denaturation of 94 °C for 3 mins; 39 cycles of denaturation at 94 °C for 30 s, annealing at 46 °C for 30 s, an extension at 72 °C for 60s, and then a final extension at 72 °C for 5 mins. The 16S amplification started with an initial denaturation of 94 °C for 3 mins; 39 cycles of denaturation at 94 °C for 30 s, annealing at 52 °C for 30 s, an extension at 72 °C for 60 s; and a final extension at 72 °C for 5 mins and 25 °C for 60 s. The amplification parameters were based on Johnson and Gosliner (2012). All PCR products that were successfully amplified were cleaned and purified using Exonuclease I – Shrimp Alkaline Phosphatase (ExoSAP) and they were either sequenced at the CCG or sent to FASMAC (Kanagawa, Japan) for sequencing in both directions.

Phylogenetic analyses

The sequences obtained were assembled, trimmed, and edited in Geneious v. 10.2.3 (Kearse et al. 2012). Publicly available COI and 16S GenBank sequences for *Goniobranchus* species were included in our dataset for analyses (Table 1). In total, 89 taxa were analyzed, and the alignment of sequences was done using MAFFT v. 7.450 (Katoh and Standley 2013) within Geneious. The alignments of each gene were trimmed to 569 and 476 base pairs, respectively, for COI and 16S. Thus, the concatenated dataset included 1,045 base pairs in total for 89 taxa.

Maximum likelihood (ML) and Bayesian inference (BI) were used to construct the phylogenetic trees among species for both markers as well as the concatenated data (COI+16S). The RAxML Next Generation (RAxML-NG) v. 1.0.2 (Kozlov et al. 2019) was used to run the ML analyses on our COI and 16S dataset using TIM1+I+G and TVM+I+G model respectively with 1000 bootstrap replications. MrBayes v. 3.2.6 (Huelsenbeck and Ronquist 2001) was used to perform the BI analyses on the same dataset using the HKY+I+G and GTR+G model for COI and 16S partitions, respectively. The best evolutionary models were determined using TOPALi (Milne et al. 2009). The Bayesian Markov chain Monte Carlo (MCMC) was run for 5×10^6 generations where chains were sampled every 200 generations. A standard 25% burn-in length was removed from the dataset, at which point the Average Standard Deviation of Split Frequency (ASDSF) was < 0.01.

Species delimitation

Automatic Barcode Gap Discovery (ABGD) (Puillandre et al. 2012) uses genetic pairwise differences to determine species-level clusters based on "barcode gaps". The ABGD analyses of our COI and 16S dataset were performed online (https://bioinfo.mnhn.fr/abi/public/abgd/abgdweb.html) and the following parameters were applied: P_{min} = 0.001, P_{max} = 0.1, Steps = 10, X = 1, and Nb bins = 20 using the Jukes-Cantor (JC69) model. The uncorrected pairwise p-distances for COI were also calculated in MEGA v. 6.06 (Tamura et al. 2013).

Morphology

Based on the ABGD analyses, selected representative specimens from each delimited species-level clade were morphologically examined. The specimens' rhinophores and gill structures were examined, as well as their reproductive systems and buccal masses. The morphologies of all specimens were also compared with all known species descriptions of *Goniobranchus* species with white mantles and various marginal bands.

The reproductive system and buccal mass for each specimen were dissected using a Nikon SMZ-U dissecting scope. The buccal mass was extracted and placed into a concentrated 10% sodium hydroxide solution for 24 hours. Connective tissues on the radula and jaw were carefully removed with the aid of a dissecting microscope. The jaw and radula were then rinsed with distilled water and mounted on a glass slide to dry. To view the radula and jaw under the scanning electron microscope, the radula and jaw were placed on a stub that was placed in a sputter coater (Cressington 108 Auto vacuum sputter coater) to cover the specimen with a thin layer of gold/palladium. For observation, we used a scanning electron microscope (Hitachi SU35), and the number and shape of the teeth were observed from the images.

The reproductive systems that were extracted from the specimens were hand drawn under a dissecting microscope (Nikon SMZ-U) with a camera lucida attached. The shape and size of the organs in the reproductive system were noted and illustrated.

Results

Phylogenetic and species delimitation analyses

A total of 35 new sequences was obtained for both COI and 16S genes (Table 1). The alignments of each gene were trimmed to 569 and 476 base pairs, respectively. Combined with sequences from GenBank, the concatenated dataset included 1,045 base pairs in total for 89 taxa. The ABGD analysis of the COI alignment recovered six species-level clades and the prior maximal distances, *P*, were stable from 0.0028 to 0.0046. The 16S dataset also recovered the same six species-level clades and the prior maximal distances, *P*, were stable from 0.0046 to 0.0077. The groups within the complex recovered were *G. albonares* (n = 4), *G. daphne* (n = 2), *G. verrieri* (n = 3), *G. preciosus* (n = 5), *G. rubrocornutus* (n = 2), *G. sinensis* (n = 18), and *G. fabulus* sp. nov. (n = 5), with interspecific *p*-COI distances ranging from 2.5–18.6% (Table 2).

In the concatenated COI+16S tree (Fig. 1), two monophyletic clades containing members of the white *Goniobranchus* with marginal bands group were recovered. The first clade, including specimens identified as *Goniobranchus albonares*, *G. collingwoodi*, *G. decorus*, *G. fidelis*, and *G. geminus*, was well-supported (0.98/-%, Bayes and ML, respectively) and its sister group, a clade which included specimens identified as *G. verrieri*, *G. rubrocornutus*, *G. preciosus*, *G. fabulus* sp. nov., *G. daphne*, and *G. sinensis* plus

Table 2. Interspecific and intraspecific range of distances among and within clades in percentages (%).

	Goniobranchus albonares	*Goniobranchus preciosus*	*Goniobranchus rubrocornutus*	*Goniobranchus sinensis*	*Goniobranchus verrieri*	*Goniobranchus fabulus* sp. nov.	*Goniobranchus daphne*
Goniobranchus albonares	1.1–5.2	–	–	–	–	–	–
Goniobranchus preciosus	15.5–18.6	0.4–2.7	–	–	–	–	–
Goniobranchus rubrocornutus	14.8–16.1	9.9–10.8	0.0	–	–	–	–
Goniobranchus sinensis	14.3–16.6	7.1–9.8	9.6–11.2	0.0–1.4	–	–	–
Goniobranchus verrieri	16.0–18.2	10.8–12.6	10.7–11.8	10.0–12.1	1.3–3.7	–	–
Goniobranchus fabulus sp. nov.	14.0–18.2	6.8–9.2	7.8–9.3	6.3–8.6	10.1–12.0	0.2–3.4	–
Goniobranchus daphne	15.3–17.5	7.4–7.9	8.9–9.0	6.7–8.5	10.8–11.4	2.5–4.5	0.5

G. albopustulosus, *G epicurius*, *G. heatherae*, *G. hunterae*, *G. rufomaculatus*, *G. splendidus*, *G. tasmaniensis*, *G.* aff. *tinctorius*, as well as *G. woodwardae* had moderate support (1/48%). The "white body and variously colored marginal bands" species formed a monophyletic group with the exception of *G. albonares*, which was closely related to *G. fidelis* that is not a "white body and variously colored marginal bands" species. However, *G. verrieri*, *G. rubrocornutus*, *G. preciosus*, *G. fabulus* sp. nov., *G. daphne*, and *G. sinensis*, which are all part of the group in question, formed a well-supported monophyletic clade (1/98%). The clade of *G. albonares* specimens was strongly supported (1/100%) and was sister to a clade of *G. collingwoodi*, *G. decorus*, *G. fidelis*, and *G. geminus*. The second main clade contained members of the white *Goniobranchus* with marginal bands group and also contained *G. albopustulosus*, *G epicurius*, *G. heatherae*, *G. hunterae*, *G. rufomaculatus*, *G. splendidus*, *G. tasmaniensis*, and *G.* aff. *tinctorius* as well as *G. woodwardae* with moderate support (1/48%). However, none of these other members of this second clade have a series of marginal bands. Within the well-supported monophyletic white *Goniobranchus* with marginal bands group subclade (1/98%), *G. verrieri* (1/89%) was sister to *G. rubrocornutus*, *G. preciosus*, *G. fabulus* sp. nov., *G. daphne*, and *G. sinensis*. A well-supported *G. preciosus* (1/83%) was sister to *G. fabulus* sp. nov., *G. daphne*, and *G. sinensis*. A well-supported subclade containing *G. fabulus* sp. nov. and *G. daphne* (1/99%) formed a sister clade to a well-supported *G. sinensis* subclade (1/100%). Additionally, there were no color morphs of any species observed that mimicked the coloration patterns of another species. This is the opposite of what has been seen in other groups of chromodorid nudibranchs, for example in *Chromodoris* (Layton et al. 2018, 2020). The confusion between the species studied here is due to a misperception regarding the morphological attributes of each species and concerning what color patterns hold constant across a species.

Morphological analyses

The species recovered from the phylogenetic and ABGD analyses are shown in Figure 1, whereas morphotypes are shown in Figures 2–4. Most of the species in this study demonstrated high levels of morphological variation. Each of *G. rubrocornutus*, *G. preciosus*, *G. fabulus* sp. nov., *G. verrieri*, and *G. sinensis* showed at

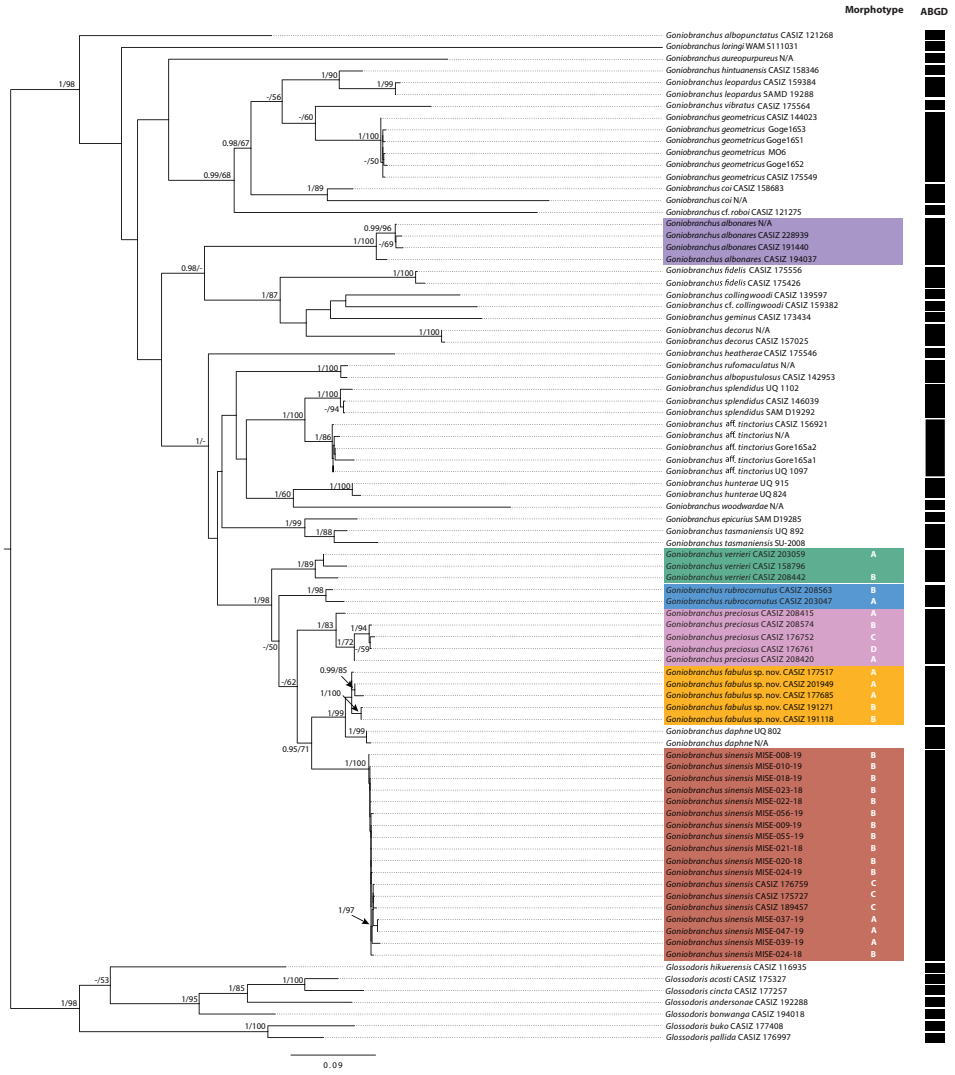

Figure 1. Molecular phylogeny based on the combined dataset (COI+16S rDNA) inferred by maximum likelihood (ML) and Bayesian inference (BI). Numbers on nodes represent Bayesian posterior probabilities (> 0.95) / ML bootstrap values (only > 50% values are shown). Black bars indicate the clade groupings of ABGD analysis on the COI + 16S dataset.

least two distinct morphotypes that had no significant genetic differences between morphotypes (Table 2).

In terms of jaw and radular morphology, all specimens had bifid rodlets and one distinctive rachidian tooth except for *G. rubrocornutus*, which is shown to have a very thin rachidian tooth that can easily pass unnoticed (Fig. 10d). In some species, while external morphology was variable, aspects of the external color pattern, radular morphology, and their reproductive anatomy exhibited clear and distinct differences, which are detailed in the following systematics section.

Systematics

Family Chromodorididae Bergh, 1891

Genus *Goniobranchus* Pease, 1866

Type species. *Doris vibrata* Pease, 1860 = *Goniobranchus vibratus* (Pease, 1860) by monotypy. Type locality: Hawai'i.

Goniobranchus albonares (Rudman, 1990)

Figures 2a, b, 5a, b, 7a–f

Chromodoris albonares Rudman, 1990: 100, 307–309, figs 26E, 35, 36; Gosliner et al. 2008: 220, second photograph from the top.

Goniobranchus albonares: Gosliner et al. 2015: 223, lower left photograph; Gosliner et al. 2018: 153, lower left photograph.

Type locality. New South Wales, Australia.

Type material. AM C156989, one specimen, west side of Northwest Solitary Island, 30.017°S, 156.267°E, Coffs Harbour, New South Wales, Australia, 6 m depth, 4 December 1988, J. & J. England, P. Edwards. Not examined in this study due to the original descriptions in Rudman (1990) being comprehensive.

Geographical distribution. Widely distributed around the tropical and subtropical Indo-Pacific Ocean (Debelius and Kuiter 2007; Gosliner 2008, 2015, 2018), Mozambique (Tibiriçá et al. 2017; Strömvoll and Jones 2019), Indonesia (Debelius and Kuiter 2007), Japan (Nakano 2018; Ono and Katou 2020), Taiwan (Jie et al. 2009), Australia (Rudman 1990), Madagascar, Philippines, Papua New Guinea (present study), New Caledonia (Hervé 2010), and Gulf of Oman (Fatemi and Attaran-Fariman 2015).

Material examined. CASIZ 228939, one specimen (2 mm preserved), subsampled for molecular data and dissected, Murals dive site, 13.688°N, 120.866°E, Maricaban Strait, Mabini (Calumpan Peninsula), Batangas Province, Luzon, Philippines, 9–22 m depth, 29 November 2018, T.M. Gosliner, 2018 Verde Island Passage Expedition. CASIZ 191440, one specimen (3 mm preserved), subsampled for molecular data, Madang Province, GPS not available, Papua New Guinea, depth not available, 26 November 2012, V. Knutson, Papua New Guinea Biodiversity Expedition 2012. CASIZ 194037, one specimen (2 mm preserved), subsampled for molecular data, Pointe Evatra, rocky bottom with areas of sand, 24.983°S, 47.083°E, South Madagascar, Madagascar, 22 m depth, 30 April 2010, *Atimo Vatae* South Madagascar Expedition.

Description. *External morphology*. Living animals 5–7 mm in length. Body opaque white, oval and elongated, with the outermost portion of the mantle edge having an orange band that gradually blends into a yellow submarginal band. Gill and rhinophores are translucent white with opaque white edges on the lamellae. Six or seven

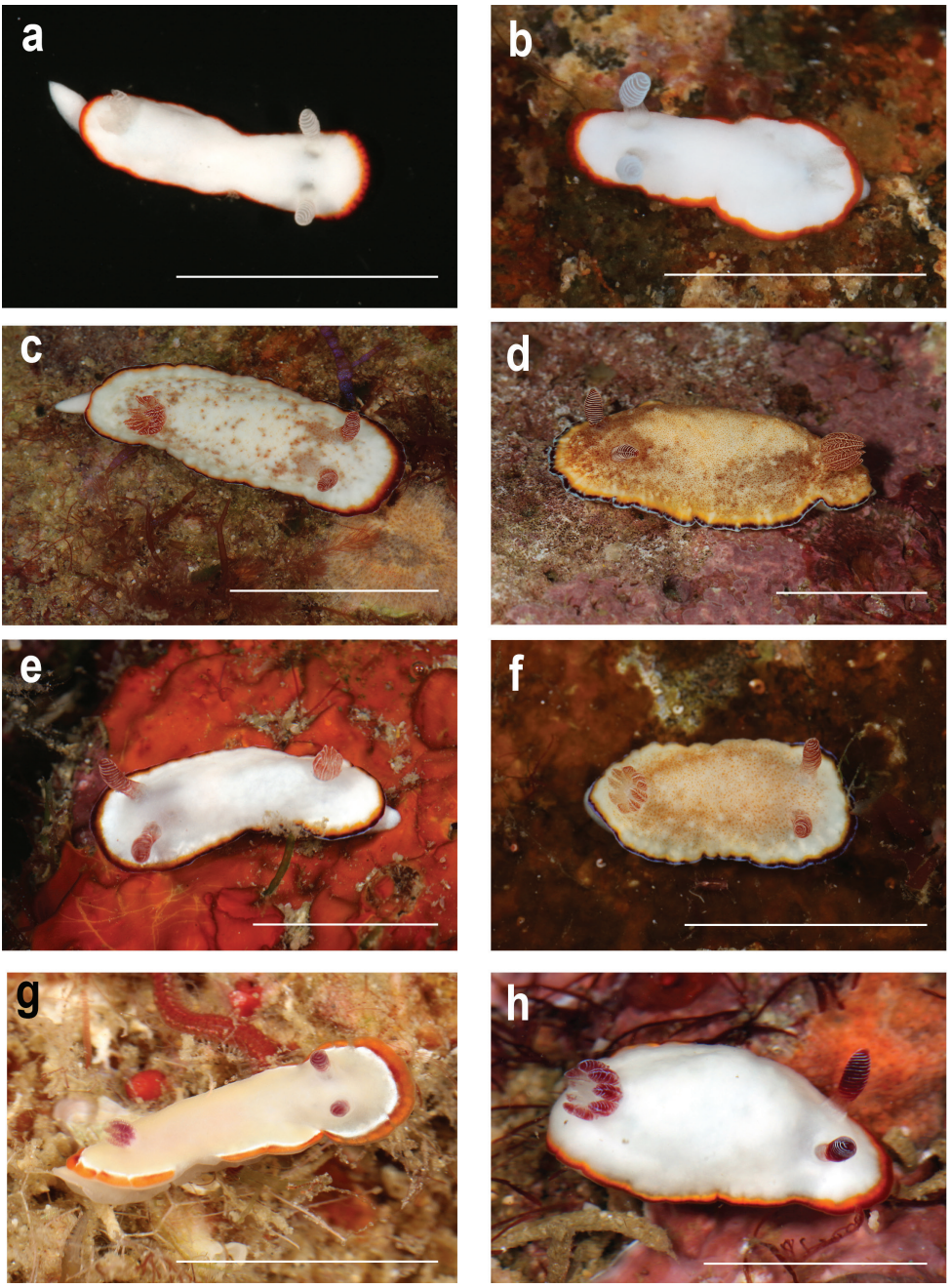

Figure 2. a, b *Goniobranchus albonares* **a** CASIZ 191440, Papua New Guinea **b** CASIZ 228939, Philippines **c–f** *Goniobranchus preciosus* **c** CASIZ 208415, Morphotype A, Philippines **d** CASIZ 208574, Morphotype B, Philippines **e** CASIZ 176752, Morphotype C, Peninsular Malaysia **f** CASIZ 176761, Morphotype D, Peninsular Malaysia **g, h** *Goniobranchus rubrocornutus* **g** CASIZ 203047, Morphotype A, Philippines **h** CASIZ 208563, Morphotype B, Philippines. Photographs TMG. Scale bars: 1 cm.

unipinnate gill branches are moderately spreading when fully extended. Rhinophores are relatively large, ~ 2× as long as the gill branches. Ten or eleven lamellae per rhinophore.

Buccal mass and radula. The muscular portion of the buccal mass ~ 2/3 the size of the oral tube length (Fig. 5a). The chitinous labial cuticle found at the anterior end of the muscular portion of the buccal mass bears bifurcated and short jaw rodlets (Fig. 7a, b). The radular formula of CASIZ 228939 is 37 × 19.1.19 (Fig. 7c). The rachidian tooth is triangular and short. The inner and outer surfaces of the inner lateral teeth have three denticles on each side of the central cusp (Fig. 7d). The central cusp on the inner lateral tooth is ~ 2× the length of the adjacent denticles. The middle lateral teeth have a short central cusp with three or four denticles (Fig. 7e). The outer lateral teeth have a rounded main cusp with three or four denticles (Fig. 7f).

Reproductive system (Fig. 5b). The long, thick, tubular ampulla narrows into a diverging short oviduct and short vas deferens. The proximal prostatic portion of the vas deferens transitions into the muscular ejaculatory portion. The ejaculatory portion narrows and elongates into a wider, long, curved penial bulb that joins with the narrow distal end of the vagina. The vagina is elongate and narrow, joining the larger, spherical bursa copulatrix and the smaller, curved receptaculum seminis at its distal end. A moderately short uterine duct emerges from the receptaculum seminis, which is adjacent to the vagina, and enters into the female gland mass. The female gland mass has small albumen and membrane glands and a large mucous gland.

Remarks. *Goniobranchus albonares* was described by Rudman (1990) from New South Wales, Australia; he described the animal as having an elongate, ovate, opaque white mantle with a bright orange band on the edge of the mantle with the inside edge of the orange band being irregular. The rhinophores and gill branches were translucent white with opaque white edges, which is a distinctive feature of this species. Also, the notum was described as smooth, ringed by an orange marginal band and a yellow submarginal band. This morphological description matches well with the *G. albonares* specimens in this study, which are quite uniform in color pattern. The vas deferens in *G. albonares* is also shorter in comparison to that of all the other white *Goniobranchus* with marginal bands species included in this study. The phylogenetic tree also showed a fully supported (1/100%) monophyly for specimens (n = 4) of this species (intraspecific distance within *G. albonares* = 1.1–5.2%; Table 2).

Goniobranchus albonares was included in this study together with all other white *Goniobranchus* with marginal bands based on Gosliner et al. (2018). However, in our concatenated phylogenetic tree, *G. albonares* is a sister clade to *G. collingwoodi*, *G. decorus*, *G. fidelis*, and *G. geminus*, and is genetically comparatively distant from the remainder of the white *Goniobranchus* species with marginal bands examined in this study (interspecific *p*-COI distances between *G. albonares* and *G. verrieri* = 16.0–18.2%; see Table 2). This suggests a case of convergent evolution of having a white body with marginal bands. Little is known about how predators perceive the color of the nudibranchs (as prey), which may provide clues to factors driving this remarkable similarity.

***Goniobranchus preciosus* (Kelaart, 1858)**
Figures 2c–f, 5c, d, 8a–f

Doris preciosa Kelaart, 1858: 98; 1883: 89.
Chromodoris preciosa: Eliot 1906: 642–643, pl. XLII, fig. 3; Eliot 1909: 92–93; Gosliner et al. 2008: 219, lower left and lower right photographs.
Goniobranchus preciosus: Gosliner et al. 2015: 222, lower left and lower right photographs; Gosliner et al. 2018: 152, lower left and lower right photographs.

Type locality. Sri Lanka (as Ceylon), Indian Ocean.

Type material. Most likely lost to science. Eliot (1906) refers to a few of Kelaart's specimens being present in the collections of the Hancock Museum (now the Great North Museum) and that many of these specimens are useless for taxonomy. A search of the collections online indicates that no specimens of *Doris preciosa* are currently held in their collection. We made comparisons to Kelaart's original drawings and description (Kelaart, 1858), as well as to updates by Eliot (1906, 1909) and Rudman (1985).

Geographical distribution. Widely distributed around the tropical and subtropical Indo-Pacific oceans (Rudman 1985; Debelius and Kuiter 2007; Coleman 2008; Gosliner et al. 2008, 2015, 2018) with specific reports from Sri Lanka (Kelaart 1858), west coast of India and the Andaman Islands (Kumar et al. 2019), Thailand (Mehrotra et al. 2021), Philippines, Indonesia, Malaysia (Gosliner et al. 2008), and Japan (Nakano 2018; Ono and Katou 2020). Records cited by Gosliner et al. (2008) from New Caledonia, Tonga, Fiji, Vanuatu, and Australia are of *Goniobranchus fabulus* sp. nov., not *G. preciosus*.

Material examined. CASIZ 208420 (morphotype A), one specimen (10 mm preserved), subsampled for molecular data, sand slope with reef, 13.522°N, 120.947°E, Manila Channel, Puerto Galera, Oriental Mindoro Province, Mindoro, Philippines, 4–22 m depth, 11 April 2015, T.M. Gosliner 2015 Verde Island Passage Expedition. CASIZ 208415 (morphotype A), one specimen (9 mm preserved), subsampled for molecular data and dissected, School Beach, 13.517°N, 120.950°E, Batangas Channel, Puerto Galera, Oriental Mindoro Province, Mindoro, Philippines, 18 m depth, 10 April 2015, T.M. Gosliner 2015 Verde Island Passage Expedition. CASIZ 208574 (morphotype B), one specimen (11 mm preserved), subsampled for molecular data and dissected, School Beach, 13.516°N, 120.950°E, Batangas Channel, Puerto Galera, Oriental Mindoro Province, Mindoro, Philippines, 6–17 m depth, 8 April 2015, T.M. Gosliner 2015 Verde Island Passage Expedition. CASIZ 176752 (morphotype C), one specimen (10 mm preserved), subsampled for molecular data, Pulau Gut, 2.664°N, 104.167°E, Pulau Tioman, South China Sea, Peninsular Malaysia, 13 m depth, 4 October 2007, T.M. Gosliner. CASIZ 176761 (morphotype D), one specimen (9 mm preserved), subsampled for molecular data, Tiger Point, 2.889°N, 104.061°E, Pulau Tioman, South China Sea, Peninsular Malaysia, 17–19 m depth, 2 October 2007, T.M. Gosliner.

Description. ***External morphology.*** Living animal approximately 15 mm in length. Body white, with low tubercles on the notum; oval and elongated, with three marginal bands on the mantle edge. There is an outermost blue band followed by a deep red submarginal band and a yellow inner submarginal band. Brownish or orange dorsal spotting may be present over the surface of the mantle. In all cases the rhinophores are translucent reddish brown with white edges on the lamellae. The same pigment extends below the rhinophore club onto the stalks of the rhinophores. Rhinophore lamellae number 12–17. Gill branches reddish brown with white lines on the rachis. Nine or ten unipinnate gill branches held erectly when the gill is fully extended. This species exhibits four distinct morphotypes in addition to the unvarying elements described above. Morphotype A (Fig. 2c) has a translucent creamy white body with fine orange spots and blotches on the notum. The outermost portion of the mantle edge is surrounded by a thin opaque bluish white band, followed by a thicker deep red band and then a yellow-orange submarginal band. Gill and rhinophores are translucent red with white edges. Morphotype B (Fig. 2d) has a translucent pale yellow body with brown spots and blotches on the notum. The outermost portion of the mantle edge is surrounded by an opaque bluish white tinged band, followed by an irregular deep red and a yellow-orange submarginal band, with all three bands having similar widths. The gill and rhinophores are translucent brown with opaque cream edges. Morphotype C (Fig. 2e) has an opaque white body with a few low tubercles. The outermost portion of the mantle edge is surrounded by a thin, opaque, bluish white band, followed by thicker deep red and yellow-orange bands. The gill and rhinophores are translucent red with opaque white edges. Morphotype D (Fig. 2f) has a creamy white translucent body with densely speckled orange spots on the notum. The outermost portion of the mantle edge is surrounded by a thin opaque bluish white tinged band, followed by irregular deep red and yellow-orange bands, all three bands having similar widths. The gill and rhinophores are translucent red with opaque white edges.

Buccal mass and radula (morphotype B). The muscular portion of the buccal mass is ~ 2× the size of the oral tube length (Fig. 5c). The chitinous labial cuticle is found at the anterior end of the muscular portion of the buccal mass, bearing long, bifurcated jaw rodlets (Fig. 8a, b). The radular formula of CASIZ 208574 is 54 × 47.1.47 (Fig. 8c). The rachidian tooth has a flame-like shape and is blunt at the tips. The inner and outer surfaces of the inner lateral teeth have three or four denticles on each side of the central cusp (Fig. 8d). The central cusp on the inner lateral tooth is ~ 2× the length of the adjacent denticles. The middle lateral teeth have a long central cusp with 5–8 denticles (Fig. 8e). The outer lateral teeth are rounded and paddle-shaped with six or seven denticles (Fig. 8f).

Reproductive system (Fig. 5d). The thick, tubular ampulla narrows into a diverging short oviduct and long vas deferens. The proximal prostatic portion of the vas deferens is narrow and convoluted, then transitions into an equally thin muscular ejaculatory portion. The narrow ejaculatory portion elongates into a wider section and again narrows prior to entering the short penial bulb, which joins with the distal end of the vagina. The vagina is short and moderately wide. It terminates at the junction of the

large, spherical bursa copulatrix, the curved, pyriform receptaculum seminis, and the uterine duct. The long narrow uterine duct emerges from junction of the vagina, bursa copulatrix, and the receptaculum seminis and enters into the female gland mass. The female gland mass has small albumen and membrane glands and a large mucous gland.

Remarks. Rudman (1985) redescribed specimens of *G. preciosus* from New Caledonia based on the description by Kelaart (1858) and the illustration in Eliot (1906) from Sri Lanka (as Ceylon). Rudman stated that Eliot's (1906) reproduction of Kelaart's drawing of *Doris preciosa* did not match the original description of *G. preciosus* by Kelaart (1858). However, Kelaart's written description and the reproduction of his drawing by Eliot (1906) clearly match the three main morphotypes of *G. preciosus* found in this study. Additionally, Eliot (1909) reported on another *G. preciosus* specimen collected by Willey in Sri Lanka that had a few obscure spots on its notum, but Eliot's notes did not mention any light bluish tinge on the outermost mantle edge. Rudman (1985) doubted that Eliot's (1909) specimen was the real *G. preciosus* due to these few obscure spots and the absence of a light bluish margin. Hence, Rudman (1985) considered his specimen from New Caledonia as *G. preciosus* based on the descriptions from both Kelaart and Eliot. However, Rudman's specimen lacks the dense red spotting described by Kelaart, but illustrated by Eliot, and that is present in the specimens studied here. Eliot's illustration matches *G. preciosus* morphotype A found in this study. Based on the phylogenetic data in this study, the morphotype that matches Kelaart's description (morphotype D; Fig. 2f) and the morphotype that matched Rudman's description (*G. fabulus* sp. nov.; Fig. 4a–c) are clearly distinct from each other. This distinction, as well as the fact that the species that Rudman identified as *G. preciosus* is not found in the Indian Ocean and appears to be restricted to the Western and Central Pacific, suggest separate species and Rudman's *G. preciosus* is herein described as G. *fabulus* sp. nov. These species have been frequently confused and often considered as a single species (e.g., Gosliner et al. 2018), but there are clear morphological distinctions as found in this study. In *G. preciosus*, the mantle always has some low tubercles, whereas the notum is smooth in *G. fabulus*. The gill branches of *G. preciosus* are more erect than those of *G. fabulus*. The gill and rhinophores of *G. precious* are reddish brown, whereas they are reddish purple in *G. fabulus*. In *G. precious* the club and stalk of the rhinophores have reddish pigment whereas in *G. fabulus* only the rhinophore club is pigmented and the stalk is the same white as the body. The two species overlap in the Philippines (present study), but *G. preciosus* is found north and westwards from the Philippines and *G. fabulus* is found to the south and eastwards from there.

Goniobranchus preciosus was recovered as a distinct species in the phylogenetic and ABGD analyses and was sister to a clade containing *G. daphne* (interspecific *p*-COI distances between *G. preciosus* and *G. daphne* = 7.4–7.9%; Table 2), *Goniobranchus fabulus* sp. nov. (interspecific *p*-COI distances between *G. preciosus* and *G. fabulus* sp. nov. = 6.8–9.2%; Table 2), and *G. sinensis* (interspecific *p*-COI distances between *G. preciosus* and *G. sinensis*.= 7.1–9.8%; Table 2). *Goniobranchus preciosus* has a high level of intraspecific morphological diversity with the presence of four morphotypes

confirmed in this study and yet showed little genetic difference (intraspecific distance within *G. preciosus* = 0.4–2.7%; Table 2). These four morphotypes have very close external morphological similarities with *G. verrieri* morphotype B and *G. sinensis*, with all of them having three marginal bands on the mantle edge and with *G. verrieri* morphotype B and some morphotypes of *G. sinensis* having spots and patches on the notum. However, *G. verrieri* morphotype B has a greatly reduced outer white band compared to the much wider bluish bands of *G. preciosus* and *G. sinensis*. Only very subtle external morphological differences separate *G. preciosus* from the other species in this study. *Goniobranchus preciosus* morphotype A has a deeper red submarginal band while *G. verrieri* morphotype B has a paler red submarginal band. *Goniobranchus preciosus* morphotype B has a pale yellow body coloration that was not observed in any other specimens in this study. *Goniobranchus preciosus* morphotype C is very similar to *G. fabulus* morphotype A and *G. sinensis* morphotype C; however, the gill and rhinophore colors are not the same: *G. preciosus* has translucent red rhinophores and gills with opaque white edges, *G. fabulus* morphotype A has reddish purple rhinophores and gills with opaque white edges, and *G. sinensis* morphotype C has translucent red rhinophores and gills with opaque reddish purple edges. *Goniobranchus preciosus* morphotype D has densely speckled orange spots on the notum and an opaque bluish white tinged band on the mantle edge and this character combination was not observed in any other specimens in this study. *Goniobranchus preciosus* morphotype D also most closely matched the original external morphology of *G. preciosus* as described by Kelaart (1858).

With regards to internal morphology, *G. preciosus* and *G. sinensis* each have a flame-shaped rachidian tooth, but differ in their external colors and morphologies. *Goniobranchus preciosus* has a tuberculate body texture, whereas *G. sinensis* has a smooth notum. The rhinophores of *G. preciosus* are reddish brown and have spots of the same color extending onto the rhinophoral stalk. In *G. sinensis*, the rhinophores have reddish purple edges along the lamellae of the club and solid reddish purple rather than scattered spots extending onto the rhinophore stalk. Both species have three marginal bands which are similar in color but in *G. preciosus* the innermost band is more yellow-orange whereas it is more yellow *in G. sinensis*. These differences in color are subtle but appear to be consistent in the specimens studied here.

The high morphological diversity of *G. preciosus* suggests two different forms of morphological adaptations. *Goniobranchus preciosus* had different color patterns within the same locality, with two different morphotypes occurring both in the Philippines and in Peninsular Malaysia. At the same time, from a regional perspective, *G. preciosus* had color patterns specific to each locality. This is not the first time such a situation has been observed in nudibranchs, as previous studies have demonstrated a form of mimicry in chromodorid nudibranchs resulting in certain chromodorid species displaying morphological variation within a locality as well as individuals with same color pattern within the same locality turning out to be different species (Padula et al. 2016; Layton et al. 2018, 2020).

***Goniobranchus rubrocornutus* (Rudman, 1985)**
Figures 2g, h, 5e, f, 9a–f

Glossodoris marginata (Pease, 1860): Baba 1938: 11–12 (misidentification).
Chromodoris rubrocornuta Rudman, 1985: 83, 283–286, figs 12F, 20A, 25, 26A; Gosliner et al. 2008: 221, bottom photograph.
Goniobranchus rubrocornutus: Gosliner et al. 2015: 224, middle right photograph; Gosliner et al. 2018: 154, middle right photograph.
Goniobranchus cf. *albonares* (Rudman, 1985): Mehrotra et al. 2021: 104, fig. 9l (misidentification).

Type locality. Hong Kong.

Type material. AM C138518, one specimen, Flynn Point, 22.467°N, 114.333°E, Hoi Ha, Hong Kong, China, depth not available, 18 April 1983, collector not available. Not examined in this study due to the original description in Rudman (1985) being sufficient for comparisons.

Geographical distribution. Widely distributed around the tropical and subtropical Indo-Pacific oceans (Debelius and Kuiter 2007; Gosliner et al. 2008, 2015, 2018; Rudman 1985) with reports from Thailand (Mehrotra et al. 2021), Malaysia, Philippines, Hong Kong, Palau, American Samoa, Marshall Islands (Gosliner et al. 2008), Japan (Nakano 2018; Ono and Katou 2020), Australia (Rudman 1985), New Caledonia (Hervé 2010), and the Marianas Islands (Carlson and Hoff 2003).

Material examined. CASIZ 203047 (morphotype A), one specimen (4 mm preserved), subsampled for molecular data and dissected, Verde Island Passage coast, 13.917°N, 120.617°E, Calatagan, Batangas Province, Luzon, Philippines, depth not available, 9 May 2014, T.M. Gosliner, 2014 Verde Island Passage Expedition. CASIZ 181235 (morphotype A), one specimen (4 mm preserved), dissected, Twin Rocks, 13.683°N, 120.883°E, Maricaban Strait, Mabini (Calumpan Peninsula), Batangas Province, Luzon, Philippines, depth not available, 22 May 2009, P. Paleracio, CAS Philippines Expedition May 2009. CASIZ 208563 (morphotype B), one specimen (3 mm preserved), subsampled for molecular data, School Beach, 13.516°N, 120.95°E, Batangas Channel, Puerto Galera, Oriental Mindoro Province, Mindoro, Philippines, 6–18 m depth, 13 April 2015, T.M. Gosliner, 2015 Verde Island Passage Expedition.

Description. ***External morphology.*** Length of living animal 7–14mm. Body oval and elongated, with two marginal bands on the mantle edge. Six to nine unipinnate gill branches, 8–14 lamellae on rhinophores. The color patterns of this species can be divided into two distinct morphotypes. Morphotype A (Fig. 2g) has a translucent creamy white body. The outermost portion of the mantle edge is surrounded by an orange band, followed by an irregular red band, followed by another irregular opaque white band. Gill branches and rhinophores are translucent, deep red with either red or white edges. Morphotype B (Fig. 2h) has an opaque white body. The outermost portion of the mantle edge is surrounded by a red band, followed by a yellow submarginal

band and both bands have similar widths. The gill and rhinophores are translucent deep red with bluish white tinged edges.

Buccal mass and radula. The muscular portion of the buccal mass approximately the same size as the oral tube length (Fig. 5e). The chitinous labial cuticle is found at the anterior end of the muscular portion of the buccal mass and bears bifurcated and short jaw rodlets (Fig. 9a, b). The radular formula of CASIZ 181235 is 39 × 27.1.27 (Fig. 9c). The rachidian tooth is thin and linear. The inner and outer surface of the inner lateral teeth have two or three denticles on each side of the central cusp (Fig. 9d). The central cusp on the inner lateral tooth is ~ 2× the length of the adjacent denticles. The middle lateral teeth have a short central cusp with 5–7 denticles (Fig. 9e). The outer lateral teeth have a rounded main cusp with 3–5 denticles (Fig. 9f).

Reproductive system (Fig. 5f). The thick, tubular ampulla narrows into a diverging short oviduct and long vas deferens. The proximal prostatic portion of the vas deferensis thin and convoluted and transitions into the muscular ejaculatory portion. The long, narrow, convoluted ejaculatory portion transitions into a wider, long penial bulb, which joins with the distal end of the vagina. The vagina is proximally narrow and elongated, transitions into a larger, spherical bursa copulatrix and large receptaculum seminis at its distal end. A moderately long uterine duct emerges from this junction of vagina, bursa copulatrix, and receptaculum seminis. The uterine duct connects the receptaculum seminis with the female gland mass. The female gland mass has smaller albumen and membrane glands and a larger mucous gland.

Remarks. In this study, *G. rubrocornutus* morphotype A matched with Rudman's (1985) *G. rubrocornutus* from Hong Kong: a creamy white translucent body with the outermost portion of the mantle edge surrounded by an orange band, followed by an irregular red band and an irregular opaque white band. The gill branches and rhinophores were translucent deep red with either red or white edges. *Goniobranchus rubrocornutus* morphotype B only has two marginal bands with the outermost red band followed by a yellow submarginal band, and this pattern does not match with Rudman's description of *G. rubrocornutus*. In this case the inner white submarginal band may simply be masked by the opaque white body color of morphotype B rather than the cream body color of morphotype A. However, in our phylogenetic and species delimitation analyses, *G. rubrocornutus* morphotype B was clustered together with morphotype A and both morphotypes did not show any genetic differences (uncorrected pairwise distance = 0.0%). Thus, morphotype B very likely represents a different color variation of *G. rubrocornutus*. Recently, molecular work has revealed the presence of mimicry adaptation in chromodorid nudibranchs (e.g., Padula et al. 2016; Layton et al. 2018). Sympatric specimens of chromodorid nudibranchs with different color patterns were found to be the same species (Layton et al. 2018), and this is also the case with our *G. rubrocornutus* morphotypes, where both morphotypes are sympatric. In this case, these variations are not likely different cases of mimicry, but simply color variants. Despite the variations observed here, few records of this species have been misidentified, with the exception of Mehrotra et al. (2021), where *G. rubrocornutus* was identified as *G.* cf. *albonares*. The specimen illustrated clearly has red rhinophores with white edging rather than white rhinophores and the orange, red, and opaque white marginal and submarginal bands that are characteristic of *G. rubrocornutus*.

***Goniobranchus sinensis* (Rudman, 1985)**
Figures 3a–d, 6a, b, 10a–f

Glossodoris marginata (Pease, 1860): Baba 1938: 11–12, fig. 8; Abe 1964: 47, pl. 21, fig. 74; Lin and Tchang 1965: 10, pl. 1, fig. 11 (misidentifications).
Chromodoris marginata (Pease, 1860): Orr 1981: 27 (misidentification)
Chromodoris sinensis Rudman, 1985: 83, 272–275, figs 12C, 13C, 14C, 15C, 18, 19; Gosliner et al. 2008: 219, bottom photograph.
Goniobranchus sinensis: Gosliner et al. 2015: 223, middle left photograph; Gosliner et al. 2018: 153, middle left photograph.

Type locality. Hong Kong.

Type material. AM C139295, one specimen, Fan Tsang Chau Island, 22.367°N, 114.400°E, Hong Kong, China, 10 m depth, 11 August 1983. Type material not examined due to high level of detailed work provided by the original description in Rudman (1985).

Geographical distribution. This species appears to be restricted to areas of the southeast Asian mainland and the islands of Japan, Taiwan, and islands off eastern Peninsular Malaysia (Debelius and Kuiter 2007; Coleman 2008; Gosliner et al. 2008, 2015, 2018) with reports from the Andaman Islands (Kumar et al. 2019), the east coast of Thailand (Mehrotra et al. 2021), the east coast of Peninsular Malaysia (present study), Japan (Nakano 2018; Ono and Katou 2020), Taiwan (Jie et al. 2009), Hong Kong (Rudman 1985), and the Gulf of Oman (Fatemi and Attaran-Fariman 2015).

Material examined. MISE-047-19 (morphotype A), one specimen, subsampled for molecular data and dissected, 31.281°N, 130.203°E, Kagoshima, Japan, 10 m depth, 14 July 2019, A. Tsuyuki. MISE-037-19 (morphotype A), one specimen, subsampled for molecular data, Sakurajima Evacuation Port Number 4, 31.552°N, 130.632°E, Kagoshima, Japan, 10 m depth, 10 July 2019, H. Kise. MISE-039-19 (morphotype A), one specimen, subsampled for molecular data, east side of Okiko-jima, 31.544°N, 130.617°E, Kagoshima, Japan, 8 m depth, 12 July 2019, G.Y. Soong. MISE-010-19 (morphotype B), one specimen, subsampled for molecular data and dissected, Tengan, 26.400°N, 127.833°E, Okinawa-jima Island, Japan, 8 m depth, 3 May 2019, G.Y. Soong. MISE-056-19 (morphotype B), one specimen, subsampled for molecular data, Tengan, 26.400°N, 127.833°E, Okinawa-jima Island, Japan, 12 m depth, 27 October 2019, G.Y. Soong. MISE-024-18 (morphotype B), one specimen, subsampled for molecular data, Tengan, 26.400°N, 127.833°E, Okinawa-jima Island, Japan, 7 m depth, 12 April 2018, G.Y. Soong. MISE-024-19 (morphotype B), one specimen, subsampled for molecular data, Tengan, 26.400°N, 127.833°E, Okinawa-jima Island, Japan, 5 m depth, 16 June 2019, Y. Kushida. MISE-009-19 (morphotype B), one specimen, subsampled for molecular data, Tengan, 26.400°N, 127.833°E, Okinawa-jima Island, Japan, 8 m depth, 3 May 2019, G.Y. Soong. MISE-055-19 (morphotype B), one specimen, subsampled for molecular data, Tengan, 26.400°N, 127.833°E, Okinawa-jima Island, Japan, 8 m depth, 27 October 2019, H. Kise. MISE-020-18 (morphotype B), one specimen, subsampled for molecular data, Tengan, 26.400°N, 127.833°E, Okinawa-jima Island, Japan, 9 m depth, 12 April 2018, G.Y. Soong. MISE-010-19 (morphotype

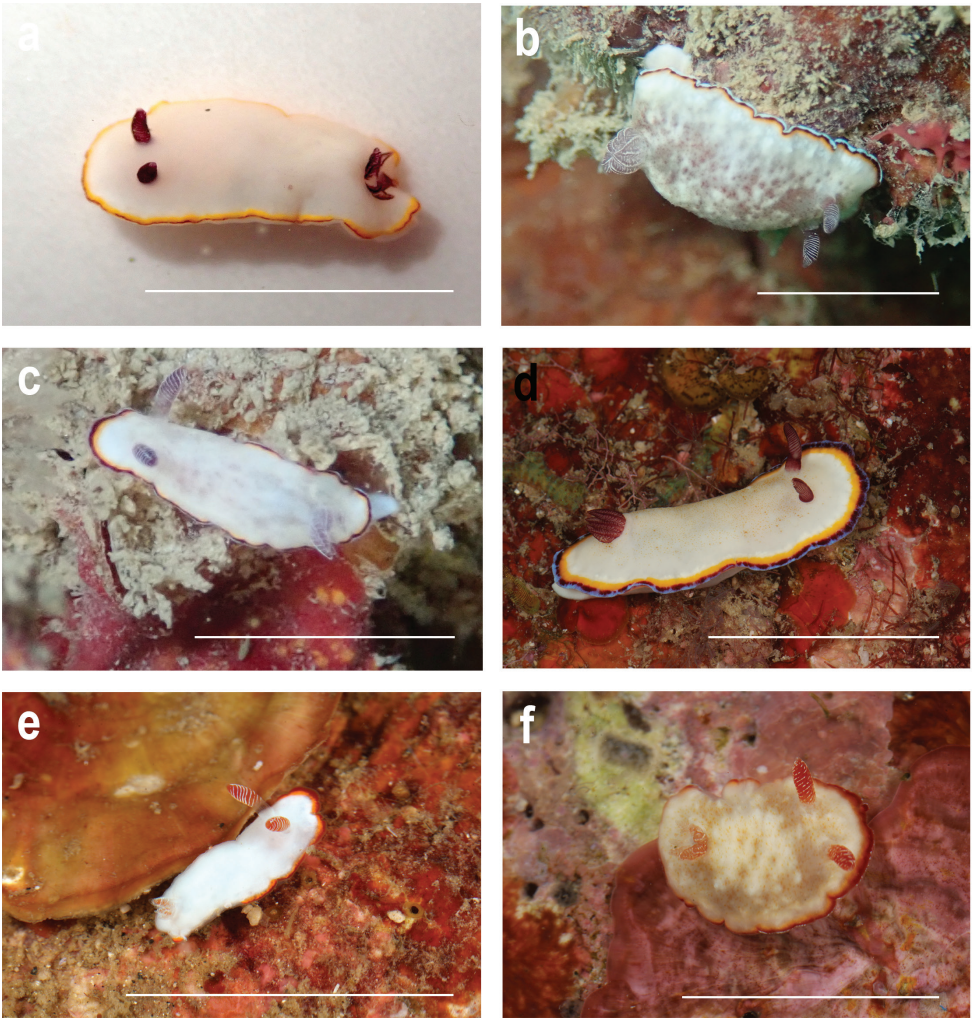

Figure 3. a–d *Goniobranchus sinensis* **a** CASIZ 176759, morphotype A, Peninsular Malaysia **b** MISE-018-19, morphotype B, Okinawa, Japan **c** MISE-55-19, morphotype B, Okinawa, Japan **d** MISE-039-19, morphotype C, Kagoshima, Japan **e, f** *Goniobranchus verrieri* **e** CASIZ 203059, morphotype A, Philippines **f** CASIZ 208442, morphotype B, Philippines. Photographs **a, e, f** TMG; **b–d** GYS. Scale bars: 1 cm.

B), one specimen, subsampled for molecular data, Tengan, 26.400°N, 127.833°E, Okinawa-jima Island, Japan, 8 m depth, 3 May 2019, G.Y. Soong. MISE-023-18 (morphotype B), one specimen, subsampled for molecular data, Tengan, 26.400°N, 127.833°E, Okinawa-jima Island, Japan, 7 m depth, 12 April 2018, G.Y. Soong. MISE-018-19 (morphotype B), one specimen, subsampled for molecular data, Red Beach, 26.447°N, 127.912°E, Okinawa-jima Island, Japan, 6 m depth, 19 May 2019, G.Y. Soong. MISE-022-18 (morphotype B), one specimen, subsampled for molecular data, Tengan, 26.400°N, 127.833°E, Okinawa-jima Island, Japan, 10 m depth, 12 April 2018, G.Y. Soong. MISE-008-19 (morphotype B), one specimen, subsampled for molecular data,

Tengan, 26.400°N, 127.833°E, Okinawa-jima Island, Japan, 8 m depth, 3 May 2019, G.Y. Soong. CASIZ 176759 (morphotype C), one specimen, subsampled for molecular data, Waterfall Bay, 2.720°N, 104.195°E, Pulau Tioman, South China Sea, Peninsular Malaysia, 14 m depth, 4 October 2007, T.M. Gosliner et al. CASIZ 175727 (morphotype C), one specimen (2 mm preserved), subsampled for molecular data, Pulau Gut, 2.664°N, 104.167°E, Pulau Tioman, South China Sea, Peninsular Malaysia. 14 m depth, 4 October 2007, T.M. Gosliner. CASIZ 189457 (morphotype C), one specimen (3 mm preserved), subsampled for molecular data, location not available, GPS data not available, Peninsular Malaysia, depth not available, 4 October 2007, T.M. Gosliner.

Description. ***External morphology.*** Living animal ~ 10 mm in length. Body smooth, without tubercles, oval and elongated, with three marginal bands on the mantle edge. Seven to ten unipinnate gill branches, 13–18 rhinophore lamellae. The species has three distinct morphotypes based on color patterns. Morphotype A (Fig. 3a) has a translucent creamy white body with no spots on the notum. The outermost portion of the mantle edge is surrounded by a thin whitish blue band, followed by one each of thicker red and yellow bands. The gill and rhinophores are translucent red with reddish purple edges. Morphotype B (Fig. 3b, c) has a translucent white body with brown spots on the notum. The outermost portion of the mantle edge is surrounded by an opaque bluish white tinged band, followed by red and yellow submarginal bands, and all three bands have similar widths. The gill and rhinophores are translucent red with opaque white edges. Morphotype C (Fig. 3d) has a creamy white but translucent body with fine orange spots on the notum. The outermost portion of the mantle edge is surrounded by a thin opaque bluish white tinged band, followed by a thicker irregular red band, and then a yellow submarginal band of similar thickness to the red band. Gill and rhinophores are translucent red with reddish purple edges.

Buccal mass and radula (morphotype A). The muscular portion of the buccal mass approximately the same size as the oral tube length (Fig. 6a). The chitinous labial cuticle found at the anterior end of the muscular portion of the buccal mass bearing bifurcated and long jaw rodlets (Fig. 10a, b). The radular formula of MISE-010-19 and MISE-047-19 (Fig. 10c) are 46 × 40.1.40 and 52 × 40.1.40, respectively. The rachidian tooth is triangular, thin, with a blunt tip. The innermost lateral teeth have two or three denticles on the inner side and 3–5 denticles on the outer side of the central cusp (Fig. 10d). The central cusp on the inner lateral tooth is elongate and ~ 2× the length of the adjacent denticles. The middle lateral teeth have a short central cusp with six or seven denticles (Fig. 10e). The outer lateral teeth have a rounded main cusp with five denticles (Fig. 10f).

Reproductive system (Fig. 6b). The thick, tubular ampulla narrows into a diverging short oviduct and long vas deferens. The proximal prostatic portion of the vas deferens is thin and convoluted and transitions into the muscular ejaculatory portion. The long, narrow, convoluted ejaculatory portion transitions into a wider and long curved penial bulb, which joins with the distal end of the vagina. The vagina is narrow and elongated and transitions into a larger, spherical bursa copulatrix and the smaller, curved receptaculum seminis at its distal end. A moderately long uterine duct emerges from this junction of vagina, bursa, and receptaculum seminis. The uterine duct con-

nects the receptaculum seminis with the female gland mass. The female gland mass has smaller albumen and membrane glands and a larger mucous gland.

Remarks. Our *G. sinensis* morphotype A specimens are the same as Rudman's (1985) specimens; all of Rudman's (1985) specimens were collected from Hong Kong. He only found one morphotype, with a translucent creamy white body and the outermost portion of the mantle edge surrounded by a thin white band, followed by one each of thicker red and yellow bands. The gill and rhinophores were translucent red with reddish purple edges. Some of the specimens he collected also had fine orange-brown specks on the notum; however, this morphological trait was observed in comparatively few of the newly collected specimens and is found in morphotype C (Fig. 3d). Rudman (1985) also synonymized specimens documented by Baba (1938) and Abe (1964) from Japan as *G. sinensis*, further supporting the identification of our specimens from Kagoshima, Japan as *G. sinensis*. Morphotype A has thus been reported from Hong Kong and Japan. In our study, we also observed two more morphotypes of *G. sinensis*: morphotype B from Okinawa, Japan and morphotype C from Peninsular Malaysia.

Goniobranchus sinensis demonstrates intraspecific variation (intraspecific *p*-COI distance within *G. sinensis* = 0.0–1.4%) in morphology based on geographic location, with specimens collected from Peninsular Malaysia, Okinawa, and mainland Japan in this study. Body patterns of nudibranchs can vary depending on environmental factors (Rudman 1991), and this may explain the morphological variation in *G. sinensis* as observed by Rudman (1991) and in the current study. Distinctive features of the external morphology are included in the remarks for *G. preciosus*, the species with which this species has been most frequently confused.

Goniobranchus verrieri **(Crosse, 1875)**

Figures 3e, f, 6c, d, 11a–f

Doris marginata Pease, 1860: 30 (junior homonym of both *Doris marginata* Montagu, 1804: 79 and *Doris marginata* Quoy & Gaimard, 1832: 255–256).
Goniodoris verrieri Crosse, 1875: 313, 314, pl. 12, fig. 5.
Chromodoris marginata: Bergh, 1880: 27, pl. 13, figs 22, 23; Risbec 1928: 133–136, fig. 33, pl. 6, fig. 4; Risbec 1953: 63–66, fig. 26; Kay 1979: 467, 468, fig. 150D.
Glossodoris verrieri: Pruvot-Fol 1951: 155.
Chromodoris verrieri: Risbec 1953: 80; Rudman 1985: 262–267, figs 12A, 13A, 14, 15A; Gosliner et al. 2008: 221, top photograph.
Chromodoris trimarginata (Winckworth, 1946): Kay and Young 1969: 205, 206, figs 45, 55 (misidentification).
Goniobranchus verrieri: Gosliner et al. 2015: 223, top right photograph; Gosliner et al. 2018: 153, top right photograph.
Chromodoris sinensis Rudman, 1985: 263, fig. 12C; Yonow 2001: 26, pl 3, fig. 6 (misidentifications).

Type locality. Noumea, New Caledonia.

Type material. Most likely lost to science. Crosse's types are deposited in the Muséum national d'Histoire naturelle (Paris), but the list of types by Valdés and Heros (1998) of Recent and fossil opisthobranchs does not mention any material of *Goniodoris verrieri* Crosse, 1875. We base our identification from Crosse's illustration (1875: pl. 12, fig. 5), which agrees with the morphological study of Rudman (1985).

Geographical distribution. Widely distributed around the tropical and subtropical Indo-Pacific oceans (Rudman 1985; Debelius 1996; Debelius and Kuiter 2007; Coleman 2008; Gosliner et al. 2008, 2015, 2018) with reports from across South Africa, Madagascar, Indonesia, Papua New Guinea, Philippines, Midway Atoll, Hawaiian Islands (Gosliner et al. 2018), Australia (Slack-Smith and Bryce 2004; Nimbs and Smith 2016), Tanzania (Rudman 1985), Thailand (Mehrotra et al. 2021), Mozambique (Strömvoll and Jones 2019), Japan (Nakano 2018; Ono and Katou 2020), Taiwan (Jie et al. 2009), New Caledonia (Hervé 2010), Marshall Islands (Rudman 1985), and Mariana Islands (Carlson and Hoff 2003).

Material examined. CASIZ 203059 (morphotype A), one specimen (3 mm preserved), subsampled for molecular data and dissected, Balibago dive site, 13.932°N, 120.611°E., Verde Island Passage Coast, Calatagan, Batangas Province, Luzon Island, Philippines, 12 m depth, 17 May 2014, S. Matsuda, 2014 Verde Island Passage Expedition. CASIZ 208442 (morphotype B), one specimen (5 mm preserved), subsampled for molecular data and dissected. Culebra (Bonito) Island, 13.617°N, 120.933°E, Maricaban Island, Tingloy, Batangas Province, Luzon, Philippines, 3–30 m depth, 18 April 2015, G. Paulay, 2015 Verde Island Passage Expedition.

Description. ***External morphology.*** Living animals approximately 11–17 mm in length. Body oval, with two marginal bands of similar widths on the mantle edge. Gill and rhinophores are translucent red with a mix of red and white edges. Four to eight unipinnate gill branches. Ten or eleven lamellae on rhinophores. The color patterns of this species can be divided into two distinct morphotypes. Morphotype A (Fig. 3e) has an opaque white body. The outermost portion of the mantle edge is surrounded by a red margin and a yellow submarginal band with both bands of similar widths. Morphotype B (Fig. 3f) has a translucent creamy white body with small orange spots on the notum. The outermost portion of the mantle edge is surrounded by a very thin opaque white band, followed by a red and a yellow submarginal band.

Buccal mass and radula (morphotype A). The muscular portion of the buccal mass is approximately the same size as the oral tube length (Fig. 6c). The chitinous labial cuticle found at the anterior end of the muscular portion of the buccal mass bearing bifurcated and short jaw rodlets (Fig. 11a, b). The radular formula of CASIZ 203059 is 37 × 28.1.28 (Fig. 11c). The rachidian tooth is flame-like in shape and short. The inner and outer surfaces of the inner lateral teeth have three denticles on each side (Fig. 11d). The central cusp on the inner lateral tooth is ~ 2× the length of the adjacent denticles. The middle lateral teeth have a short central cusp with approximately four or five denticles (Fig. 11e). The outer lateral teeth have a rounded tooth shaped with ~ 2–4 denticles (Fig. 11f).

Reproductive system (Fig. 6d). The thick, tubular ampulla narrows into a diverging short oviduct and long vas deferens. The proximal prostatic portion of the vas deferens is wide and convoluted and transitions into the muscular ejaculatory portion.

The long, narrow, convoluted ejaculatory portion transitions into a wider, long penial bulb, which joins with the distal end of the vagina. The thick muscular vagina is elongated and transitions into a larger, spherical bursa copulatrix. At this junction of the vagina and bursa copulatrix, the smaller pyriform receptaculum seminis also connects. The moderately long uterine duct that emerges from the junction of the vagina, bursa copulatrix, and receptaculum seminis enters into the female gland mass. This uterine duct junction also extends proximally on one side and includes a larger portion of the vagina. The female gland mass has small albumen and membrane glands and a large mucous gland.

Remarks. *Goniobranchus verrieri* was originally described by Crosse (1875) from New Caledonia. The species had been previously described by Pease (1860) as *Doris marginata* from Hawai'i. However, the name *Doris marginata* was pre-occupied: several different species had been given the same name and *Goniobranchus verrieri* is the next available name for this species. Crosse described the animal as having a white body and the mantle edged in a light red margin and a yellow tinged submarginal band. This description matches the external morphology of the *G. verrieri* morphotype A in this study and specimens studied by Rudman (1985).

Goniobranchus verrieri morphotype B has a creamy translucent body with small orange spots on the notum and three marginal bands on mantle edge. Although this pattern did not match with the original description of *G. verrieri*, the phylogenetic and species delimitation analyses in this study showed that *G. verrieri* morphotype B is clustered with morphotype A. Based on this result, we consider morphotype B a color variation of *G. verrieri*. Both morphotypes also showed little genetic differences (intraspecific *p*-COI distance within *G. verrieri* = 1.3–3.7%), also suggesting that *G. verrieri* has morphological variation, similarly observed in some other white *Goniobranchus* species with marginal bands in this study. The vast majority of specimens of *G. verrieri* closely resemble morphotype A and there has been relatively little confusion of this species with others that have a white body and marginal bands. Spotted specimens of *G. verrieri* could be confused with *G. preciosus*, but have a more spreading gill plume whereas *G. preciosus* always have an erect gill plume.

Goniobranchus fabulus **Soong & Gosliner, sp. nov.**

http://zoobank.org/A8690AEB-E87C-4F2D-985F-98404B87644A
Figures 4a–d, 6e, f, 12a–f

Chromodoris preciosa (Kelaart, 1858): Rudman 1985: figs 12b, 13b, 17; Gosliner et al. 2008: 219, upper right photo (misidentifications).

Goniobranchus preciosus (Kelaart, 1858): Gosliner et al. 2015: 222, lower middle right photo; Gosliner et al. 2018: 152: middle right photo (misidentifications).

Type material. ***Holotype*****:** CASIZ 191271 (morphotype B), one specimen (5 mm preserved), subsampled for molecular data and dissected. Siar Island, 5.187°S, 145.807°E,

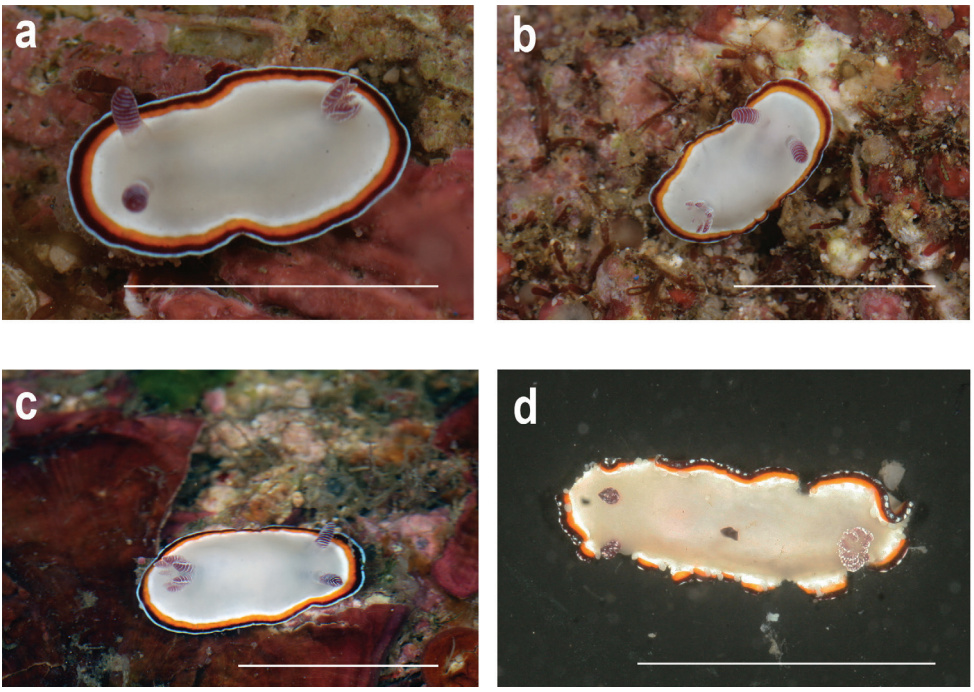

Figure 4. *Goniobranchus fabulus* sp. nov. **a** CASIZ 177517, morphotype A, Philippines **b** CASIZ 177685, morphotype A, Philippines **c** CASIZ 201949, morphotype A, Philippines **d** CASIZ 191118, morphotype B, Papua New Guinea. Photographs TMG. Scale bars: 1 cm.

Madang Province, Papua New Guinea, depth not available, 16 November 2012, V. Knutson, Papua New Guinea Biodiversity Expedition 2012.

***Paratypes*:** CASIZ 177517 (morphotype A), one specimen (3 mm preserved), subsampled for molecular data, Arthur's Rock, 13.417°N, 120.517°E, Maricaban Strait, Mabini (Calumpan Peninsula), Batangas Province, Luzon, Philippines, 3 m depth, 21 March 2008, T.M. Gosliner et al., Philippines Expedition March 2008. CASIZ 177685 (morphotype A), one specimen (6 mm preserved), subsampled for molecular data, Bethlehem Channel, 13.672°N, 120.841°E, Bethlehem, Maricaban Island, Batangas Province, Philippines, 15 m depth, 20 April 2008, T.M. Gosliner. CASIZ 201949 (morphotype A), one specimen (5 mm preserved), subsampled for molecular data, Lago de Oro Hotel, 13.917°N, 120.616°E, Verde Island Passage coast, Calatagan, Batangas Province, Luzon Island, Philippines, 2 m depth, 19 May 2014, VIP Team, 2014 Verde Island Passage Expedition. CASIZ 191118 (morphotype B), one specimen (4 mm preserved), subsampled for molecular data, Mangroves, GPS, Madang Province, Papua New Guinea, 3 m depth, 10 November 2012, Papua New Guinea Biodiversity Expedition 2012.

Geographical distribution. This species appears to be restricted to the western and southern central Pacific tropics (Gosliner et al. 2008, 2015, 2018) with reports from the Philippines (present study), Japan (Nakano 2018), Papua New Guinea, New Caledonia, Tonga, Vanuatu (Gosliner et al. 2008), Australia, and Fiji (Rudman 1985).

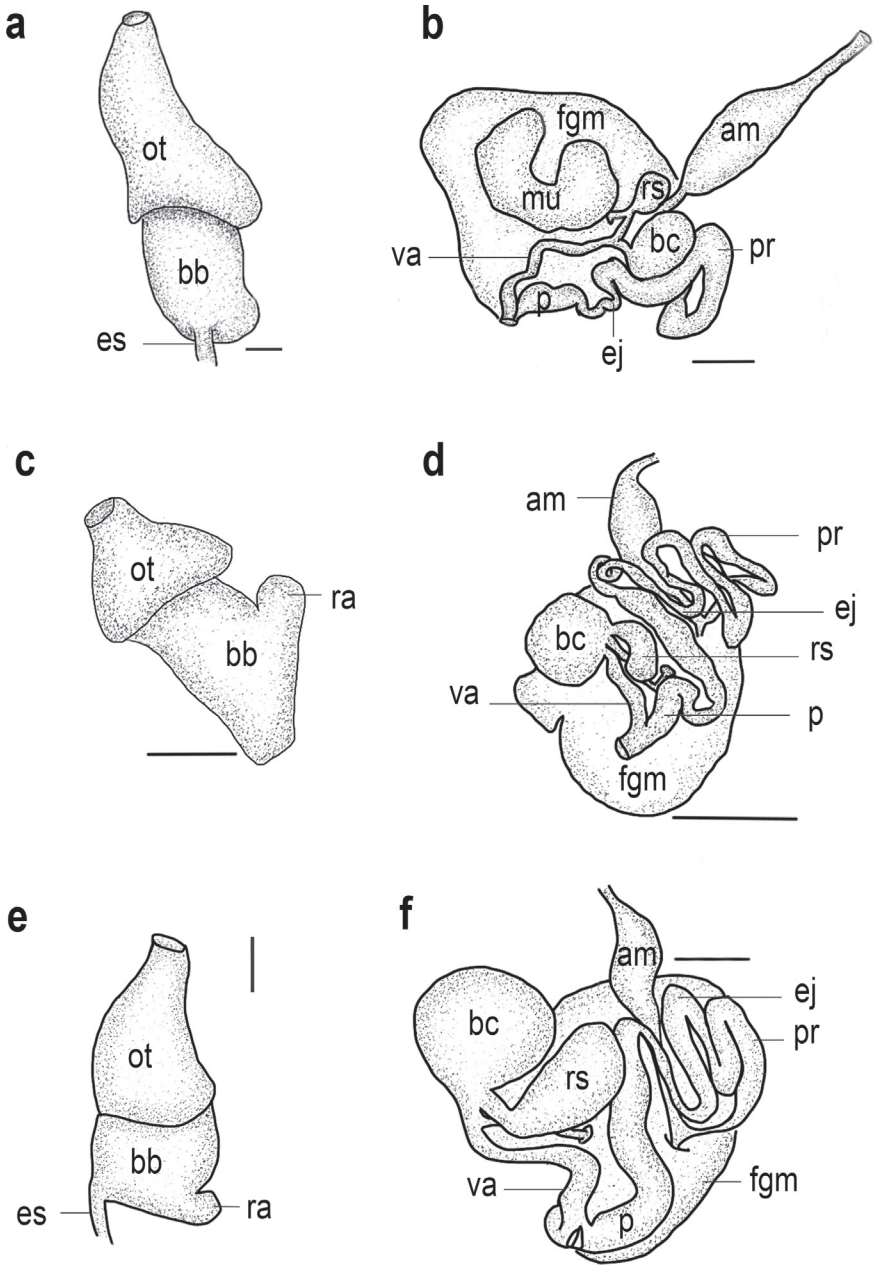

Figure 5. a buccal mass of *Goniobranchus albonares*, CASIZ 228939 **b** reproductive system of *Goniobranchus albonares*, CASIZ 228939 **c** buccal mass of *Goniobranchus preciosus*, CASIZ 208574 **d** reproductive system of *Goniobranchus preciosus*, CASIZ 208574 **e** buccal mass of *Goniobranchus rubrocornutus*, CASIZ 203047 **f** reproductive system of *Goniobranchus rubrocornutus*, CASIZ 203047. Abbreviations: am, ampulla; bb, buccal bulb; bc, bursa copulatrix; ej, ejaculatory duct; es, esophagus; fgm, female gland mass; ot, oral tube; p, penis; pr, prostate; ra, radular sac; rs, receptaculum seminis; va, vagina; mu, mucous gland. Scale bars: 0.1 mm (**a, b, e, f**); 1 mm (**c, d**).

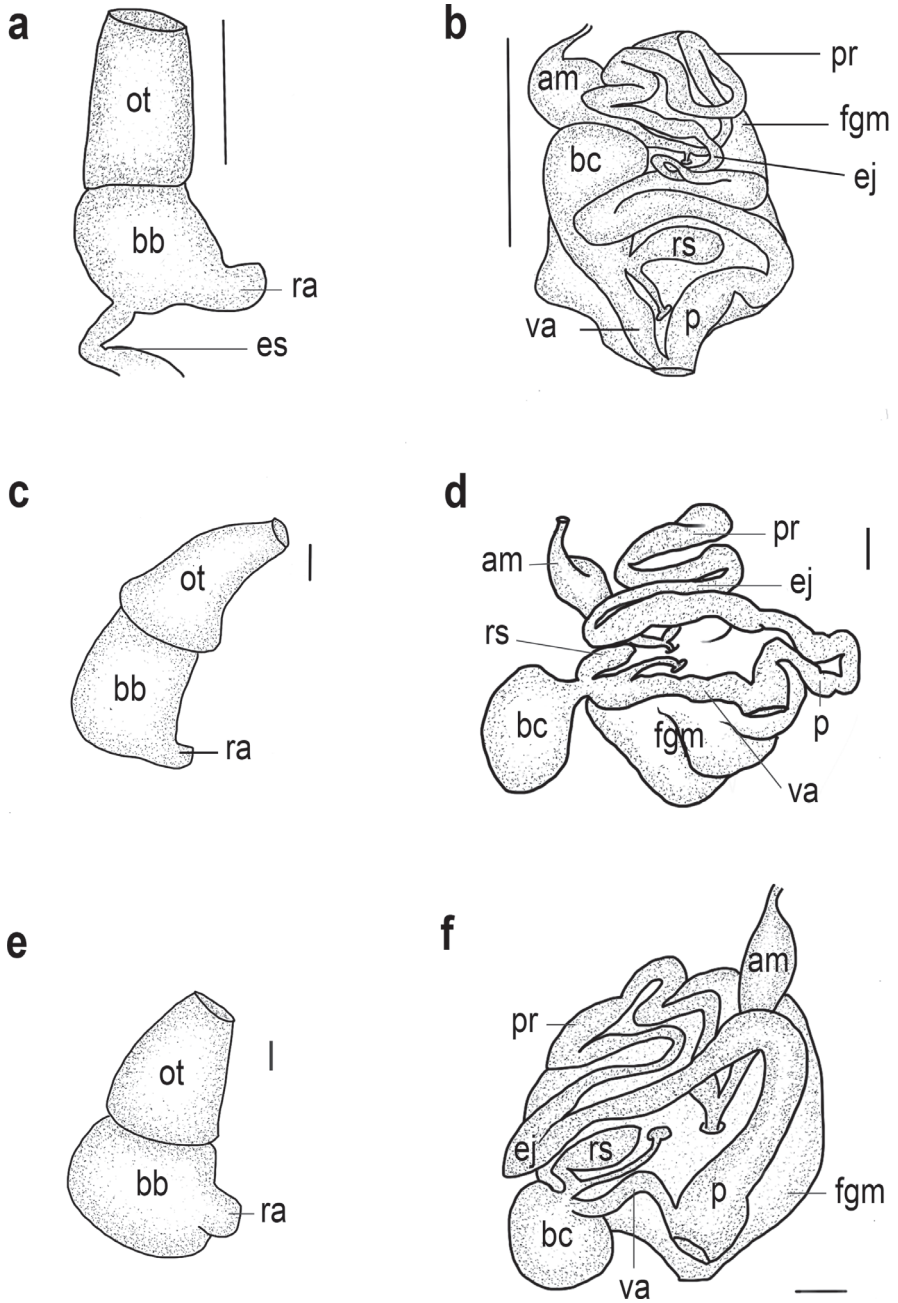

Figure 6. a buccal mass of *Goniobranchus sinensis*, MISE-047-19 **b** reproductive system of *Goniobranchus sinensis*, MISE-047-19 **c** buccal mass of *Goniobranchus verrieri*, CASIZ 203059 **d** reproductive system of *Goniobranchus verrieri*, CASIZ 203059 **e** bBuccal mass of *Goniobranchus fabulus* sp. nov., CASIZ 191271 **f** reproductive system of *Goniobranchus fabulus* sp. nov., CASIZ 191271. Abbreviations: am, ampulla; bb, buccal bulb; bc, bursa copulatrix; ej, ejaculatory duct; es, esophagus; fgm, female gland mass; ot, oral tube; p, penis; pr, prostate; ra, radular sac; rs, receptaculum seminis; va, vagina. Scale bars: 0.1 mm (**c, d, e, f**); 1 mm (**a, b**).

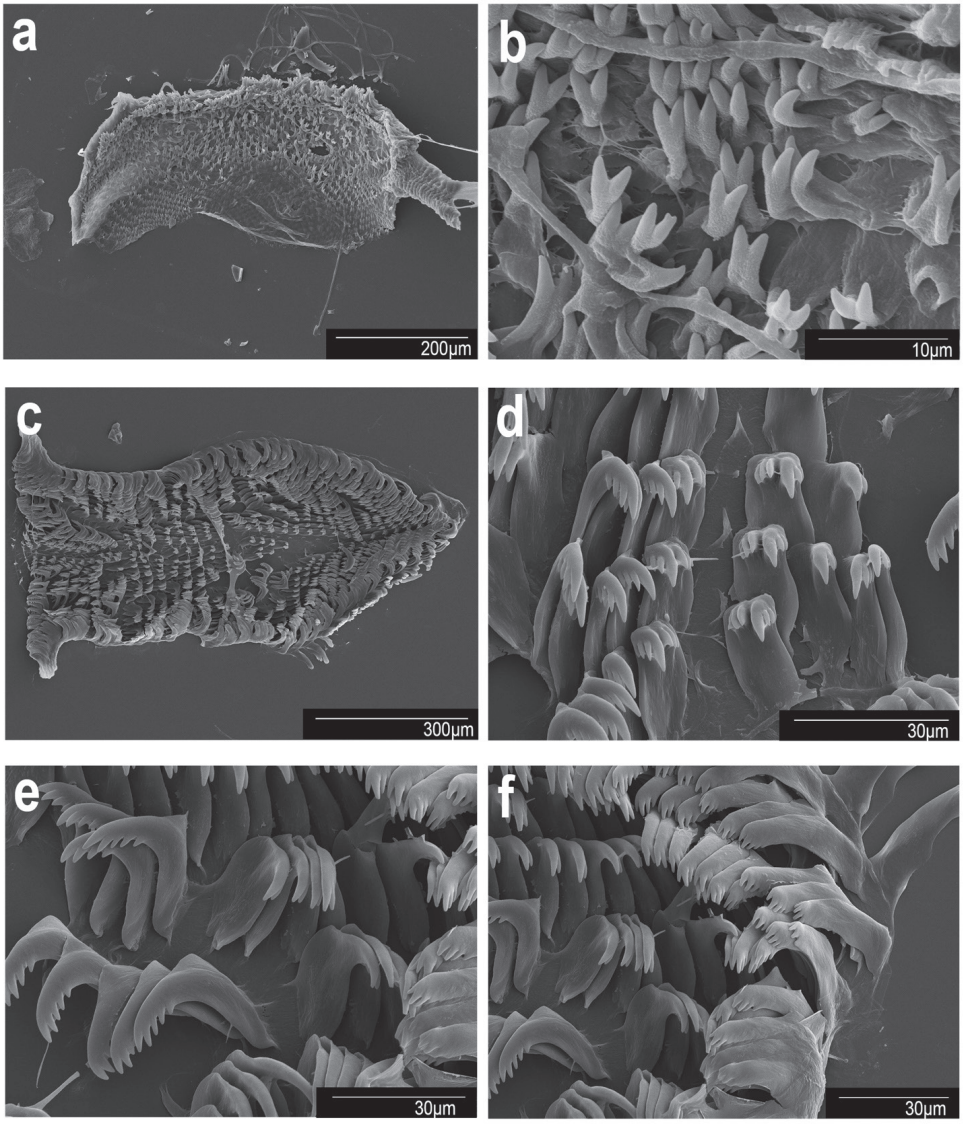

Figure 7. Scanning electron micrographs. *Goniobranchus albonares*, CASIZ 228939, Philippines **a** jaw **b** jaw rodlets **c** radula **d** central teeth **e** mid-lateral teeth **f** outer lateral teeth.

Description. ***External morphology.*** Living animals 12–18 mm in length. Body oval with three marginal bands on the mantle edge. Notum smooth with no apparent spots. Six to ten unipinnate gill branches. Eleven or twelve lamellae on rhinophores. The color pattern exhibits two distinct morphotypes. Morphotype A (Fig. 4a–c) has a creamy opaque white body. The outermost portion of the mantle edge is tinged an opaque bluish white, followed by a deep red band, followed by a yellow submarginal band, and then an opaque white band, with all bands having similar widths.

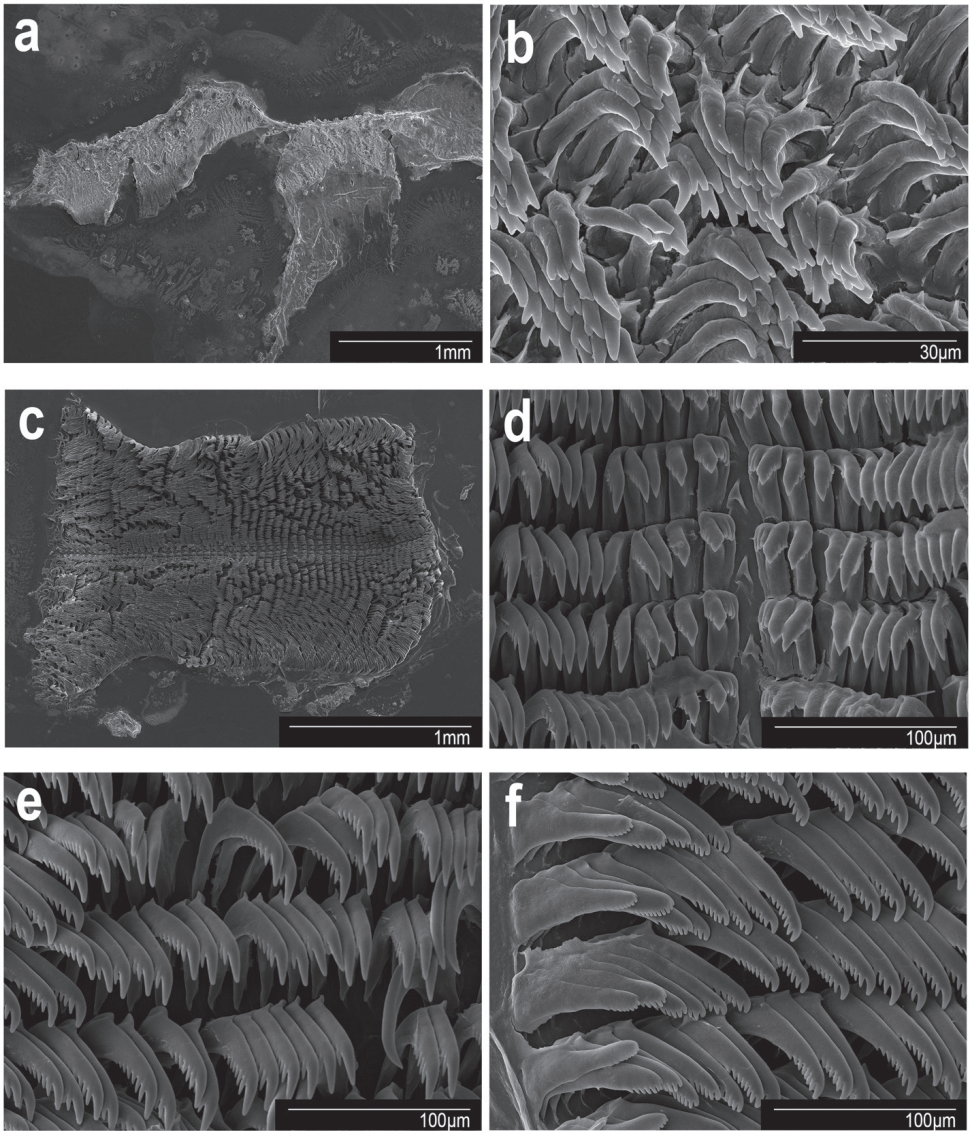

Figure 8. Scanning electron micrographs. *Goniobranchus preciosus*, CASIZ 208574, Philippines **a** jaw **b** jaw rodlets **c** radula **d** central teeth **e** mid-lateral teeth **f** outer lateral teeth.

Gill branches and rhinophores are reddish purple with white edges. Morphotype B (Fig. 4d) has an opaque creamy white body. The outermost portion of the mantle edge is surrounded by a speckled opaque white band, followed by a deep red band, a yellow submarginal band, and then an innermost opaque white band. The gill and rhinophores are reddish purple with white edges and opaque white speckles.

Buccal mass and radula (morphotype B). The muscular portion of the buccal mass is approximately the same size as the oral tube length (Fig. 6e). The chitinous labial cuticle

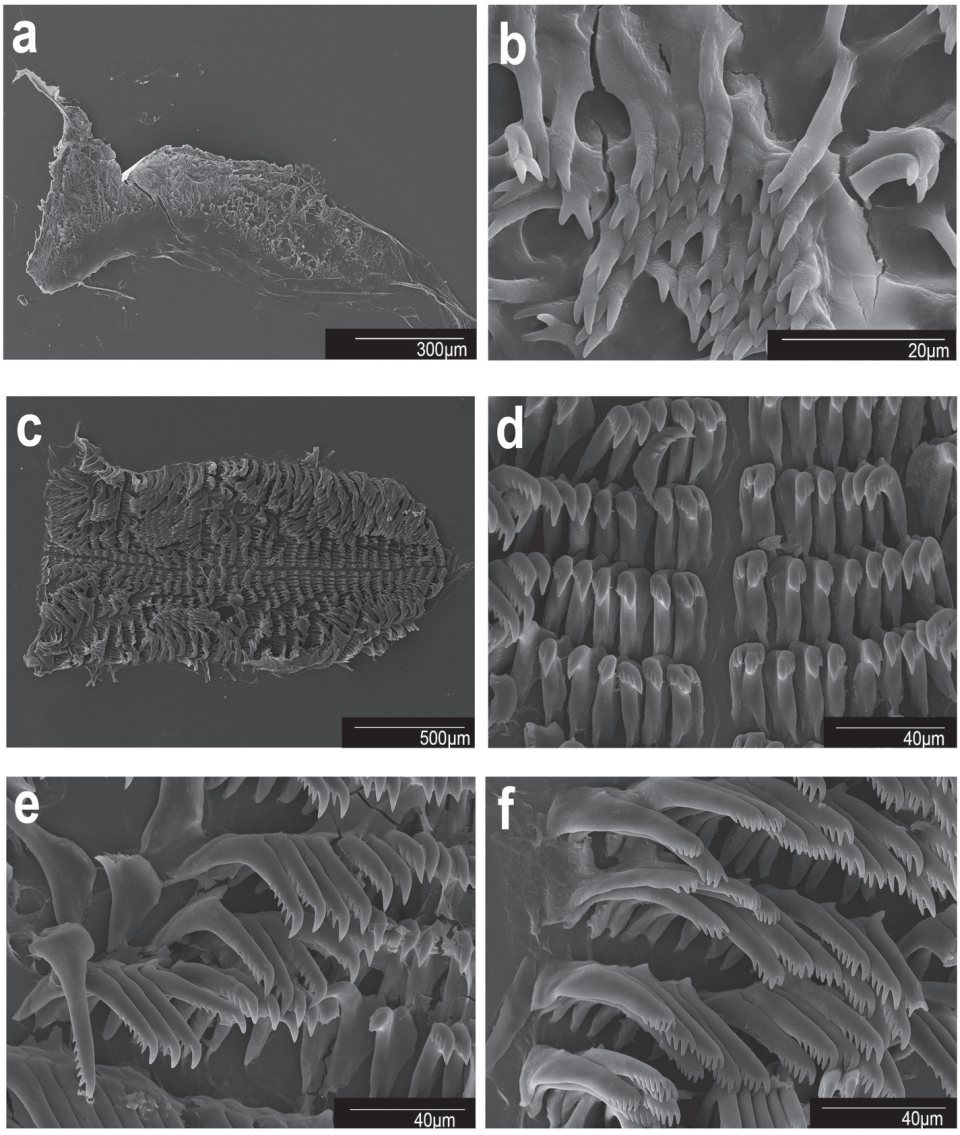

Figure 9. Scanning electron micrographs. *Goniobranchus rubrocornutus*, CASIZ 203047, Philippines. **a** jaw **b** jaw rodlets **c** radula **d** central teeth **e** mid-lateral teeth **f** outer lateral teeth.

found at the anterior end of the muscular portion of the buccal mass and bears bifurcated and short jaw rodlets (Fig. 12a, b). The radular formula of CASIZ 191271 is 42 × 35.1.35 (Fig. 12c). The rachidian tooth is triangular. The innermost lateral teeth have two denticles on the inner side of the cusp and three or four denticles on the outer side (Fig. 12d). The central cusp on the inner lateral tooth is elongate and ~ 2× the length of the adjacent denticles. The middle lateral teeth have an elongated central cusp with 5–7 denticles (Fig. 12e). The outer lateral teeth have a rounded tooth with 2–5 denticles (Fig. 12f).

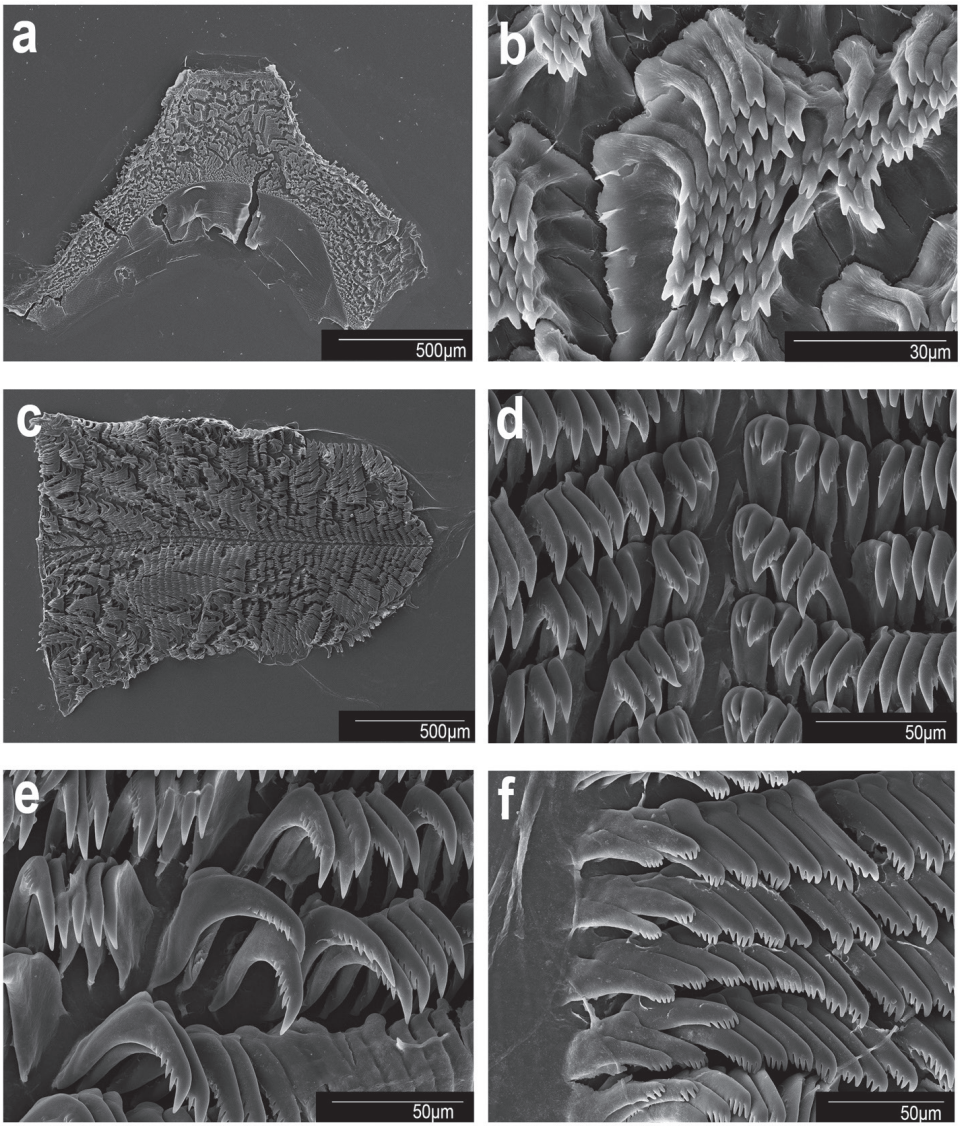

Figure 10. Scanning electron micrographs. *Goniobranchus sinensis*, MISE-047-19, Kagoshima, Japan. **a** jaw **b** jaw rodlets **c** radula **d** central teeth **e** mid-lateral teeth **f** outer lateral teeth.

Reproductive system (Fig. 6f). The thin, tubular ampulla narrows into a diverging short oviduct and long vas deferens. The proximal prostatic portion of the vas deferens is thin and convoluted and transitions into the muscular ejaculatory portion. The long, narrow, convoluted ejaculatory portion transitions into a wider, long penial bulb, which joins with the moderately wide distal end of the vagina. The vagina is elongate and narrow, joining the larger, spherical bursa copulatrix and the smaller, curved receptaculum seminis at its distal end. A moderately long uterine duct that emerges from

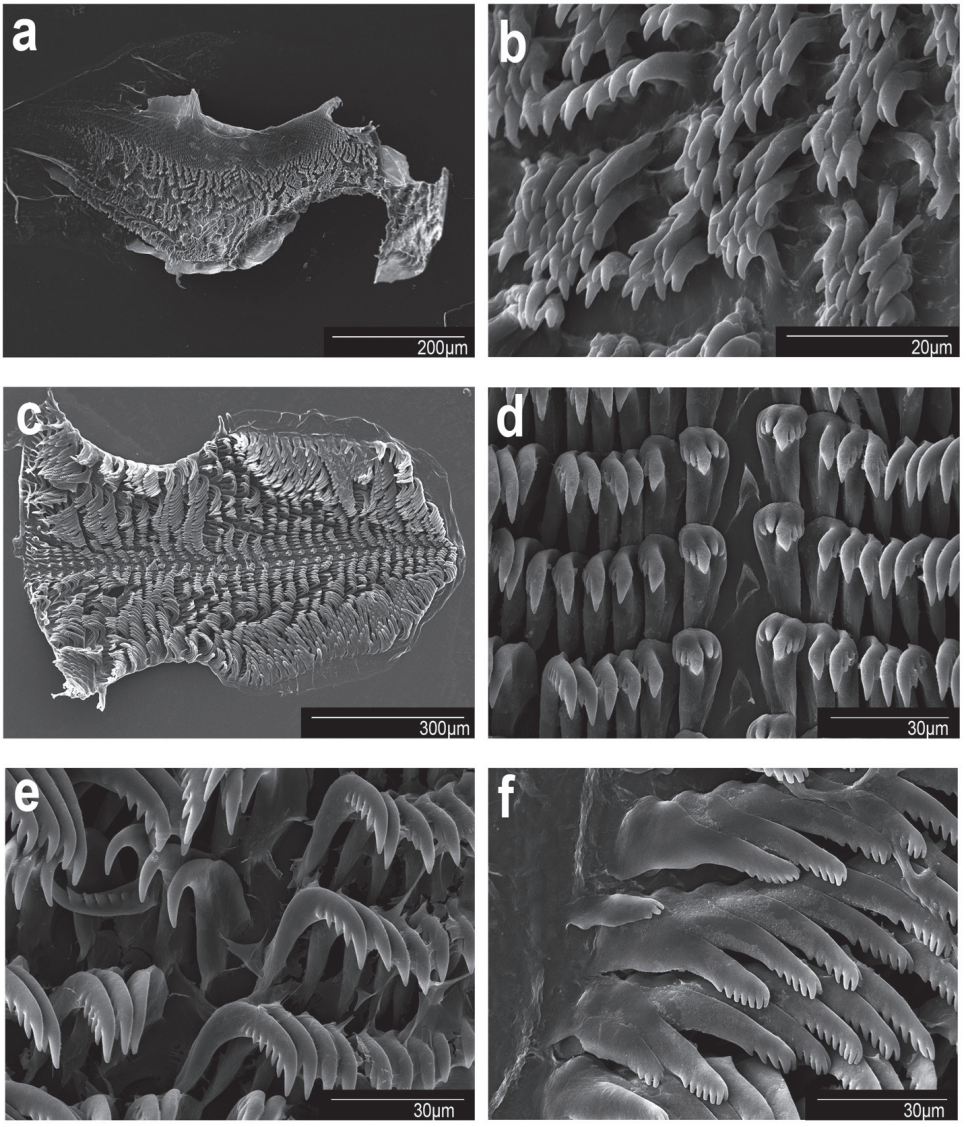

Figure 11. Scanning electron micrographs. *Goniobranchus verrieri*, CASIZ 203059, Philippines. **a** jaw **b** jaw rodlets **c** radula **d** central teeth **e** mid-lateral teeth **f** outer lateral teeth.

this junction of vagina, bursa copulatrix, and receptaculum seminis. The uterine duct connects the receptaculum seminis with the female gland mass. The female gland mass has smaller albumen and membrane glands and a larger mucous gland.

Etymology. *Goniobranchus fabulus* sp. nov. is named after the Latin word which, in one translation, means a small bean, in reference to the body shape of the nudibranch.

Remarks. *Goniobranchus fabulus* sp. nov. was recovered as a sister species to *G. daphne* in our phylogenetic analyses, with an interspecific distance of 2.5–4.5%

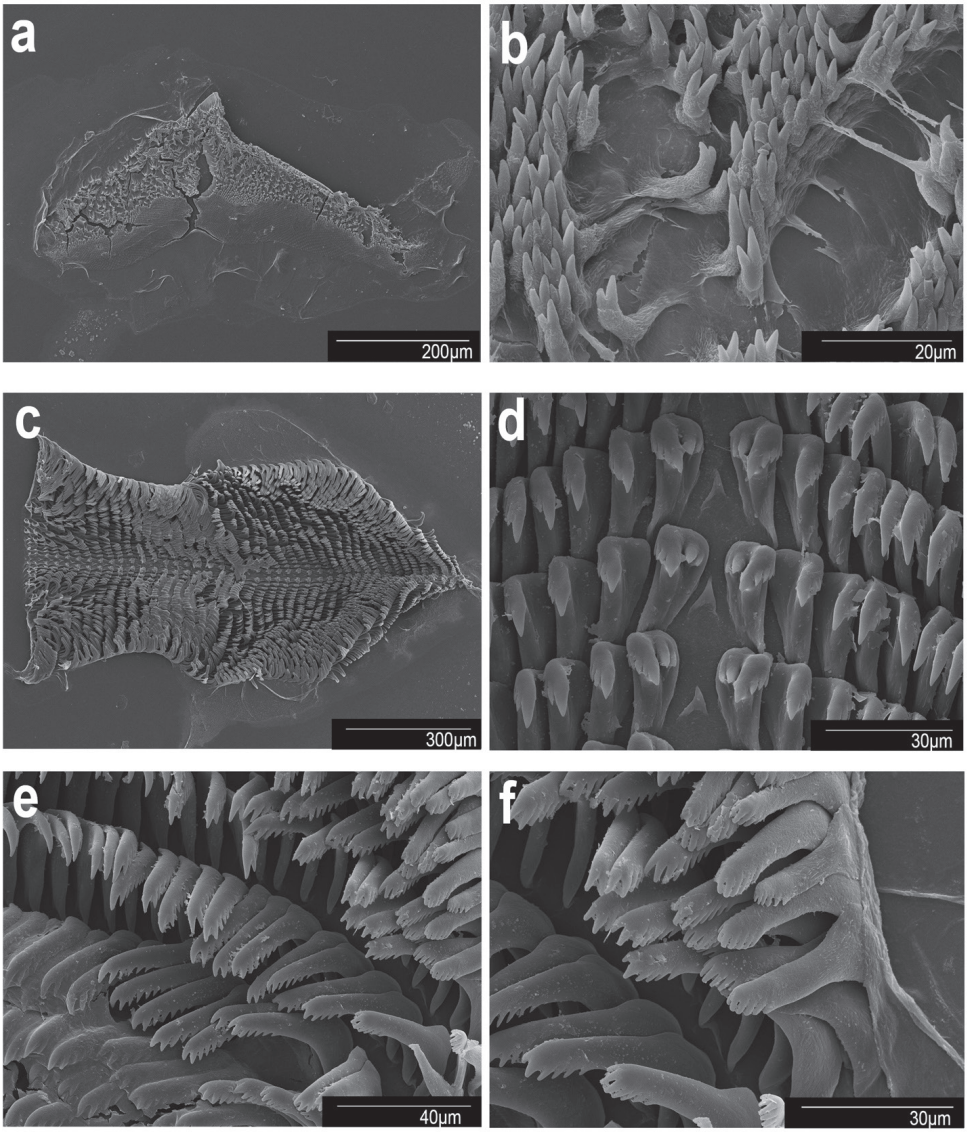

Figure 12. Scanning electron micrographs. *Goniobranchus fabulus* sp. nov., CASIZ 191271, Philippines. **a** jaw **b** jaw rodlets **c** radula **d** central teeth **e** mid-lateral teeth **f** outer lateral teeth.

(Table 2). *Goniobranchus daphne* possess red spots of different sizes on the notum and can only be found in the Australian waters.

Goniobranchus fabulus sp. nov. morphotype A in our study matches well with Rudman's (1985) description of *Goniobranchus preciosus* from New Caledonia based on morphological characteristics. However, in our opinion the morphological characteristics of *G. preciosus* sensu Rudman did not match with the original description of *G. preciosus* and our specimen sequences are also genetically distinct from *G. preciosus* in this study (inter-

specific *p*-COI distance between *G. fabulus* and *G. preciosus* = 6.8–9.2%) (Fig. 1; Table 2). Hence, we have assigned *G. preciosus* sensu Rudman (1985) to *G. fabulus* sp. nov.

Goniobranchus fabulus sp. nov. morphotype B is slightly different from morphotype A in having opaque white speckles all over the gills and around the outermost edge of the mantle. This morphotype is only known from Papua New Guinea (Wakeling 2001; Gosliner et al. 2018). There is little genetic difference between the two morphotypes (intraspecific *p*-COI distances within *G. fabulus* sp. nov. = 0.2–3.4%). Confusion of this species with *G. preciosus* is discussed in the remarks section of *G. preciosus*.

Discussion

Goniobranchus fabulus sp. nov. is known from the Philippines south and eastwards to Australia, Fiji, and Tonga. Many of the other species in this study are found in the Coral Triangle with overlap specifically in the Philippines; however, due to different geographical distributions, morphological differences, and the addition of new molecular data from this study, the six species examined here can be considered distinct.

As with other groups within Chromodorididae, the results of this study show that white *Goniobranchus* species with various marginal bands can be difficult to accurately identify based solely on external morphology due to similar color patterns. Although color pattern differences were distinct between species in this study, color pattern variations within species were also observed. In our study, *G. verrieri*, *G. preciosus*, *G. rubrocornutus*, *G. sinensis*, and *G. fabulus* sp. nov. displayed color polymorphism. Previous studies on chromodorid nudibranchs have also confirmed polymorphism (Padula et al. 2016; Layton et al. 2018, 2020), hypothesized to be due to Müllerian mimicry in which the nudibranchs mimic one another as protection from predators (Rudman 1991; Cheney et al. 2016). However, the mechanisms that cause color and pattern polymorphism in the white *Goniobranchus* with marginal bands species in this study need further examination.

Despite these issues of variability, color and pattern still play important roles in the identification of many nudibranchs, and in at least some *Goniobranchus* species. Based on previous research, putative *Goniobranchus* species that can be identified based on color patterns include *G. splendidus* (Wilson et al. 2016) and the red reticulate species *G.* sp. 1, *G.* sp. 2, *G.* sp. 3, and *G.* sp. 4 from Soong et al. (2020). Additionally, color and pattern-based identification was shown to be useful in all of the species studied here. However, many of the white *Goniobranchus* species with marginal bands are pseudocryptic and have intraspecific color variation which complicates identification, but subtle yet consistent elements of color pattern provide unambiguous features that permit identification of species. This intraspecific color variation was observed in *G. verrieri*, *G. preciosus*, *G. sinensis*, *G. rubrocornutus*, and *G. fabulus* sp. nov. in this study, as well as *G.* sp. 5 in Soong et al. (2020). Thus, based on this study and previous research, at least six molecularly confirmed *Goniobranchus* species have intraspecific color variation, showing that despite confusing color patterns, there are specific morphological characteristics that provide diagnostic features for species identifications. Internal morphological data can help delineate species in *Goniobranchus* and *Chromodoris* (Rudman

1984) and, additionally, molecular data has been able to recover multiple putative species within *Goniobranchus* and other Chromodorididae groups formerly thought to be single species (Matsuda and Gosliner 2018a, 2018b; Layton et al. 2018; Soong et al. 2020; this study). Our study further supports the importance of integrative systematics that both color patterns and internal morphological data is needed with molecular data to aid in nudibranch identification and taxonomy.

Based on the phylogenetic tree in this study (Fig. 1), *Goniobranchus albonares* was recovered within another clade different from the rest of the white *Goniobranchus* with marginal bands. Most of the white *Goniobranchus* with marginal bands species in this study possibly inherited their white body color with variously colored marginal bands from a common ancestor, except for *G. albonares*, which likely evolved its color pattern independently and convergently. *Goniobranchus albonares* is very widespread, found in the western Indian Ocean to the western Pacific. Throughout its range, members of the other species with variously colored marginal bands (e.g., *G. daphne*, *G. sinensis*, *G. fabulus*, *G. preciosus*, *G. verrieri*) are ubiquitous and sympatric, ensuring that their mimetic pattern will be present together with other similarly appearing species (Rudman 1985). Gosliner (2001) also noted that a species of polyclad flatworm (*Pseudoceros* sp.) mimicked *Chromodoris preciosa* (*Goniobranchus fabulus* sp. nov. of this study) and that the nudibranchs were far less palatable than the flatworms, suggesting this was a case of Müllerian mimicry.

Well-studied chromodorid nudibranch groups continue to reveal the presence of cryptic species through molecular phylogenetic analyses (Layton et al. 2018). In this study, our examination of *Goniobranchus* species with a white mantle and various marginal bands recovered seven species groups (*G. preciosus*, *G. albonares*, *G. rubrocornutus*, *G. daphne*, *G. verrieri*, *G. fabulus* sp. nov., and *G. sinensis*) of white species with marginal bands. In the past, there has been some confusion regarding the appearance and taxonomy of the *Goniobranchus* species with white mantles and variously colored margins (Rudman 1985; Gosliner et al. 2008, 2015, 2018). Aside from the species and morphotypes examined in this study, there are other described white *Goniobranchus* species with various marginal bands [*G. trimarginatus* (Winckworth, 1946) and *G. galactos* (Rudman & Johnson, 1985)], as well as unidentified morphotypes with white mantles and various marginal bands based on online images (Sea Slug Forum) and field guide books (e.g., Gosliner et al. 2018: 152–154; Nakano 2018: 292–294; Ono and Katou 2020: 195, 196, 200, 202), all of which remain to be examined. There are also white *Goniobranchus* with marginal bands known from Hawai'i (Pittman and Fiene 1998), the Marshall Islands (Gosliner et al. 2018: 153, *G.* sp. 26), western Thailand (Gosliner et al. 2018: 153, *G.* sp. 29), New South Wales, Australia (Harasti 2003), the Red Sea (Yonow 1989, 2008), Gulf of Oman (Mayes 2007), the Indian Ocean (Bidgrain 2006), and the South Pacific Ocean (Stenhouse 2000; Potter 2001, 2005). Together, these records suggest a much wider distribution and diversity for this group, and thus further examination is urgently needed to fill in biogeographical gaps and the phylogenetic tree. Therefore, examination of all other described *Goniobranchus* species with these color patterns as well as of other morphotypes, are needed to better understand the relationships between species, and to infer their evolutionary relationships more clearly and better establish robust intraspecific variability thresholds.

Acknowledgements

We would like to thank Aoi Tsuyuki (Hokkaido University), Dr Hiroki Kise, and Dr Yuka Kushida (both University of Ryukyus) for assisting in specimen collection from Okinawa and Kagoshima, Japan. Dr Takuma Fujii (Kagoshima University) is thanked for providing specimens from Amami Oshima, Japan. We are grateful to Dr Angelo Poliseno, Dr Gaelle Quere, as well as Dr Daisuke Uyeno and Midori Matsuoka (both Kagoshima University) for providing logistics and funding for field work in Kagoshima, Japan.

This research was supported by a grant from the National Science Foundation: DEB 1257630 grant to Terrence Gosliner, Kent Carpenter, Richard Mooi, Luiz Rocha, and Gary Williams. This collaborative research involved the following partners in the Philippines: former Secretary of Agriculture Proceso J. Alcala; former Philippine Consul General Marciano Paynor and the Consular staff in San Francisco; former Bureau of Fisheries and Aquatic Resources (BFAR) Director Attorney Asis G. Perez; BFAR colleagues, especially Attorney Analiza Vitug, Ludivina Labe; National Fisheries and Research Development Institute (NFRDI) colleagues, especially Director Drusila Bayate and November Romena; U.S. Embassy staff, especially Heath Bailey, Richard Bakewell and Maria Theresa N. Villa; staff of the Department of Foreign Affairs; University of the Philippines (UP) administrators and colleagues including former UP President Alfredo Pascual, former Vice President Giselle Concepción, Dr Annette Meñez; the staff of the National Museum of the Philippines, especially Dr Jeremy Barns, Anna Labrador and Marivene Manuel Santos. We also thank Boy Venus, Joy Napeñas, Peri Paleracio, Alexis Principe, the staff of Atlantis Dive Resort Puerto Galera (especially Gordon Strahan, Andy Pope, Marco Inocencio, Stephen Lamont, P.J. Aristorenas), Kati Eschweiler and the other staff of the 3P Resort Romblon, Ipat Luna, Anne Hazel Javier, Jay-o Castillo, Arvel Malubag, and Mary Lou Salcedo. Lastly, our sincere thanks are extended to our fellow Academy and Filipino teammates on the expeditions. All the specimens from the Philippines were collected under our Gratuitous Permits (GP-0077-14, GP-0085-15) from the shallow waters of the municipalities of Mabini, Tingloy, Calatagan, Romblon, and Puerto Galera. This is part of the joint Department of Agriculture-NFRDI-California Academy of Sciences Memorandum of Agreement for the ongoing implementation of the National Science Foundation-funded biodiversity expedition in the Verde Island Passage. The specimens were collected in accordance with the terms and conditions of the gratuitous permit and under the supervision of our partners from BFAR Fisheries Regulatory and Quarantine Division and NFRDI.

We would like to send thanks to the Vanuatu expedition and Philippe Bouchet, Marta Pola, Angél Valdés, and Yolanda Camacho-Garcia for collecting specimens used in this study. In addition, we are grateful to Gustav Paulay and Amanda Bemis for lending several specimens for molecular sequencing. The Department of Invertebrate Zoology collection staff and the Center for Comparative Genomics at the California Academy of Sciences are thanked for all the help and support.

Material for some of several of the species studied here were kindly provided by Dr Philippe Bouchet (Muséum national d'Histoire naturelle, Paris; MNHN). The Madang expedition specimens were obtained during the *Our Planet Reviewed* Papua Niugini expedition organized by MNHN, Pro Natura International (PNI), Institut de Recherche pour le Développement (IRD), and the University of Papua New Guinea (UPNG), Principal Investigators Philippe Bouchet, Claude Payri, and Sarah Samadi. The organizers acknowledge funding from the Total Foundation, Prince Albert II of Monaco Foundation, Fondation EDF, Stavros Niarchos Foundation, and Entrepose Contracting, and in-kind support from the Divine Word University (DWU). The expedition operated under a permit delivered by the Papua New Guinea Department of Environment and Conservation. The *Atimo Vatae* expedition to South Madagascar (Principal Investigator, Philippe Bouchet) formed part of a cluster of Mozambique-Madagascar expeditions funded by the Total Foundation, Prince Albert II of Monaco Foundation, Stavros Niarchos Foundation, with additional support from the Richard Lounsbery Foundation and Triballat, under *Our Planet Reviewed*, a joint initiative of MNHN and PNI in partnership with Institut d'Halieutique et des Sciences Marines, University of Toliara (IH.SM) and the Madagascar bureau of Wildlife Conservation Society (WCS). Institut de Recherche pour le Développement (IRD) deployed its research catamaran *Antéa.*

We would also like to thank the reviewers, Dr Manuel Caballer (American University of Paris) and Prof. Dr Heike Wägele (Zoological Research Museum Alexander Koenig), for their thorough and helpful comments, which undoubtedly have contributed to a better manuscript. Finally, we would like to thank editor Dr Nathalie Yonow for her guidance.

References

Abe T (1964) Opisthobranchia of Toyama Bay and Adjacent Waters. Hokuryu-kan, Tokyo, 99 pp.

Baba K (1938) Opisthobranchia of Kii, Middle Japan. Journal of the Department of Agriculture, Kyushu Imperial University 6: 1–19. https://doi.org/10.5109/22587

Bergh LSR (1880) Nudibranchien. Nachträge und Ergänzungen. In: Semper C (Ed.) Reisen im Archipel der Philippinen. Malacologische Untersuchungen. Band 2, Theil 4. Supplement 1: 1–78. https://www.biodiversitylibrary.org/page/14356032

Bergh LSR (1891) Die cryptobranchiaten Dorididen. Zoologische Jahrbücher, Abtheilung für Systematik Geographie und Biologie der Thiere 6: 103–144. https://www.biodiversitylibrary.org/page/10194699

Bidgrain P (2006) *Chromodoris verrieri* from Reunion Island. Sea Slug Forum. http://www.seaslugforum.net/find/16411 [accessed 12 September 2020]

Bonomo LJ, Gosliner TM (2020) Adding stars to the *Chromodoris* (Nudibranchia, Chromodorididae) galaxy with the description of four new species. Zootaxa 4819(3): 401–435. https://doi.org/10.11646/zootaxa.4819.3.1

Carlson C, Hoff PJ (2003) The opisthobranchs of the Mariana Islands. Micronesica 35–36: 272–295. http://micronesica.org/sites/default/files/14-opisthos.pdf

Cheney KL, White A, Mudianta W, Winters AE, Quezada M, Capon RJ, Mollo E, Garson MJ (2016) Choose your weaponry: selective storage of a single toxic compound, Latrunculin A, by closely related nudibranch molluscs. PLoS ONE 11(1): e0145134. https://doi.org/10.1371/journal.pone.0145134

Coleman N (2008) Nudibranchs Encyclopedia: Catalogue of Asia/Indo-Pacific Sea Slugs. Neville Coleman's Underwater Geographic Pty Limited, Queensland, 416 pp.

Crosse JCH (1875) Description de nudibranches inédits, provenant de la Nouvelle-Calédonie, avec le catalogue des espèces actuellement connues. Journal de Conchyliologie 23: 305–322. https://www.biodiversitylibrary.org/page/15674851

Debelius H (1996) Nudibranchs and Sea Snails. IKAN-Unterwasserarchiv, Frankfurt, 321 pp.

Debelius H, Kuiter RH (2007) Nudibranchs of the World. IKAN-Unterwasserarchiv, Frankfurt, 360 pp.

Eliot CNE (1906) On the nudibranchs of southern India and Ceylon, with special reference to the drawings by Kelaart and the collections belonging to Alder and Hancock preserved in the Hancock Museum at Newcastle-on-Tyne. Proceedings of the Zoological Society of London 1906: 636–691. https://www.biodiversitylibrary.org/page/31208359

Eliot CNE (1909) Notes on a collection of nudibranchs from Ceylon. Spolia Zeylanica 6: 79–95. https://www.biodiversitylibrary.org/page/59022094

Epstein HE, Hallas JM, Johnson RF, Lopez A, Gosliner TM (2019) Reading between the lines: revealing cryptic species diversity and colour patterns in *Hypselodoris* nudibranchs (Mollusca: Heterobranchia: Chromodorididae). Zoological Journal of the Linnean Society 186(1): 116–189. https://doi.org/10.1093/zoolinnean/zly048

Fatemi Y, Attaran-Fariman (2015) Checklist of the opisthobranchs (Heterobranchia: Gastropoda) along the Iranian coasts of the Gulf of Oman. Journal of Biodiversity and Environmental Sciences 6(3): 1–7. https://www.innspub.net/wp-content/uploads/2015/03/JBES-Vol6No3-p1-7.pdf

Folmer O, Black M, Hoeh W, Lutz R, Vrijenhoek R (1994) DNA primers for amplification of mitochondrial cytochrome c oxidase subunit I from diverse metazoan invertebrates. Molecular Marine Biology and Biotechnology 3(5): 294–299.

Gosliner T (2001) Aposematic coloration and mimicry in opisthobranch mollusks: new phylogenetic and experimental data. Bollettino Malacologico 37: 143–150. https://www.biodiversitylibrary.org/page/51214700

Gosliner T, Behrens D, Valdés Á (2008) Indo-Pacific Nudibranchs and Sea Slugs: A Field Guide to the World's Most Diverse Fauna. Sea Challengers/California Academy of Sciences, Gig Harbor/San Francisco, 426 pp.

Gosliner T, Valdés Á, Behrens D (2015) Nudibranch & Sea Slug Identification Indo-Pacific. First edition. New World Publications, Jacksonville, 408 pp.

Gosliner TM, Valdés Á, Behrens DW (2018) Nudibranch and Sea Slug Identification: Indo-Pacific. Second edition. New World Publications, Jacksonville, 451 pp.

Harasti D (2003) *Chromodoris verrieri* from Nelson Bay. Sea Slug Forum. http://www.seaslugforum.net/find/9244 [accessed on 12 September 2020]

Hervé JF (2010) Guide des Nudibranches de Nouvelle-Calédonie. Catherine Ledru, Nouvelle-Calédonie, 400 pp.

Huelsenbeck JP, Ronquist F (2001) MrBayes: Bayesian inference of phylogeny. Bioinformatics 17: 754–755. https://doi.org/10.1093/bioinformatics/17.8.754

Johnson RF, Gosliner TM (2012) Traditional taxonomic groupings mask evolutionary history: a molecular phylogeny and new classification of the chromodorid nudibranchs. PLoS ONE 7(4): 29–31. https://doi.org/10.1371/journal.pone.0033479

Jie WB, Chan CY, Wu SK (2009) Taiwan Nudibranchs. National Museum of Marine Biology and Aquarium, Pingtung, 309 pp.

Kay EA, Young DK (1969) The Doridacea (Opisthobranchia; Mollusca) of the Hawaiian Islands. Pacific Science 23: 172–231. https://scholarspace.manoa.hawaii.edu/bitstream/10125/3322/v23n2-172-231.pdf

Kay EA (1979) Hawaiian Marine Shells. Reef and Shore Fauna of Hawaii. Section 4: Mollusca. Bernice Pauahi Bishop Museum Special Publications, Honolulu, 653 pp.

Katoh K, Standley DM (2013) MAFFT multiple sequence alignment software version 7: improvements in performance and usability. Molecular Biology and Evolution 30(4): 772–780. https://doi.org/10.1093/molbev/mst010

Kearse M, Moir R, Wilson A, Stones-Havas S, Cheung M, Sturrock S, Buxton S, Cooper A, Markowitz S, Duran C, Thierer T, Ashton B, Meintjes P, Drummond A (2012) Geneious basic: an integrated and extendable desktop software platform for the organization and analysis of sequence data. Bioinformatics 28(12): 1647–1649. https://doi.org/10.1093/bioinformatics/bts199

Kelaart EF (1858) Descriptions of new and little known species of Ceylon nudibranchiate molluscs and zoophytes. Journal of the Ceylon Branch of the Royal Asiatic Society, Colombo 3(1): 84–139. https://www.biodiversitylibrary.org/page/43940429

Korshunova T, Fletcher K, Picton B, Lundin K, Kashio S, Sanamyan N, Sanamyan K, Padula V, Schrödl M, Martynov A (2020) The Emperor's *Cadlina*, hidden diversity and gill cavity evolution: new insights for the taxonomy and phylogeny of dorid nudibranchs (Mollusca: Gastropoda). Zoological Journal of the Linnean Society 189(3): 762–827. https://doi.org/10.1093/zoolinnean/zlz126

Kozlov AM, Darriba D, Flouri T, Morel B, Stamakis A (2019) RAxML-NG: a fast, scalable, and user-friendly tool for maximum likelihood phylogenetic inference. Bioinformatics 35(21): 4453–4455. https://doi.org/10.1093/bioinformatics/btz305

Kumar JSY, Venkatraman C, Shrinivaasu S, Raghunathan, C (2019). New records of Opisthobranchs (Mollusca: Gastropoda) from Gulf of Mannar, India. Indian Journal of Geo Marine Sciences 48(10): 1508–1515. http://nopr.niscair.res.in/handle/123456789/51165

Layton KKS, Gosliner TM, Wilson NG (2018) Flexible colour patterns obscure identification and mimicry in Indo-Pacific *Chromodoris* nudibranchs (Gastropoda: Chromodorididae). Molecular Phylogenetics and Evolution 128: 27–36. https://doi.org/10.1016/j.ympev.2018.02.008

Layton KKS, Carvajal JI, Wilson NG (2020) Mimicry and mitonuclear discordance in nudibranchs: New insights from exon capture phylogenomics. Ecology and Evolution 10: 11966–11982. https://doi.org/10.1002/ece3.6727

Lin GY, Tchang S (1965) Opisthobranchia from the intertidal zone of Hainan Island, China. Oceanologia et Limnologia Sinica 7: 1–20.

Matsuda SB, Gosliner TM (2018) Glossing over cryptic species: descriptions of four new species of *Glossodoris* and three new species of *Doriprismatica* (Nudibranchia: Chromodorididae). Zootaxa 4444(5): 501–529. https://doi.org/10.11646/zootaxa.4444.5.1

Matsuda SB, Gosliner TM (2018) Molecular phylogeny of *Glossodoris* (Ehrenberg, 1831) nudibranchs and related genera reveals cryptic and pseudocryptic species complexes. Cladistics 34: 41–56. https://doi.org/10.1111/cla.12194

Mayes B (2007) *Chromodoris verrieri?* from Oman. Sea Slug Forum. http://www.seaslugforum.net/find/19690 [accessed on 12 September 2020]

Mehrotra R, Caballer Gutiérrez MA, Scott C, Monchanin C, Viyakarn V, Chavanich, S (2021) An updated inventory of sea slugs from Koh Tao, Thailand, with notes on their ecology and a dramatic biodiversity increase for Thai waters. ZooKeys 1042: 73–188. https://doi.or/10.3897/zookeys.1042.64474

Milne I, Lindner D, Bayer M, Husmeier D, McGuire G, Marshall DF, Wright F (2009) Topali v2. Bioinformatics 25(1): 126–127. https://doi.org/10.1093/bioinformatics/btn575

MolluscaBase (2021) *Goniobranchus* Pease, 1866. World Register of Marine Species. http://www.marinespecies.org/aphia.php?p=taxdetails&id=558453 [accessed on 1 December 2021]

Nakano R (2018) Field Guide to Sea Slugs and Nudibranchs of Japan. Bun-ichi Co., Tokyo, 544 pp.

Nimbs MJ, Smith SDA (2016) An illustrated inventory of the sea slugs of New South Wales, Australia (Gastropoda: Heterobranchia). Proceedings of the Royal Society of Victoria 128: 44–113. https://doi.org/10.1071/RS16011

Ono A, Katou S (2020) Nudibranch and Sea Slug Illustrated. Seibundo-shinkosha, Tokyo, 591 pp.

Orr J (1981) Hong Kong Nudibranchs. Urban Council, Hong Kong, 82 pp.

Padula V, Bahia J, Stöger I, Camacho-García Y, Malaquias MAE, Cervera JL, Schrödl M (2016) A test of color-based taxonomy in nudibranchs: molecular phylogeny and species delimitation of the *Felimida clenchi* (Mollusca: Chromodorididae) species complex. Molecular Phylogenetics and Evolution 103: 215–229. https://doi.org/10.1016/j.ympev.2016.07.019

Palumbi S, Martin A, Romano S, McMillan WO, Stice L, Grabowski G (1991) The simple fool's guide to PCR version 2.0. Department of Zoology and Kewalo Marine Laboratory, University of Hawaii, Honolulu, 45 pp.

Palumbi SR (1996) Nucleic acids II: the polymerase chain reaction. In: Hillis D, Moritz C, Mable BK (Eds) Molecular Systematics (Second Edition). Sinauer Associates, Sunderland, 205–248.

Pease WH (1860) Descriptions of new species of Mollusca from the Sandwich Islands. Proceedings of the Zoological Society of London 28: 18–36; 141–148. https://www.biodiversitylibrary.org/page/12866516

Pease WH (1866) Remarks on Nudibranchiata inhabiting the Pacific islands, with descriptions of two new genera. American Journal of Conchology 2: 204–208. https://www.biodiversitylibrary.org/page/15841170

Pittman C, Fiene P (1998) *Goniobranchus verrieri*. Sea slugs of Hawaii. http://seaslugsofhawaii.com/species/Goniobranchus-verrieri-a.html [accessed on 12 September 2020]

Potter B (2001) *Chromodoris preciosa* from Solomon Ids. Sea Slug Forum. http://www.seaslugforum.net/find/3232 [accessed on 12 September 2020]

Potter B (2005) *Chromodoris verrieri* from Solomon Ids. Sea Slug Forum. http://www.seaslug-forum.net/find/13526 [accessed on 12 September 2020]

Pruvot-Fol A (1951) Revision du genre *Glossodoris* Ehrenberg. Journal de Conchyliologie 91:76–164.

Puillandre N, Lambert A, Brouillet S, Achaz G (2012) ABGD, automatic barcode gap discovery for primary species delimitation. Molecular Ecology 21(8): 1864–1877. https://doi.org/10.1111/j.1365-294x.2011.05239.x

Risbec J (1928) Contribution à l'étude des nudibranches Néo-Calédoniens. Faune des Colonies Françaises T. 2, fasc. 1. Société d'éditions géographiques, maritimes et colonials, Paris, 328 pp.

Risbec J (1953) Mollusques Nudibranches de la Nouvelle Calédonie. Faune de l'Union Française, 15. ed. ORSTOM et Larose, Paris, 189 pp.

Rudman WB (1973) Chromodorid opisthohranch Mollusca from the Indo-West Pacific. Zoological Journal of the Linnean Society 52(3): 175–199. https://doi.org/10.1111/j.1096-3642.1984.tb01174.x

Rudman WB (1984) The Chromodorididae (Opisthobranchia: Mollusca) of the Indo-West Pacific: a review of the genera. Zoological Journal of the Linnean Society 81(2–3): 115–273. https://doi.org/10.1111/j.1096-3642.1984.tb01174.x

Rudman WB (1985) The Chromodorididae (Opisthobranchia: Mollusca) of the Indo-West Pacific: *Chromodoris aureomarginata*, *C. verrieri* and *C. fidelis* color groups. Zoological Journal of the Linnean Society 83: 241–299. https://doi.org/10.1111/j.1096-3642.1985.tb00875.x

Rudman WB (1990) The Chromodorididae (Opisthobranchia: Mollusca) of the Indo-West Pacific: further species of *Glossodoris*, *Thorunna* and the *Chromodoris aureomarginata* color group. Zoological Journal of the Linnean Society 100: 263–326. https://doi.org/10.1111/j.1096-3642.1990.tb01864.x

Rudman WB (1991) Purpose in pattern: the evolution of color in chromodorid nudibranchs. Journal of Molluscan Studies 57: 5–21. https://doi.org/10.1093/mollus/57.Supplement_Part_4.5

Slack-Smith SM, Bryce CW (2004) A survey of the benthic molluscs of the Dampier Archipelago, Western Australia. Records of the Western Australian Museum Supplement 66: 221–245. https://doi.org/10.18195/issn.0313-122x.66.2004.219-245

Soong GY, Wilson NG, Reimer JD (2020) A species complex within the red-reticulate *Goniobranchus* Pease, 1866 (Nudibranchia: Doridina: Chromodorididae). Marine Biodiversity 50: e25. https://doi.org/10.1007/s12526-020-01048-w

Sørensen CG, Rauch C, Pola M, Malaquias MAE (2020) Integrative taxonomy reveals a cryptic species of the nudibranch genus *Polycera* (Polyceridae) in European waters. Journal of the Marine Biological Association of the United Kingdom 100(5): 733–753. https://doi.org/10.1017/S0025315420000612

Stenhouse V (2000) *Chromodoris preciosa* from Vanuatu. Sea Slug Forum. http://www.seaslug-forum.net/find/1604 [accessed on 12 September 2020]

Strömvoll J, Jones G (2019) A Guide to the Sea Slugs of the Maputaland Coast. Ponta do Ouro Partal Marine Reserve, Back to Basics Adventure, Southern Underwater Research Group, Swedish International Development Cooperation Agency, Western Indian Ocean Marine Science Association, Johannesburg, 105 pp.

Tamura K, Stecher G, Peterson D, Filipski A, Kumar S (2013) MEGA6: molecular evolutionary genetics analysis version 6.0. Molecular Biology and Evolution 30(12): 2725–2729. https://doi.org/10.1093/molbev/mst197

Tibiriçá Y, Pola M, Cervera JL (2017) Astonishing diversity revealed: an annotated and illustrated inventory of Nudipleura (Gastropoda: Heterobranchia) from Mozambique. Zootaxa 4359(1): 1–133. https://doi.org/10.11646/zootaxa.4359.1.1

Valdés Á, Heros V (1998). The types of recent and certain fossil opisthobranch molluscs in the Muséum national d'Histoire naturelle, Paris. Zoosystema 20(4): 695–742. https://www.biodiversitylibrary.org/page/56146062

Wakeling M (2001) *Chromodoris preciosa*. Sea Slug Forum. http://www.seaslugforum.net/find/5321 [accessed on 3 September 2020]

Wilson NG, Winters AE, Cheney KL (2016) Tropical range extension for the temperate, endemic south-eastern Australian nudibranch *Goniobranchus splendidus* (Angas, 1864). Diversity 8(3): e16. https://doi.org/10.3390/d8030016

Winckworth HC (1946) *Glossodoris* from Bombay. Proceedings of the Malacological Society of London 26: 155–160. https://academic.oup.com/mollus/article-pdf/26/6/155/3774636/26-6-155.pdf

Yonow N (1989) Red Sea Opisthobranchia. 2. The family Chromodorididae (Mollusca, Nudibranchia). Fauna of Saudi Arabia 10: 290–309.

Yonow N (2001) Results of the Rumphius Biohistorical Expedition to Ambon (1990). Part 11. Doridacea of the families Chromodorididae and Hexabranchidae (Mollusca, Gastropoda, Opisthobranchia, Nudibranchia), including additional Moluccan material. Zoologische Mededelingen 75(1): 1–50. https://repository.naturalis.nl/pub/217432

Yonow N (2008) Red Sea Sea Slugs. Pensoft Publications, Sofia/Moscow, 304 pp.